Development of Life Cycle Assessment Based Air Quality Modeling and Decision Support System for the Mining Industry

Zunaira Asif

A Thesis
In the Department
of
Building, Civil and Environmental Engineering

Presented in Partial Fulfillment of the Requirements
For the Degree of
Doctor of Philosophy (Civil Engineering) at
Concordia University
Montreal, Quebec, Canada

June 2018

CONCORDIA UNIVERSITY
SCHOOL OF GRADUATE STUDIES

This is to certify that the thesis prepared

By: Zunaira Asif

Entitled: Development of Life Cycle Assessment Based Air Quality Modeling and Decision Support System for the Mining Industry

and submitted in partial fulfillment of the requirements for the degree of

Doctor of Philosophy (Civil Engineering)

complies with the regulations of the University and meets the accepted standards with respect to originality and quality.

Signed by the final examining committee:

Dr. Javad Dargahi — Chair

Dr. Rehan Sadiq — External Examiner

Dr. Mingyuan Chen — External to Program

Dr. Maria Elektorowicz — Examiner

Dr. Amruthur S. Ramamurthy — Examiner

Dr. Zhi Chen — Thesis Supervisor

Approved by

Dr. Ashutosh Bagchi, Chair of Department

15 August 2018

Dr. Amir Asif, Dean, Faculty of Engineering and Computer Science

ABSTRACT

Development of Life Cycle Assessment Based Air Quality Modeling and Decision Support System for the Mining Industry

Zunaira Asif, Ph.D.
Concordia University, 2018

Air quality in mining region has been facing many challenges due to lack of understanding of atmospheric factors and physical removal mechanism. Mining operations emit various types of pollutants which could violate the environmental guidelines. The development of an integrated approach is conceptualized in this thesis as life cycle assessment based air quality modeling system (LCAQMS) for the mining industry. LCAQMS consists of four primary models which are: (1) life cycle inventory model, (2) artificial neural network model, (3) mining-zone air dispersion model, and (4) decision analysis model. A graphical user interface (GUI) is built to integrate primary models to understand the pollutant's fate from its generation (emission inventory) to its management (control decisions). The life cycle inventory (LCI) model is developed to determine emission inventory using inverse matrix method, and defined characterization methods are investigated to assess the environmental impact. Artificial neural network model is developed to analyze carbon footprints (CO_2 equivalent) using backpropagation method. Mining-zone air dispersion model (MADM) is developed to generate the predicted concentration of air pollutants at various receptor levels by considering the deposition effect. The meteorological factors based on atmospheric stability conditions are determined by employing the Pasquill-Turner method (PTM). The decision analysis model comprises multi-criteria decision analysis (MCDA) method and air pollution control model (APCM) to provide air pollution control alternatives and optimize the cost-effective solutions, respectively. Monte Carlo simulation accomplishes the uncertainties in the system. Moreover, an environmental risk assessment (ERA) method is extended by integrating the APCM with a fuzzy set. The applicability of LCAQMS is explored through three different case

studies of open-pit metal mining in North America. Inventory results first show the air emission load for each mining activity and allow to evaluate the emission impact by linking the inventory to each impact category. Then this study helps to quantify the carbon footprints for the gold and copper mines. Also, prediction of significant pollutants such as PM_{10}, $PM_{2.5}$, SO_2, and NO_x at ground level has been calculated. The results depict that dry deposition is a dominate physical removal mechanism in the mining area. The LCAQMS results are evaluated with the monitoring field values, particularly MADM results are statistically tested against California puff (CALPUFF) model. Additionally, atmospheric stability is examined by analyzing the relationship between modeled $PM_{2.5}$ concentrations and mixing height based on seasonal variation and the diurnal cycle. In conclusion, LCAQMS can serve as a useful tool for the stakeholders to assess the impact, predict the air quality, and aid planners to minimize the pollutants at a marginal cost by suggesting control pollution techniques.

ACKNOWLEDGEMENTS

I would like to thank and acknowledge my supervisor, Dr. Zhi Chen, for his guidance, and patience throughout my Ph.D. program. His academic opinions have helped me establish a solid foundation for my research and encouraged me to furnish my best effort, leading to the successful completion of this dissertation. His support and suggestions on my work and future plans are invaluable. I am indebted to him for his availability, inspiration, and optimism.

I am also grateful to all the other members of my committee: Dr. Maria Elektorowicz, Dr. A.S Ramamurthy, and Dr. Mingyuan Chen for their valuable pieces of advice and help. I would especially like to thank Dr. Rehan Sadiq for contributing his time and offering valuable comments on my research work.

Foremost, I would like to express my sincere gratitude to my parents, my siblings Aroosha, Saira, and Zeeshan for their unconditional support and encouragement. Finally, my thanks go to my husband Bilal Khan who made this long journey much easier. This thesis is simply impossible without his support and help.

Last but not the least, I wish to extend my deepest appreciation to all my friends, group fellows Jinxin Dong, Ali Zakar, and my colleagues who have directly or indirectly helped me to complete this thesis.

TABLE OF CONTENTS

LIST OF TABLES

LIST OF FIGURES

LIST OF SYMBOLS

Section 3.2

α	scaling vector
β	environmental load vector
f_h	transfer function
g'	reference inventory vector
H	impact vector
H_{normal}	reference impact vector
i_c	impact category
j'	process unit
M	technology matrix
M^{-1}	inverse matrix of M
N	environmental intervention matrix
n	number of pattern
p	demand vector
q	characteristic matrix
s	sample size
w_{ij}	connection weights between the input (i) and hidden layer (j)
w_{jk}	connection weights between the hidden (j) and output neurons (k)
$y\hat{}$	predicted response (M)
σ_s	Standard deviation of samples

Section 3.3

a, b, c, d	power law exponent
C	pollutant concentration (M/L^3)
C_o	initial pollutant concentration (M/L^3)
C_f	field observed concentration (M/L^3)
C_m	modeling predicted concentration (M/L^3)

D_B	Brownian diffusivity (L^2/t)
d_p	particle diameter (L)
E	pollutant emission rate due to mining activities (M/t)
F	buoyancy flux(L^4/t^2)
f_i	fraction of particles
h	mixing height (L)
H	effective plume height (L)
hs	physical stack height (L)
ΔH	plume rise (L)
J	deposition flux (M/L^2t)
k	von Karman constant
k_x, k_y, k_z	eddy diffusivity coefficient in x, y and z direction (L^2/t)
L	Monin–Obukhov length (L)
L_y	lateral spread parameter in the (crosswind) distance
L_z	vertical spread parameter in vertical direction
P	precipitation rate (L/t)
P_o	reference precipitation rate (L/t)
Q	emission rate (M/t)
R	term used for sinks (M/L^3t)
r	radius of the stack (L)
r_a	aerodynamic resistance (t/L)
r_d	deposition layer resistance (t/L)
S	slip correction factor
Sc	Schmidt number
S_o	term used for source (M/L^3t)
St	stokes number
t	time (t)
T_a	ambient air temperature (K)

T_s	temperature at the source (K)
u, v, w	average wind speed component (L/t)
u	wind speed (L/t)
u_o	frictional velocity (L/t)
V_d	deposition velocity (L/t)
V_s	stack exit velocity (L/t)
V_{df}	deposition velocity for fine particles (L/t)
V_{dc}	deposition velocity for coarse particles (L/t)
W	gravitational settling velocity (L/t)
x_2, a_1, a_2, a_3	slip correction constants
x, y, z	Cartesian coordinates (L)
Z	receptor height or height above the ground (L)
z_d	deposition reference height (L)
z_o	surface roughness length (L)
$\sigma_x, \sigma_y, \sigma_z$	standard deviation in x, y and z direction (L)
μ	viscosity of air (L^2/t)
ρ	particle density (M/L^3)
ρ_a	air density (M/L^3)
Λ	scavenging ratio (1/t)
λ	wet scavenging coefficient (1/t)
σ_o, σ_p	standard deviations of the field observed and modeling predicted concentration (statistical value)

Section 3.4

α_s	solar altitude
β_s	area latitude
δ_s	solar declination angle
γ_s	solar hourly angle
σ_θ	horizontal fluctuation of the wind direction
f	Coriolis parameter
Θ	earth's rotation (1/t)

ψ	latitude (L)
S_f	surface heat flux (KL/t)
T_v	virtual temperature (K)
ω	mixing ratio

Section 3.5

A	evaluation matrix consists of alternatives (actions)
B	utility matrix
d_i	difference between ranks of criteria weights and alternatives values
I	multicriteria preference index
S_j	weights of criterion
Sp	spearman rank correlation coefficient
$Y\ (x_i, x_k)$	degree of the preference of one alternative (x_i) with respect to another alternative ($x_{k)}$
Φ^+	positive flow of alternatives
Φ^+	negative flow of alternatives

Section 3.6

C_{ij}	total cost of treatment j of pollutant p for activity ($/M)
d_t	dispersion transfer function (t/L^3)
L_p	Air quality standard of pollutant p (M/L^3)
Pf	probability density function
P_r	annual production of metal (M)
X_{ij}	metal produced after controlled treatment option j at source i (M/t)
Z_t	treatment cost ($/t)
σ^2	Variance
η	efficiency of a controlled treatment (%)
$\mu_{G1}, \mu_{G2}, \mu_{G3}$	membership functions

Section 5.2

a_m	mining area (L^2)
c_d	capacity of dumpers/unloader (M)
d_h	hole diameter (L)
d_r	number of days with at least precipitation (t)
f	frequency (holes/day)
h_d	drop height of a loader (L)
k_c	emission coefficients of particles
k_p	particle size multiplier
l	size of loader (L^3)
m	moisture content (%)
pt	percentage of time wind speed is greater than 5.4m/s
s_i	silt content (%)
v_s	average vehicle speed (L/t)
Vt	total distance covered by vehicle (L)
x_f	frequency of loading
y_f	frequency of unloading

Section 5.4

C_B	background concentration (M/L^3)

LIST OF ACRONYMS

ABL	Atmospheric boundary layer
ADE	Advection-diffusion equation
AHP	Analytical hierarchy process
AERMOD	American meteorological society/environmental protection agency regulatory model
ANN	Artificial neural network
AP	Air pollution
APCM	Air pollution control model
BATs	Best available technologies
BH	Baghouse
BPANN	Back propagation artificial neural network
CALMET	California Meteorological model
CALPUFF	California Puff (model)
CFD	Computational fluid dynamics
CMLCA	Chain management by life cycle assessment
CST	Concentrated solar thermal (technology)
DM	Decision-maker
DOC	Diesel oxidation catalyst
DS	Dust suppressant
DTE	Dispersion transfer function
EDIP	Environmental development of industrial products
EIA	Environmental impact assessment
EIO	Economic input-output
ELECTRE	Elimination and choice translating reality
EP	Electrostatic precipitator
ERA	Environmental risk assessment
FAME	Fatty acid methyl ester
FC	Fuel consumption
FDM	Fugitive dust model

FGR	Flue gas recirculation
Gabi	Ganzheitliche Bilanz (german word means Holistic Balance)
GAIA	Geometrical Analysis for Interactive Decision Aid
GHG	Greenhouse gas
GILTT	Generalized integral Laplace transform technique
GSH	Gas sparged hydro-cyclone
IOA	Input-output analysis
ILDC	International reference life cycle data system
ISC	Industrial source complex
LCA	Life cycle assessment
LCAMM	Life cycle assessment and artificial neural networking model of mining
LCAQMS	Life cycle assessment-based air quality modeling system
LCIA	Life cycle impact assessment
LCI	Life cycle inventory
LNB	Low NOx burner
LP	Long term performance
MADM	Mining-zone air dispersion model
MAUT	Multi-attribute utility theory
MCDA	Multicriteria decision analysis
MCS	Monte Carlo simulation
MILP	Mixed-integer linear programming
MSE	Mean square error
NAAQO	National ambient air quality objectives
NAAQS	National ambient air quality standards
NAPS	National air pollution surveillance
NOAA	National oceanic and atmospheric administration
NRI	Net radiation index
OD	Operating duration

PBL	Planetary boundary layer
PDF	Probability density function
PFD	Process flow diagram
PGM	Pasquill-Gifford method
PM	Particulate matter
PROMETHEE	Preference ranking organization method for enrichment of evaluations
PTM	Pasquill–Turner method
SCR	Selective catalytic reduction
SEM	Standard error of the mean
SNCR	Selective non-catalytic reduction
TRACI	Tool for the reduction and assessment of chemical and other environmental impacts
TSP	Total suspended particles
ULSD	Ultra low sulfur diesel
VOCs	Volatile organic compounds
WHO	World health organization
WS	Wet scrubbers

CHAPTER 1 INTRODUCTION

1.1 Background

The mining industry contributes significantly to the economy in North America primarily Canada, USA, etc. Mining operations, however, emit various types of pollutants that have significant impacts on the environment. In a recent inclusive assessment of the worst environmental pollution issues, among the four of the world's top ten pollution sources were the activities associated with mining operations, including gold mining; metal smelting and processing (Ericson et al., 2008). The concerned environmental challenge in the mining sector is vulnerability to the air quality due to emissions of pollutants such as particulate matter (PM_{10} and $PM_{2.5}$) nitrogen oxide (NO_x), sulfur oxide (SO_x), and greenhouse gas (GHG) emissions from various activities of mine (Mining Association Canada Report, 2012; National Pollutant Release Inventory, 2013). In mining, the extraction and transformation of metals such as gold, silver, and copper create risks of negative impacts on the environment and the surrounding communities. The potential air pollutants during construction and operational phase of the mining are dust and particulate matter (PM_{10} and $PM_{2.5}$). Particulate emissions are primarily associated with fugitive dust that comes from the usage of heavy equipment such as haul truck, windblown dust from mineral stockpiles, drilling, loading and blasting activities, etc. During the mining operations, vegetation is usually removed, in return making the land vulnerable to the effect of weather, causing particulates to become airborne through the wind erosion. Sometimes metals (such as arsenic, lead, mercury, nickel, etc.) which are the part of ore or produced during processing or recovery activities in the mine also become the part of particulates and responsible for the health effect in the downwind area (Soriano et al., 2012).

At both workplace and residential areas, these airborne particles are adversely affecting the health by contributing to illnesses. For instance, damaging the lungs, respiratory tract and causing skin diseases by absorbing into the skin (Leili et al., 2008).

Also, many reagents used in processes of mining can be responsible for air pollutants such as SO_2 produced during the process of cyanide destruction and fuel consumption. Fuel combustion is also responsible for the release of carbon monoxide (CO) and nitrogen oxide (NO_x). Carbon dioxide (CO_2) derived mainly from on-site fuel combustion, explosive detonation, and from off-site power generation at the energy production sources, contributed to the increment of carbon footprints.

With increasing environmental awareness, more and more mining companies are showing their interest to address the air quality problems and carbon credits and to identify appropriate corrective measures to improve the environmental sustainability of their processes. Two approaches could be used to analyze this issue. A life cycle assessment (LCA) approach, which helps to develop the emission inventory and to scrutinize the environmental impact based on technology's life cycle perspective. Another one is air quality modeling, which is used to predict pollutant concentrations. Before examining the air quality, it is equally important to have an effective inventory of the mining system.

Emission inventories of mines are generally far complicated than those established for other industries because of variability in mining activities. From the last few years, many researchers studied to develop inventories by the help of life cycle assessment (LCA) modeling in the mining industry (Durucan et al., 2006; Norgate and Haque, 2010; Awuah-Offei and Adekpedjou, 2011; Ingwersen, 2011; Norgate and Haque, 2012; Northey et al., 2013; Nuss and Eckelman, 2014). Unfortunately, LCA use in assessing metal mining processes has not been much publicly available, as evidenced by limited published literature on LCA applications in mining (Awuah-Offei and Adekpedjou, 2011; Durucan et al., 2006; Norgate and Haque, 2010). This situation also stands for metal mining such as gold and copper (Ingwersen, 2011; Norgate and Haque, 2012). In these LCA studies, a little emphasis has been given on greenhouse gases or air pollutants that could be generated from the processing of the metal in the context of the allocation of environmental burdens. In other words, the mining system has been mostly discussed concerning acid mine drainage and handling of tailings (Reid et al., 2009). Most of the studies depicted that some specific mines and their inventories were

mostly reported in aggregated form (pre-allocated values), and which makes it difficult to carry it forward for further investigation (Nuss and Eckelman, 2014). However, LCA studies are mostly lacking in detailed representation of variables used in a linear or non-linear system for flows analysis. Thus, it is significant to include maximum dependent variables which are directly responsible for environmental burden in the mining industry. There are various tools available commercially for conducting LCA and supporting the application of LCA for different industries. Examples include NIRE-LCA (Narita et al., 2005), Quick LCA in Japan (Quick LCA, 2015), SimaPro in the Netherlands (Li and Guan, 2009), open LCA in Europe (OpenLCA, 2016) and GaBi in Germany (Hendrickson et al., 1997). These tools can be used for studying LCA in the mining industry. For instance, SimaPro was used during the study of copper-zinc underground mine in Quebec (Reid et al., 2009) and gold mining in Peru, United States (Ingwersen, 2011). Gabi was used to studying overburden in the mining sector (Worldsteel Association report, 2014). All the mentioned LCA tools are very efficient. However, very costly and most of them associated with European databases, which is one of the significant disadvantages. To overcome this shortcoming, mostly tools are linked with ecoinvent 2.2 and 3.1 databases (ecoinvent, 2016). Thus, recently this database is updated with nonferrous metal mining such as gold and silver but have geographical limitations.

To strengthen the assessment of the complex mining system, an improved and integrated approach to quantify the greenhouse gases and carbon footprints based on life cycle thinking needs to be developed and implemented. Thus, the artificial neural network models (ANN) are capable of reflecting the underlying linear and nonlinear relationship amongst the air pollution data and further predict the future concentration by training the past data. In recent years, the application of ANN models has been applied successfully to assess the air quality (Tecer, 2007). Moreover, it seems to be a worthy choice because it shows remarkable performance while dealing with complex interactions within the given input parameters (Baawain and Al-Serihi, 2014). In particular, the back-propagation algorithm among ANN models performs better when dealing with the mixture of linear and nonlinear systems such as the pollution-climatic phenomenon (Baawain and Al-Serihi, 2014). Recently, some researchers applied ANN

in the field of mining to predict dust and particulate matter (Lal and Tripathy, 2012; Patra et al., 2016; Roy et al., 2011a; Tecer, 2007). ANN models are glimpsed as efficient tools for predicting the air quality and a more promising approach in systematically preparing the data while focusing on dealing with limitations like missing data. However, insufficient work is available in the field of metal mining. Therefore, the present study conceived the possibility to predict the carbon footprint analysis in terms of CO_2 equivalent emission as the midpoint impact analysis with varying greenhouse gases and fuel consumption.

Mining operations obtain air quality permits before starting any new project, construction or expansion. The impact assessment also involves prediction of pollutant concentration emitting due to existing various mining operations. Some attempts have been made previously to create mine targeted air dispersion model based on mathematical techniques, but a very few validated with testing at mine sites (Bhaskar and Ramani, 1988; Reed et al., 2002; Silvester et al., 2009). Numerous air quality models such as box model, Gaussian model, the Eulerian model, and the Lagrangian model have been reported to be used for the prediction of air quality for the mining industry (Reed et al., 2002). The methods mentioned above have some limitations when applied to the mining system. For air quality assessment, the traditional mathematical models do not incorporate emission rates from various mining activities. Moreover, most of the models are mainly centered around the particulate matter and ignore other gaseous air pollutants which are sometimes as important if not more important than the particulate emissions from these processes (Silvester et al., 2009; Trivedi et al., 2009). The past studies also concluded that most models share common assumptions and consequently produced results based on the analysis of the single source at the mining site (Badr and Harion, 2007; Pereira et al., 1997) and over prediction analysis (Fishwick and Scorgie, 2011; Neshuku, 2012). These studies concluded that there is a need to take a holistic approach to understanding air pollution from various mining operations, including multi-pollutants identification and physical removal mechanism such as deposition. In general, Gaussian-based models are easier to implement with relatively minimum requirements for the meteorological data and computational effort. Despite

the usefulness models as mentioned earlier, there is a continue quest to contribute more in the field of mining with the advanced Gaussian algorithms.

Air quality deterioration has been increasingly drawing researchers' attention over the past few decades to identify appropriate corrective measures to improve the environmental sustainability of their processes. Two approaches have been used to analyze this issue. One is the direct application of abatement technology to reduce the air pollution, based on the quantities of pollutant's concentration in the effluent stream. The second approach is to develop a decision tool to control air pollution and effective management in a stochastic manner. Many control technologies have been widely studied and practically used in the mining sector based on the environmental protection agency (EPA) guidelines, such as desulfurization of fuel, electrostatic precipitators, and baghouse to reduce particulate matter, etc. However, the present study, the focus is on the second approach, as this strategy complements the first approach by including treatment options while minimizing economic resources for their implementation. Selecting the suitable optimal technology for a mine site is a critical task because most environmental decision making (i.e., the selection process) involves multiple criteria and conflicting objectives (e.g., minimizing pollution and cost while maximizing production) (Kiker et al., 2005; Sadiq and Tesfamariam, 2009). Moreover, a huge database is required, and input information for each objective is often represented in qualitative or quantitative form, which is difficult to understand and thus intensify the decision-making process (Tesfamariam and Sadiq, 2006). Multiple criteria decision analysis (MCDA) methods deal with such problems whose alternatives are predefined and multiple criteria based ranking to evaluate the alternatives (Betrie et al., 2013). The recent advances in optimization theory and its applications have enabled the decision makers to develop the systematic tools to control environmental problems by using mathematical programming techniques (Cristóbal et al., 2012; Grandinetti et al., 2007). Unfortunately, there have been uncertainties associated with the air dispersion model. The stochastic uncertainties due to the variation of inputs or randomness inherent such as several determinative parameters related to contaminant concentration and meteorological conditions including wind speed and direction, vertical and horizontal dispersion coefficients and topographical site conditions. The probability theory

(Monte Carlo method) is used mostly to address random variability in parameters using probability distribution/density function (Kaya and Kahraman, 2009). Furthermore, environmental risk, because of output data (pollutant concentration), need to be seriously evaluated which may lead to the violation of the environmental guidelines and aids in decision making management. More attention is being paid to the fuzzy-set concept for addressing regional air pollution problems (Onkal-Engin et al., 2004; Ping et al., 2010).

Consequently, development of a life cycle assessment based air quality modeling system (LCAQMS) for mining is proposed and applied practically to the mining field. The system integrates inverse matrix which is used to develop air emission inventory; characterization method to assess the environmental implications; artificial neural network model for carbon footprint analysis; an advance Gaussian algorithm for air dispersion modeling to predict the pollutant concentration at receptor level; Pasquill–Turner method (PTM) to determine the atmospheric stability; multicriteria decision analysis tool to provide alternatives for treatment technologies and air pollution control model to optimize the cost of treatment system. The uncertainties in the model are handled with the fuzzy-based environmental risk assessment method using Monte Carlo simulation. The model has a single graphical user interface and shared data storage.

1.2 Research Objectives

The aim of this study is to conceptualize the life cycle assessment based air quality modeling (LCAQMS) and decision support system and implement it to the three different open-pit metal mining sites in North America to explore the feasibility of the system. The modeling system is comprised of mathematical equations and analytical solutions which help to generate emission inventory emanating from the mining activities; assess the environmental midpoint-impacts; carbon footprint analysis of the mining; predict the air pollutants at ground level; determine various meteorological factors based on atmospheric stability and choice of best cost-effective treatment technology of air pollution. Specifically, this thesis has the following objectives:

1. To develop an integrated life cycle assessment and artificial neural network model for mining (LCAMM) to determine the pollutant's emission inventory, impact assessment and carbon footprints for the metal mining industry.
2. To develop a mining-zone air dispersion model (MADM) which allows to predict the pollutant's concentration at downwind distance and to investigate the effect of deposition on the predicted concentration. The concentration gradient (k-theory) plume algorithm is modified by incorporating mining emission rates to determine the transport and removal mechanism of the dispersed pollutant.
3. To investigate the effect of vertical dispersion based on atmospheric stability under different seasonal variation and diurnal patterns using Pasquill–Turner method (PTM).
4. To develop the decision support system by ranking the alternatives and to choose the cost-effective treatment techniques. Two different approaches are used to explore the applicability of the system. One is the development of multi-criteria decision analysis (MCDA) to rank the alternatives. The other is to develop an optimization model based on linear programming for mining-air pollution control planning called as air pollution control model (APCM) as the next stage of decision analysis.
5. To develop the LCAQMS graphical user interface and implement it to the open pit metal mining site for testing an integrated system.

1.3 Thesis Organization

This thesis is organized into ten chapters as shown in Figure 1.1.

Chapter 1 introduces the research background, states the research problems, specifies the research objectives, and briefly introduces the research methodologies.

Chapter 2 provides a brief review regarding air pollution in mining, life cycle assessment modeling, application of artificial neural networking in air pollution, air

quality modeling in mining and decision analysis methods which assist in the management of air pollution.

Chapter 3 describes the methodologies for developing LCA based air quality modeling system (LCAQMS) for assessing, predicting and managing air pollution in the mining sector. The system integrates life cycle inventory and artificial neural network model which is used to generate the source inventory and impact assessment. Then the development of meteorological model and mining-zone air dispersion model is conceptualized which assist in predicting the air pollution. In addition, decision analysis system including multi-criteria decision analysis and air pollution control model is developed to manage the air pollution. A graphical user interface is built to provide LCAQMS as an integrated system.

Chapter 4 represents the implementation of the first two modules of LCAQMS: life cycle inventory (LCI), and artificial neural network (ANN) model. The integrated modeling approach is used to determine air emission load for each mining activity and to evaluate the emission impact by linking the life cycle inventory to each impact category. Furthermore, ANN model is applied to simulate the carbon footprint analysis for the gold mining site (mine A), Ontario, Canada.

Chapter 5 depicts the implementation of the third module of LCAQMS as mining-zone air dispersion model (MADM) to predict air pollutants concentration in the mining region while considering the deposition effect. The feasibility of MADM is explored through a case study in a gold mine (mine B), British Columbia, Canada. The studied pollutants are PM_{10}, $PM_{2.5}$, NO_x and six heavy metals (As, Pb, Hg, Cd, Zn, Cr). The modeling results are also validated with the monitoring data and statistically evaluated with CALPUFF.

Chapter 6 determines various meteorological factors based on atmospheric stability by employing Pasquill-Turner method (PTM) indices using net radiation index and wind speed. PTM method is integrated with MADM to predict the effect of vertical

dispersion on $PM_{2.5}$ concentration under the different stability patterns in a copper mining area (mine C), Utah, USA.

Chapter 7 represents the fourth module of LCAQMS to manage air pollution by ranking the alternatives of control methods. The study helps in reducing air pollution and carbon footprints by implementing the multi-criteria decision analysis (MCDA) method in a copper-gold mine (mine B), British Columbia, Canada. Three categories which are the reduction of dust control equipment, reduction in fuel consumption to minimize carbon footprint and cyanide destruction methods are selected for the study.

Chapter 8 describes the way to select the cost-effective solution and environmental risk assessment by exploring the applicability of air pollution control model through a case study of an open pit copper mine (mine C), Utah, USA. Results are analyzed to select the optimized treatment technology for $PM_{2.5}$, PM_{10}, NO_x, and SO_2. Moreover, air quality is analyzed by integrating the system with a fuzzy set.

Chapter 9 presents an implementation of an integrated LCA based air quality modeling system (LCAQMS) and decision support in an open pit copper mining (mine C), Utah, USA as a combined system using graphical user interface. Prediction of four significant pollutants (PM_{10}, $PM_{2.5}$, SO_2, NO_2) is studied along with the greenhouse gases for carbon footprints analysis. The system is further evaluated with field data.

Chapter 10 presents the conclusions and contributions as well as the recommendations for further research.

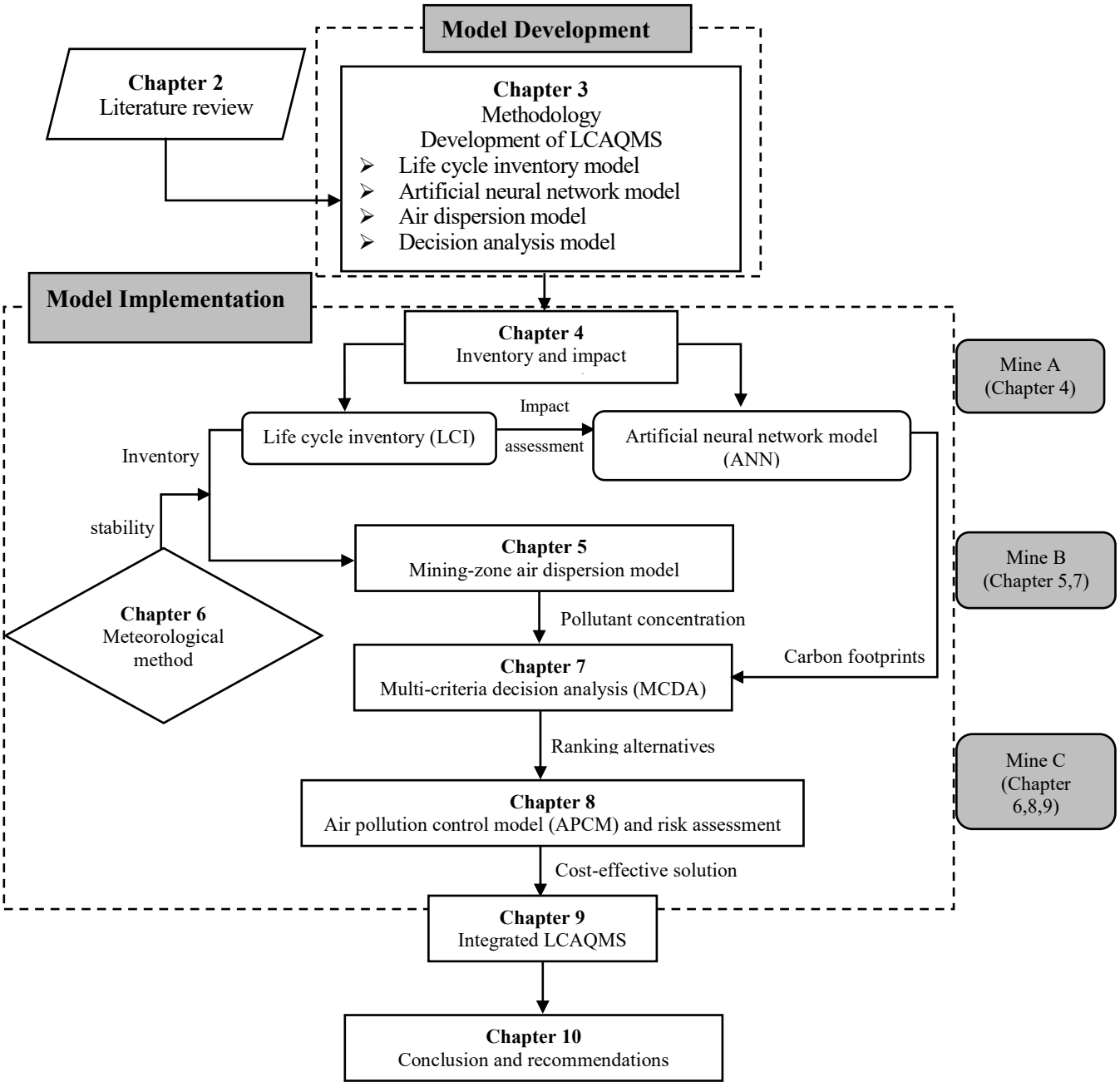

Figure 1.1 Thesis organization

CHAPTER 2 LITERATURE REVIEW

2.1 Air Pollution in the Mining Region

Air quality management in the mining industry is a complex task, mainly due to the wide range of sources, the fact that these sources are highly variable, difficult to measure, and site-specific concerning drilling holes, pit area, moisture contents, etc. The primary air quality issues related to mining are mainly particulate impact. Dust is a significant concern for open pit mines, and many surface mines employ a variety of techniques to control and manage dust. Other air pollutants which may generate during mining activities are CO_2, NO_x, SO_2 and heavy metals concentrations (Asif and Chen, 2016).

January 1, 2013, has been considered as the beginning of a new era in the fight against greenhouse gases and climate change in Québec, the period of the western climate initiative's (WCI) carbon market. Industries that emit 25,000 metric tons or more of CO_2 equivalent a year are subject to the cap and trade system for the first compliance period (2013–2014). Fossil fuel distributors will also be subject to the system in the coming years when the second compliance period begins. The third compliance period will extend from 2018 to 2020 (Technical overview Quebec Report, 2013). Electricity use and fuel consumption are mainly responsible for just over half of the GHG emissions which indicates that attempts to lessen the environmental impact should focus on these two stages (Norgate and Haque, 2012).

Poor air quality in the mines can lead to occupational illness and health hazardous for the surrounding community. For instance, sixty-nine mine workers died from occupational diseases, including cancer and skin allergies, according to claims accepted by the workplace safety and insurance board (WSIB) of Ontario between 2008 and 2013 (Ontario Ministry of Labour, 2013). Based on national pollutant release inventory (NPRI) report 2013, between 1998 and 2011, the mining sector has made considerable progress in reducing emissions of air pollutants, i.e., SO_2 (52.0 %) and NO_x (28.4 %). However, emissions of particulate matter increased in the mining as well as in rock

quarrying subsector especially PM_{10} levels increased by 0.03 % for the same period and by 13.9% between 2008 and 2011, whereas NO_x levels increased by 24.2 % between 2008 and 2011 (CIEEDAC, 2015). The increased level of airborne particulate matter resulted from various operational activities including drilling, blasting, crushing, loading, hauling, and transferring to belts. Likewise, open-pit mining, waste rock stockpiling, and open dumped solid waste are significant potential sources of dust/windblown PM_{10}. Similarly, the percentage of NO_x increased due to fuel and diesel consumption by heavy equipment used during haulage, drilling, maintenance, personnel transportation, generators, and heating and cooling. Conversely, the decline in SO_2 and NO_x emissions can be attributed in part to federal and provincial government regulatory initiatives such as the implementation of the Canada-wide acid rain strategy for post-2000, as well as treaties with the USA on SO_2 emission caps. The reduction of SO_2 can also be attributed to the use of low-sulfur fuels, advanced technologies, pollution control equipment for base-metal smelters, and proper mine closures (National Pollutant Release Inventory, 2013).

Mine can be operated in various ways including such as open cast, underground methods, surface stripping and hydraulic leaching (Norgate and Haque, 2010). Whereas, mostly metal mining such as gold, copper, silver, etc., classified into underground mining or open pit mining to extract the ore, followed by crushing, grinding, recovery processing such as flotation or cyanidation to extract the gold and formation of concentrate (Norgate and Haque, 2012). In some cases, a combination of open pit and underground mining occurs, although usually sequentially in the mine life-cycle, rather than simultaneously. At underground mines, the leading causes of dust emissions are the stockpiling, tailings area, and load-out facilities. Whereas, at open pit mines, the same sources exist, including some additional activities such as drilling, loading, haulage, and from a greater extent of surface disturbance and exposure (Asif and Chen, 2016).

2.2 Life Cycle Assessment (LCA) for the Mining Process

The LCA methodology is based on International Organization for Standardization (ISO) (14040 and 14044) guidelines. At present, methodologies comprise four phases (Awuah-Offei and Adekpedjou, 2011; ISO., 2006):

- Goal and scope definition
- Life cycle Inventory Analysis
- Impact Assessment
- Interpretation

The reason for carrying out the first step of the LCA is defining the scope of the study and setting the system boundaries and the level of detail. The next step is inventory analysis, and this phase deals with collecting the data to meet the objectives of the LCA study by producing output data, i.e., inventory of the studied system. Possible data sources include for example measurements on the production site and existing databases. The purpose of the third phase, life cycle impact assessment (LCIA), is to convert the life cycle inventory (LCI) results in the related environmental impacts. In next section, further detail of the LCA phases is discussed.

2.2.1 Life cycle inventory analysis and database for mining

Availability of data is an essential concern in conducting LCA as most of the data necessary for this work is unavailable directly and little information accessed to the public domains. The mining sector has been facing this challenge. Some life cycle inventory (LCI) data on coal and ferrous metals have been available to the LCA studies for many years, either directly from industrial sector or through LCI databases provided by academic and consulting groups (e.g., Gabi, ecoinvent, National Renewal Energy Laboratory (NREL) and the ELCD databases). Mostly mining data comprised the following activities: energy flows during mining operations, fuel consumption for instance in the form of electricity usage or diesel; information on mining infrastructure and the chemicals used in metal recovery processes. Some of the databases may

consider inputs from the actual ground resources and emissions to air, soil, and groundwater. While, in other traditional databases, pollutant emission rates are only partially included or not available at all. Even in the most advanced databases, there are not any features like operational activities, location-based data availability and mining/processing method (Durucan et al., 2006; Lesage et al., 2006). All LCA models whether commercially available or not followed the EPA and ISO defined methods (EPA, 2006; ISO, 2006). The four primary methods which have been used for inventory development are (1) process flow diagram method (PFD), (2) matrix method, (3) input-output analysis method (IOA), and hybrid method (Heijungs and Sun, 2002).

Process flow diagram (PFD) method is the first LCI method which appeared in early LCA studies, and it is still in use under various LCA applications nowadays. PFD shows the way processes of a product system are interlinked through commodity flows. In PFD, boxes generally represent processes and directs the commodity flows. Each process is expressed as a ratio between inputs and outputs. The values of commodities fulfilling a particular functional unit is obtained in order to calculate LCI of any system, by multiplying with the environmental interventions (Suh and Huppes, 2002).

Heijungs and Sun, (2002) first time introduced the matrix based LCIA method (matrix method). This method utilizes a system of linear equations to solve an environmental inventory problem. Using matrix algebra operations and arranging the economic and environmental flows in matrix forms, the final cumulative environmental loads are calculated (Lu, 2006). The detailed computational skills of the matrix method were developed and modified by Cooper, (2003). As compared to other methods, this method can deal with the detailed LCA system with a better understanding of internally recurring unit processes (Gwak et al., 2003; Heijungs et al., 2006).

Input-output analysis (IOA) method was first introduced by Wassily Leontief in the 19th century (Lu, 2006). IOA was primarily designed for economic dependencies in industrial sector but can serve environmental analysis as well. A table is used in an IOA method, and environmental data is added to quantify the environmental burdens for each sector per unit of money inflow to that sector. The costing data, as well as the

environmental data, are expressed as average values over the whole industrial sector. The similar approach is used in one of the commercially available model economic input-output analysis EIO-LCA (Economics and Ecology, 2009). IOA, in contrast, yields a complete system but is overly aggregated and hence unspecific (Heijungs et al., 2010).

Integration of PFD and IOA by combining the strengths of both is generally called the hybrid method (Lenzen, 2002). So far hybrid LCIA method has been adopted in some LCA case studies (Economics and Ecology, 2009). In detail, hybrid LCIA method can be distinguished as tiered hybrid analysis, IOA-based hybrid analysis and integrated hybrid analysis (Suh et al., 2004). For LCI analysis, a large quantity of data is needed to collect. In practical LCA applications, it is difficult to collect data of every unit, and there must exist some missing data, which is vital sometimes depending upon the goal of the study (Geldermann et al., 2000; González et al., 2002).
Summary of all the methods with limitations and other features are mentioned in Table 2.1.

Table 2.1 Summary of LCI methods (Suh and Huppes, 2002)

	Based on process analysis			
Items	Process flow diagram	Matrix method	Input-output based LC1	Hybrid LCI
Data requirement	commodity and environmental flows per process		commodity and environmental flows per sector/process	
Uncertainty of source data	low	low	medium-high	depends
Technological system boundary	complete	complete	medium-poor	depends
Simplicity of application	simple	simple and detail	simple	complex
Required computational tools	excel or similar	Matrix inversion (MATLAB or Mathematica)	Excel or similar	Matrix inversion (Mathematica)
Examples	many available	CMLCA	EIOLCA	MIET+LCA

In this thesis, an inverse matrix method is used to determine the air pollution inventory for the mining industry. In comparison, this method is detailed and simple to use with a better understanding of LCA system (Gwak et al., 2003; Heijungs et al., 2006).

2.2.2 Methods for LCA impact assessment

There are various LCIA methodologies that can be applied. They can differ in the impact categories, selection of indicators, and in their geographical focus. The choice of the most suitable LCIA methodology is case-specific. The following Table 2.2 gives information for the variety of the appropriate methods, including:

- Chain management life cycle assessment (CMLCA) 2002
- Eco-indicator 99
- Environmental development of industrial products (EDIP97 and EDIP2003)
- International reference life cycle data system (ILCD)
- IMPACT 2002+
- Recipe
- Tool for the reduction and assessment of chemical and other environmental impacts (TRACI)
- USEtox

Table 2.2 Various environmental assessment methods and their impact categories

Methods	Climate Change	Acidification	Photochemical Oxidation	Particulate Matter	Freshwater toxicity	Human toxicity	Terrestrial toxicity	Land use	Normalization factor	Reference
CMLCA (baseline)	✓	✓	✓	-	✓	✓	✓	-	Europe Netherlands, West Europe, Worldwide	(CMLCA, 2015)
CMLCA (non-baseline)	✓	✓	✓	-	✓	✓	✓	✓		
Eco-indicator 99	✓	✓	✓	✓	✓	✓	✓	✓	Europe EI 99	(Eco-indicator, 2016)
ILCD 2011 endpoint	✓	✓	✓	✓	-	-	-	✓	Europe	(ILCD, 2015)
ILCD 2011	✓	✓	✓	✓	✓	✓	✓	✓	Europe	
Recipe Endpoint	✓	✓	✓	✓	✓	✓	✓	✓	Worldwide	(Recipe, 2016)
Recipe Midpoint	✓	✓	✓	✓	✓	✓	✓	✓	Europe, worldwide	
TRACI 2.1	✓	✓	✓	✓	✓	✓	✓	-	USA, Canada	(Bare et al., 2003; TRACI, 2016)
USEtox	-	-	-	-	✓	✓	✓	-	USA	(USEtox, 2015)
EDIP	-	✓	✓	-	✓	✓	✓	-	Denmark	(EDIP, 2016)
IMPACT 2002+	✓	-	-	-	-	✓	✓	✓	--	(IMPACT, 2002)

As shown in Table 2.2, every method has its impact category and characteristics factor. Each method seeks to establish a linkage between a system and potential impacts. The key to assess the actual impact is using an appropriate set of characterization factor. Many characterization factors are established based on the studies conducted in Europe, and only a few are based on global studies such as CMLCA, Recipe, and TRACI. Therefore, selection of method depends upon the relevancy of characterization factors to the site-specific case studies.

2.3 Application of Artificial Neural Network (ANN) Method

Artificial Neural Network (ANN) models have been applied to assess the air quality from the past data. These studies have proven that neural networks are preferable modeling system for air quality prediction in comparison with other regression-based statistical models (Chan and Jian, 2013; Cheng et al., 2012; Gobakis

et al., 2011). In particular, ANNs, the back propagation implements when dealing with the combination of linear and nonlinear systems such as the air pollution phenomenon (Tecer, 2007). Zhang et al., (2013) applied an ANN model to predict the concentration of ambient respirable particulate matter (PM_{10}) observed in a city of China. McKendry, (2002) made a comparative analysis of traditional regression models and neural network for maximum, average and daily ozone and particulate matter (PM_{10} and $PM_{2.5}$) forecasting. Goyal and Kumar, (2013) also studied ANN for predicting the dust concentration.

Even more, application of ANN in the field of mining to predict air quality is very new, but up till now applied to predict particulate matter and dust (Lal and Tripathy, 2012; Patra et al., 2016; Roy et al., 2011a; Tecer, 2007). Tecer, (2007) predicted particulate matter and sulfur dioxide in a coastal mining area in Turkey using ANN. The results showed that ANN could efficiently be used in the analysis and prediction of air quality. Roy et al., (2011) compared multiple regression and neural network models for assessment of blasting dust at a large surface coal mine. The results showed that the neural network could produce better results than multiple regression models. Lal and Tripathy, (2012) studied ANN to estimate particulate matter (PM) concentration inside an opencast mine and relate it to the local meteorological parameters. Patra et al., (2016) developed ANN model for the copper mining to assess the concentration of particulate matter.

2.4 Air Quality Modeling for the Mining Area

Numerous air quality models such as box model, Gaussian model, the Eulerian model, and the Lagrangian model have been reported to be used for the prediction of air quality for the mining industry in the past few years (Reed et al., 2002). The box model is simple to use, and it is assumed that the air-shed is in the shape of a box with the homogenous concentration. Although this model has been considered as a useful tool, it has some limitations. As box model itself is designed to examine the air dispersion on regional instead of the local scale. Modeling assumption could affect the results due to its inability to deal with spatial information (Cecala et al., 2012).

The Gaussian models are the most used models in the mining industry. They are based upon the assumption that the pollutant will disperse according to a normal statistical distribution. Cole and Fabrick, (1984) studied escape of dust mass fraction by modifying the Gaussian algorithm to pit retention-mathematical model but did not show validation results with the field. Pereira et al., (1997) discussed predicting of dust concentrations from the stockpiles of an open pit mine in Portugal. Then Atkinson et al., (1996) established industrial source complex- 3 model (ISC3) and modeling results were compared with actual measurements in surface coal mining. It was based on point source Gaussian equation designed for flat and complex terrain and can predict CO, NO_x, SO_x, Pb, and PM_{10} (Atkinson et al., 1996). Later on, over-prediction of ISC3 was reported by Cole and Zapert, (1995) (PM_{10} 87 % over predicted) and (Huertas et al., 2012). Reed et al., (2002) modified ISC3 model and termed as "dynamic component program". The research included the two mines (i.e. coal and stone quarry), but the major limitation was that only haul trucks were considered in the study to predict particulate matter. Chaulya et al., (2003) and Trivedi et al., (2009) used fugitive dust model (FDM) to study total suspended particulate for an opencast mining system. However, FDM is not suitable for other pollutants. American Meteorological Society/Environmental Protection Agency Regulatory Model (AERMOD) is the next generation air dispersion model based on the Gaussian plume approach. It applies to industrial and complex terrain sources. Its usage in the field of mining is very new (Huertas et al., 2012; Neshuku, 2012; Tartakovsky et al., 2013). AERMOD is based on a simple Gaussian algorithm and able to predict the concentration of pollutants up to 50 km (Tartakovsky et al., 2013). However, recent studies show that AERMOD is not suitable for calm conditions or during low wind speed conditions (Neshuku, 2012).

Eulerian models are used to solve conservation of mass equation for a given pollutant. However, the equations used in this model are complicated to solve and can deal with one pollutant at a time. Bhandari et al., (2004) also developed a model for predicting plume dispersion from blasting operations based on the Eulerian mathematical algorithm. The study has many uncertainties, and the results are not validated with field observations. Similarly, Silvester et al., (2009) studied the

dispersion of mineral dust particles due to rock blasting activity under neutral conditions using computational fluid dynamics (CFD) model. CFD helps to analyze airflow modeling and identify hotspots in visual graphics. However, it requires a vast amount of data, and its application in mining field is limited (Baklanov, 2000).

Lagrangian models are applied to predict pollutant dispersion based upon a shifting reference grid (such as prevailing wind direction or plume direction). This mathematical model has limitations when its modeling results are compared with monitoring measurements. Because of the dynamic nature of the model, observed values are generally calculated at stationary points, while the model predicts pollutant concentration concerning moving reference grid which makes it difficult to validate the model during initial use. California Puff model (CALPUFF) has been used to analyze the impact of particulate matter because of mining activities (Arregoces et al., 2016; Fishwick and Scorgie, 2011).

To conclude, despite their usefulness, these existing models are limited in their abilities when applied to the field of mining to predict the concentration of air pollutants. In general, Gaussian models are easier to implement with relatively minimum requirements for the meteorological data and computational effort. Even so, their application neglects the physical removal mechanism in the atmosphere.

2.4.1 Advancement in K-theory Gaussian algorithm

Pollutants emitted into the atmosphere may be eliminated by some natural processes. One of the important removal mechanisms is settling of the particle as dry deposition onto the surface of the earth due to gravitational effect. A single parameter is used to model dry deposition such as deposition velocity. If removal mechanisms are ignored, the Gaussian plume is considered as the basic algorithm to calculate the predicted concentrations of the dispersed pollutants from a point source. However, results would be more precise and closer to the field observations by considering dry deposition. Unfortunately, a paucity of literature were reported to consider the dry settling (Ermak, 1977; Costa et al., 2006; Moreira et al., 2006; Shankar Rao, 2007).

Efforts have been made to modify the Gaussian model by using the gradient transport K- theory by many researchers in the past. The authenticity of K-theory depends on the way eddy diffusivity is dogged based on the turbulence in the atmospheric boundary layer (ABL) and the ability of the model to replicate the observed diffusion data. Many numerical solutions were proposed regarding eddy diffusivity, but their work restricted to the specific case study or ignoring the settling effect. Ermak, (1977) solved analytically three dimensions advection-diffusion equation (ADE) with eddy diffusivity as a function of downwind distance with dry deposition and gravitational settling. In recent years, new approaches like simple Laplace transform, generalized integral Laplace transform technique (GILTT) have been used for solving advection-diffusion equation (Moreira et al., 2005; Wortmann et al., 2005; Buske et al., 2007; Tirabassi et al., 2009). Moreira et al., (2006) gave semi-analytical solution for ADE by using Laplace transform technique depending on eddy diffusivity and vertical turbulent velocity. Moreira et al., (2009) modified the study by using GILT numerical solutions for two-dimensional ADE. (Sharan and Modani, 2007) discussed a mathematical model by using Fourier transforms and eigenfunction expansion for a steady state three-dimensional ADE. A step forward was taken by Essa et al., (2014) who developed a simple and new analytical solution based on the advanced Gaussian algorithm by using the separable variable technique. There is a need to focus on the eddy diffusivity as an important parameter in the model together with dry deposition for the mining sector to assess the air pollution.

2.4.2 Meteorological parameters and atmospheric stability

The climatic conditions at the source site play an integral role in selecting various meteorological factors. Among all significant parameters (such as horizontal wind, atmospheric stability, terrain effects, etc.) atmospheric stability is one of the most crucial factors which tend to alter the boundary conditions and fundamentals of any dispersion model by considering the turbulence and dispersion of pollutants (Zhang et al., 2015). Moreover, atmospheric stability is also related to the two primary factors which are the lapse rate and wind speed (Hassoon et al., 2014). Thus, it can be

characterized by using several methods, for instance, empirical approach, the flux or gradient Richardson number and Monin-Obukhov length method. These methods share the common scheme while having different indicators for atmospheric motions mainly convective and mechanical turbulence (Essa et al., 2006).

Many scientists used an empirical approach to determine the atmospheric stability because it involves a minimum number of parameters required and proven to be a most reliable method. One of the empirical methods is Pasquill-Gifford method (PGM) for estimating atmospheric stability proposed by Pasquill in 1961 (Turner, 1997). In PGM, stability is classified into six different categories (from A to F). In this classification, it is assumed that net radiation is the important indicator in the surface layer (the layer near the ground up to the height of the roughness length) to observe the turbulence. Whereas, net radiation could be calculated based on insolation number (incoming solar radiation), wind speed and sky conditions (cloud cover at day and night) (Hunter, 2012). This method has been further modified and revised by Turner (1964) called as Pasquill–Turner method (PTM) by incorporating incoming solar radiation regarding solar altitude, cloud cover and cloud ceiling height which helps to determine the net radiation index (NRI) (Turner, 1964). This method distributes the atmospheric stability into seven distinct categories instead of six (from A to G or 1 to 7) by using NRI and wind speed. Thus, PTM helps to classify stability for both types of turbulence (convective and mechanical) in a boundary layer.

The atmospheric conditions are divided into three main categories which are stable, neutral and unstable based on wind speed and turbulence. For example, stable conditions are encountered mostly during clear nights with no vertical mixing and convective turbulence. Usually having weak wind speed and mechanical turbulence is reduced. In contrast, when convective turbulence dominates, unstable conditions appear and mostly happen in the daytime. Whereas, neutral conditions create when mechanical turbulence tends to increase, and thermal turbulence starts decreasing (Bhattacharjee et al., 2016; Kaimal and Finnigan, 1994; Zannetti, 2013). This type of state occurs during a day-night shift with strong winds. However, various studies reported that the percentage distribution of atmospheric stability of any area also

depends on both the day and night climatic conditions and seasonal variation (Nassar et al., 2010; Tecer et al., 2008). Most of the planetary boundary layer (PBL) climatic factors are dependent on these three primary stability conditions (Ashrafi and Hoshyaripour, 2010). One of the most critical parameters, which helps to define the limit on the vertical diffusion of plumes within the PBL is the mixing height or the mixing depth (The mixing height is the layer of the lower atmosphere where mixing occurs). This layer also tends to be the part of turbulence and diffusion of the pollutant (Baklanov et al., 2005; Fisher, 2002; Garland and Branson, 1976). Therefore, the mixing height is considered to appear during neutral and unstable conditions and to be undefined during stable conditions. Other foremost factors which are related to stability conditions are PBL height, roughness length, frictional velocity, Monin-Obukhov length, surface heat flux and variance of the wind components (Diez et al., 2014; García-Díaz and Gozalvez-Zafrilla, 2012). Therefore, these parameters provide the foundation of almost every air dispersion model and Gaussian algorithms. Hence, choice of parameters and empirical equations related to these factors make a huge difference in the features of the model.

2.4.3 CALPUFF application in the mining industry

CALPUFF is a non-steady, Lagrangian based puff modeling system for the simulation of air pollution dispersion distributed by the Atmospheric Studies Group at TRC Solutions. The model can perform estimation of deposition and concentration patterns for air pollutants by considering the effects of varying meteorological conditions. The concentrations pattern follows the puff as it crosses over or near a receptor point (Zhou et al., 2003). The model has a preprocessing module which is called as (California meteorological model) CALMET model used for generating meteorological input data for the model, such as wind and temperature profiles in a gridded model. It has applicability for complex terrain and can deal with different pollutants, including particulate matter. The function of the CALPUFF model is to simulate the effects of temporally and spatially varying meteorological conditions that occur more often over long pollutant transport distances > 50 km (Zhou et al., 2003). Macintosh et al., (2010) used CALPUFF to study dust in zinc smelter in a complex

terrain shows that this model is suitable to analyze a long-term impact of pollutants in the near field. Fishwick and Scorgie, (2011) applied CALPUFF to the large surface mine and concluded that model results tended to overpredict higher range 24-hour average ground level PM_{10} concentrations. Atabi et al., (2016) studied CALPUFF modeling performance is better than AERMOD for a gas refinery in complex terrain.

2.5 Decision Analysis Methods

2.5.1 Multicriteria decision analysis

Air pollution control technologies in mining are categorized into source control or using alternative method during mining activities. Multiple criteria decision analysis (MCDA) methods deal with such problems whose alternatives are predefined and multiple criteria based ranking to evaluate the alternatives (Sadiq and Tesfamariam, 2009). There are many methods available for MCDA classified into three different categories, i.e., elementary, utility theory, and outranking (Belton and Stewart, 2002). The elementary methods identify least preferred alternative based on the performance and suitable for reducing the number of options into potential alternatives. However, this category is not suitable for resolving those environmental problems that involve many criteria and alternatives (Kiker et al., 2005). Maxmin and conjunctive are the examples of elementary methods. Utility theory methods are based on a value function for each criterion to evaluate alternatives and to aggregate the value of each criterion in order to identify the most suitable alternative (Keeney and Raiffa, 1993). Examples of these methods include multi-attribute utility theory (MAUT) and analytical hierarchy process (AHP). The third category of MCDA is outranking methods which involve all the possible alternatives by pair building up some binary relation (to evaluate the performance of the outranking character of one alternative over another alternative), and then exploit this relation in an appropriate way to obtain the final recommendations, sort alternatives into groups, or rank them (Belton and Stewart, 2002). Examples of outranking methods include ELECTRE (Elimination and choice translating reality), PROMETHEE (preference ranking organization method for enrichment of evaluations), and other methods.

In the past, the details of MCDA methods and its applications regarding environmental decision making was studied by Kiker et al., (2005) and Huang et al., (2011). Recently, Yang et al., (2012) have developed a simulation-based fuzzy multi-criteria decision analysis to select remedial alternatives for a benzene-contaminated site. Some researchers use MCDA to analyze problems in the field of air pollution (Nikolić et al., 2010). Whereas, literature available in the context of mining is scarce. Elevli and Demirci, (2004) studied multi-criteria choice of ore transport system for Turkish mines for economic analysis. Bogdanovic et al., (2012) used integrated AHP and PROMETHEE method to study alternative mining method based on technical and economic indicators. Betrie et al., (2013) provided a framework for selecting remedial alternatives for acid drainage issue in British Columbia mining system, based on MCDA approach. Mladineo et al., (2015) developed MCDA support system for project management at the mining site. However, all the studies up till now mostly prefer technical and economical aspect and ignore the environmental analysis in the mining sector. There is no published study available on selecting alternative methods to reduce air pollution in mining.

2.5.2 Optimization for air pollution control planning

Shaban et al., (1996) developed optimization model using mixed-integer linear programming (MILP) to reduce the particular pollution based on the available maximum budget in urea plant. Grandinetti et al., (2007) studied a multi-objective linear programming model to identify the best available technologies (BATs) in a manufacturing industry. Ren et al., (2010) developed a multi-objective model based on linear programming (LP) for the design of a distributed energy system that minimizes the energy cost and CO_2 emissions. Cristóbal et al., (2012) used mixed integer non-linear programming for the optimal design of pollution control devices in coal-fired plants. Chen et al., (2015) developed robust fuzzy linear programming for coal-burning power plants and the kilns to suggest total suspended particulates (TSP) pollution control technique. Thus, simplification is motivated by the numerical difficulties associated with the optimization of nonlinear models, which are more difficult to handle than linear programming formulations. The complexity simulation is another major

limitation of multi-objective functions using non-linear programming. Long-term planning to control air pollution includes the consideration of objective, optimum cost analysis, and risk assessment to achieve a balance of technical and economic feasibility to improve the environmental quality. Past studies mostly focused on the pollutant emissions and ignored the meteorological variabilities (Ma and Zhang, 2002). Whereas, the pollutant concentration at downwind distance depends on not only the source emission but also dynamic meteorological conditions of that area. To overcome this issue, dispersion transfer function (DTE) could be integrated into a model as one of the constraints (Liu et al., 2003). The transfer coefficient or DTE can be determined by modifying the simple Gaussian model.

2.5.3 Probabilistic decision analysis and risk assessment

The probability theory (Monte Carlo method) is used mostly to address random variability in parameters using probability distribution/density function (Kaya and Kahraman, 2009). While imprecise uncertainties because of lacking information considered as cognitive uncertainty. Fuzzy set methods/logic has been successfully applied to solve such issues, and membership function is used to characterize the vagueness in data (Gopal et al., 2016). The consequences of temporal and spatial variations of environmental conditions lead to violating the guidelines and shift the uncertainties from probabilistic to possibility due to the vagueness of data. Whereas, the literature on contaminant concentrations in ambient air predicted from any mathematical simulation model usually discussed only probabilistic uncertainties due to the variations in modeling input parameters (Kaya and Kahraman, 2011). This practice leads to difficulties in direct implementation of the deterministic environmental guidelines because of the existence of both types of uncertainties.

Furthermore, environmental risk, because of output data (pollutant concentration), need to be seriously evaluated which may lead to the violation of the environmental guidelines and aids in decision making management. More attention is being paid to the fuzzy-set concept for addressing regional air pollution problems. Onkal-Engin et al., (2004) assessed urban air quality in Istanbul using a fuzzy synthetic evaluation.

Upadhyaya and Dashore, (2011) used fuzzy approach to calculate air quality index of different cities in USA, China, and Mexico. Liu et al., (2003) used robust fuzzy programming for regional air pollution control. The hybrid integrated approach considering both stochastic and fuzzy method is used by Ping et al., (2010) for risk assessment of ambient air quality of SO_2 in a thermal power station in Atlantic Canada. The developed approaches can offer an effective method of assessing risk and quantify uncertainties in air quality modeling. However, there is need to implement this approach in the field of mining industries by integrating optimization technique with hybrid fuzzy risk assessment.

2.6 Summary

In this chapter, different life cycle assessment methods, artificial neural networking, air dispersion models and decision analysis approaches are studied as well as their potential in the field of mining is investigated. Life cycle modeling particularly inventory development models in the field of mining have specific challenges to overcome such as lacking the detailed representation of variables used in a system for impact analysis. Most studies failed to represent the pollutant emission rate around the mining activities. The considerable challenges in the air dispersion modeling when applied to the field of mining in most of the past reported studies are mainly centered around the single source or a single pollutant. These studies concluded that there is need to take a holistic approach to understanding air pollution from various mining operations, and considering the effect of meteorological parameters. Artificial neural networking models have been used from the past few years in predicting air pollutants. Its application in the field of mining to predict carbon footprints would be a new direction. Dispersion modeling is an integral component of air quality assessment, and particularly during the mine planning phase where such models can be used to inform on the location of specific activities, and the controls required to manage air emissions adequately. Some researchers used decision analysis to analyze problems in the field of air pollution. However, there is need to develop a modeling approach to select alternative methods to reduce air pollution in mining. Therefore, a new system seems to be required to overcome the existing challenges while reducing the pollutant

emission in the mining field. Mines need the consolidation of air quality management into a single, integrated air quality modeling system which could address all potential sources, source inventories, relative impacts, abatement measures and risk assessment methods.

CHAPTER 3 METHODOLOGY

3.1 Development of a LCA Based Air Quality Modeling System (LCAQMS) for Mining-Conceptualization

The mining system is conceptualized concerning all the potential air pollutants and the mining technical data including meteorological conditions. This conceptualization is reflected in the architecture of framework chosen for the models. LCA based air quality modeling system (LCAQMS) consists of four primary models which help to generate inventory, assess the impacts, carbon footprints analysis, predict the air pollutants at ground level, and selection of best alternative technology. Consequently, LCAQMS includes life cycle inventory model, artificial neural network model, mining-zone air dispersion model, and decision analysis model. The decision analysis model comprises multi-criteria decision analysis tool, and air pollution control model. as shown in Figure 3.1. The primary methods applied in the development of LCAQMS herein include:

- An integrated life cycle and artificial neural networking model for mining (LCAMM) which comprises two main modules:
  - Life cycle inventory model which utilizes an inverse matrix method as a life cycle assessment (LCA) tool and characterization method to assess the midpoint environmental impacts such as climate change, particulate matter formation, etc.
  - Artificial neural networking model for mining based on back propagation artificial neural network (BPANN) algorithm to investigate the carbon footprints from various energy resources and greenhouse gases in mining.

- Mining-zone air dispersion model (MADM) based on an advanced Gaussian algorithm to determine predicted concentration of pollutants at ground level. MADM also includes features of physical removal mechanisms such as particle settling, dry and wet deposition. Moreover, Pasquill-Turner method (PTM) is used

to determine the atmospheric stability conditions, which help to investigate the meteorological parameters using an empirical approach.

- A decision support system which comprises further two modules:
  - Preference ranking organization method for enrichment evaluation (PROMETHEE) method to select the best treatment technology for air pollution at the mining site. Furthermore, PROMETHEE method is integrated with AHP to determine the weighting for each criterion.
  - Optimization method by developing the air pollution control model using linear programming with an objective function (minimize cost) and multi-constraints. Fuzzy risk assessment method is used to examine environmental air quality guidelines.

- Monte Carlo simulation (MCS) which assist in investigating the uncertainties in the model including all inputs (wind speed, emission rate) and output (predicted concentrations). Besides the system development that integrates the above methods, statistical analysis and model performance is evaluated with the field data by comparing the modeling results with the monitoring values.

Linear method, statistical approach, analytical Gaussian-based simulation, outranking method, single objective-optimization and fuzzy set approach is used to develop the integrated LCAQMS. The goal of the study is to combine mining and air dispersion disciplines by integrating with the field database and mathematical simulations. In general, model aims to provide a user-friendly interface by combining the life cycle assessment, prediction models, decision-making tools and a database for data storage and management. For implementation of the developed system, it is employed to assess the air quality condition in the open pit mining system.

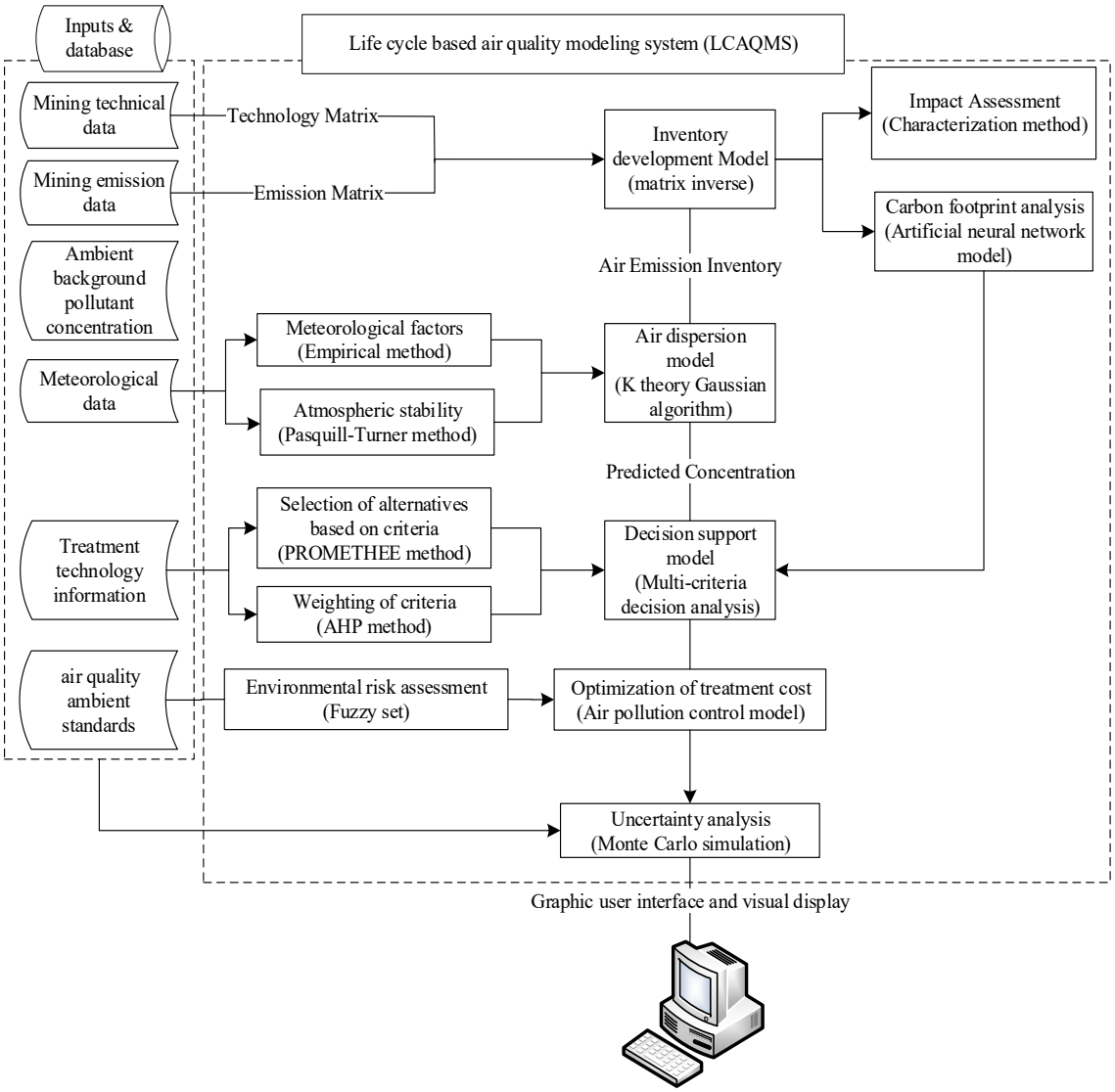

Figure 3.1 Flow chart of life cycle assessment based air quality modeling system (LCAQMS) for mining

3.2 An Integrated Life Cycle and Artificial Neural Networking Model for Mining (LCAMM)

3.2.1 Development of LCAMM

LCAMM is designed as a framework for life cycle environmental analysis of a mining system in the context of air pollution and carbon footprint analysis. The scope is to include all activities from the stage of the ore extraction to the waste handling. In the first module, all the technical and air emission data are used as input of technology

matrix which is used to compute the scalar vector. Consequently, emission load matrix is constructed based on the estimated emissions. The scalar matrix and emission load matrix is multiplied to produce air pollution inventory. In the second module of the model, back propagation algorithm is used in ANN modeling to stimulate CO_2 eq. by utilizing greenhouse emission data (CO_2, CH_4, and N_2O) fuel consumption and operating duration. For assessing other midpoint impacts, five environmental indicators are used depending upon the type of potential pollutant produced. Mainly climate change, acidification, photochemical oxidant formation and particulate matter formation are used for characterization of data by using TRACI (tool for reduction and assessment of chemicals and other environmental impacts) method.

3.2.2 Development of mining life cycle inventory (LCI) model

This phase of the LCAMM comprises two principal activities i.e. identification and quantification of the technical and environmental data. Firstly, the processing unit is considered as a functional unit, since it plays a vital role by providing the basis on which alternative options and different scenarios are compared. For example, if heap leaching method is considered instead of carbon in pulp, the only change would take place in the functional unit, and rest of the activities remain the same. System boundaries are identified (see Figure 3.2) to ensure that all the relevant parts of the system are involved. The study comprises of general principles of ISO 14040-49 series of standards for LCA and adapting them where appropriate to the unique situation of the open pit as well as can be used for underground mining system. The mining system is categorized into three subsystems: First ore extraction, then ore processing and last waste handling. In this thesis, the functional unit is expressed in terms of mass instead of energy. A mass-based functional unit is easy to work with since mining industries typically report their production information by mass. Also, it is the practice in the mining sector that material inputs either waste products or pollutant emissions are expressed based on a unit mass of product (typically tons) (Durucan et al., 2006).

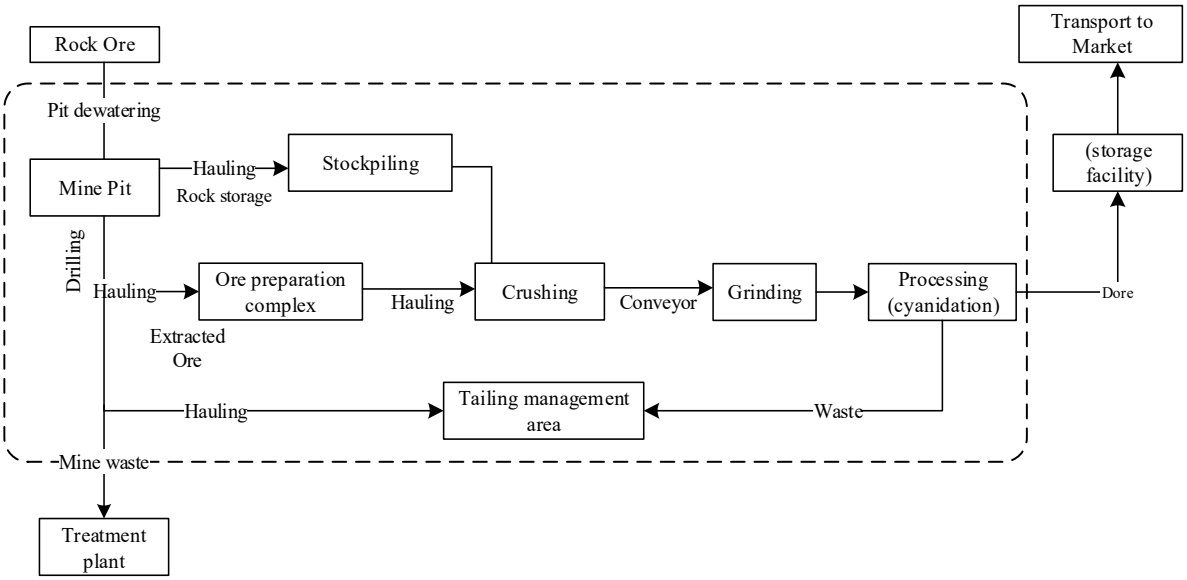

Figure 3.2 Overview of mining processes and system boundaries

Note: *Extraction* of ore from mine pit including drilling, pit dewatering activities; *ore processing* for gold including ore preparation, crushing, grinding, cyanidation and concentrating; *waste handling* includes stockpiling, tailing management area.

The technical, processing and energy flows per unit activity are together considered as an economical flow which is arranged in the technology matrix "*M*" and the environmental flows in the environmental intervention matrix "*N*". In both matrices *M* and *N*, columns represent the processes and rows are the flows. Each process in the matrix is represented by demand vector "*p*", and boundary conditions for the economic flows at the system boundary are expressed by the scaling vector "*α*". Thus, the scaling vector α can be derived as (Heijungs and Suh, 2006):

$$M \,.\, \alpha = p \tag{3.1}$$

$$\alpha = M^{-1} P \tag{3.2}$$

M represents a square matrix, and M^{-1} is the inverse matrix of *M*. Items in the system boundary vector *α* are the absolute values of the economic flows, which cross the system boundary. Each item in the demand vector *p* is the scaling factor

corresponding to the unit process. Then, the final environmental load vector β can be obtained by using the environmental intervention matrix N as (Cooper, 2003):

$$\beta = N\ (\alpha) \quad \text{or}$$
$$\beta = N\ .\ (M^{-1}p) \tag{3.3}$$

For example, the two units produced 10 kWh and 0kWh of electricity respectively which is generated by the consumption of 100 liters of fuel (crude oil). The demand vector involves 1000 kWh of electricity. It scales up the factor of fuel consumption by "2" because 200 liters is needed to generate 1000kWh of electricity for unit 1. The consumption is showing a negative sign.

$$M = \begin{bmatrix} \text{Fuel} & : -2 & 100 \\ \text{Electricity} & : 10 & 0 \end{bmatrix} \rightarrow M^{-1}p = \begin{bmatrix} 0 & 0.1 \\ 0.01 & 0.002 \end{bmatrix} . \begin{bmatrix} 0 \\ 1000 \end{bmatrix} \rightarrow \alpha = \begin{bmatrix} 100 \\ 2 \end{bmatrix}$$

Thus, CO_2 emitted during this activity from unit one and two are 1 and 10 kg respectively. The final environmental load can be calculated by interacting the calculated scalar vector and environmental intervention matrix as follows:

$$N\alpha = \begin{bmatrix} 1 \\ 10 \end{bmatrix} \begin{bmatrix} 100 \\ 2 \end{bmatrix} \rightarrow \beta = 1 \times 100 + 10 \times 2 = 120$$

The same (above-mentioned example) matrix concept is applied during the development of an inventory model at the larger scale by including 10-unit activities and for 10 emission pollutants, which also simply the calculations by categorizing the matrix as 10 by 10 square matrix. All input tables are compiled an excel spreadsheet, and then data is imported to MATLAB 2015 R edition, where all the formulas are applied, and LCAMM inventory model is developed. The process activities used in the computational structure of matrix-based inventory are divided into ten groups based on their function and availability of data:

1. Ore removal

2. Drilling
3. Handling
4. Hauling
5. Crushing and conveying
6. Milling and grinding
7. Processing
8. Tailing area
9. Pit dewatering
10. Stockpiling

Groups 2, 3,4 and 9 are the sub-activities of ore extraction from the rock removal to surface mine pit. Whereas, group 4 involving trucks hauling distance and their routes. Group 5 comprises of crusher and conveyor, as both are interconnected for the purpose to crush the metal ore to the small size and transport to miller through the conveyor. Group 6 included milling and grinder. Thus, group 5, 6 and 7 are under the category of processing which includes metal extraction process such as to extract the gold from the ore by using cyanide solution and removing impurities. Group 8 and 10 are the subdivision of waste handling.

3.2.3 Mining impact assessment method

Impact assessment is defined as assembling the environmental burdens, which are quantified in the inventory analysis, into a limited set of environmental impact categories. This phase has several steps, which include classification, characterization, normalization, and weighting. In terms of the ISO standard (14042:2000) classification and characterization are compulsory, while the other steps are optional (Finkbeiner et al., 2006). Classification comprises of the emissions from the life cycle inventory into impact categories according to the pollutant's ability to contribute to different environmental problems (Baumann and Tillman, 2004). For instance, sulfur dioxide (SO_2) can be assigned to acidification while carbon dioxide (CO_2) and methane (CH_4) can be assigned to climate change (Norgate and Haque, 2010). In each category, units of expressions are different based on the pollutants involved in that impact. In the

impact category of climate change, characterization factors are expressed in terms of kg CO_2-equivalent mainly due to greenhouse gases, and this would represent midpoint modeling. However, ANN modeling is integrated for further investigation of carbon footprint analysis in the mining industry. Every method has its impact category and characteristics factor which seeks to establish a linkage between a system and potential impacts. Many characterization factors are established based on the studies conducted in Europe, and only a few are based on worldwide studies such as CMLCA, Recipe, and tool for the reduction and assessment of chemical and other environmental impacts (TRACI). Therefore, selection of method depends upon the relevancy of characterization factors to the site-specific case studies. For this thesis, all impact categories were embodied at midpoint level adapted from TRACI, CMLCA, and Recipe methodology. An expression used in LCAMM for characterization is (Baumann and Tillman, 2004):

$$H_{ic} = \sum_{j'} (q_{ic})\, \beta_{j'} \tag{3.4}$$

where H is an impact vector, q is a characteristic matrix, β is environmental load vector, ic represents impact category and j' is a representation of process unit.

The formula used in LCAMM into various impact categories assumes the form:

$$H = q \,.\, \beta \tag{3.5}$$
$$\text{as } q = (q_1 \mid q_2 \mid \ldots\ldots)$$

Normalization puts the significance of the characterization results in context, by relating the environmental burdens of a mining system to the overall burden in its surroundings ecosystem mostly during a reference period. In LCAMM background pollutant concentration data for the site is used to normalize the output values, following expression is included based on matrix method approach:

$$H_{normal} = q \,.\, g' \,(\beta \rightarrow g') \tag{3.6}$$

where H_{normal} indicates reference impact vector and g' represents reference inventory vector. (Notice the use of the " ' ", for the fact that system related interventions are usually expressed in terms of a kilogram (kg) while the load for a reference period is expressed in kg/year).

3.2.4 Development of back propagation artificial neural network (BPANN) for mining carbon footprint analysis

Artificial neural networking is a mathematical construct that emulates the processes to aid in recognizing pattern and predictions based upon past database. ANN have usually described in terms of numbers and types of connections between discrete processing elements called neurons and the learning rules when data is presented to the network for analysis. The advantage to using ANN lies in their capacity to solve linear and nonlinear problems. In order to study carbon credit and its relationship with the greenhouse gases, the separate data set is required for training, testing, and validation of the model. It is worth to mention that there is no universal rule to determine the size of the data set and the data set is divided among the three categories randomly. For this study, the percentage of the division of the dataset is as follows:

- Training Dataset-70%
- Testing Dataset-15%
- Validation Dataset-15%

Back-propagation (BP) is selected for carbon footprint modeling, which uses the back-propagation algorithm as the gradient descent technique to minimize the network error. Each layer in the BP has several neurons which are equal to the number of the inputs and outputs of the system. The architecture of a feed-forward neural network has layers between the input and the output layers. These layers are considered as hidden layers and represent a set of parallel processing units (or nodes). The function of the hidden layer is to allow the network to identify the relevant patterns in the data and to carry out the complex nonlinear mapping between the input and the output variables. Initially, each input is weighted with a small arbitrary value. The input data, during the

training of a network, are propagated in a feed-forward manner to produce output, based on the weights and predefined transfer function. The prediction error is then calculated from the difference between the produced output and the actual output. The weights of the links could be adjusted to minimize the prediction errors according to the training algorithm being used.

The network reflects well trained when the sum of all the errors in the network reaches minimum based on trial and error method. The algorithm used in the constructed model for training is Levenberg-Marquardt (trainlm) in this study since the TRAINLM is faster than other back-propagation algorithms that are used to update weights and bias (MathWorks-trainlm, 2015). The purpose of using application of the BPANN model in this study is to train the most generalized neural network rather than the one that optimally fitted the training set. The transfer function of the hidden layer and output layer neurons is the hyperbolic tangent function. As can be seen in Figure 3.3, the input variables are multiplied by the connection weights (w_{ij}) between the input and hidden layer. The weighted signals and bias from the input neurons are summed by the hidden neurons and then projected through a transfer function (f_h). The results of the function (f_h) are weighted by the connection weights (w_{jk}) between the hidden and output neurons and sent to the output nodes. The output transfer function (f_o) is then projected by the output neurons. The output of this neuron is the predicted response ($y\hat{}$) (Dieterle, 2003). There can be different neural networking structures possible by using different variables as inputs. For instance, to build the ANN model for the mining sector, a three-layered architecture, is constructed to predict the concentration of particles. The architecture primarily consists of five input variables such as fuel consumption (x_1), CO_2 (x_2), N_2O (x_3), CH_4 (x_4) and operating hours of equipment (x_5) depending upon the site conditions and database (Cooper and Alley, 2002) and one output i.e.CO_2 equivalent kg. The rationale for the use of a BPANN is to provide insight into the importance of mining and greenhouse gases by visually examining the weights between the layers.

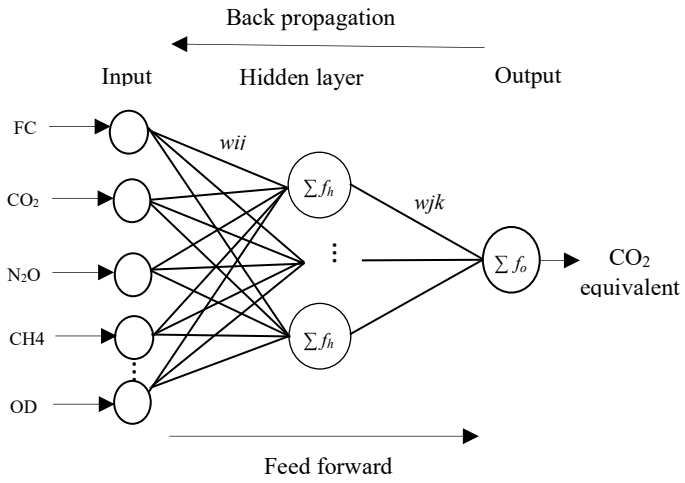

Figure 3.3 Architecture of feedforward back propagation ANN for carbon footprint prediction for metal mining

3.2.5 Performance of LCAMM model

The standard error of the mean (SEM) is the standard deviation of the sample means an estimate of a population mean. It is usually determined by the sample standard deviation (σ_s) divided by the square root of the sample size (s) expressed by using the following equation (Wortmann et al., 2005):

$$\text{SEM} = \frac{\sigma_s}{\sqrt{s}} \tag{3.7}$$

The optimum structure of the BPANN model is determined based on the minimum mean square error (MSE) of the training and validation data sets. MSE is used as a statistical approach to network training. The MSE is defined as (Moreira et al., 2009):

$$\text{MSE} = \frac{1}{n}\sum_{i=1}^{n}(target_i - output_i)^2 \tag{3.8}$$

where n is the number of patterns, target is the desired output (monitoring values) for the i-th pattern, and output (modeling values) is the predicted value for the i-th

pattern. SEM is used during LCA impact analysis, and MSE is used for BPANN analysis.

3.3 Development of Mining-Zone Air Dispersion Model (MADM)

In the proposed mining-zone air dispersion modeling (MADM) approach, there are three components of input database including geographical, meteorological and air emission inventory as shown in Figure 3.4. The geographical database included mining infrastructure, digital maps, land usage data, elevation dataset and surface roughness length within the modeling domain. Whereas, meteorological data included surface air as well as upper air data depending upon the requirement of the project. The surface air set included wind speed, direction of the wind, ambient temperature, precipitation rate, stability class, relative humidity, etc. The upper air set also included temperature, elevation, pressure, and cloud formation. The air emission inventory data is determined using LCI model. The included parameters are emission rate from the sampling points, stack height, stack diameter, exhaust temperature, exhaust exit velocity, and plume rise. For statistical evaluation normalized mean square error, correlation coefficient, and fractional bias equations are used. Visual graphs for other results are then plotted in Excel/Sigma plot, and golden software surfer V13 is used to produce contour mapping.

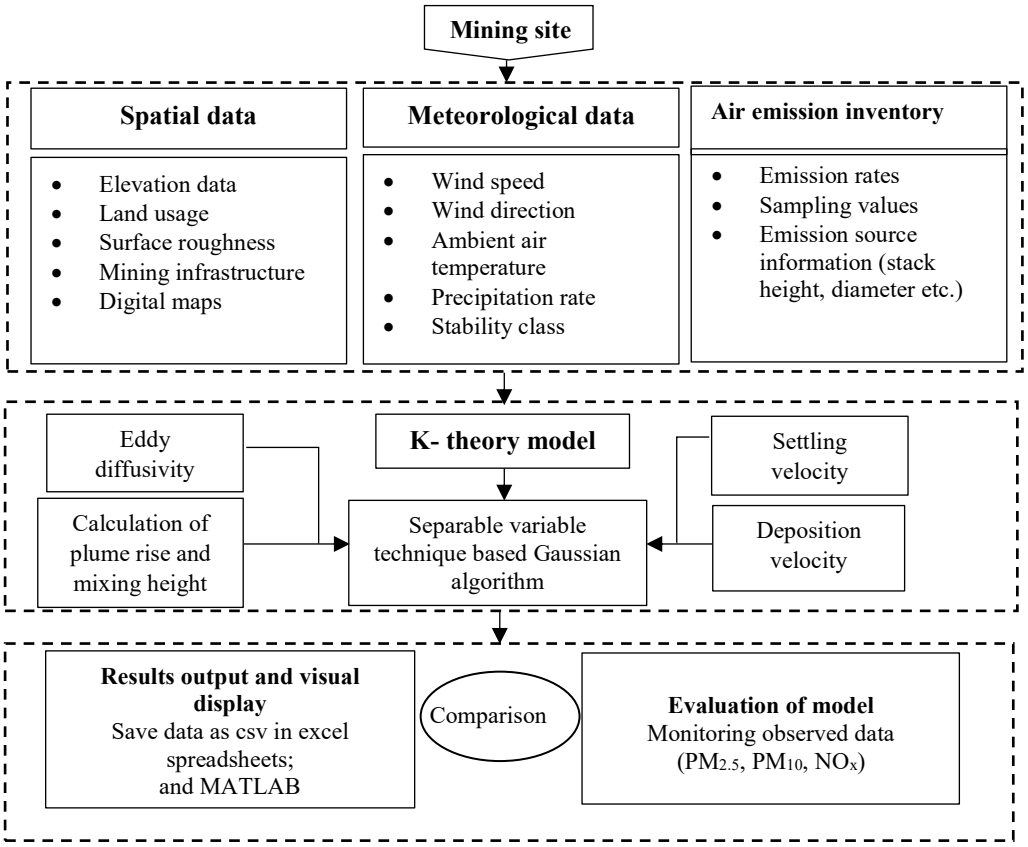

Figure 3.4 MADM depicting conceptualization and implementation of the proposed model

3.3.1 K-theory based Gaussian plume algorithm

The dispersion of pollutants from various point sources in the mining sector can be determined using simple advection-diffusion equation. A Cartesian coordinate system is used to represent *x*, *y* and *z*-axis in the direction of the wind (constant), along with the crosswind direction and in the vertical direction respectively. The governing equation for the pollutant transport is expressed as follows (Essa et al., 2014):

$$\frac{\partial c}{\partial t}+u\frac{\partial c}{\partial x}+v\frac{\partial c}{\partial y}+w\frac{\partial c}{\partial z}=\frac{\partial}{\partial x}(k_x\frac{\partial c}{\partial x})+\frac{\partial}{\partial y}(k_y\ \frac{\partial c}{\partial y})+\frac{\partial}{\partial z}(\mathrm{k}_z\frac{\partial c}{\partial z})+R+S_o \qquad (3.9)$$

whereas C is the pollutant concentration (g/m^3) at any time t (sec) and at any location (x, y, z); k is the eddy diffusivity coefficient in x (k_x), y (k_y) and z(k_z) direction (m^2/s); u, v and w are the average wind speed component (m/s); R is the term used for sinks (g/m^{3}s) and S_o used for the sources (g/m^{3}s).

Equation (3.9) can be solved by considering some assumptions like i) neglecting the sources and sinks for the current situation thus, S=0; R= 0, ii) at steady state $\frac{\partial c}{\partial t} =$ 0, iii) the wind is blowing in x-direction only so v=w=0, iv) transport of contamination in x-direction is outweighed due to the wind as compared to eddy flux in the same direction, $u\frac{\partial c}{\partial x} >> \frac{\partial}{\partial x} k_x \frac{\partial c}{\partial x}$ Hence, equation (3.9) reduced to the following expression:

$$u\frac{\partial c}{\partial x} = \frac{\partial}{\partial y}\left(k_y \frac{\partial c}{\partial y}\right) + \frac{\partial}{\partial z}\left(k_z \frac{\partial c}{\partial z}\right) \tag{3.10}$$

Assuming when the plume is released from the source considering the same coordinates system then coefficients of eddy diffusivity can be calculated by using standard deviation as follows:

$$\sigma_x^2 = 2\,t\,k_x ; \sigma_y^2 = 2\,t\,k_y ; \sigma_z^2 = 2\,t\,k_z \tag{3.11}$$

Following is the equation used to calculate standard deviation (m) (Sharan and Modani, 2007):

$$\sigma_y = c\,x^d ; \sigma_z = a\,x^b \tag{3.12}$$

where a, b, c and d are the power-law exponent.

By considering the Gaussian concentration in crosswind direction in a three-dimensional state is modified as (Moreira et al., 2009):

$$C(x, y, z, t) = C(x, z) \frac{1}{(4\pi\, t\, k_y)^{\frac{1}{2}}} exp\left(-\frac{y^2}{2(2\, t\, k_y)}\right) \tag{3.13}$$

where $C(x, z)$ is an integrated concentration in crosswind direction (g/m^2) and y is the crosswind distance from the plume centerline (m).

When $C(x, z) = 0$, x and y approaches to $+/-\infty$; z approaches to $+\infty$ then equation (3.10) becomes:

$$u \frac{\partial c\ (x, z)}{\partial x} = \frac{\partial}{\partial z}\left(k_z \frac{\partial c\ (x, z)}{\partial z}\right) \tag{3.14}$$

The upper limit of the domain is extended to $z=\infty$ when $C(x, z) \rightarrow 0$ then the law of conservation of flux in an analysis of the air dispersion system is as follows (Chandra and Katiyar, 2011):

$$uC\left(0, z\right) = Q\, \delta(Z - h) \tag{3.15}$$

whereas δ represents dirac delta function, h is the mixing height, and Q represents the emission rate (g/sec).

3.3.2 Settling and deposition velocity

The deposition flux (J) of pollutant onto the ground is proportional to the ambient air $J_{(x,\ y,\ z)} = [k_z \frac{\partial c}{\partial z} + WC]_{\ z\rightarrow 0} = V_d\, C(x,\ z)\big|_{\ z\rightarrow 0}$; and the pollutants are removed by contacting the top of the height of mixing layer, i.e., $C(x, z) = 0$ at $Z = h$; based on Stokes law, the gravitational settling velocity (W) is represented as follows (Essa et al., 2007):

$$W = \frac{(\rho - \rho_a)\, g\, d_p^2\, C_s}{18\mu} S \tag{3.16}$$

where ρ is the particle density (g/cm^3); ρ_a is the air density (g/cm^3); g represents gravitational acceleration (m/s^2); d_p is particle diameter (μm); C_s is the air unit conversion constant (cm^2/μm^2); μ represents air viscosity (g/cm/s); S is the slip correction factor. Following is the expression for slip correction formula (Chandra and Katiyar, 2011):

$$S = 1 + \frac{a_1 + a_2\,[exp\,(a_3 d_p / x_2)]}{d_p\,(10)^{-4}} \tag{3.17}$$

whereas x_2, a_1, a_2, and a_3 are the slip correction constants with values of 6.5x 10^{-6}, 1.257, 0.4, and 0.55 x 10^{-4}, respectively. dp is the particle diameter (μm).

The deposition velocity is expressed as the gravitational settling velocity using the following equation (Moreira et al., 2010):

$$V_d = \frac{1}{r_a + r_d + r_a\, r_d W} + W \tag{3.18}$$

where r_a is an aerodynamic resistance (s/m), and r_d is the deposition layer resistance (s/m)

For stable conditions ($L > 0$) an aerodynamic resistance is expressed as (Atkinson et al., 1996):

$$r_a = \frac{1}{k u_o}\left[ln\left(\frac{z_d}{z_o}\right) + 4.7\left(\frac{Z}{L}\right)\right] \tag{3.19}$$

For unstable conditions ($L< 0$) an aerodynamic resistance is expressed as (Atkinson et al., 1996):

$$r_a = \frac{1}{ku_0} ln \left(\frac{[\{1+16(\frac{z}{L})^{\frac{1}{2}}-1\}\{1+16(\frac{z_o}{L})^{\frac{1}{2}}+1\}]}{[\{1+16(\frac{z}{L})^{\frac{1}{2}}+1\}\{1+16(\frac{z_o}{L})^{\frac{1}{2}}-1\}]} \right) \quad (3.20)$$

whereas u_o is the friction velocity (m/s), k is the von Karman constant with value 0.4, Z is the height above ground (m), L is the Monin–Obukhov length (m), z_d is the deposition reference height (≈10 m), and z_o is the surface roughness length (m).

For neutral conditions an aerodynamic resistance is expressed as (Atkinson et al., 1996):

$$r_a = \frac{1}{ku_o} \left[ln \left(\frac{z_d}{z_o} \right) \right] \quad (3.21)$$

Follow by equation (3.18) deposition resistance (r_d) includes the Schmidt number, parameterizes the effects of Brownian motion is expressed as (EPA, 2004):

$$r_d = \frac{1}{\{(Sc)^{-2/3}+(10)^{-3/st}\}u_o} \quad (3.22)$$

whereas Sc is the Schmidt number ($Sc= \mu/D_B$; dimensionless), μ is the viscosity of air (≈0.15 cm^2/s), D_B is the Brownian diffusivity (cm^2/s) of the pollutant in the air; this term controls the deposition rate for small size particles. St is the stokes number ($St = (W/g)(u_o^2/\mu)$; dimensionless), and g is the acceleration due to gravity. St is a measure of the importance of inertial impaction, which tends to dominate for intermediate- sized particles in the 2–20-μm-diameter size range. The expression for Brownian diffusivity of the pollutants (Sharan and Modani, 2007):

$$D_B = 8.09 \times 10^{-10} \left(\frac{T_a \, S}{d_p} \right) \tag{3.23}$$

where *Ta* (K) is the ambient air temperature, d_p is the particle diameter, and *S* is the slip correction factor. If settling velocity of the particles is very small so that particles are not well transported across the deposition layer by Brownian motion, then these particles have minimal deposition velocities and calculate as follows (Visscher, 2014):

$$V_d = f_i \, V_{df} + (1 - f_i) \, V_{dc} \tag{3.24}$$

whereas *fi* is the fraction of particles smaller than 2.5 μm in diameter; V_{df} is the deposition velocity for fine particles, with *W* set to zero; V_{dc} is the deposition velocity of coarse particles.

The wet deposition rate of pollutant is proportional to the scavenging ratio (Wang et al., 2014):

$$\Lambda = \lambda \left(\frac{P}{P_o} \right) \tag{3.25}$$

whereas Λ represents the scavenging ratio (sec^{-1}); λ is the wet scavenging coefficient (sec^{-1}), which depends on the characteristics of the pollutant as well as the nature of precipitation; P_o is the reference precipitation rate, which is usually taken as (1mm/hr); *P* is the precipitation rate taken as mm/hr (Wang et al., 2014). The scavenging coefficients are influenced by pollutant characteristics such as reactivity for particles or gases, size distribution for particles and the nature of precipitation such as liquid or frozen.

3.3.3 Mining-zone air dispersion model (MADM)

In order to observe the contamination at the receptor site, it is assumed that plume is released into the atmosphere and in downwind direction, the plume is diluted by the wind. Whereas, in a crosswind and vertical direction, the plume follows the mechanism of an eddy diffusivity and can be written as:

$$C_o = \frac{E}{u} L_y L_z \tag{3.26}$$

whereas C_o is the initial pollutant concentration (g/m^3), E is the pollutant emission rate (g/s), and u is the wind speed (m/s). L_y is the lateral spread parameter in the (crosswind) distance, and L_z is the vertical spread parameter in the vertical direction and expressed as follows:

$$L_y = exp\,(-\frac{y^2}{2\sigma_y^2})\;; \tag{3.27a}$$

$$L_z = exp\,(-\frac{1}{2}\frac{(Z-H)^2}{\sigma_z^2}) \tag{3.27b}$$

In practice, if there is no plume deposition to the ground, the plume is reflected which leads to the addition of vertical direction component which is (Z+H). When the plume is confined within mixing layer, then an infinite number of plume reflection can occur and by modifying it with using the following equation adapted from Visscher, (2014):

$$C(x,y,z) = \sum_{n=i} \frac{E_i}{2\pi u \sigma_y \sigma_z} \exp\,(-\frac{y^2}{2\sigma_y^2}) \sum_{j=-\infty}^{+\infty} \left[exp\{\frac{-1}{2}\frac{[Z-(H+2jh)]^2}{\sigma_z^2}) + exp\{-\frac{1}{2}(\frac{[Z+(H+2jh)]^2}{\sigma_z^2})\} \right] \tag{3.28}$$

whereas h is the height of the mixing layer. j is mostly limited to +/-1 and 0. After a few reflections, the plume dispersion is sufficient to fill the entire mixing layer homogenously. Where H is the effective source height (m), and Z is the receptor height or height above the ground (m). E is the emission rate per unit activity "i" (g/s). The effective plume height H which is equal to the physical stack height (hs) plus the plume rise, i.e., ΔH which is estimated by using the following equation based on Brigg's formula (Carson and Moses, 1969):

$$\Delta H = 1.6\, F^{\frac{1}{3}} u^{-1} (10\, h_s)^{\frac{2}{3}} \tag{3.29}$$

where F is buoyancy flux (m^4/s^2); u is the average wind speed (m/s), and hs is the physical stack height (m). F is calculated by using the following expression (Rao, 1981):

$$F = \frac{\Delta T}{T_s} g v_s r^2 \tag{3.30}$$

where T_s, g, V_s, and r are the temperature at the source (K), gravitational acceleration (m/s^2), stack exit velocity (m/s) and radius (m) of the stack respectively; $\Delta T = T_s - T_a$, where T_a is the local/ ambient air temperature (K).

3.3.4 Mining-zone air dispersion model with deposition

The dry deposition of the dispersing pollutants on the ground is considered through boundary conditions and by assuming that the eddy diffusivity depends only on the effective height (Z) above the ground and takes the form (Sharan and Modani, 2007):

$$k_z = k\, u_o x \tag{3.31}$$

whereas k is von Karman constant with a constant value of 0.4 and u_o is the frictional velocity (m. sec^{-1}) mostly taken as 0.1 of wind velocity). Thus, equation (3.14) is modified as follows:

$$u\frac{\partial c\,(x,z)}{\partial x} = \frac{\partial}{\partial z}\left(\frac{\partial c\,(x,z)}{\partial z}\right) k u_o x \tag{3.32}$$

For air dispersion at the mining site, the Gaussian algorithm based on the separable variable technique approach (Essa et al., 2014) is considered to find the predicted concentration and then modified it with emission rate dependent on the mining activities to get the (pseudo) non-steady analytical solution:

$$C(x,y,z,t) = \sum_{n=i} \frac{E_i}{u\,h(4\pi\,t\,k_y)^{\frac{1}{2}}} exp\left(-\frac{y^2}{4\,t\,k_y}\right) exp\left\{-\frac{v_d}{k\,u_o}\left(\frac{(Z-h)}{x} - \frac{v_d}{2u}\right)\right\} \tag{3.33}$$

where E is the emission rate per unit activity (g/s), and V_d is the dry deposition velocity (m/s). Z is the reference height (m) and h is the mixing height (m).

To quantify the dry deposition, the dry deposition flux F_d ($\mu g/m^2 s$) is correlated to the concentration C ($\mu g/m^3$) at a given reference height and calculated as (Liu et al., 2016):

$$F_d = -V_d\,C \tag{3.34}$$

The negative sign shows the downward flux.

In case of wet deposition, below-cloud scavenging is used, and it is assumed that all parts of the plume are depleted to an equal extent because of precipitation. Thus, the process follows the first order in the pollutant concentration (Rao, 1981):

$$C = C_o exp\,(-\Lambda t) \tag{3.35}$$

where t is the plume time traveled (sec), and C_o is the initial average concentration of pollutant ($\mu g/m^3$) which can be calculated using equation (3.24).

3.3.5 Statistical method to evaluate MADM performance

In order to evaluate the modeling result, it's essential to check the agreement between the observed field value and model predicted values. The most commonly used evaluation method was applied for testing the model (Moreira et al., 2005; Essa et al., 2014).

(a) The normalized mean square error (NMSE) is calculated as

$$\text{NMSE}=\frac{\overline{(C_m - C_f)^2}}{\overline{C_m}.\overline{C_f}} \tag{3.36}$$

whereas C_f and C_m are the observed and modeling predicted concentrations, respectively. It informs on the overall deviations between the modeled and field observed concentrations. The NMSE value close to zero is the indication of a good model.

(b) The correlation coefficient (COR) is calculated as

$$\text{COR} = \frac{\overline{(C_m - \overline{C_m})(C_f - \overline{C_f})}}{\sigma_o \sigma_p} \tag{3.37}$$

where σ_o and σ_p are the standard deviations of the field observed, and modeling predicted concentrations, respectively. The range of COR lies between -1 and 1 and for good performance of a model COR should be close to 1.

(c) The fractional bias (FB) is given by

$$FB = \frac{1}{0.5}\left(\frac{\overline{C_f} - \overline{C_m}}{\overline{C_f} + \overline{C_m}}\right) \quad (3.38)$$

It gives status to the tendency of the model to over predict or underestimate the value as compared to field observed concentrations. A good model should have a value close to zero.

3.4 Modeling Framework for Determination of Meteorological Factors

The modeling framework is conceptualized and structured as two main modules. 1) PTM method to estimate the atmospheric stability; 2) Empirical equations to determine the meteorological parameters based on stability conditions as shown in Figure 3.5. The stability is mainly based on the wind speed and net radiation index. The stability conditions allow estimating the set of meteorological factors by using empirical equations. The degree of stability helps to calculate the standard deviation and mixing height for the dispersion model. Moreover, many significant parameters (such as mixing height, deposition velocity, frictional velocity, etc.) are an integral part of the dispersion model and are determined based on these meteorological factors. These parameters vary from site to site depending upon the ambient temperature profile, wind speed, solar altitude and local weather conditions. Furthermore, the sky condition includes cloud cover such as scattered, overcast, etc. and their height from the ground.

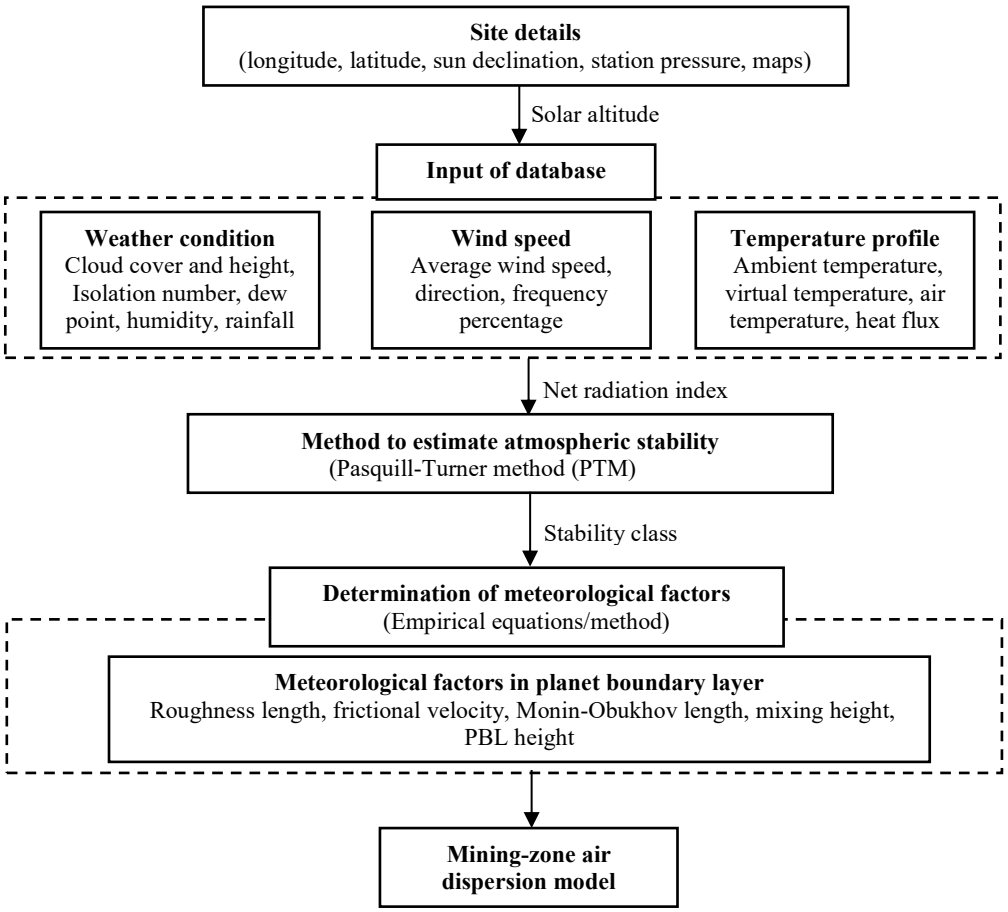

Figure 3.5 Flow chart depicting modeling framework to estimate atmospheric stability and meteorological factor

3.4.1 Method to estimate atmospheric stability

Pasquill-Turner method (PTM) is used to estimate the stability class. This is one of the numerical approaches which comprises of net radiation index (NRI) and wind speed (knots) to determine the suitable class for atmospheric stability as shown in Table 3.1 (Essa et al., 2006). NRI is (the index showing the net radiation which is the balance between incoming and outgoing solar radiation) determined by solar insolation number and sky condition (cloud cover and ceiling height). Whereas, solar insolation number is obtained by solar altitude using Table 3.2 (Ashrafi and Hoshyaripour, 2008). The solar altitude (α_s) is expressed as follows:

$$cos\,(\alpha_s)=sin\,(\beta_s).\,sin\,(\delta_s)+cos\,(\beta_s).\,cos\,(\delta_s).\,cos\,(\gamma_s) \quad (3.39)$$

whereas β_s represents the area latitude, δ_s shows solar declination angle and γ_s is the solar hourly angle. NOAA solar position calculator is used to calculate solar declination (degree) for each day for any time and location by providing its coordinate (NOAA calculator, 2017).

Table 3.1 Atmospheric stability with respect to wind speed and NRI (Ashrafi and Hoshyaripour, 2010)

Wind speed	**Net radiation Index (NRI)**						
(Knots)	**4**	**3**	**2**	**1**	**0**	**-1**	**-2**
0-1	1	1	2	3	4	6	7
2-3	1	2	2	3	4	6	7
4-5	1	2	3	4	4	5	6
6	2	2	3	4	4	5	6
7	2	2	3	4	4	4	5
8-9	2	3	3	4	4	4	5
10	3	3	4	4	4	4	5
11	3	3	4	4	4	4	4
12	3	4	4	4	4	4	4

extremely unstable =1; unstable= 2; slightly unstable=3; neutral= 4; slightly stable 5; stable=6; extremely stable= 7

Table 3. 2 Insolation class number as a function of solar altitude

Solar Altitude	Insolation	Insolation class number
60< α_s	Strong	4
35< α_s <60	Moderate	3
15< α_s <35	Slight	2
α_s <15	Weak	1

To assign NRI to each day and night separately the following procedure is used based on cloud cover in okta and ceiling height of the clouds. (Oktas is the unit measurement to quantify the cloudiness; Clear sky= 0; Few clouds = 1 to 2 oktas; Scattered clouds = 3 to 4 oktas; Broken clouds = 5 to 7 oktas; Overcast sky = 8 oktas).

(1) when the total cloud cover is 8 oktas, and the ceiling height of cloud base is less than 7000 ft then the index value is 0.

(a) *At night time*

(2) If the total cloud cover is ≤3 oktas then index value is -2, and if the cloud cover is >3 oktas then -1

(b) *At day time*

(3) Assign 1 to 4 isolation number based on the solar altitude using Table 2. However, the NRI should be corrected as follows:

I. If the total cloud cover is ≤4 oktas, then used isolation number as provided in Table 2.
II. If the cloud cover is >4 oktas then ceiling height of cloud base should be observed as mentioned below:
Isolation number -2; if ceiling <7000 ft
Isolation number -1; if ceiling ≥7000 ft but <16000 ft
III. If the total cloud cover is 8 oktas and the ceiling height is ≥7000 ft, then 1 is subtracted from isolation number.
IV. If the corrected value is less than 1, then NRI is considered equal to 1.

3.4.2 Empirical methods for selecting meteorological factors

The selection of empirical equation to determine the meteorological factors depends on the three main conditions which are stable, unstable and neutral.

(a) *Mixing height*

Mixing height (*h*) is the fundamental factor that is used to determine the volume available for pollutant dispersion due to mechanical and convective turbulence. Past studies observed that rapid changes of mixing height occurred after the sunset and at sunrise (Roy et al., 2011). The dispersion of pollutants could be highly sensitive to the changes in this height. Moreover, higher the mixing height, the higher is the volume availability for the dispersion of the pollutant. Following expressions are used to determine the mixing height (Helmis et al., 2012):

For unstable condition $$h = \frac{1}{2}[12\text{-}\ (\sigma_\theta \frac{u}{u_o})^3 L] \quad (3.40)$$

whereas u is the wind speed (m/s); σ_θ is the horizontal fluctuation of the wind direction; u_o is the frictional velocity (m/s) and L is the Monin-Obukhov length (m).

For stable condition $$h = \text{const.} \sqrt{\frac{u_o}{f} L} \quad (3.41)$$

For neutral condition $$h = 0.3 \frac{u_o}{f} \quad (3.42)$$

whereas, the value of constant is mostly used as 0.4, f is the Coriolis parameter usually determined as $f = 2\Theta sin\ (\psi)$ (where Θ is the earth's rotation rate (s^{-1}), and ψ is the latitude).

(b) *Frictional velocity, surface roughness, and Monin-Obukhov length*

In convective boundary layer (CBL) the calculations of frictional velocity depend on the reference measurement height for the wind in the surface height (z). Following expressions are used to measure frictional velocity (Kim, 2010):

For unstable condition $$u_o = 0.4[\frac{z}{(1\text{-}15(\frac{z}{L}))^{-1/4}}] \frac{\Delta u}{\Delta z} \quad (3.43)$$

Whereas, z is the height above the ground or surface height and Z_o is the surface roughness (m).

For stable condition $$u_o = 0.4(\frac{u}{ln[\frac{z}{z_o}]} + 5\frac{z}{L}) \quad (3.44)$$

for neutral condition $$u_o = 0.4\left(\frac{u}{\ln\left[\frac{Z}{z_o}\right]}\right) \quad (3.45)$$

The surface roughness (Z_o) is important to consider the development of models which are ranging from microscale to macroscale. Thus, $z_0 = \epsilon/30$; where ϵ is the height of obstacles in the study or wind profile method is used to estimate the surface roughness length. The topography of an area especially category of terrain, manmade and natural obstacles are described by its roughness length. Also, by increasing the height of roughness elements will increase the Reynolds stresses for the wind flow and radically alter the vertical wind shear (Barnes et al., 2014). (see values of surface roughness length by land use and different seasons in appendix Table A-1).

The Monin-Obukhov length (L) is that height at which turbulence is generated more by buoyancy than by wind shear. The Obukhov length is defined by the following expression (Latini et al., 2000):

$$L = \frac{-T_v\, u_o^3}{g\, k\, S_f} \quad (3.46)$$

where S_f is the surface heat flux (K m/s), g is acceleration due to gravity (m/s^2), T_v is virtual temperature (K) [$T_V = (1+0.61\omega)\, Ta$; where, ω is the mixing ratio, Ta is the ambient temperature], and k is the von-Karman constant. For stable night, L can also be determined using $L = 1.1\text{x } 10^3\, (u_o)^2$ (Visscher, 2014).

(c) *Wind direction and wind speed*

Wind direction determines the flow direction in which the pollutants are transported in the atmosphere. In this thesis, WRPLOT view tool is used to develop wind rose which helps to predict the wind direction (WRPLOT, 2017). Moreover, percentage frequency is generated to distribute the wind speed into different categorizes. The wind speed is one of the significant meteorological parameters in

dispersion modeling. Wind speed also influences the initial dilution of the plume leaving a source, the stronger the wind speed, the pollutant gets more diluted. Consequently, the lower the concentrations at the ground level and vice versa. Surface roughness alterations to the average flow affect diffusivities and the average wind speed. For neutral conditions eq. (3.45) is rearranged and can be used to calculate the wind speed. Following equations expressed the wind speed profiling (during $7z_0$ to mixing height (h)) in MADM during stable conditions (Tecer et al., 2008):

$$u = \frac{u_o}{k}\left[ln\frac{Z}{z_o} - 17exp\left(-0.29\frac{Z}{L}\right) + 17exp\left(-0.29\frac{Z}{L}\right)\right] \tag{3.47}$$

The above-mentioned equation is only valid for extreme stable conditions, and it can be reduced to eq. (3.44) during slightly stable conditions. Below $7z_o$, the following equation can be used (Kim, 2010):

$$u = \frac{z}{7z_o}u_{7z_o} \tag{3.48}$$

where u_{7zo} is the wind speed at height $7z_o$; At height more than h, the wind speed is at $z=h$.

3.5 Development of Multi-Criteria Decision Analysis System

The proposed integrated decision analysis system comprises of two methods: (1) selection of best alternative technology using PROMETHEE; (2) selection of best criteria and determination of criteria weights using AHP. In this research, PROMETHEE method was applied to a mine site. PROMETHEE method comprises PROMETHEE I and II for partial ranking and complete ranking respectively. The method involves calculation of net outranking flow value (Φ) that indicates the balance between the positive and negative outranking flows. The more positive the net flow, the better the alternative would be selected (Gurumurthy and Kodali, 2008). Whereas, PROMETHEE I provide a partial ranking of the alternatives. The selection approach

consists of four basic stages: 1) identification of alternative methods considered as actions in the context of the objectives at the data gathering stage. 2) defining the criteria and assigning values which assist in evaluating the options. 3) analysis of data with the PROMETHEE method by determining the preference functions and parameters. 4) Finally, the decision-making stage in which the best mining method is selected based on rankings of alternatives.

As there is no defined method in PROMETHEE analysis to decide the weights, for this purpose AHP method is applied, to select the best criterion and generate weights using the pairwise method. Visual PROMETHEE tool is applied to conduct complete ranking and sensitivity analysis through stability interval or random walking weight method using visual PROMETHEE tool. Also, GAIA (Geometrical Analysis for Interactive Decision Aid) plane is applied to analyze the results further. The schematic demonstration of the proposed approach is presented in Figure 3.6.

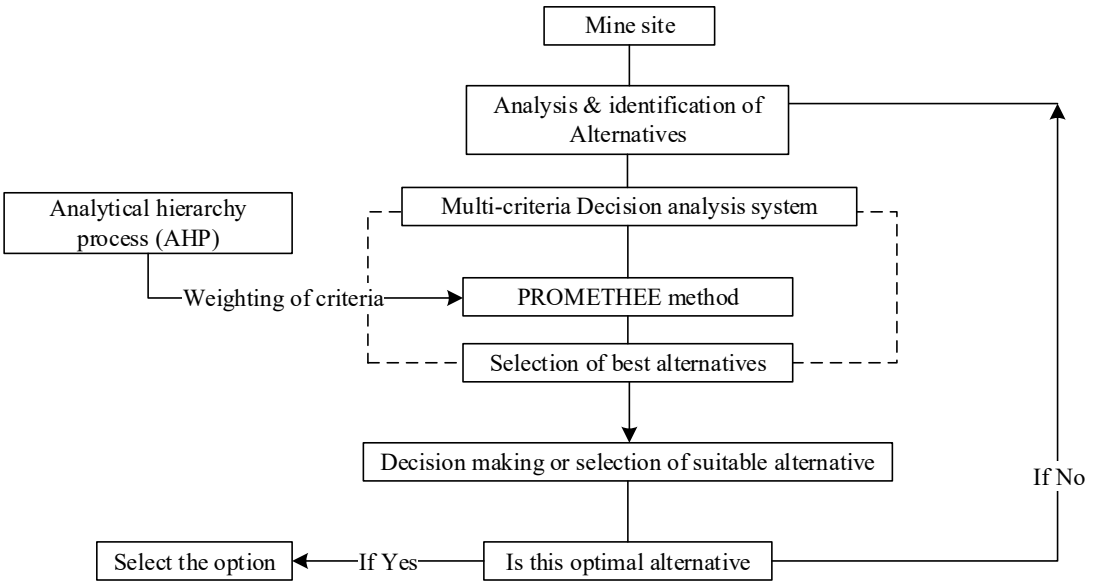

Figure 3.6 Proposed framework for selecting the suitable alternative to minimize air pollution at mine sites

3.5.1 PROMETHEE method

Preference Ranking Organization Method for Enrichment Evaluation (PROMETHEE) is one of the outranking methods suitable for a finite set of alternatives. Input for the PROMETHEE method comprises of matrix "*A*" consisting of a set of all the potential alternatives options (actions) concerning each criterion as shown in eq. (3.49). Based on evaluation matrix, the alternatives are compared to every single criterion. The results are then expressed in terms of preference functions with a range from 0 to 1.

$$A=\begin{pmatrix} A_{11}A_{12}.... & A_{1j}.... & A_{1m} \\ A_{i1}A_{i2}.... & A_{ij}.... & A_{im} \\ A_{n1}A_{n2}... & A_{nj}.... & A_{nm} \end{pmatrix} \tag{3.49}$$

where A_{ij}, i=1……m; j=1…..n, represents the values of alternative i according to criterion j. After constructing the evaluation-matrix A, another matrix B also called as utility matrix is constructed based on the results of matrix A. The matrix B is given as:

$$B=\begin{pmatrix} B_{11}B_{12}.... & B_{1j}.... & B_{1m} \\ B_{i1}B_{i2}.... & B_{ij}.... & B_{im} \\ B_{n1}B_{n2}... & B_{nj}.... & B_{nm} \end{pmatrix} \tag{3.50}$$

where B_{ij} indicates the utility of alternative i according to criterion j, and it is given as a function of A_{ij} as follows (Belton and Stewart, 2002):

$$B_{ij} = f(A_{ij}) \tag{3.51}$$

The function $Y(x_i, x_k)$ represents the degree of the preference of one alternative "x_i" with respect to another alternative "x_k", $k \in (1,2,\ldots n)$ and such that;

$Y(x_i, x_k) = 0$ shows no difference or preference of one alternative x_i over another x_k,

$Y(x_i, x_k) \sim 0$ indicates weak preference of x_i over x_k,

$Y(x_i, x_k) \sim 1$ represents the strong preference of x_i over x_k,

$Y(x_i, x_k) = 1$ shows strict preference of x_i over x_k.

A new matrix is constructed by multiplying preferences with the criteria's weights and assigning the single values. In the matrix, the sum of all the row represents the strength of an alternative (x_i). The sum of all the column represents how much an alternative is dominated by another one (x_k). A linear ranking is calculated by subtracting the x_i value from the x_i value (Belton and Stewart, 2002) expressed as follows:

$$d_i B = A(x_i) - A(x_k) \tag{3.52}$$

whereas $A(x_i)$ is the value of alternative i.

Multicriteria preference index (I) is expressed as the weighted average of the preferred function $Y(x_i,x_k)$ (Clímaco and Craveirinha, 2005):

$$I(x, x_i) = \sum_{j=1}^{k} \frac{S_j \, Y(x_i, x_k)}{S_j} \tag{3.53}$$

S_j represents weights of criterion determined by AHP method.

$I(x_i,x_k)$ shows the degree of preference of the alternative x_i over alternative x_k.

$I(x_i,x_k) \approx 0$ represents a weak preference of x_i over alternative x_k for all the criteria,

$I(x_i,x_k) \approx 1$ denotes a strong preference of x_i over alternative x_k for all the criteria

The PROMETHEE method consists of positive flow (Φ^+) and negative flow (Φ^-) for each treatment technology concerning the given weight for each criterion. The higher the positive flow ($\Phi^+ \rightarrow 1$), the better the alternative would be selected and the other way around. The negative outranking flow represents how much each option is

outranked. The positive and negative flows are expressed as follows (Macharis et al., 2004):

$$\Phi^{+}(x_i) = \sum_{k=1}^{m} I(x_i, x_k) \tag{3.54}$$

$$\Phi^{-}(x_i) = \sum_{k=1}^{m} I(x_k, x_i) \tag{3.55}$$

3.5.2 Analytical hierarchy process (AHP) method

For this modeling approach, AHP is integrated into the framework only to generate weight by using pairwise comparison. The method of generating weight consists of the following steps (Polat et al., 2016):

- Identification of criteria to produce weight.
- Make a pairwise comparison for each criterion.
- Computation of Eigenvalues and vectors to determine a normalized weight for each criterion.

3.5.3 Probabilistic multicriteria decision analysis

In this study, a stochastic approach has been incorporated in the MCDA framework using Monte Carlo Simulation (MCS) method. A random data was generated to select the suitable weights of each criterion and represented the weights as probability distribution function. For each combination of weights, PROMETHEE method was run to get the net flow of alternatives. A distribution function was defined and randomly sampled for 1000 times using the MCS technique. For each iteration, PROMETHEE model was run to generate the flow values against each criterion. The final results of output flows of each alternative and weights of the criteria were ranked, and then correlation coefficients were estimated using Spearman rank correlation (*Sp*) method, which is expressed as follows (Betrie et al., 2013):

$$Sp = 1 - \frac{6 - \sum_{i=1}^{n} d_i^2}{(n^3 - n)} \tag{3.56}$$

whereas d_i is the difference between ranks of criteria weights and alternatives values. n is the number of MCS sampling. The estimated coefficient values lie between -1 to +1 and usually multiplied by 100 to normalize the results and expressed as percentage contribution.

3.6 Integrated Air Pollution Control and Risk Assessment Model

The modeling framework comprises two main modules. First is optimization module in which an air pollution control model (APCM) is developed based on (a) constructing single objective function and multi constraints using linear programming, (b) to determine air dispersion function through the mining-zone air dispersion model as a meteorological variable in the air quality constraint. Second is integrated risk assessment in which attempt is made to link the stochastic uncertainty analysis approach through the concept of fuzzy risk analysis. Consequently, an integrated environmental risk assessment approach is developed which is based on (c) Monte Carlo simulation for the fate of pollutant in the study domain through the mining-zone air dispersion model (MADM); (d) examination of pollutant concentrations based on the simulation results concerning probability density functions; (e) quantification of environmental quality guidelines using fuzzy risk assessment.

The integrated APCM and fuzzy risk assessment can be conceptualized using a framework as shown in Figure 3.7. The objective function of APCM is solved in Excel solver by running the model every time for different pollutants and various controlling technologies.

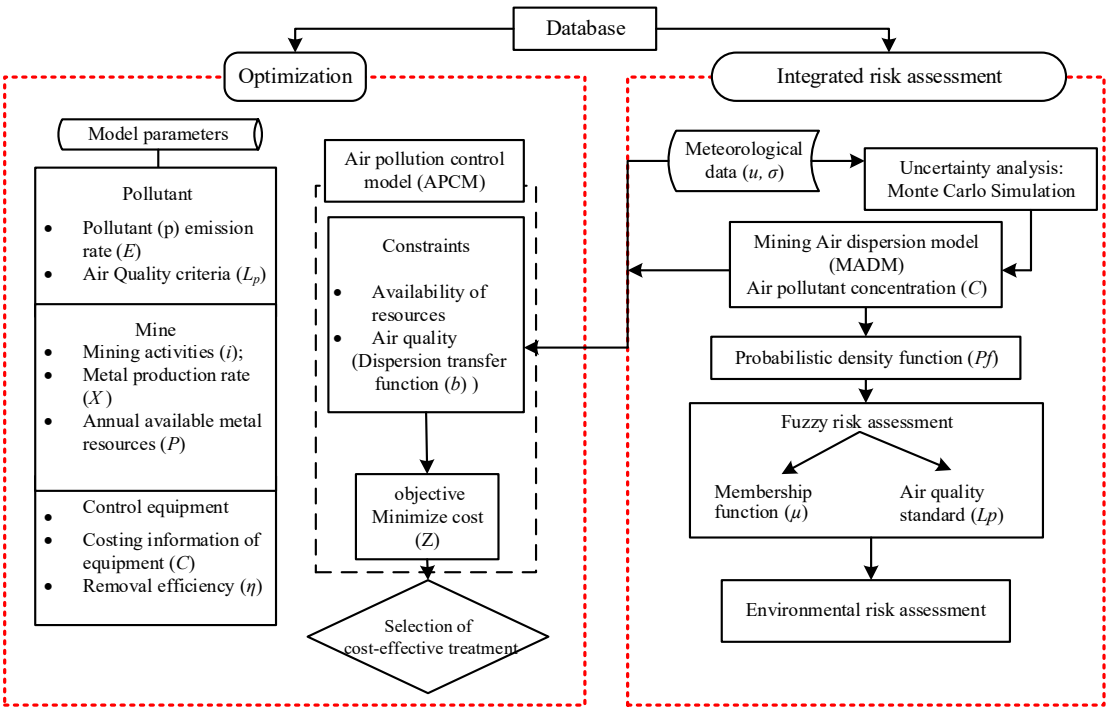

Figure 3.7 A framework to conceptualize an integrated optimization and simulation approach for air pollution control model under uncertainty analysis

3.6.1 Development of air pollution control model (APCM)

Various control emissions technologies are employed to evaluate the best treatment technology for air pollutants. The emission of the pollutant (p) should not exceed the limitation environmental guideline at the optimum cost while the production of metal does not exceed the available resources. The emission of the pollutant is summarized through various mining activities ($i_{1\text{-}10}$) based on average yearly contribution. The mining activities included in this research are mining pit, hauling, crushing and conveying, milling and grinding unit, a processing unit, tailing area, power plant and stockpiling area.

There are certain assumptions which must be made to relate the appropriate variables and to solve the complex problems. It is assumed that: (1) There is the specific number of source activities instead of a single point source. For each type of source (i :1-n) have the same pollutant's concentration limitation and cost of treatment

equipment. (2) The optimized model is simulated for a specified period with the subject to change in direct and indirect costing value in future. (3) The limitation of concentration of a pollutant is determined based on the national ambient air quality standards (NAAQS). 4. The treatment technologies should be listed down and identified.

The mathematical model is formulated as follows:

(a) *Objective function*

The objective is to minimize the treatment cost Z_t (\$/yr). The model includes m mining activities and n treatment methods using the following expression:

$$Z_t = \sum_{i=1-n}^{m} \sum_{j=1}^{n} C_{ij} . X_{ij} \qquad (3.57)$$

whereas C_{ij} is the total cost of treatment j of pollutant p for activity i per production of metal (\$/production); X_{ij} is the metal produced after controlled treatment option j at source i (tons/year). The total cost of any treatment j included direct cost as well as Indirect cost. The direct cost of treatment including purchased cost, installment cost and operating cost and indirect cost is the indirect cost of treatment includes maintenance cost, labor cost.

(b) *Constraints*

i. Availability of resources

A monetary benefit of optimizing the effective treatment strategy could equally provide information about the metal production depending upon the resources available. This constraint helps decision makers to evaluate the treatment options according to the production from each mining activity. If the production after treatment exceeded the annual resources, then the benefit of selecting the suitable technology is

not feasible. Thus, one of the most policy-relevant feature and constraint is not to exceed the available resources.

$$\sum_{j=1}^{n} a_{ij} . X_{ij} \leq Pr \tag{3.58}$$

Pr is the annual- available resources of metal (tons). The coefficient a_{ij} is equal to 1 if control *j* is applicable or feasible at source *i* and 0 if not suitable for the pollutant. Whereas, $X_{ij} \geq 0$.

ii. Air quality

This constraint represents the air quality and pollutant concentration relationship. Air pollutant dispersion transfer function is formulated by modifying Gaussian air quality dispersion model equation (3.28). As, in this study, it is assumed that distribution of air pollutants dispersion is along the centerline. Thus, the dispersion transfer function d_t (sec/m^3) is expressed as follows (Liu et al., 2003):

$$d_t = \sum_{i}^{m} \frac{1}{\pi u \sigma_y \sigma_z} exp(-\frac{y^2}{2\sigma_y^2} - \frac{H^2}{2\sigma_z^2}) \tag{3.59}$$

whereas *u* is the average wind speed (m/sec), *H* is the effective height (m) from source "*i*", *y* is the distance from the centerline (m), σ_y and σ_z are standard deviations of dispersion in x and y-direction (m). Thus, the following form to be used in the air quality constraint:

$$C = d_t \ . E_i \ (X_{ij}) \tag{3.60}$$

whereas *C* is the pollutant concentration at the certain downwind distance (μg/m^3) and E_i is the emission rate (kg/tonn). Moreover, d_t and *E* are considered as technology coefficients in air quality constraint, and X_{ij} is the unknown variable.

The constraint of air quality is formulated as follows:

$$\sum_{i=1-n}^{m} \sum_{j=1}^{n} (1-\eta_j)\, E_{ijp} .\, d_{t\,ij} \,.\, X_{ij} \geq L_p \tag{3.61}$$

whereas η is the efficiency of control method j at source i. The emission rate of pollutant p from source i with control j is E_{ijp}. Whereas, L_p is the standard for each pollutant p.

3.7 Uncertainty Analysis and Risk Assessment

3.7.1 Monte Carlo simulation (MCS)

MCS is a conceptually direct approach to dealing with stochastic uncertainties by generating a large quantity of random realizations of inputs of each random parameter, solving dispersion transfer equation and pollutant's concentration using the mean and standard deviation results from across all the realizations to obtain a sample distribution for the solution (Li et al., 2007). To adequately represent the range of all possible input variables in a Monte Carlo analysis, several hundred iterations of the calculations are required. As a result, the sampling results can then be evaluated in probability density function (PDF). The primary elements of the MCS include PDFs, a random number generator, a sampling rule, error estimation and variance reduction techniques. In the Monte Carlo model, there are different probability density functions (PDFs) available, such as normal, exponential, Gumbel, triangular, etc. (Qin and Huang, 2009). In this study, a normal PDF method is used to analyze the uncertainties. Following expression is used to represents the normal distribution function (Ma and Zhang, 2002):

$$Pf(x) = \frac{1}{\sigma\sqrt{2\pi}} exp - \frac{(x_r - \bar{x})^2}{2\sigma^2} \tag{3.62}$$

whereas x_r is the random variable of any parameter, Pf is the probability density function, σ is the standard deviation, $\bar{x}$ is the average value of x_r and σ^2 is a variance.

3.7.2 Fuzzy set based environmental risk assessment

A fuzzy set is any set that allows its members to have different grades of membership (membership function) in the interval [0, 1]. In specific, a fuzzy set is a pair (G, μ) where G is a set and for each $x \in G$, $\mu(x)$ is the grade of membership of x. The triangular membership function is one of the most simple and popular approaches to employ for generating values of the membership function. The detailed risk characterization relative to a source can usually be regulated through environmental-guideline risk assessment (ERA) (Liao and Hou, 2015). The environmental-guideline-based risk (ER) is defined as the potential for violation of environmental regulations. To facilitate a guideline environmental risk analysis, the guidelines are categorized into three fuzzy sets in this study as ‘‘strict" (lowest possible value), ‘‘medium" (most flexible or credible value) and ‘‘loose' (highest possible value). An element mapping to the value 1 describes a fully included member or medium value, any number that less than the lowest possible value or greater than the highest possible is not included in the fuzzy set and thus mapping to the value 0. Values strictly between 0 and 1 characterize the fuzzy members, and they could be obtained by linear interpolation. Let μ_{G1} ($f(x)$), $\mu_{G2}(f(x))$ and $\mu_{G3}(f(x))$ be the membership functions of the fuzzy sets "low-risk" (loose), "medium-risk" (medium) and "high-risk" (strict), respectively. Then these can be defined as follows in order to characterize such linguistic variables (Ping et al., 2010).

$$\mu_{G1}(\phi) = \begin{cases} 1 & \text{when } \phi \in [0, a] \\ f_G(\phi) & \text{when } \phi \in [a, b] \\ 0 & \text{otherwise} \end{cases} \tag{3.63}$$

whereas $\phi = f(x)$

$$\mu_{G2}\ (\phi) = \begin{cases} 1 & \text{when} \phi = b \\ g_B(\phi) & \text{when} \phi \in [a,\ b] \\ h_B(\phi) & \text{when} \phi \in [b,\ c] \\ 0 & \text{otherwise} \end{cases} \tag{3.64}$$

$$\mu_{G3}(\phi) = \begin{cases} f_G(\phi) & \text{when } \phi \in [b, c] \\ 1 & \text{when } \phi = c \\ 0 & \text{otherwise} \end{cases} \tag{3.65}$$

Given the wide variability in air pollution quality standards, their applicability must be further addressed. Uncertainties associated with a standard's practicability involves imprecise concepts that cannot be solved through probabilistic approach. However, such issues can be resolved using fuzzy logic (Chen et al. 2003 and 2010). Moreover, too strict standard may lead to the impracticality and may difficult to implement. Whereas, it would also risky to select a loose standard. Thus, fuzzy approach provides bases for calculating membership function for different standards.

3.7.3 Integrated risk assessment

The uncertainties exist in two ways which are the variation in pollutant concentration levels and the suitability of environmental standards. The first type of uncertainties is quantified using Monte Carlo simulation, while the second one is addressed by the fuzzy-set technique. MCS for the integrated risk assessment includes probability density function (PDF), model outputs for PDF and the risk assessment. In the present study, Gaussian based predictions that examine the pollutant's concentration, in conjunction with the environmental guidelines for protection of air quality, is used to quantify the risk. Implementation of the integrated gaussian based simulation and risk assessment under uncertainty needs MCS to identify the pollutant concentration based on probability distribution function as shown in Figure 3.8. In order to quantify risks, it is necessary to specify the distribution of pollutants in the

environment, and related uncertainties along with the method of risk evaluation. Thus, the characterization of the risk is calculated as probabilistic risk assessment which refers to the generation of distributions of risk representing uncertainty. In a developed framework environmental risk can be expressed as $Pf\,(C > L_p)$, where C denotes the concentration of any pollutant (random variable), L_p is the standard for each pollutant p (prescribed safety limit of the pollutant p), and Pf denotes probability. More specifically, the environmental risk could be expressed as $Pf = P(C > L_p)$. Thus, the risk can be expressed as follows (Ping et al., 2010):

$$Pf = P(C > L_p) = \int_0^{\infty} \left\{ \int_0^{c} \mathrm{f}_{C,L_p}(C, L_p)\, d\, L_p \right\} d\, C \tag{3.66}$$

If random number L_p can be defined by some local or ambient environmental guidelines or objectives (i.e., if $L_p = L_o$), then the risk can be quantified as follows:

$$Pf = P(C > L_o) = \int_{L_o}^{\infty} f_C(C)\, dC \tag{3.67}$$

If different guidelines are adopted to describe pollutant concentration, then different risk-assessment results will be derived from implementing proposed stochastic risk. In other ways, the environmental guidelines are selected based on fuzzy approach. For contamination risk assessment, the ERA approach is to compare the contaminant concentration with the corresponding quality standard. By Monte Carlo simulation, the probability (Pf) under which the contaminant concentration exceeds the quality standard can be described as follows (Qin and Huang, 2009):

$$Pf = P(C > L_o) = 1 - F(L_o) \tag{3.68}$$

where C is the pollutant concentration, and L_o is the air quality standard. $F(L_o)$ is the cumulative distribution function (CDF) of contaminant concentration which can be obtained from Monte Carlo simulation results.

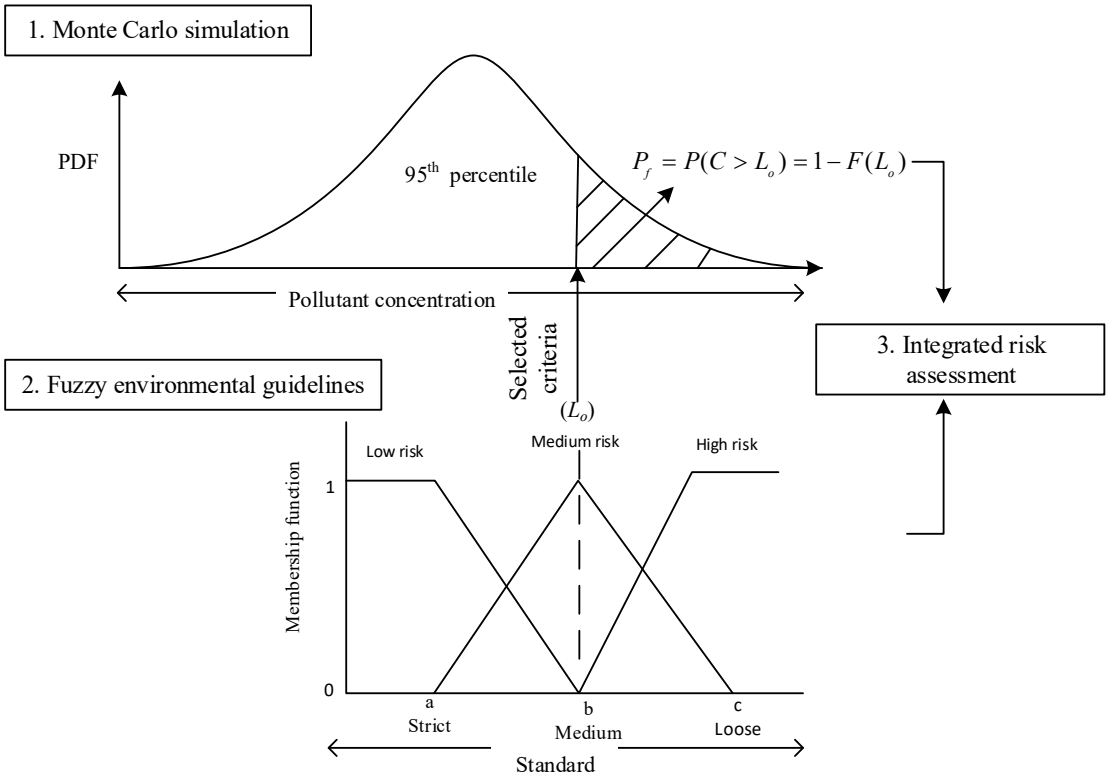

Figure 3.8 Steps of risk evaluation using fuzzy-stochastic risk assessment approach

Subsequently, environmental standard is selected which lead to the probability risk (R)= P_f of violating the standard using eq. (3.68). Lets L_o= 10 µg/m^3 is the criterion for the $PM_{2.5}$ then the $R = P$ (C>10). At the same time, suitability of this standard can be determined by quantifying the risk. MCS is used for quantifying system uncertainties, with the modeling outputs serving as the basis for risk quantification. After generating certain sets of random samples for each pollutant, the distribution of predicted concentrations can be calculated by the Gaussian model. The distribution results can then be used to define 5th and 95th percentile concentrations.

3.8 Development of Graphical User Interface

LCAQMS for the mining is developed using the C sharp and visual basic programming language in visual studio 2015 and integrated with the inverse matrix and backpropagation artificial neural network (BPANN) model, Gaussian algorithm, and visual PROMETHEE tool. The original data are processed through the MATLAB that represents the algorithms of the models, and the results of the models are subsequently displayed and stored in excel files. The algorithm of BPANN model is packaged as a dynamic link library (*.dll) by using the MATLAB Compiler. The mining site data and emission inventory from the life cycle modeling are considered as inputs for MADM model. All the equations are solved in excel, and then data is imported to MATLAB complier. The input data and all the variables representing alternatives are prepared in the matrix form, and the output can be directly imported to excel as csv format. However, visual graphs prepared through this tool can be used in raw with little improvement. The models have a single graphical user interface and share a common data storage as shown in Figure 3.9.

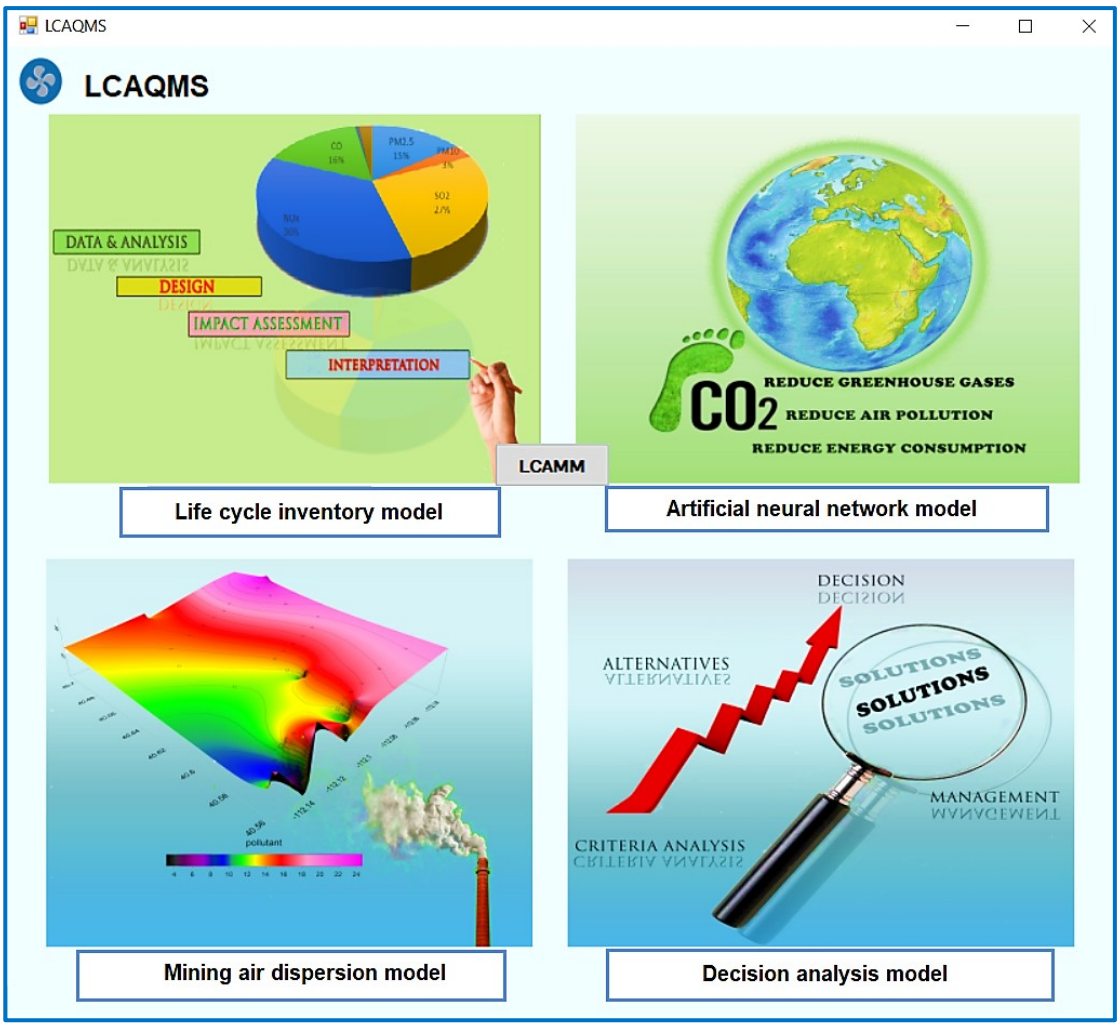

Figure 3.9 Graphical user interface for the LCAQMS model

The module of a life cycle model comprised two sub models which are inventory development model and characterization method for impact assessment. The module has two main pages showing inputs and outputs. The input page allows users to select the technology variables, pollutants, and units. The technology and emission intervention matrix generates by clicking their buttons. The excel sheet appears which allow entering quantitative information related to all variables as shown in Figure 3.10 (a). All the inputs data are stored in the database, and calculated results can be obtained by clicking "Run Matrix and load". The impact assessment is analyzed by selecting any of the characterization methods. The users can choose to display the environmental

indicators and normalized the results by uploading background data of pollutants. An additional option is provided to link the emission inventory with the mining activities.

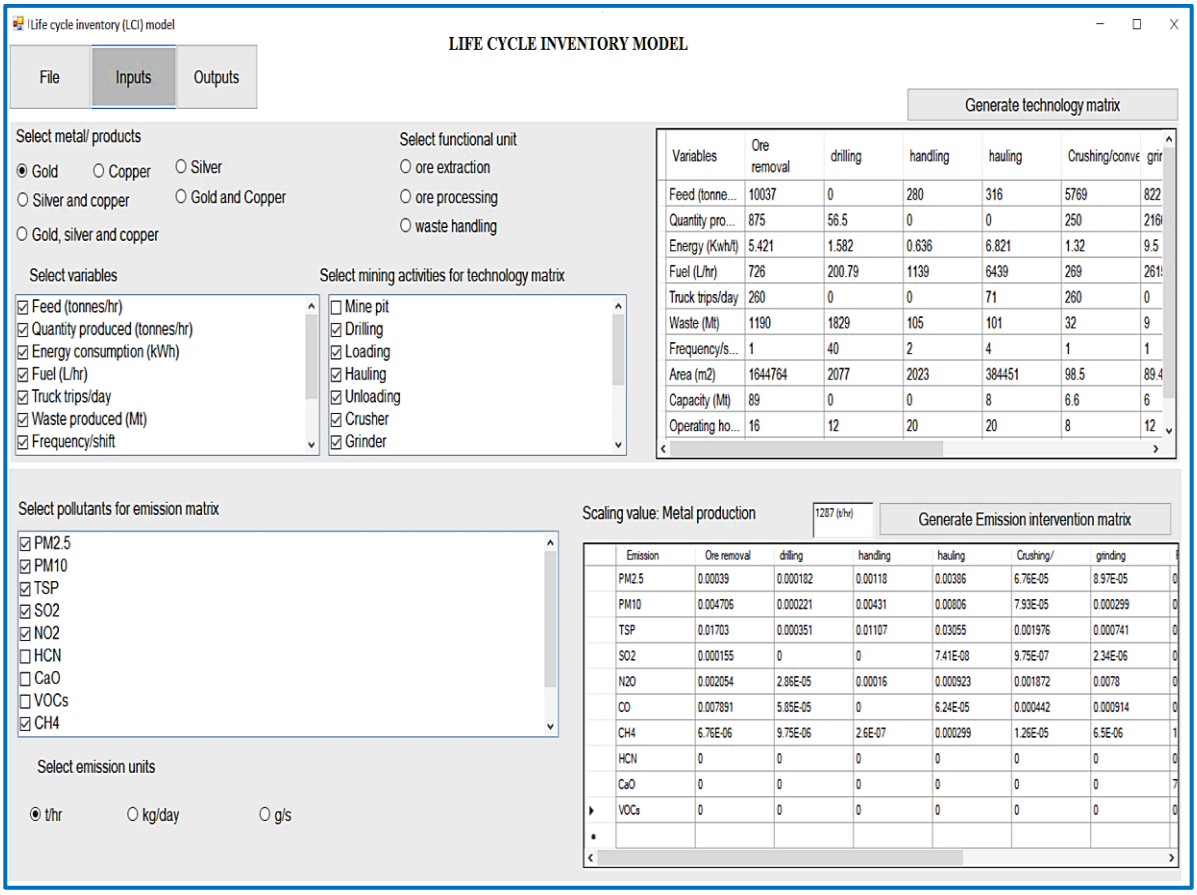

(a)

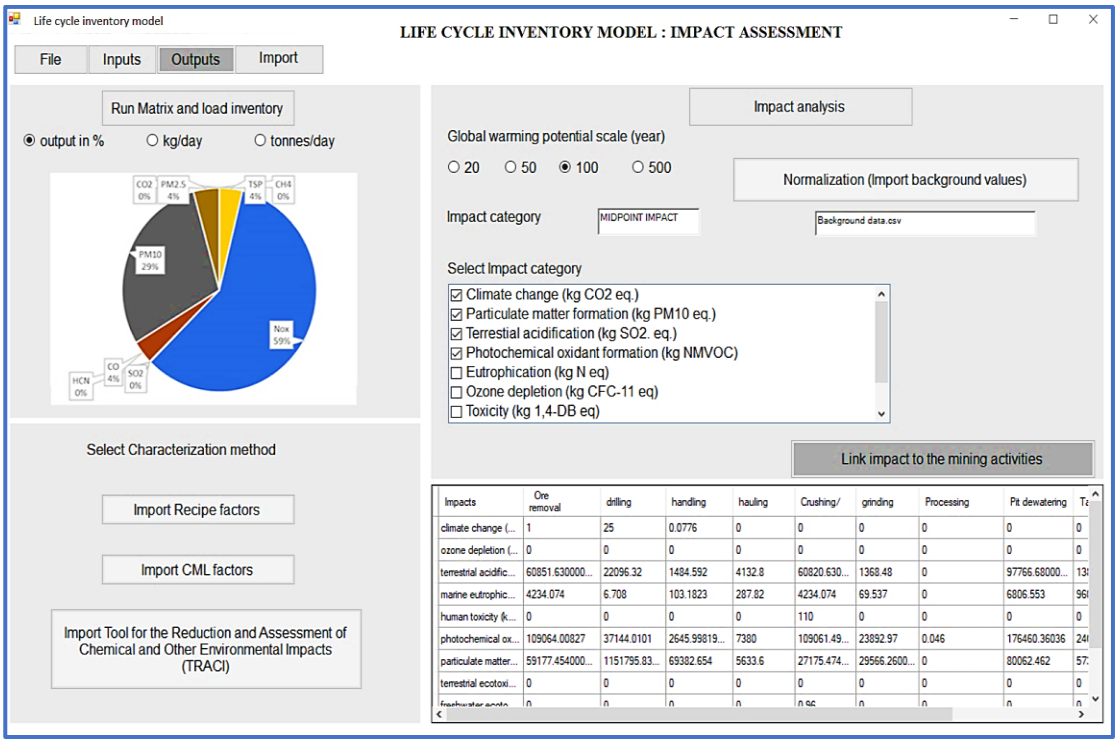

(b)

Figure 3.10 User interface of a life cycle inventory model module (a) inputs (b) outputs and impact assessment

The carbon footprints module comprises ANN model which consists of training data, validation and testing data. This module can perform the training of the data and prediction using the neural networking algorithm. The initial step is to import the data as csv files by clicking the "Load" button. The attributes are selected based on the preferences such as the distribution of sampling data, number of input layers, hidden neurons and variables. The data can be linked to the MATLAB compiler and run using MATLAB ANN. The results can be seen by clicking the load button. Figure 3.11 shows an example when the model stops running after 10 epochs (An epoch is a represents the number of times all of the training values are used once to update the weights.) and mean square error is obtained after every time training stops or after fixed iterations. The regression analysis can also be performed by comparing the predicting and monitoring values. After each training and prediction, the results could be exported to csv files.

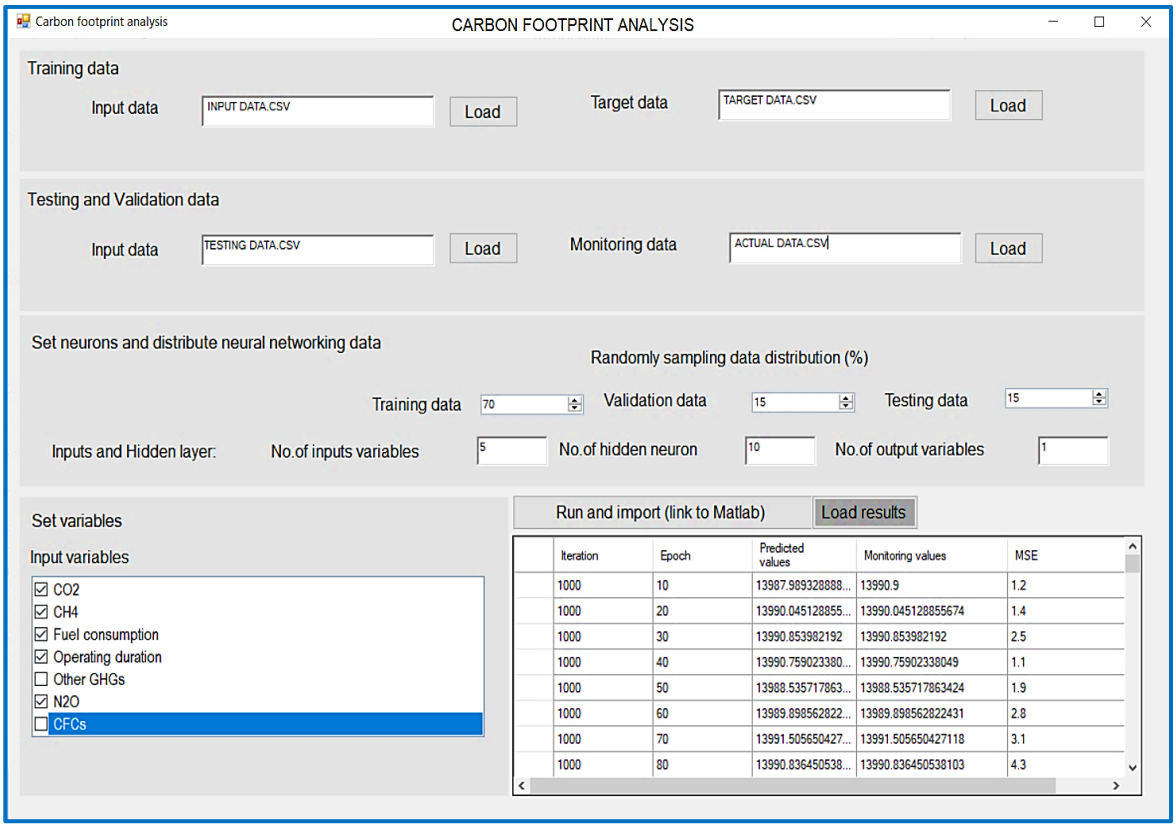

Figure 3.11 User interface of carbon footprint analysis module

An air quality module consists of mining-zone air dispersion model (MADM) which allows users to input source information, receptor site information and meteorological parameters. The interface can import the daily average values of the parameters and detailed 24 hrs data as csv files. By clicking "Calculate atmospheric stability", Stability class is obtained. Other parameters such as settling velocity, mixing height, deposition velocity is obtained by clicking the button "Calculate parameters and save results to database". The predicted modeling values are obtained by running the model. The results are automatically imported from excel to the interface showing major input columns and predicted concentration column. The "Load contour" button is linked to the surfer tool, by clicking it the contour maps based on the final results is produced and shown in the interface. However, users can do the modification by selecting the scales, filling the contours and labeling the maps as shown in Figure 3.12.

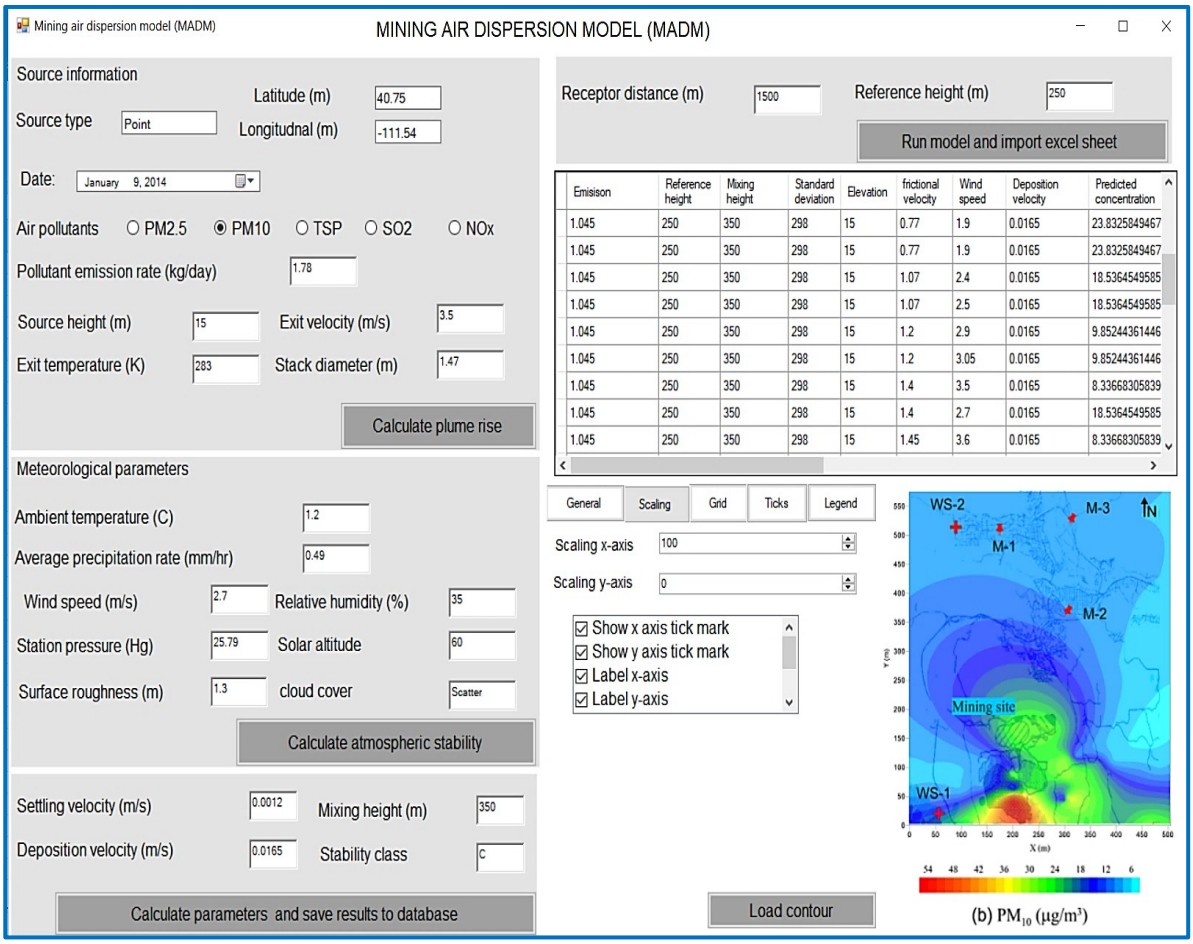

Figure 3.12 User interface of an air quality module

The decision analysis model comprises two sub-models which are multi-criteria decision analysis model and optimization model as shown in Figure 3.13. The interface allows selecting the alternatives and criteria. The criteria weights are calculated by clicking "Calculate weights using AHP". The users can assign scoring to the alternatives by clicking button "Assign scoring using PROMETHEE". Both above-mentioned buttons are linked to the excel sheets. The net flows of alternatives or negative and positive flows of alternatives can be calculated using PROMETHEE tool which is linked with the buttons "Calculate net flows of alternatives" and "Calculate positive/negative flows of alternative". Moreover, sensitivity analysis and uncertainty analysis can also be determined and results are saved as csv by loading results. An optimization module consists of air pollution control model. A single objective function is assigned by the user and multi-constraints can be selected from the list by checking

the box. The pollutant concentration calculated using MADM model can be imported as csv files. The ambient air quality criteria or guidelines can also be imported. All the input data is linked to the excel spread sheets and the model run as an excel solver add on which is linked to the button “Solve”. The final results can be imported by clicking the button and save all the results to the database. Furthermore, the probability distribution of the input and modeling results can be analyzed, and fuzzy risk assessment is performed by clicking the provided buttons in the interface.

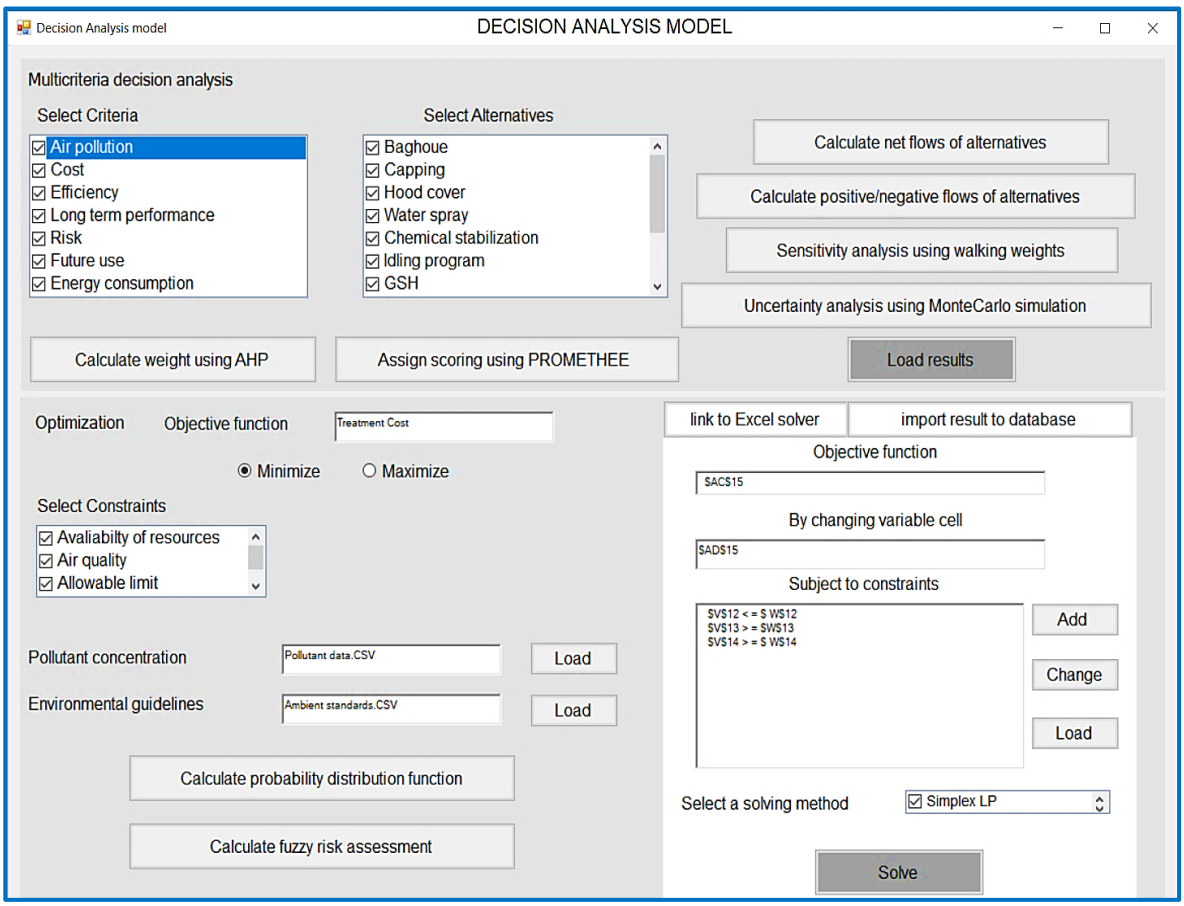

Figure 3.13 User interface of a decision analysis model module

3.8.1 Spatial and temporal scales

Features of LCAQMS includes all the technical data from the mining site and real time atmospheric conditions in addition to the emission data per unit mining activities. The three-dimensional values could be produced by considering x, y and z directions.

The LCAQMS model also implies variable grid cells depending on the boundary conditions at the inventory development stage. Moreover, values can be predicted at different distances after the mining source from C_{0km} to C_{30km} depending upon the availability of stability conditions. For vertical reference height, modeling values can be generated at various points until concentration get sufficiently dispersed. Usually, the coupling of all primary and sub level models increases the computational demand. However, in the inventory model, the input variables are fixed, and other unnecessary parameters are eliminated using cut-off criteria rules in LCA. For air dispersion model, daily (24 hrs) data is used along with the local weather station data. Precisely, real-time meteorological data is critical to be used to get the predicted modeled value on the specific day of the month or year.

3.8.2 Management of model structure and input values

The parameters and variables are selected from the field and literature studies, technical reports and mining companies. In the case of open-pit metal mining, variables defining the contribution of pollutants are determined by mining corporations and government database. The technology matrix included ten variables divided as processing flows [feed (tons/hr), quantity produced (tons/hr) and waste produced (tons/hr)]; technical flows [Area (m^2), capacity of unit (Mt), frequency of activity per shift (number), truck trips per shift (number) and operating hours per shift (hr)] and energy flows [fuel consumption (L/hr) and energy consumption (kWh/t). The environmental flows comprise of potential pollutants produced and may vary from mine to mine and then compiled in matrix forms. Calculations based on underlying environmental indicators for impact assessment. For example, characterization factors when linked with emission loads (inventory), give results in terms of impact. This relationship is used to determine the midpoint impact analysis in the first module of the model. Because of inherent variability and nature of the processes, only greenhouse gases are used to calculate the carbon credit for the mine using artificial neural network algorithm.

In the proposed mining-zone air dispersion modeling (MADM) approach, there are three components of input database including geographical, meteorological and air emission inventory from the LCA output as shown in Figure 3.4. The geographical database included digital maps, land usage data, elevation dataset, surface roughness length and processed into gridded surface within the modeling domain. Whereas, meteorological data included the wind speed, direction of the wind, ambient temperature, precipitation rate, stability class, etc. The source related parameters are emission rate from the sampling points, stack height, stack diameter, exhaust temperature, exhaust exit velocity and plume rise. These data sets are spatially allocated and stored in the database of MADM in the corresponding compartment and saved as Excel spreadsheet. MADM has been embedded in a MATLAB edition 2015R for linear regression. Visual graphs for other results are then plotted in Excel/Sigma plot, and golden software surfer V13 is used to produce contour mapping.

For multi-criteria decision analysis, all the outputs from MADM and BPANN are carefully evaluated to find the potential air pollution issue in the mine which helps to find the best possible alternatives. Criteria to evaluate each alternative are identified to ensure the objective of the decision analysis method. The data for each criterion is obtained from literature studies and different mining reports by experts. The chosen criteria for decision system are minimize the air pollution, minimize the cost, maximize the extraction rate or efficiency, maximize the sustainable performance, minimize the risk associated with the pollutants, minimize the quantity required for chemicals and application rate in context of dust suppressants, maximize the future use and minimize the energy/fuel consumption. Whereas, alternatives could be identified based on the field study and target group such as minimize dust and reduce carbon footprints.

3.8.3 Model performance evaluation

Uncertainty, sensitivity and statistical analysis in LCAQMS model is performed while considering input data, boundary conditions, data for verification, missing data and output concentrations. Following are the task performed to improve the performance of the model:

- The variables included at the stage of inventory development are chosen based on careful analysis and understanding of the mining activities and limited by the availability of input data. Thus, other irrelevant variables are eliminated using cut-off criteria rule in LCA.
- During carbon footprint analysis, a lot of processes, directly and indirectly contribute towards carbon credits. Artificial neural network algorithm is selected to avoid any uncertainty because of missing values and nonlinear relationships.
- Uncertainty in boundary conditions may affect the analytical solutions. However, for K-theory Gaussian algorithm boundary conditions, assumptions are made based on the past air dispersion models and literature studies.
- The ranking of alternatives is profoundly influenced by the allocation of weights to criteria as well as alternatives which may contribute to uncertainties. This issue is overcome through net flow of alternatives by conducting the sensitivity analysis using walking weights as a unique feature in the visual PROMETHEE tool and Spearman rank correlation coefficient.
- The uncertainties exist during risk assessment in two ways which are the variation in pollutant concentration levels and the suitability of environmental standards. The first type of uncertainties is quantified using Monte Carlo simulation, while the second one is addressed by the fuzzy-set technique. The uncertainty analysis in the inputs such as meteorological parameters (wind speed), is analyzed using Monte Carlo simulation. Moreover, output concentrations are distributed as probability density function to avoid the uncertainty in the final results.
- Model performance is statistically evaluated at each step during the development of different modules of the LCAQMS by considering the mean square error, standard error, normalized mean square error, fractional bias and correlation coefficient.

3.8.4 Model application and users

Integrated environmental models are usually complex and when designed to produce quantitative results, are often accessible only to experienced modelers. For

LCAQMS modeling, the model aims to be used by the site and design engineers in the mining industry. The model has been integrated to run with various treatment options for air and different atmospheric conditions relevant to management questions and stakeholder concerns. Model output is analyzed to provide scientific and visual interpretations for stakeholders, including regional environmental managers.

3.9 Summary

In this chapter, an integrated approach is conceptualized as LCA based air quality modeling system (LCAQMS) for the mining. This chapter focuses on incorporating air quality modeling to understand the severity of air pollution in mining and developing an integrated system for mining- related decision support for the field applications. The system integrates inverse matrix which is used to develop air emission inventory, characterization method to assess the environmental implications and back propagation artificial neural network model for carbon footprint analysis. The K-theory based Gaussian algorithm is used to develop the mining-zone air dispersion model (MADM) while considering the physical removal mechanism. Pasquill-Turner method (PTM) is integrated into the system to investigate the meteorological parameters using an empirical approach. The multi-criteria decision analysis (MCDA) method is developed to provide alternatives to air pollution treatment based on multi-criteria using PROMETHEE method. An AHP method is integrated with PROMETHEE to assign the weights to all participated criteria and scoring to the alternatives. Furthermore, an air pollution control model is developed based on single objective function with multi-constraints to optimize the treatment cost of treatment using linear programming. A probabilistic decision analysis method is constructed using Monte Carlo Simulation (MCS) to perform uncertainty analysis. A fuzzy-based risk assessment approach is developed to evaluate the environmental risk arising from multiple air pollutants predicted by MADM.

CHAPTER 4 AN INTEGRATED LIFE CYCLE AND ARTIFICIAL NEURAL NETWORKING MODEL FOR MINING (LCAMM)

4.1 Overview of the Study Area: An Open-Pit Gold Mine Study, Ontario, Canada

Mine "A" which is an open pit mine located in the northeast of Ontario, Canada with gold production from 475 to 525 thousand ounces per year as shown in Figure 4.1. At present, mining is being carried out using a gravity technique, cyanidation recovery techniques, and carbon-in-pulp processing facility with the production rate of 55,000 tons/day. The grinding circuit comprises two parallel lines, each having one sag mill and one ball mill. The gravity circuit is used for recovery of the gold. The remaining gold in the ore is sent to cyanidation process followed by carbon in pulp recovery method. After carbon stripping, the gold is finally processed through electro-winning cells stage before the gold pouring stage with 92 % of overall gold recovery.

Figure 4.1 Mine A site overview

4.2 Data Preparation and Model Implementation

4.2.1 LCAMM computation

For each mining activity included in the study, data were collected through the survey, the environmental impact assessment (EIA) reports, companies' websites and government reports of gold mining industries in Canada were incorporated in LCI databases. Ecoinvent 2.2 and 3.1 is the only database having information on metal mining in North American countries (especially Canada and USA) was also included in this study to build more profound and detailed inventory inputs. The average monthly data were collected over the four years' period from 2011 to 2015 from various sources in mine A as shown in Table 4.1.

Table 4.1 Input data sources and database

Input data type	Sources	References
Mining technical data	Mine A	Technical reports
Pollutant emission data	Monitoring stations of mine A (2011 to 2015: average daily)	Environment and sustainability reports
Other mining data	Ecoinvent 2.2 and 3.1 databases	(ecoinvent, 2016)
Characterization factors adopted from three different methods	CMLCA database: International EPD system: default environmental impact categories for CMLCA database	(CMLCA, 2015)
	TRACI: USEPA	(TRACI, 2016)
	Recipe (Dutch National Institute for Public Health and the Environment (RIVM))	(Recipe, 2016)
Equipment sizing and dimension information	Metso company: product details and sizing	(Mesto, 2016)
Greenhouse data	Environment and climate change Canada: Greenhouse gas emissions reporting program Facility Greenhouse Gas (GHG) Data base:756 samples (year: 2014 and 2015)	(ECC, 2017)
Fuel consumption	Caterpillar performance handbook; fuel consumption data from Mine A	(Caterpillar, 2010)

All the data is stored in excel spreadsheets in the matrix form and divided into two main parts concerning mining activities.

1. Technical information stored as a technology matrix
2. Air emission data stored as an environmental intervention matrix

Table 4.2 shows the technology matrix which is comprised of positive flows such as quantity produced, waste generated, and those with numbers (frequency per shift, truck trips per shift, etc.). The flows with a negative sign represents consumption such as fuel, energy, area utilization, and ore consumption as feed. Depending upon the size of the particles required, the specification of the crusher, conveyor belt and grinders were selected. For example, in this study the specification of HPT cone crushers was adopted; such as for 185 (mm) coarse,125 (mm) medium and 95 (mm) fine particles feed,19 (mm),16 (mm) and 13 (mm) discharge were available respectively, with 250 (tons/hr) capacity at the rate of 160 (kW) energy consumption. The conveyor belt of 12 x 27 ft with the capacity of 200 (tons/hr) was used which could operate 8 hours per shift. Similarly, for grinding, Ball mill's values were adopted. For instance, for 6 (tons/hr) output capacity, 20 (mm) feeding size was selected which could have potential to discharge of 0.07-4 (mm) (Mesto, 2016).

The truck trips were between the two activities like from ore removal, i.e., mine pit to the crusher and from ore removal to stockpiling. It is worth to mention that stockpiling is the storage place for rocks before handling or discharge. Thus, trips can be from the stockpiling to different stations including handling of ore. If the hauling is between two activities, the number of trips were evenly distributed among them. For processing unit, energy, fuel consumption, the area provided were based on the sum of activities in that unit such as cyanidation process comprises of adsorption columns, electro-winning cells and cyanide destruction unit. Take this into consideration that this process is mentioned for this study and might be different for other mines. Figure 3.10 (a, b) in Chapter 3, represents the user interface inputs of Table 4.2 and Table 4.3.

Table 4.2 Technology matrix for gold mining site A

Variables	Ore removal	drilling	handling	hauling	Crushing /conveyor	grinding	Processing unit	Pit dewatering	Tailing area	Stockpiling
Feed (t/hr)	10,037	0	280	316	5769	822	1000	0	2716	982
Quantity produced (t/hr)	875	56.5	0	0	250	21666	1278.3	0	0	0
Energy (Kwh/t)	5.421	1.582	0.636	6.821	1.320	9.5	9.472	1.527	1.754	0
Fuel (L/hr)	726	200.79	1139	6439	269	2615	2615	271	87	0
Truck trips/day	260	0	0	71	260	0	0	0	35	250
Waste (Mt)	1190	1829	105	101	32	9	18	5	298	6
Frequency/shift	1	40	2	4	1	1	1	1	2	4
Area (m^2)	164476	2077	2023	384451	98.5	89.4	8093	0	217175	448930
Capacity (Mt)	89	0	0	8	6.6	6	20	0	303	7
Operating hours	16	12	20	20	8	12	25	6	0	8

Note: All values are supposed to put in the model with negative sign except quantity produced, trucks/trip, waste, frequency/shift and operating hours;
Functional unit: 1278 (t/hr) of metal produced during processing;
Zero value indicated that this variable is not related to the particular activity.

Following Table 4.3 represents the input for emission load per unit activity. All direct and indirect emission rates are added as a single input for each pollutant.

Table 4.3 Emission intervention matrix for the mine site A

Emission (t/hr)	Ore removal	drilling	handling	hauling	Crushing/ Conveyor	grinding	Processing unit	Pit dewatering	Tailing area	Stockpiling
$PM_{2.5}$	0.00039	0.00018	0.00118	0.00386	6.76E-05	8.97E-05	0.00156	7.8E-06	3.8E-05	0.000559
PM10	0.004706	0.00022	0.00431	0.00806	7.93E-05	0.000299	0.00195	7.8E-06	0.00024	0.001989
TSP	0.01703	0.00035	0.01107	0.03055	0.001976	0.000741	0.002717	7.8E-06	0.00035	0.004979
SO_2	0.000155	0	0	7.41E08	9.75E-07	2.34E-06	0.00416	9.75E-07	0	0
N_2O	0.002054	2.86E-05	0.00016	0.00093	0.001872	0.0078	0.001001	0.000572	0	0
CO	0.007891	5.85E-05	0	6.2E-05	0.000442	0.000914	0.000534	0.000403	0	0
CH_4	6.76E-06	9.75E-06	2.6E-07	0.00029	1.26E-05	6.5E-06	1.3E-08	0.000013	0	0
HCN	0	0	0	0	0	0	0.000195	0	0	0
CaO	0	0	0	0	0	0	7.41E-05	0	0	0
VOCs	0	0	0	0	0	0	0.00065	0	0	0

Note: Zero value indicated that there is no emission with respect to activity

4.2.2 Structure composition for artificial neural network method

The data used for carbon footprint analysis were obtained from mine A. Three greenhouse gases were selected for this study, i.e., CO_2, CH_4, and N_2O. Also, two other parameters, i.e., fuel consumption (FC) and operating days (OD) were chosen for input variables in ANN. There were 756 samples collected from different equipment and those mining activities which were fuel dependent. The sampling data for the five variables over the period of two years (2014 and 2015) were chosen. Following Table 4.4 shows the input for ANN as an example of the collected samples. The data can be directly imported to the user interface as CVS excel sheets as shown in Figure 3.11.

Table 4.4 Inputs for ANN computation

Items	fuel consumed (L/hr)	CO_2 (kg/hr)	N_2O (kg/hr)	CH_4 (kg/hr)	operating days (hours)
crush engine 1	269.000	707.470	0.108	0.036	8760
screening engine 1	36.000	94.680	0.014	0.005	8761
crush engine 2	269.000	707.470	0.108	0.036	6441
screening engine 2	36.000	94.680	0.014	0.005	4661
pump engine	87.000	228.810	0.035	0.012	8701
pit dewatering	271.000	712.730	0.108	0.036	8652
Sum of all generator	4165.200	10954.476	1.666	0.554	8771
Drilling	200.799	528.102	0.080	0.027	5225
Loading	1139.726	2997.479	0.456	0.152	4884
Hauling	6439.840	16936.780	2.576	0.856	8780
pit maintenance	726.027	1909.452	0.290	0.097	3789
Bulldozer	232.000	610.160	0.093	0.031	3847
wheel loader	492.000	1293.960	0.197	0.065	4412
hydraulic shovel	144.000	378.720	0.058	0.019	5190

Note: Emission factor for diesel fuel (CO_2 =2663 (g/L) N_2O =0.4 (g/L) and CH_4 =0.133 (g/L)); for gasoline (CO_2 =2289 (g/L) N_2O =0.05 (g/L) and CH_4 =2.7 (g/L)); for propane (CO_2 =1510 (g/L) N_2O =0.108 (g/L) and CH_4 =0.024 (g/L); global warming potential (GWP) for CO_2 =1, N_2O =298; and CH_4 =25 (Caterpillar, 2010)

4.3 Results

4.3.1 Inventory development

The scaling vectors calculated through technology inverse matrix were multiplied by emission load matrix to generate environmental emissions inventory. Figure 4.2 illustrates an example of the output emission inventory that is obtained from all the air emission load calculated from environmental intervention matrix by following the methodology of LCAMM inventory model. The inventory result shows that the mine "A" contributed 49.6 % of TSP of the total environmental load. Whereas, rest of the burden was due to PM_{10} (20%), $PM_{2.5}$ (14.7%), N_2O (7.1%), CO (6.1%), SO_2 (1.3%), HCN (0.6%), CH_4 (0.4%), CaO (0.2%) and VOCs (0.06%). Most dust generated from natural activities at a mining site such as heavy machinery, bulldozing, blasting, and hauling of trucks on unpaved roads. Moreover, PM_{10} is also generated when the wind blows over different types of stockpiles. PM_{10} and $PM_{2.5}$ are produced mainly from mobile equipment and vehicle exhausts. The reason behind the percentage contribution of N_2O may emanate as the by-product in the post-blast gas of ammonium nitrate-based explosive (contribution of N_2O values due to blasting were added in ore removal

activity). In addition, thousands of liters/years fuel is consumed in mine A along with five diesel generators of 1200kW which were mainly responsible for N_2O and CO_2 production. However, CO_2 production is discussed separately under carbon footprint analysis. Whereas, CO is produced due to heavy equipment used during processing of ore. Even though, 390 kg/hour of SO_2 is usually used with the mixture of air to destroy HCN produced during processing of metal ore. The generation rate for SO_2 is less as it counts only if excess amount emitted remaining after cyanide destruction. Since SO_2 treatment is used by this mine for removal of HCN, this leads to 0.6 % contribution towards emission load. As this mine is facilitated with a baghouse as air pollution treatment equipment, there are chances for other toxic gases emissions. During data collection, it is found that lime bins are being used along with baghouse in the mine A, which is responsible for the generation of 0.2 % CaO in the air. CH_4 is also considered as a greenhouse gas which may produce because of fuel consumption such as diesel, gasoline, and propane. Usually, the presence of VOCs is more profound during smelting of ferrous metals. Thus, in this study there are very few traces of VOCs found which are almost considered negligible.

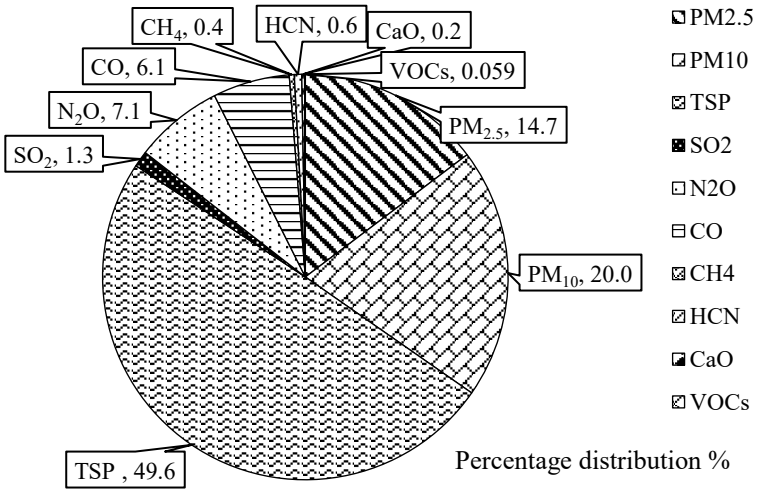

Figure 4.2 LCAMM environmental air pollutant life cycle inventory for mine A

4.3.2 Midpoint impact analysis

Life cycle impact assessment of all the air pollutants was calculated through TRACI, CMLCA, and Recipe characterization used in LCAMM to observe all the possible impacts. Figure 4.3 presents the midpoint modeling results of impact categories for the gold mine A using above mentioned assessment method. Moreover, the analysis also expressed the results regarding impacts when characterization factors linked with the emission loads. Climate change is not discussed during midpoint impact analysis as it is tested during simulation of carbon footprint analysis using ANN.

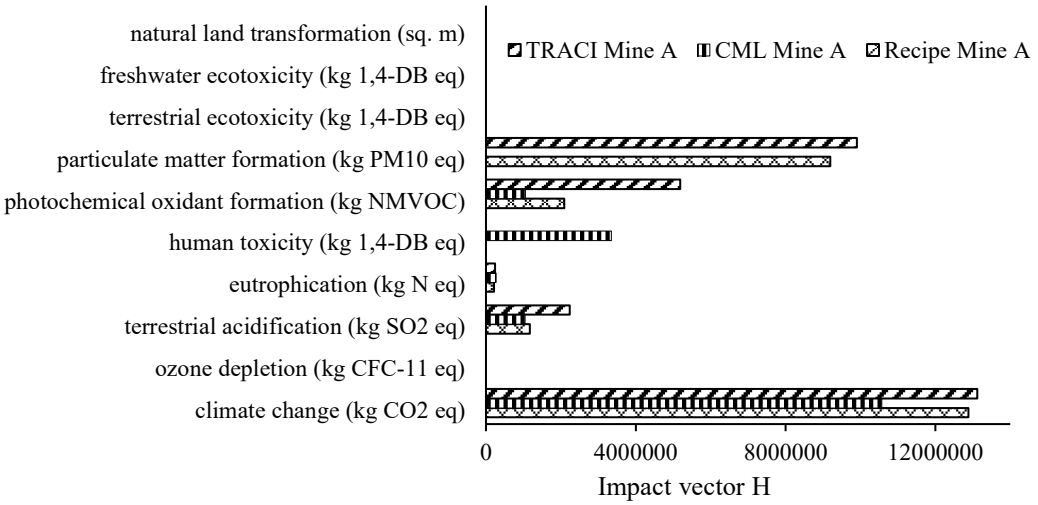

Figure 4.3 Midpoint impact modeling for a mining impact assessment

It is also possible to attribute the calculated impacts to each activity and trace it back to the unit processes that are responsible for generating them by using any of the assessment methods in LCAMM. As an example, TRACI and CMLCA based significant impacts are summarized in Figure 4.4 such as the formation of particulate matter, human toxicity, photochemical oxidant formation and acidification regarding mine A. Mostly results were normalized to the midpoint level concerning any of the suitable methods (e.g., CMLCA, Recipe, and TRACI world 2000 data). For this study, instead of using adopted reference values from the defined method, data were

normalized based on the background emissions data at the mine site A as Figure 4.4 shows the results after normalization the data. The standard error of the mean (SEM) was determined for each category illustrating ±0.0009 for particulate matter formation, ±0.00052 for acidification, ±0.00017 for human toxicity and ± 0.000095 for photochemical oxidant formation.

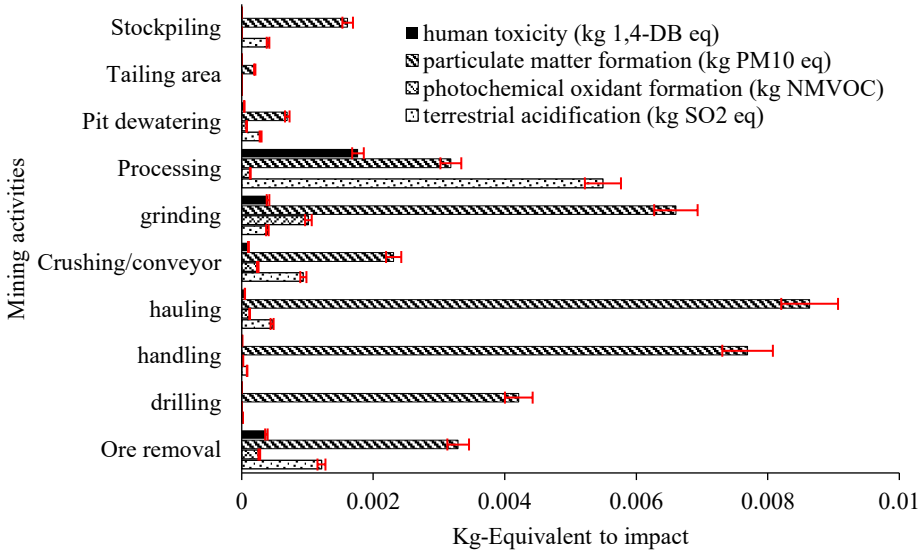

Figure 4.4 Normalized Impact assessment per unit process for gold mine A

4.3.3 Evaluation of carbon footprint analysis

Five scenarios were established by the availability of data and which may directly subsidize the carbon credit as shown in Table 4.5. The input variable subsequently decreased one by one in descending order to construct different possibilities and combination. Different combinations based on various nodes were performed through ANN model for each scenario. Consequently, structures of ANN models were constructed and tested to determine the optimum number of hidden neurons or nodes. Among the five scenarios, the one that uses all the five variables as model input showed the highest prediction performance in the testing data set, with the values of R^2 and MSE were 0.86 and 0.63. For validation set, third scenario (FC, CO_2, N_2O) showed the highest performance based on the R^2 value =0.90. However, its MSE was 47 % more

as compared to the first scenario (FC, CO_2, N_2O, CH_4, OD). Thus, only considering the regression coefficient might not be the exact representation of the data. That's why by considering both the regression coefficient and mean square error the first scenario has been awarded as the best performance in the validation set category. Similarly, for the testing set, even though the last scenario (FC) was showing a minimum mean square error, i.e., 0.25, the first scenario was the sensible choice with R^2 =0.87 and MSE=0.35 values. In conclusion, the topology of this model has five neurons in the input layer, ten neurons in the hidden layer and one neuron in the output layer.

Table 4.5 Scenarios of various input variables for the carbon footprint simulation

		Training set		Validation set		Testing set	
Input variables	Structure	R^2	MSE	R^2	MSE	R^2	MSE
FC, CO_2, N_2O, CH_4, OD	5-10-1	0.86	0.63	0.89	0.48	0.87	0.35
FC, CO_2, N_2O, CH_4,	4-8-1	0.83	1.7	0.80	0.63	0.78	1.3
FC, CO_2, N_2O	3-7-1	0.87	0.97	0.90	0.91	0.79	0.58
FC, CO_2	2-5-1	0.85	0.74	0.79	0.7	0.80	0.65
FC	1-4-1	0.84	0.84	0.75	0.55	0.76	0.25

The BPANN predictions reproduce the measured values satisfactorily. The stop criteria for the neural network training algorithm (LM) in this study were to achieve the maximum number of iterations (1000). Figure 4.5 depicts the comparison of modeled and measured values of CO_2 eq. (tons). Various simulations were performed during training, validation and testing data sets for the optimal selection of the model. All the measured and modeled values were based on the average values of CO_2 eq. (tons) over the two years' period. The intercepts of the regression line of training data set, validation data set and testing data set are 0.004, 0.0039 and 0.0031 respectively.

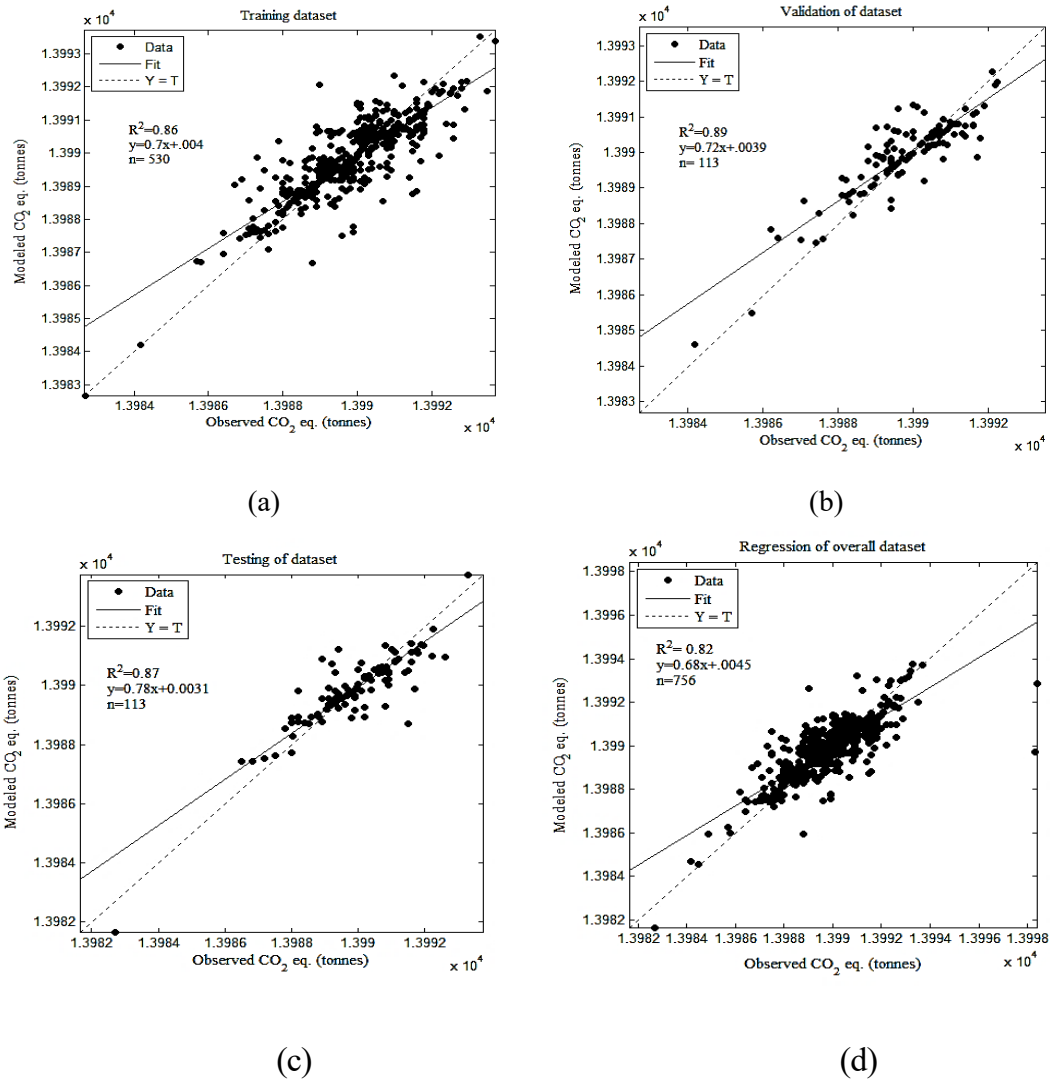

Figure 4.5 Comparison of the modeled and measured values of CO_2 eq. (tons) in (a) training data set, (b) validation data set and (c) testing data set (d) overall dataset

4.4 Discussion

This study confirms that one of the advantages of matrix inverse method is that the results can be quickly obtained to understand and evaluate the emission inventory. Although, the scope of the present study is limited to the air pollutants, for the open pit mining method. Whereas, one can apply the same framework to study other mining methods such as underground mining. In this study, average emission rate of each pollutant was considered which is most suitable for such type of life cycle modeling.

However, end of life stages and recycling effect were not discussed during this study. In this mining site, cyanidation was the primary metal extraction technique. For other open pit mines, any of the hydrometallurgical method such as heap leaching, in-situ leaching or pyro-metallurgical process such as refining, or roasting could be used. This work shows that most of the impact in this mine was mainly because of particulate matter formation. This trend may be notably altered if emission rates after removal efficiency of treatment techniques such as water spraying, wet drilling, dust suppression system, etc., would be added to the model (Asif et al., 2018c). It may also vary from mine to mine. Also, particulate matter significantly contributed to the midpoint impact because of hauling, handling of ore, milling/grinding, drilling and stockpiling.

LCAMM features are enhanced by adding BPANN algorithm for simulation of carbon footprint analysis. This study confirms that the BPANN is the best choice for analyzing non- linear input variables. ANN models were run in a managed way on the trial and error basis by adjusting various alternatives to find the optimal structure such as weight updates, some hidden layers and different epochs (events) as shown in Figure 3.11 (chapter 3). The optimum number of the nodes are selected based on the availability of the training data and hit and trial (Lal and Tripathy, 2012). Apart from these, no rules of thumb exist in the selection of dataset for training, testing, and validation of a neural network model.

As shown in Table 4.6, the range of CO_2 eq. concentration in the training, validation and testing data set was 13988- 13999, 13984-13998, and 13994-13998 tons respectively. The standard deviation of the validation and training data sets were also higher than that of the testing data set. Moreover, the data were statistically evaluated in Table 4.6. The range of true population along with confident interval for training, validation, training and the overall dataset is 13990.76 to 13993.2 tons (C.I ±1.24), 13988.27 to 13991.73 tons (C.I ±1.73), 13992.25 to 13993.75 tons (C.I ±0.75) and 13993.17 to 13994.83 (C.I ±0.83) respectively. It is noteworthy that true range for the modeling result is different from the normal range. This study confirms that true range is a better representation of the data because of the confident interval.

Table 4.6 Statistical properties of CO_2 eq. concentration in training, validation, testing and overall data sets for optimal model

CO_2 eq. (tons)	Training set	Validation set	Testing set	Overall set
Number of samples	530	113	113	756
R^2	0.86	0.89	0.87	0.82
Mean	1.3992E+04	1.3990E+04	1.3993E+04	1.3994E+04
Minimum	1.3988E+04	1.3984E+04	1.3994E+04	1.3990E+04
Maximum	1.3999E+04	1.3998E+04	1.3998E+04	1.3998E+04
Median	1.3900E+04	1.3900E+04	1.3990E+04	1.3992E+04
Mode	1.3991E+04	1.3990E+04	1.3980E+04	1.3990E+01
Standard deviation	3.68	2.5	1.08	2.47
Confident interval (C.I) 95%	±1.24	±1.73	±0.75	±0.83

4.5 Summary

The developed LCAMM modeling approach has been examined to produce air emission inventory, midpoint impact assessment and predicted carbon footprint analysis in terms of CO_2 eq. (tons) for the open pit gold mining, Ontario, Canada. LCAMM comprises of life cycle inventory model (inverse matrix method) and carbon footprint analysis model (BPANN algorithm). The inventory results could be further used as input for mining-zone air dispersion modeling in next stages of the LCAQMS modeling. The midpoint impact assessment shows that particulate matter formation is the primary issue of this mine. The modeling results of carbon footprints were compared with the monitoring values. Good agreement was acquired during the analysis. Hence, LCAMM is the first module of the LCAQMS which could deliver an effective air pollution assessment at the mining site and local scale. The approach would help the stakeholders or site engineers to adopt suitable measurements during the initial stages of the project and afterward.

CHAPTER 5 AIR QUALITY MODELING FOR MINING

5.1 Overview of the Study Area: A Copper-Gold Mine, British Columbia, Canada

The case study mine "B" is a copper-gold mine, located in Canada comprises of 2000 ha area. In the vicinity, there are residential areas situated in the north-west (NW) and north-east (NE) of the mining site at the distance of approximately 10 to 12 km as shown in Figure 5.1. The study area is in the semi-arid zone having average precipitation of 235 mm annually with usually light winter snow. The area has extremely cold winters and warm summers where temperatures can reach 38°C. During the winter, short periods of cold weather can occur where temperatures drop to as low as -39^{0}C. The site is covered in grassland and deciduous forest, and above 900 (mean above sea level) the grassland gives way to a continuous forest cover.

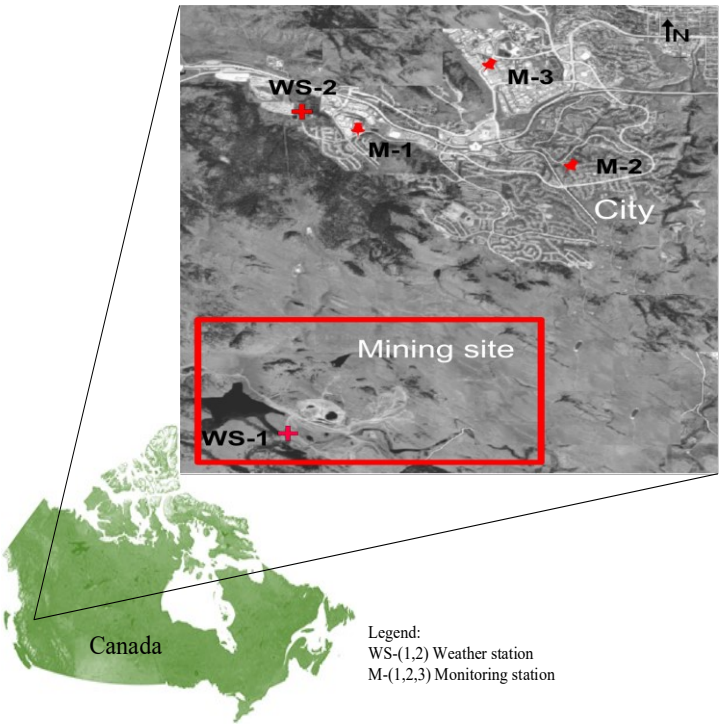

Figure 5.1 Mine B and monitoring station locations

5.2 Data Preparation and Resources

The data were collected from the 2010 to 2014 period of the mine to evaluate emission of dust, particulate matter, gaseous pollutants and heavy metals from various mining activities. The average emission data (g/s) were collected from different mining source activities. Four targeted pollutants TSP, $PM_{2.5}$, PM_{10}, NO_2 and six heavy metals as airborne particulate (As, Pb, Hg, Zn, Cd, and Cr) were selected for this study. However, for evaluation of modeling results only $PM_{2.5}$, PM_{10}, NO_2 monitoring data were available. The monitoring station M-1, M-2 and M-3 were chosen at the distance of 7 km (NW), 12 km(NNE-NE) and 10 km (NE-ENE) respectively to validate the model results. The 24 hrs (daily) monitoring data from the year 2010 to 2014 were obtained from the National Air Pollution Surveillance (NAPS) Network database, Canada (NAPS, 2015) and Ministry of the Environment, British Columbia (MOE BC, 2017), which allowed detailed evaluation. The input data were subdivided into spatial information, meteorological data, and emission rates based on mining activities. Table 5.1 shows the general weather information for the site. All parameters such as, stability class, cloud cover, solar altitude, wind speed, precipitation rate, etc., are saved to user interface database (see Figure 3.12).

Table 5.1 Meteorological data for the mining site

Months	Temperature	Dew point	Precipitation rate	RH
Average (2010-2014)	^{0}C	C	mm	%
January	-4.5	-4.5	15.5	84.1
February	-2.4	-8.2	10.1	75.2
March	1.5	-2.0	14.1	67.2
April	6.5	1	19.8	57.2
May	11.1	5.3	33	56.7
June	14.7	5.1	45	60.9
July	18.7	6.0	27	46.7
August	17.8	7.7	25.6	48.4
September	12.9	6.3	18.2	55.1
October	5.6	1.3	11.1	69.7
November	-0.1	-2.4	30.8	81.7
December	-4.9	-7.5	28.9	84.1
Mean	6.4	1.2	23.2	64.3
Standard deviation	0.6	0.78	1.7	2.0

Source: (Environment Canada, 2016)

5.2.1 Spatial and meteorological data

The digital maps and UTM coordinates along with national elevation dataset were obtained directly from the company X. The 24 hrs (daily) meteorological data included ambient temperature, wind speed, direction, frequency distribution were extracted from the real-time two different airport stations WS-1 (NW) and WS-2 (SSW) (Environment Canada, 2016). The annual average wind speed during the period of study was 2.3 m/s. The graphs for wind class frequency distribution (based on 24 hrs data) are generated by software WRPLOT view freeware 8.00 (WRPLOT, 2017). (The frequency distribution of wind and wind rose of mining site are presented in Figure 5.2). Most of the direction of the wind prevailing form west and south. The frequency distribution based on 24 hrs data reveals that there is highest percentage frequency of 0.50-2.1 (m/s) wind speed with an average of 0.09 to 0.17 % calm conditions (year: 2010 to 2014).

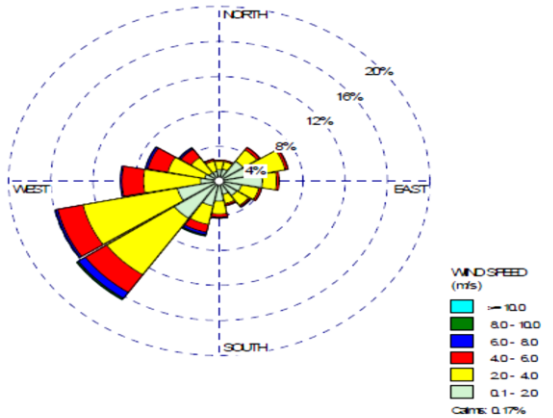

(a)

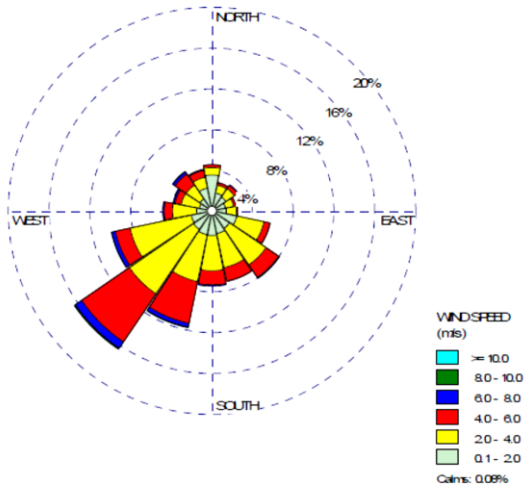

(b)

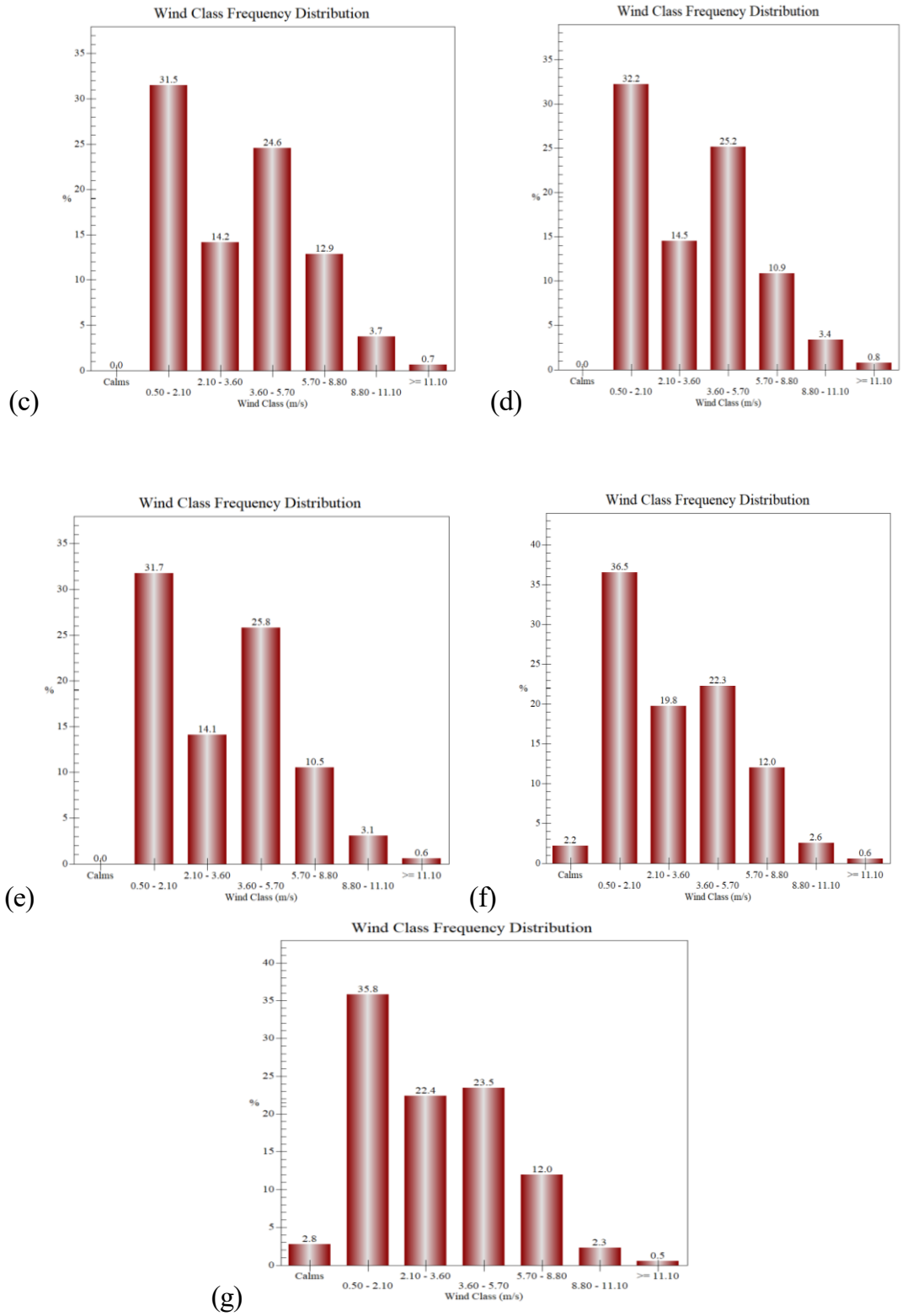

Figure 5.2 (a) Windrose at WS-1; (b) windrose at WS-2 (based on 24 hr (average data from 2010-2014); wind class frequency distributon (based on 24 hrs (individually for each year)genertd by software WRPLOT view freeware 8.00 (c) in 2010; (d) in 2011; (e) in 2012; (f) in 2013; (g) in 2014.

The atmospheric stability was determined using the meteorological method based on Pasquill-Turner method (PTM) (Ashrafi and Hoshyaripour, 2010). Figure 5.3 (a) illustrates atmospheric stability pattern of this site and depicting neutral class (D) is dominant among all classes. Figure 3.5 (b) represents the mixing height values based on seasonal variation and different times of the day. Mixing height is the depth of vertical mixing or dispersion of pollutants above the ground level (EPA, 2006, 1995). It affects on the pollutant concentration (for more detail see Chapter 6, section 6.4.3). In this study, the maximum mixing height achieved during summer evening (6:00 pm) is 1280 m. Whereas, during winter, it varies from 380 (6:00 pm) to 430m (midnight). Other than summer, maximum mixing height is observed during the spring and fall (12:00 pm) afternoon. Hence, for each cold month, mixing height is small with a chance of high pollutant concentration and vice versa. This result elucidates the fact that high would be the mixing depth, more possibilities for the dispersion of the pollutants (Asif et al., 2018a).

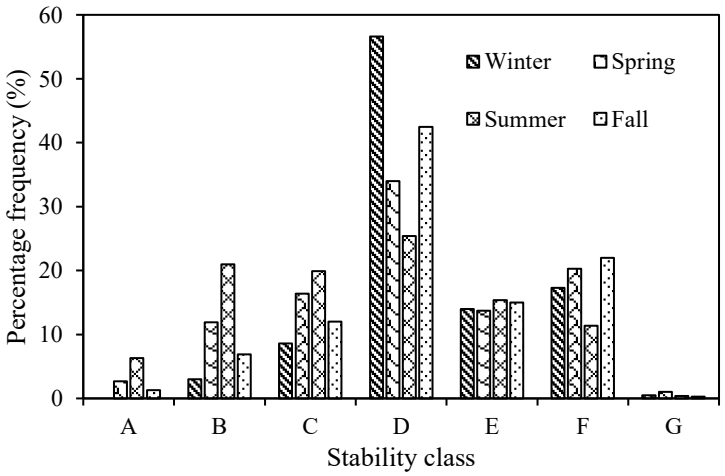

(a)

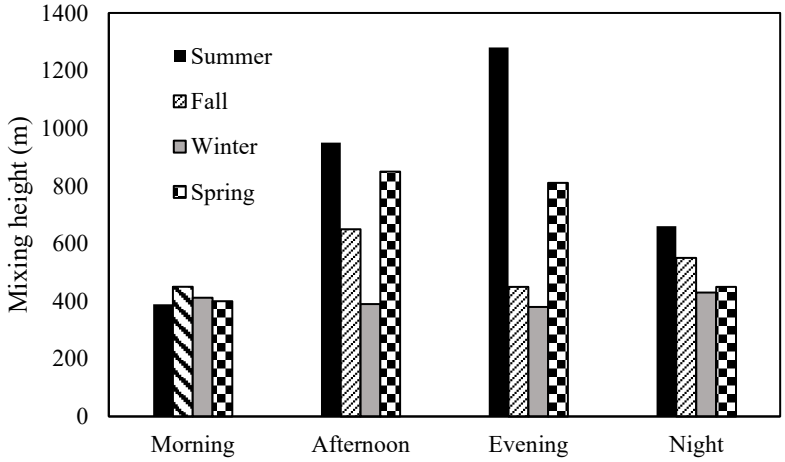

(b)

Figure 5.3 (a) Atmospheric stability distribution percentage at mining site; (b) Mixing height in different seasons and duration of the day

5.2.2 Determination of the emission rate

A set of nine empirical formulas were selected to calculate the emission rate for the mining site for each mining activity (see Table 5.2). The following chosen mining activities fall into the category of point sources, line sources, and fugitive emissions.

- drilling
- handling of piles
- ore loading
- waste loading
- unloading
- hauling included unpaved roads and truck roads
- crushing
- open pit escape

The data for the parameters used in the empirical formula such as drilling holes per day, holes diameter, and metal production were gathered from the technical reports of the mining. Each dataset concerning each activity has been segregated and stored in the database accordingly. The wind erosion impact on dust emission has also been included

in the empirical equation set for the mining activities due to its recent emphasis and impacting on the settling of the dust particles (Saxton and Chandler, 2000). During the data collection, it was found that dust, PM_{10}, and $PM_{2.5}$ were the significant pollutants from various mining activities. Therefore, heavy metals emissions data were collected based on total mine emission and as a part of particulate matter (PM). Whereas, TSP, NO_x and other gaseous emission rates are determined based on life cycle inventory model.

Table 5.2 Empirical method and estimated emission rate for particulate matter

Activities	Empirical equations (Chandra and Katiyar, 2011)	Emission rate	
		PM_{10} (g/sec)	$PM_{2.5}$ (g/sec)
Drilling	$E=0.0325\,k_c\left[\frac{(100-m)\,s_i\,u}{(100-s_i)\,m}\right]^{0.1}\left(d_h f\right)^{0.3}$	0.192	0.192
Handling of piles	$E=k_c\left[k_p\,(.0016)\left(\frac{u}{2.2}\right)^{1.3}\right]\left(\frac{2}{m}\right)^{1/1.4}$	4.33	1.36
Ore loading	$E=\left[\left\{\frac{(100-m)}{m}\right\}^{0.1}\left\{\frac{s_i}{(100-s_i)}\right\}^{0.3} h_d{}^{0.2}\left\{\frac{u}{(0.2+1.05u)}\right\}\left\{\frac{x_f l}{(15.4+0.87x_f l)}\right\}\right]k_c$	1.523	0.7
Overburden loading	$E=\left[0.018 f_i\left\{\frac{(100-m)}{m}\right\}^{1.4}\left\{\frac{s_i}{(100-s_i)}\right\}^{0.4}\left(uh_d x_f l\right)^{0.1}\right]$	2.11	0.03
Unloading	$E=\left[1.76 h_d{}^{1/2}\left\{\frac{(100-m)}{m}\right\}^{0.2}\left\{\frac{s_i}{(100-s_i)}\right\}^{2} u^{0.8}\left(c_d y_f\right)^{0.1}\right]k_c$	0.94	0.08
Hauling (per meter)	$E=\left[\left\{\frac{(100-m)}{m}\right\}^{0.8}\left\{\frac{s_i}{(100-s_i)}\right\}^{0.1} u^{0.3}\left\{2663+0.1\left(v_s+f\,c_d\right)\right\}10^{-6}\right]V_t\,k_c$	8.9	0.0117
Open pit Escape	$E=\left[2.4\left\{\frac{(100-m)}{m}\right\}^{0.8}\left\{\frac{a_m . s_i}{(100-s_i)}\right\}^{0.1}\left\{\frac{u}{(4+66u)}\right\}10^{-4}\right]P_r\,f_i$	3.2	0.4
Crushing	$E=P_r . k_c$	0.524	0.06
Wind erosion	$E=\left\{1.9 k_c f_i\left(\frac{s_i}{1.5}\right)365\left[\left(365-d_r\right)\frac{1}{235}\right]\left(\frac{pt}{15}\right)\right\}a$	0.078	0.019

Note: parameters, units and symbols used are: E= emission rate (g/s); P_r= metal production (Mt/year); m = moisture content (%); s_i= silt content (%); u= wind speed (m/s); f= frequency (holes/day); d_h= hole diameter (mm); h_d= drop height of a loader (m); l= size of loader (m^3); v_s= average vehicle speed (m/s); a_m= mining area (km^2); c_d= capacity of dumpers/unloader (ton); y_f= frequency of unloading (no./h); x_f= frequency of loading (no./h); k_c= emission coefficient (PM_{10} fraction: 0.4; $PM_{2.5}$ fraction: 0.1); d_r= number of days with at least precipitation of 0.254 mm per year; pt=percentage of time that wind speed is greater than 5.4 m/s; kp= particle size multiplier (dimensionless); f_i= PM_{10} fraction: 0.35; $PM_{2.5}$ fraction: 0.11; Vt= total distance covered by vehicle, t= time or duration. The moisture content values are obtained from NOAA website Soil moisture: (http://www.cpc.noaa.gov/soilmst/leaky_glb.htm).

5.3 Results

5.3.1 Distribution of pollutants among mining activities

PM_{10} and $PM_{2.5}$ both particulate matters were produced from the various mining activities. As shown in Figure 5.4, handling and storage of piles at the mining site during the operational phase, contributed most of the PM_{10} (22 $\mu g/m^3$) in the air among all the point and fugitive sources. $PM_{2.5}$ (12.2 $\mu g/m^3$) was also produced more during the handling of piles as compared to the other mining source. Primary crushing emission data was used for this study and responsible for generating 15 ($\mu g/m^3$) PM_{10} and 11.3 ($\mu g/m^3$) $PM_{2.5}$. Wind erosion is drifting dispersion of the dust particulates and contributing 9.8 % of the total PM_{10} and 10.9 % of total $PM_{2.5}$ in the air. Wind erosion and atmospheric particulate emissions are influenced by a variety of factors including atmospheric conditions, usage of land, vegetation cover, and other geographical characteristics. The contribution because of wind erosion varies from site to site. Hauling is not showing as much influence in dispersion as expected because of the values mentioned here are in per meters. If total haul distance and a total number of trips during the mining is considered, this factor would be likely potential to produce more emissions. Thus, as far as activities are concerned, the maximum concentration of particulate matters in ambient air was due to the handling of the piles, waste loading/unloading, and crushing.

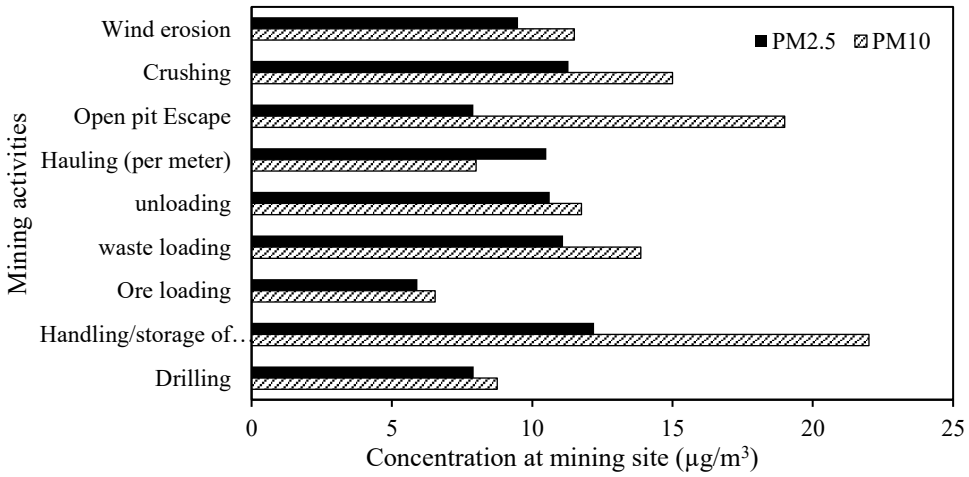

Figure 5.4 PM_{10} and $PM_{2.5}$ predicted concentration distribution among different mining activities

5.3.2 Predicted concentration of heavy metals at various receptor

Using MADM model, six heavy metals (As, Pb, Hg, Cd, Zn, Cr) concentrations have been predicted at certain receptor locations. The intervals of the distance have been selected such that the identified concentrations were readily evaluated with the observed values of the monitoring station located within the same domain. Figure 5.5 described the exponential fall of all the predicted values with the distance from the source. However, the quantity of the pollutant's concentration produced at the mining site is one of the criteria that how far the pollutant could travel. Based on annual average concentration, Zn was quantitatively more as compared to other pollutants, so it would go hardly beyond 20 km but in minimal quantity. Whereas, others did not travel beyond 10 km due to its less emission at the source. All the heavy metals generated at the mining site met the air quality standards of Level A. (Level A is the maximum desirable level; Pb and Zn= 1 μg/m^3, Cd and Cr = 0.05 μg/m^3, As= 0.1 μg/m^3 (Soriano et al., 2012)).

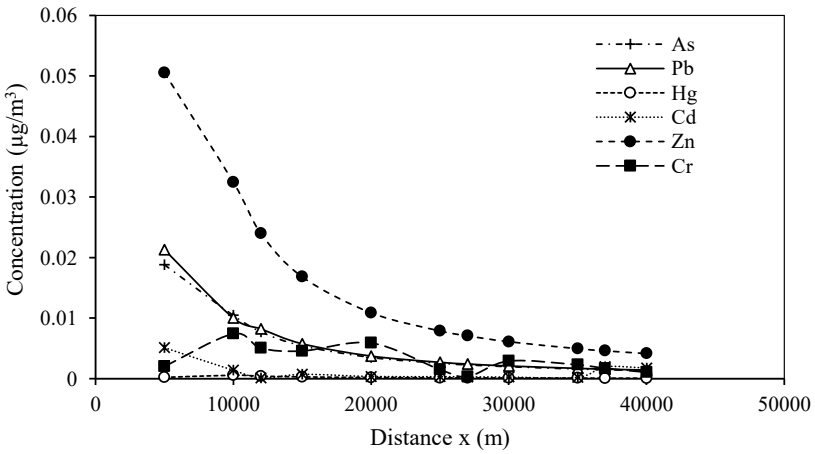

Figure 5.5 Heavy metal concentration at downwind distances (average annual)

5.3.3 Evaluation of model with the field observation

The MADM simulation was examined and evaluated by comparing the modeling results with the observations values of monitoring stations (M-1, M-2, and M-3) under

the same environmental conditions using the 24hrs (daily data) from the March 2010 to December 2014. The modeling results for $PM_{2.5}$, PM_{10}, and NO_2 were considered for regression analysis. Since the monitoring values for heavy metals were not available, they were not included for the model evaluation. Figure 5.6 (a, b, c, d, e, f, g) illustrates the comparison of all the observed and modeled values at the monitoring station M-1, M-2 and M-3. The coefficient of determination (R^2) was 0.71 for NO_2, 0.96 for $PM_{2.5}$ and PM_{10} it was 0.819 at M-1. Similarly, at M-2, NO_2 and $PM_{2.5}$ show R^2 values of 0.89 and 0.783 respectively. Moreover, at M-3, $PM_{2.5}$ and PM_{10} show R^2 value 0.725, and 0.71 respectively. This correlation value indicates that model can generate predicted results using selected input parameter at other sampling stations.

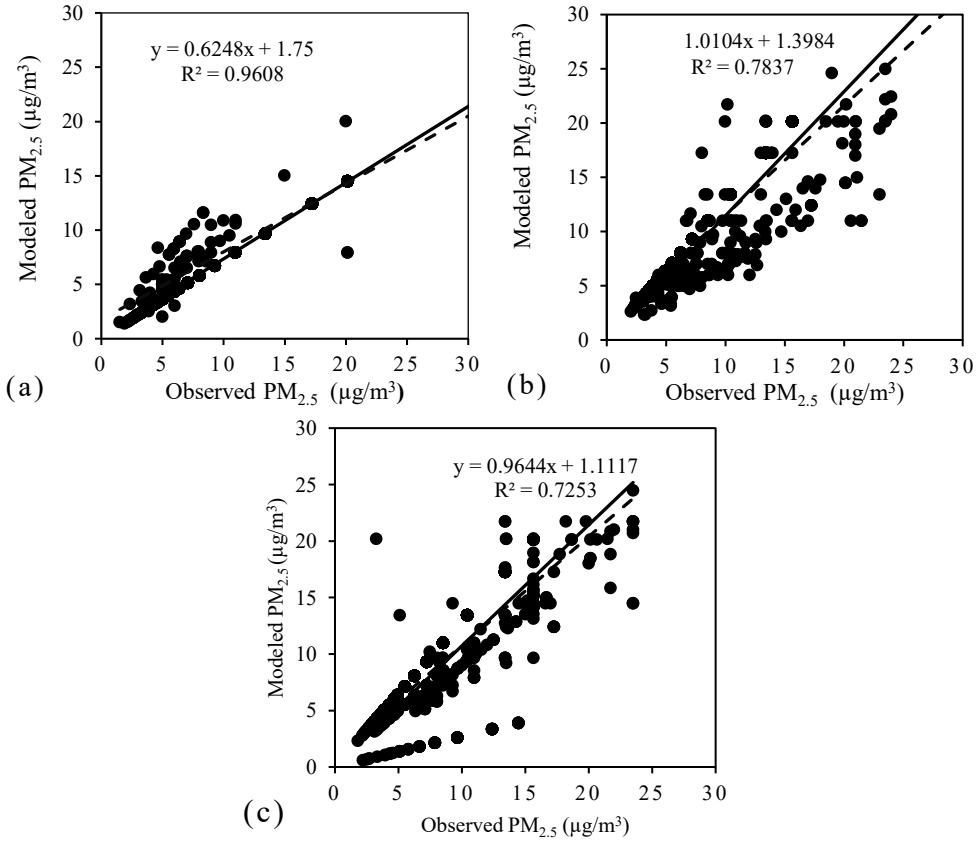

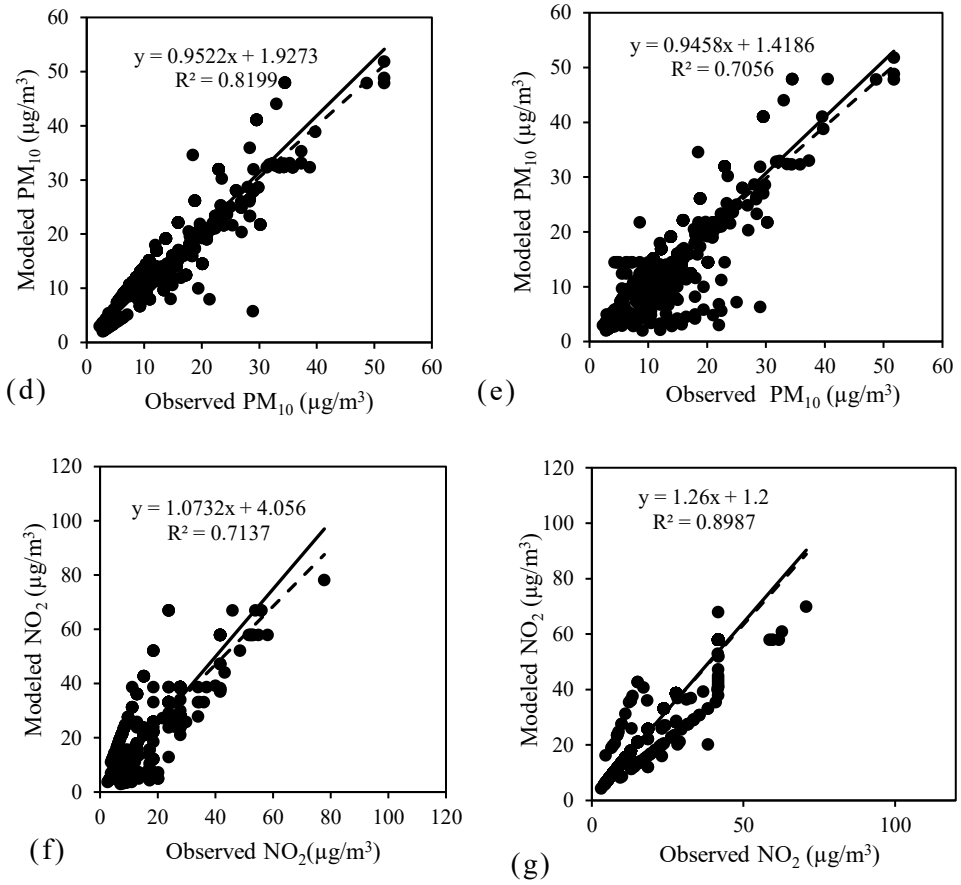

Figure 5.6 Correlation between modeling and monitoring values (a) $PM_{2.5}$ at M-1; (b) $PM_{2.5}$ at M-2; (c) $PM_{2.5}$ at M-3; (d) PM_{10} at M-1; (e) PM_{10} at M-3; (f) NO_2 at M-1; (g) NO_2 at M-2

Figure 5.7 (a, b, c, d) shows the contour map representing latitude values at y-axis and the longitudinal interval at the x-axis. $PM_{2.5}$, PM_{10}, TSP, and NO_2 predicted concentrations are shown over the sitemap to analyze the plume profile. Maximum values for pollutants were observed only at the source. The predicted concentration gradually reduced as traveled as a plume away from the source.

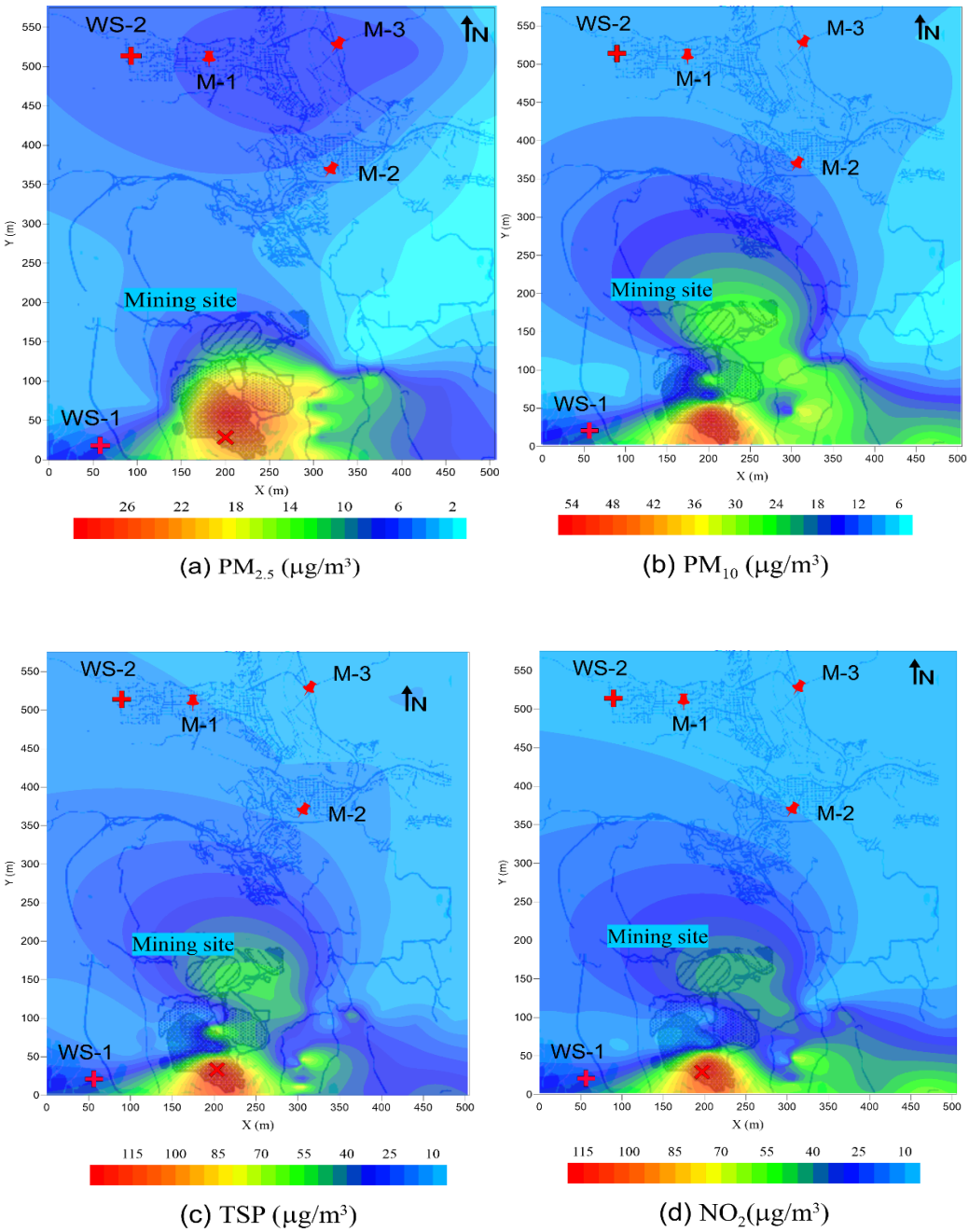

Figure 5.7 Contour mapping of air quality pollutant concentrations for mine B based on 24 (hrs) average from 2010 to 2014 for (a) $PM_{2.5}$; (b) PM_{10}; (c) TSP; (d) NO_2

5.3.4 Comparison between MADM and CALPUFF

Figure 5. 8 (a, b, c, d) represents the modeling predicted concentrations under various stability conditions and their comparison with CALPUFF. For PM_{10}, there is a very slight difference in the modeled values of both the models for stable, unstable and neutral conditions. Whereas, for $PM_{2.5}$ and NO_2 the difference is prominent for stable and neutral conditions. The difference in values is among 25^{th} percentile modeling values for stable conditions (3.1 $\mu g/m^3$) and 75^{th} percentile for unstable condition (2 $\mu g/m^3$) using CALPUFF. Similarly, for TSP, there is a slight difference noticed for the stable state and neutral condition, but 75^{th} percentile values of unstable condition showing more difference (4.2 $\mu g/m^3$) between the two models. Thus, all the predicted concentrations using CALPUFF are slightly higher than MADM except for NO_2 at neutral condition (difference of 5.6 $\mu g/m^3$ among 75^{th} percentile modeling values). However, all the values met the air quality ambient standard except $PM_{2.5}$ (for environmental guidelines see Table 8.3 in chapter 8). Figure 5.8 depicts that during stable conditions, both models show that maximum values and 75^{th} percentile values are higher than the air quality standards. Both models capture the maximum predicted concentration over the defined period.

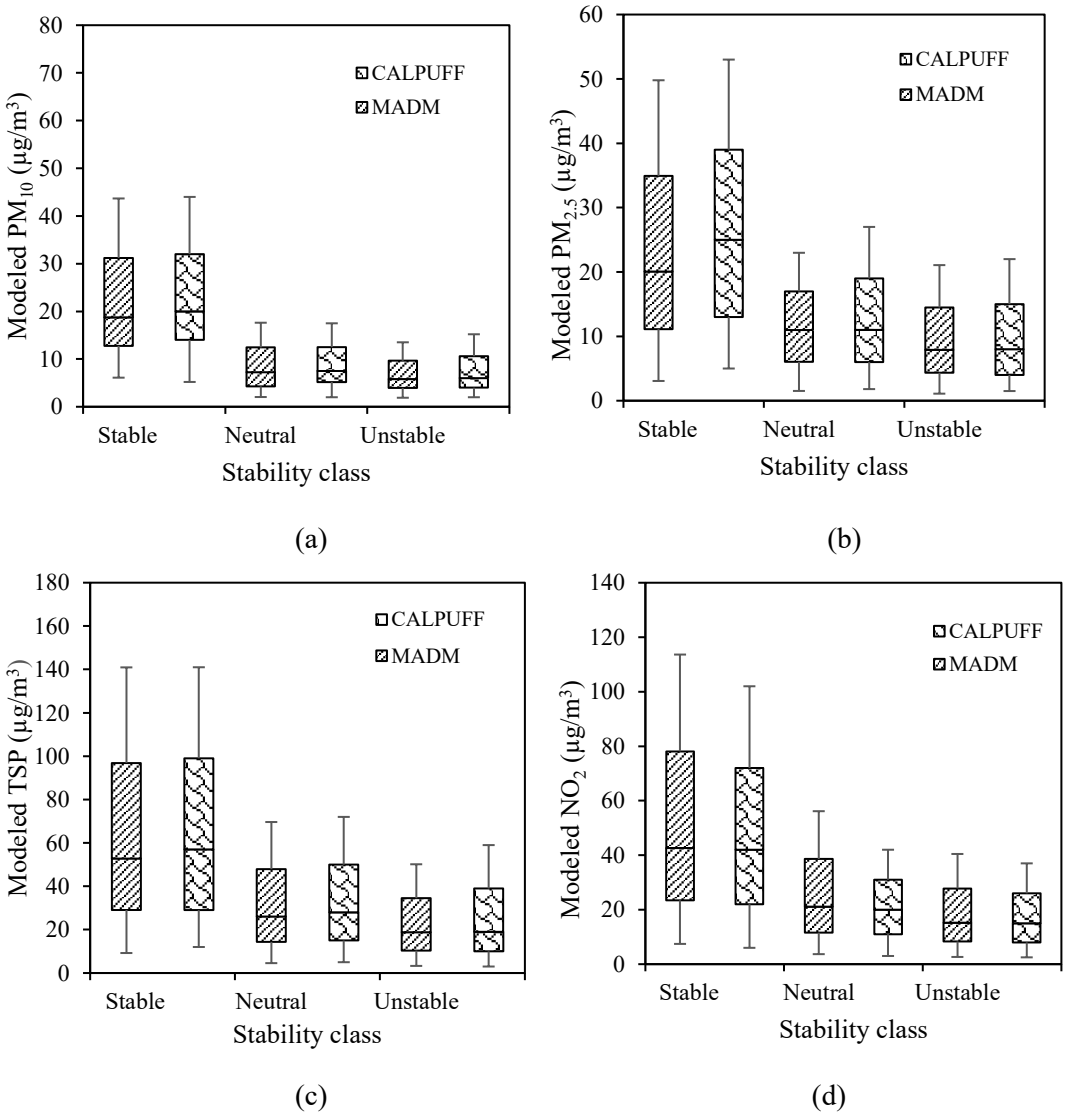

Figure 5.8 Modeling predicted concentrations under various stability conditions and comparison with CALPUFF (a) PM_{10}; (b) $PM_{2.5}$; (c)TSP; (d) NO_2

The lines divided the group is called quartiles. The middle line is called median of the data, which also divides the box into two parts. The middle box is known as inter-quartiles, showing 50% of the data. The upper line of the box is known as upper-quartiles, which represents 75th percentile of the data. The lower quartiles represent 25th percentile of the data. The minimum and maximum ranges outside the 50 % of the box is called as lower and upper whiskers.

The deposition flux is analyzed for dust considering PM coarse (which included the range ≤ 10 µm). The calculated dry deposition velocity of PM coarse is 4.67 cm/s. Both CALPUFF and MADM dust fall deposition flux is compared for different months of the year 2012-2014 (based on 24hr average data). Figure 5.9 shows the maximum deposition flux is obtained in February followed by March. The second highest

deposition flux is captured in the fall season (September). Whereas, soon after the March, there is very minimum deposition determined in April. The reason behind this is might be the neutral conditions with mixing height from 810 to 850 m during afternoon and evening in the spring season. There is very minimum deposition predicted in July and April. Overall CALPUFF is showing more deposition flux as compared to MADM for February, March, and June. However, the average percentage of dry days was 71 % and wet days were 29 % of the days per year for this site. The reason behind this is that the study area lies in the semi-arid zone with 13% moderate precipitation rate annually.

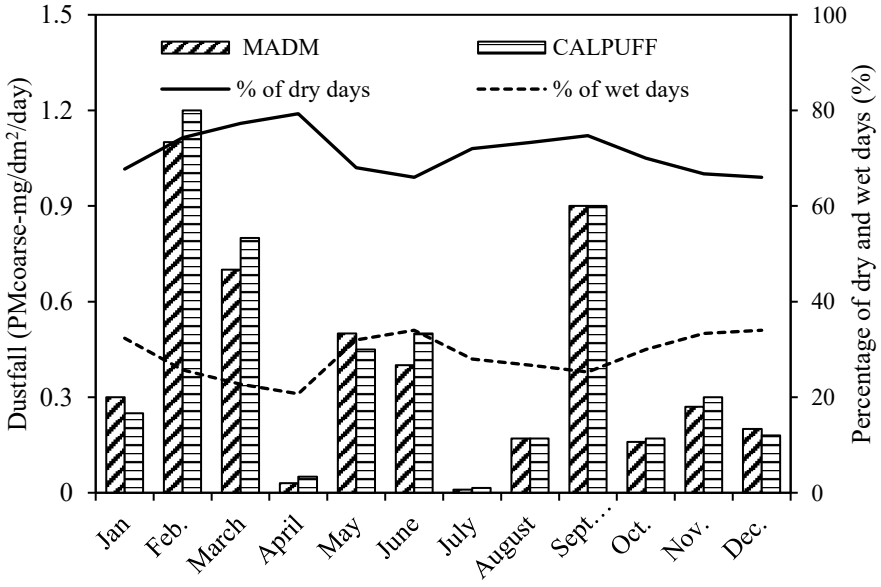

Figure 5.9 Dust fall deposition flux modeling comparison with CALPUFF

To assure that the results provided by MADM are reasonable, the performance of MADM model was also statistically evaluated against the CALPUFF model. Both models were run at the same boundary and atmospheric conditions to study the air quality and predicted the concentration of $PM_{2.5}$, PM_{10}, and NO_2 at the downwind monitoring station M-1. The presented results were obtained from the operational data (2012 to 2014) of the selected mine. Table 5.3 point out that a satisfactory agreement was achieved for the MADM method by analyzing the NMSE and FB values near zero, and COR values represented results around 1 for all the three pollutants. Whereas,

CALPUFF model showing the FB value, (1.49) indicated the overprediction of the PM_{10}. This result is comparable with Fishwick and Scorgie (2011) study which concluded that CALPUFF model results tended to over predict the PM_{10} values when applied to the large surface mine. However, it is noticed that for $PM_{2.5}$ and PM_{10}, MADM model simulates better in contrast to NO_2 modeling. To encapsulate, overall MADM produced statistically agreeable results in the case of all the three target pollutants.

Table 5.3 Statistical evaluation and comparison between MADM and CALPUFF

Pollutants	Models	NMSE	COR	FB
Indicator for good performance*		≅ zero	≅ one	≅ zero
$PM_{2.5}$	MADM	0.13	0.79	0.01
	CALPUFF	0.15	0.78	0.02
PM_{10}	MADM	0.22	0.82	0.31
	CALPUFF	0.15	0.84	1.49
NO_x	MADM	0.26	0.71	0.52
	CALPUFF	0.44	0.88	0.08

*(Moreira et al., 2010; Essa et al., 2014); Note: - sign means over estimation

5.4 Discussion

The broadness of the analysis scope makes it almost impossible to avoid dealing with persistent uncertainties with a wide range of input sources, meteorological factors, terrain effect, boundary conditions, data for verification and missing data. The probabilistic approach has been used to analyze the emission inputs (g/s) and meteorological data (wind speed). MADM can include surface conditions such as the surface roughness length (Z_o). Surface roughness affects the vertical profiles of wind and temperature and the dispersion rates in the surface layer and is a significant variable in assessing dispersion at receptor sites. The values of Z_o vary for land cover types such as green forest land (1.3m), urban build up and mixed forest (1m), and barren land (0.3m) in summer (Barnes et al., 2014). These values can be seasonally varied depending on other factors such as snow cover (0.2m). The value of surface roughness is normally distributed while considering the surface roughness distribution range (0.0001-1.3m) (Manomaiphiboon and Russell, 2004). However, MADM model can manually allow entering terrain elevation data from topographical maps or digital maps

(Canadian Digital Elevation Data (CDED, 2017)). Whereas, CALPUFF can derive terrain data directly from GEO. DAT files. The resolution selected for this case study is 250 m (Tartakovsky et al., 2013).

MADM with site-specific information on emission release and meteorological wind data predicted concentrations at the receptor level. The monitoring stations in the residential area are considered as an approximation of "background" concentration to improve the model performance by analyzing simulation ratio observed concentration (see Table 5.4). Values greater than unity indicate over prediction, while values less than unity indicate under prediction. Thus, if the percentage of underprediction is less then the percentage of overprediction, there is no need to add the background concentration and vice versa. For instance, $PM_{2.5}$ at M-1 shows 11% underprediction predicted concentrations as compared to 4 % overprediction by considering background concentrations. This analysis suggests that adding the background $PM_{2.5}$ concentration (+2.7μg/m^3) helps to improve the performance and to increase R^2 from 0.90 to 0.96 statistically. Similarly, at other monitoring stations, M-2 and M-3 indicate 3 % and 1.7% underprediction performance respectively. Whereas, overpredicts the results by 16 % and 21% respectively after considering background concentrations (4.3 μg/m^3 at M-2 and 5.3 μg/m^3 at M-3). This result depicts that there is no need to add the background concentrations around and at M-2 and M-3. For PM_{10} and NO_2, the model performance at M-3 and M-2 show improvement in the percentage of underprediction by 21-22% by considering background concentrations (9.6 and 10.8 μg/m^3 respectively). Whereas, at M-1 for both the pollutant (PM_{10} and NO_2) there is no need to add any background values. Consequently, this analysis suggests that the limitations of the MADM model to calculate dispersion away from the mining site underestimates of concentrations in certain areas, where many sources with a high emission rate are in the vicinity. Moreover, using a constant value for the "background" concentrations does not seem to be accurate enough, and more background detail is required to estimate the emission loads for each receptor.

Table 5.4 Model performance with and without background concentration

Pollutants	Stations	MADM[1] (μg/m^3)		Monitoring[2] value	Performance (Modeled/Observed)	
(μg/m^3)	ID	without C_B	with C_B	(μg/m^3)	without C_B	with C_B
$PM_{2.5}$	M-1	15.0	17.7	17	0.88	1.04
	M-2	20.7	25	21.5	0.96	1.16
	M-3	22.1	27.4	22.5	0.98	1.21
PM_{10}	M-1	48.4	58	45	1.07	1.28
	M-2	30.7	41.5	49.1	0.62	0.84
NO_2	M-1	54.8	65.6	55	0.99	1.19
	M-2	30.7	41.5	50	0.61	0.83

Note: C_B is background concentrations

(for more information see supplementary information Table A-2); 1,2 average predicted concentration-24 hr average;

The estimated deposition velocity for dust is 4.67 cm/s (included range of particles ≤ 10 μm) which is calculated based on the settling velocity (W), aerodynamic resistance (r_a) and Brownian transport or quasi-laminar layer resistance (r_d) (Asif et al., 2018b). Whereas, deposition velocity of $PM_{2.5}$ (V_d= 1.67 cm/s) is determined separately based on the fraction of size ranges. The predicted concentration of pollutant based on these velocities are compared with the literature reported velocities for $PM_{2.5}$ and PM_{10}. Figure 5.10 represents the deposition flux at different distances (m) based on different V_d. For PM (coarse: $PM_{2.5}$-PM_{10}) two velocities were considered including modeling velocity (4.67 cm/s) and V_d literature value by Zhu et al., (2016) (normal period deposition velocity: 4.88 cm/s). Figure 5.10 depicts that modeling velocity and literature reported velocity are close to each other. Similarly, for $PM_{2.5}$, two V_d values were considered, and the results confirm that the modeling value (1.56 cm/s) based on settling velocity is close to calculated V_d of 1.50 cm/s by Zhu et al., (2016). Thus, the results suggest that V_d which is calculated for PM is larger than the $PM_{2.5}$.

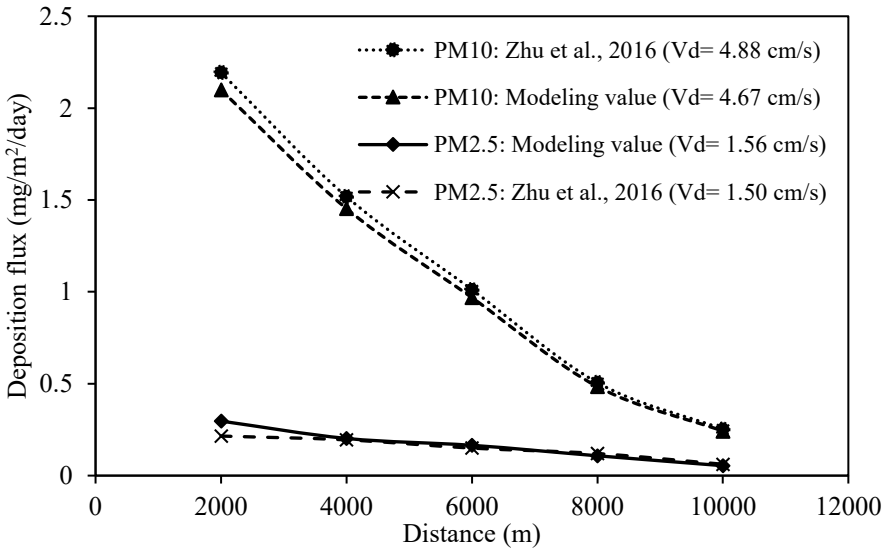

Figure 5.10 Comparison of dry deposition velocities for PM_{10} and $PM_{2.5}$ with the literature value

The use of MADM is an advantage when used for air quality assessment in a mining industry because it avoids incurring in long computation time and the approach used in this model contributes towards the importance of deposition phenomena while using a simple algorithm. It is important to keep in mind that the end users of MADM might not certainly be high-skilled computer users and could be unaware of air quality modeling. Therefore, MADM would be further improved using simple terminology and next chapters 7-8, air pollution management is discussed based on pollutant concentrations. In this study, regression analysis and statistical model performance are evaluated with field data. It is recommended to calibrate this model by doing uncertainty analysis for all the parameters. For future work, it is recommended to incorporate downwash algorithm in the model by extending the features of the model to engulf the wind circulation effect around buildings in the residential area. Moreover, the model can be integrated with CFD model to get further insight of the air dispersion in the mining pit area.

5.5 Summary

The developed MADM has been examined through exploring its application to a mining site in Canada. The model provides values as the predicted concentrations of PM_{10}, $PM_{2.5}$, TSP, NO_2 and six heavy metals (As, Pb, Hg, Cd, Zn, Cr) at various receptor locations. The model shows that neutral stability conditions are dominant for the study site. The maximum mixing height is achieved (1280 m) during the evening of summer, and minimum mixing height (380 m) is attained during the evening of winter. The dust fall (PM coarse) deposition flux is maximum during February and March with the deposition velocity of 4.67 cm/s. The results were evaluated with the monitoring field values, revealing a good agreement for the target air pollutants with R-squared ranging from 0.72 to 0.96 for $PM_{2.5}$; 0.71 to 0.82 for PM_{10} and from 0.71 to 0.89 for NO_2. The analyses illustrate that presented algorithm in this model can be used to assess air quality for the mining site in a systematic way. The comparison of MADM and CALPUFF modeling values were made for four different pollutants ($PM_{2.5}$, PM_{10}, TSP, and NO_2) under three different atmospheric stability classes (stable, neutral and unstable). Further, MADM results were statistically tested against CALPUFF for the air pollutants, and model performance is found satisfactory.

CHAPTER 6 DETERMINATION OF ATMOSPHERIC STABILITY IN THE MINING REGION

6.1 A Case Study of $PM_{2.5}$ in the Open-Pit Mining Area, Utah, USA

The source of the emission was taken as smelter and refinery of a large open pit copper mine "C" in Utah state, USA, with 233.63 tons/year of $PM_{2.5}$ contribution into the air (Utah, 2017). The study area features as semi-arid to sub-humid zone. The temperatures are extreme having cold temperatures in winter because of its elevation, and a very hot summer (The same case study is used in Chapter 8 and 9).

6.2 Data Collection and Preparation

The hourly $PM_{2.5}$ emission data were collected for the year 2015 from the copper mine. Meteorological data were obtained from the National Oceanic and Atmospheric Administration (NOAA) for the nearest monitoring station 40^0 42' 30.96" latitude and -112^0 5' 40.92" longitude. The weather data included cloud cover, ceiling height of clouds, wind speed at 10m, direction, temperature, surface heat flux, rainfall and humidity. Thus, daily data was prepared for the year 2015 by taking an average of hourly data for each month. The data were separated for day and night and seasonal basis. The average temperature of the area is 12.7 ^{0}C. The average monthly input data is presented in Table 6.1, showing average temperature, wind speed, dew point, relative humidity, actual station pressure, and surface heat flux. However, a virtual temperature is required while determining Monin-Obukhov length. Moreover, the mixing ratio was calculated using online tool for this site (NOAA, 2017). The observational $PM_{2.5}$ hourly data were collected for this station from Utah air monitoring network (Utah, 2017) to validate the results obtained through the mining-zone air dispersion model (MADM).

Table 6.1 Average input data for ambient atmospheric condition at a copper mining site

Months	Temperature	Dew point	Actual station pressure	Saturated mixing ratio[1]	actual mixing ratio[1]	Relative humidity	Virtual temperature[2]	Wind speed	Surface heat flux[3]
units	ºC	C	Hg	g/kg	g/kg	%	C	m/s	kWh/m^2/d
Jan	1.2	-12.1	25.79	4.8	1.72	38	1.56	2.01	2.7
Feb	6.6	-1.6	25.78	7.02	3.88	55.2	7.26	3.2	4
March	9.8	-1.11	25.82	8.75	4.03	46.09	10.39	3.3	5.6
April	11.3	-4.44	25.66	9.7	3.16	32.54	11.84	4.11	7.3
May	15.5	4.4	25.63	12.86	6.07	47.19	16.57	3.62	8.8
June	25.2	6.11	25.66	23.8	7.09	29.67	26.49	3.39	10
July	25.1	12.2	25.72	23.74	10.32	43.47	26.98	3.71	10.1
August	25.3	22.2	25.73	23.9	21.11	82.42	29.14	3.69	9.2
Sept.	21.5	19.44	25.71	18.9	16.54	87.49	24.47	4.11	7.6
Oct.	15.8	5.5	25.76	13.08	6.53	49.93	16.95	3.2	5.5
Nov.	4.3	1.11	25.75	5.99	4.76	79.39	5.11	3.79	3.2
Dec.	-0.44	-10	25.72	4.25	2.05	48.21	-0.1	3.21	2.3

[1]Calculated using NOAA calculator, available at https://www.weather.gov/epz/wxcalc_mixingratio
[2]Calculated using $T_{Virtual} = (1+0.61\omega)Ta$; where mixing ratio ($\omega$) and ambient temperature (Ta)
[3] Data collected form NOAA

6.3 Selection of Meteorological Factors

The meteorological parameters were determined based on the stability atmospheric conditions (For more detail see Chapter 3, section 3.4). The crucial factors used during the research are PBL height, mixing height, roughness length, frictional velocity, and Monin-Obukhov length. These factors determined the boundary conditions for the MADM. Moreover, selection of empirical equation depends on the three primary conditions which are stable, unstable and neutral. Mixing height is the fundamental factor that is used to determine the volume available of pollutant dispersion due to mechanical and convective turbulence. Past studies observed that rapid changes of mixing height occurred after the sunset and at sunrise (Baklanov et al., 2005). The dispersion of pollutants could be highly sensitive to the changes in this height. Moreover, higher the mixing height, the higher is the volume available for the dispersion of the pollutant. The surface roughness is significant to consider the development of models which are ranging from microscale to macroscale. The topography of an area especially category of terrain, humanmade and natural obstacles are described by its roughness length. Also, by increasing the height of roughness elements will increase the Reynolds stresses for the wind flow and radically alter the

vertical wind shear (Martano, 2000). These alterations to the average flow affect diffusivities and the average wind speed. Though in this study, roughness length is used to calculate the frictional velocity. In convective boundary layer (CBL) the calculations of frictional velocity and Monin-Obukhov length depends on the reference measurement height for the wind in the surface layer (*S*). Typically, a 10-m height for a reference is chosen. However, depending upon the roughness length, the accepting range for wind speed data is also changed. Above 50-m, the wind measurements are likely to be above the surface layer. Therefore, an upper limit of 100-m could be imposed for reference wind speed and temperature measurements for computing the friction velocity and Monin-Obukhov length. If cloud cover measurement is not available, Richardson number method can be applied to stable conditions by using temperature gradient technique or lapse rate (In this study, insolation and cloud cover method is used). The calculations of meteorological parameters, and atmospheric stability shares same module of user interface under mining-zone air dispersion model (see Figure 3.12).

6.4 Results

6.4.1 Atmospheric stability pattern

By implementing PTM method, the results reveal that the stable condition (class F) appear most of the time of the year based on the percentage relative frequency distribution. Whereas, unstable (class B) is the second dominant condition (21%) followed by slightly stable (16%) and slightly unstable (14%) patterns as shown in Figure 6.1.

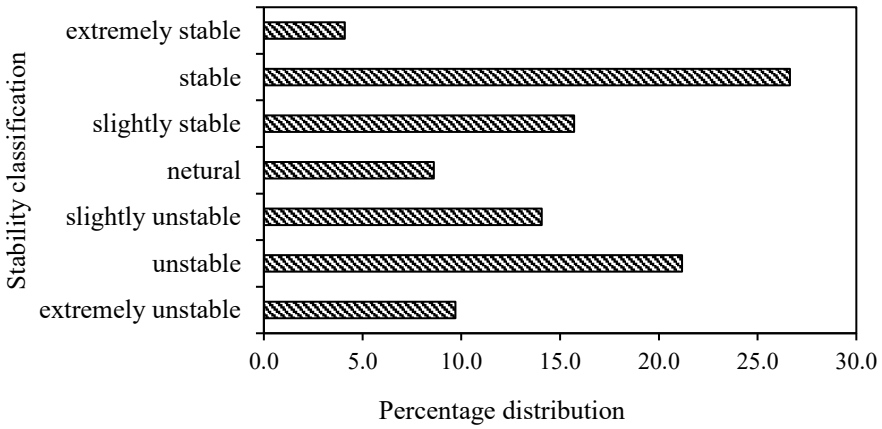

Figure 6.1 Percentage distribution of stability classification

Moreover, it is equally important to find the diurnal pattern of the area to observe the variation of the atmospheric stability concerning day and night. Figure 6.2 illustrates the distribution of data between day and night time showing that unstable is dominant (27%) during the day which approves the presence of solar radiations. Thus, the clear sky at night is represented with stability condition and with the probability of inversion occurrence. It is also noticed that during daytime only classes (A to C) of instability are present which never appeared at night. Similarly, none of the stability classes are occurred (E to G) during the daytime. Though, neutral class (D) happened during both the time periods. Regarding NRI, value from 0 to -2 indices is the only representatives for night time.

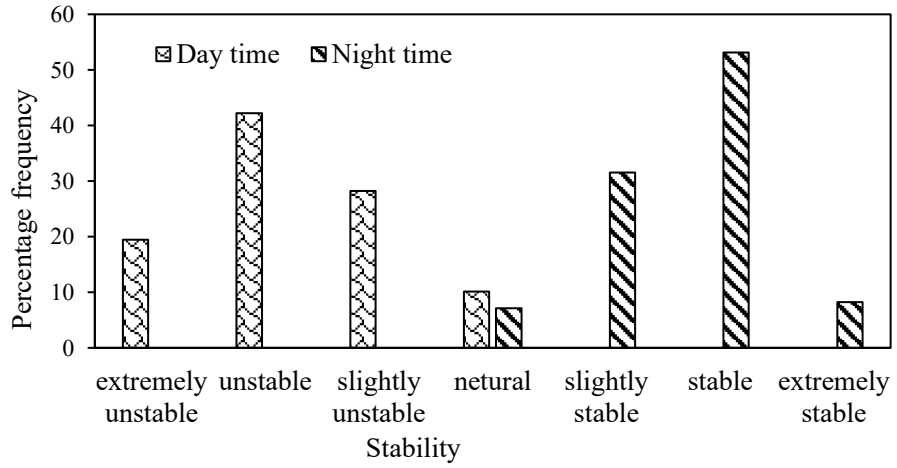

Figure 6.2 Diurnal stability pattern analysis

6.4.2 Seasonal variation

Four different seasons, winter (December to February), spring (March to May), summer (June to August) and fall (September to November), were compared to determine the atmospheric stability along with the diurnal pattern. As depicted in Table 6.2, winter is the most stable (class F) at night with 54.9 % frequency occurrence followed by spring (51%), summer (47.2%) and fall (42.8%). Moreover, extremely stable condition (class G) is also dominant in winter (19.8%) as compared to the other seasons (fall= 8.8%, spring= 3.2% and summer = 0.9%). It is noteworthy that during the daytime, winter is showing the extremely unstable conditions with 51.2 % of frequency. Whereas, spring is dominant for moderately unstable atmosphere (class B= 61.9%) followed by fall (52.7%). Summer is having slightly unstable conditions (50%) during the daytime. Also, summer season has the most neutral condition (23.9%) during the day as compared to all other seasons. Hence, neutral condition shares both day and night time of each season.

Table 6.2 Percentage frequency distribution for seasonal and monthly stability pattern

Atmospheric stability	Class	Winter (Dec-Feb.)		Summer (June-Aug.)		Fall (Sep.- Nov.)		Spring (Mar.-May)	
		Day	Night	Day	Night	Day	Night	Day	Night
Extremely unstable	A	51.2	0	0	0	20.8	0	0	0
Unstable	B	34.5	0	26.1	0	52.7	0	61.9	0
Slightly unstable	C	13.2	0	50	0	17.6	0	31.5	0
Neutral	D	1.1	6.6	23.9	7.8	8.8	7.7	6.5	6.5
Slightly stable	E	0	18.7	0	44.1	0	40.6	0	39.3
Stable	F	0	54.9	0	47.2	0	42.8	0	51
Extremely stable	G	0	19.8	0	0.9	0	8.8	0	3.2

6.4.3 Effect of atmospheric stability on $PM_{2.5}$

The ground-level $PM_{2.5}$ concentration based on monthly variations and diurnal stability patterns are presented in Figure 6.3. As discussed in previous sections, because of stable conditions at night time, $PM_{2.5}$ concentration is higher at night and may accumulate most of the time. In the aspect of seasons, the month of January shows the maximum concentration of $PM_{2.5}$ (28 $\mu g/m^3$). However, this concentration starts

decreasing when colder months shift towards warmer months of the year. Whereas, during the day, $PM_{2.5}$ concentration is relatively high for June (15.8 $\mu g/m^3$) as compared to the other months. This is explained by the fact that insolation is maximum for this warm month of the summer season with less strong winds. Consequently, there are more chances of air pollution due to a high concentration of $PM_{2.5}$ in the cold month at night and during the high insolation with low wind speed during the day.

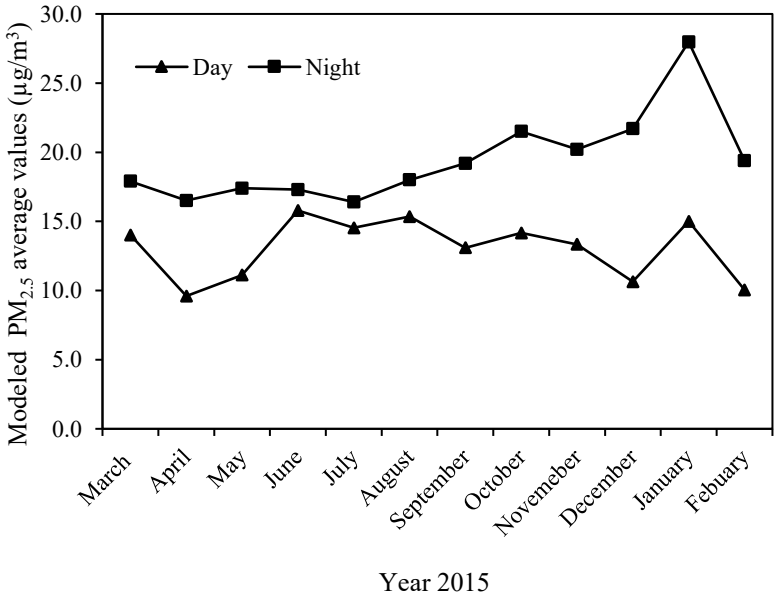

Figure 6.3 $PM_{2.5}$ concentration based on monthly variation and diurnal pattern

To address the question that what would be the effect on $PM_{2.5}$ concentration under different stability scenario? Further investigation was done by predicting the daily concentration of $PM_{2.5}$ for seven (A to G) classes of atmospheric stability. Figure 6.4 shows the statistical distribution of modeled $PM_{2.5}$ concentration for each class. The daily average modeling concentrations of $PM_{2.5}$ were obtained by simulating air dispersion model for 360 samples. The reference line shows national ambient air quality standard (NAAQS) for 24 hr based $PM_{2.5}$ concentration which is 35 ($\mu g/m^3$). The samples exceeded the standard value under the conditions of slightly stable (class E) and extremely stable (class G). Whereas, comparison of spatial variability shows that rest of the spread of $PM_{2.5}$ concentration met the air quality standard. The least $PM_{2.5}$ concentration simulated values were generated under the extremely unstable (class A)

and unstable (class B) scenario. The spread of concentration for neutral (class D) and stable (class F) conditions have almost similar lower quartile (25th percentile of data) but different median (50th percentile) and upper/lower whisker (75th percentile) values. There is a significant difference in $PM_{2.5}$ concentration for each classification including 25th, 50th and 75th percentile of spread data. Thus, long-term stability can lead to air pollution.

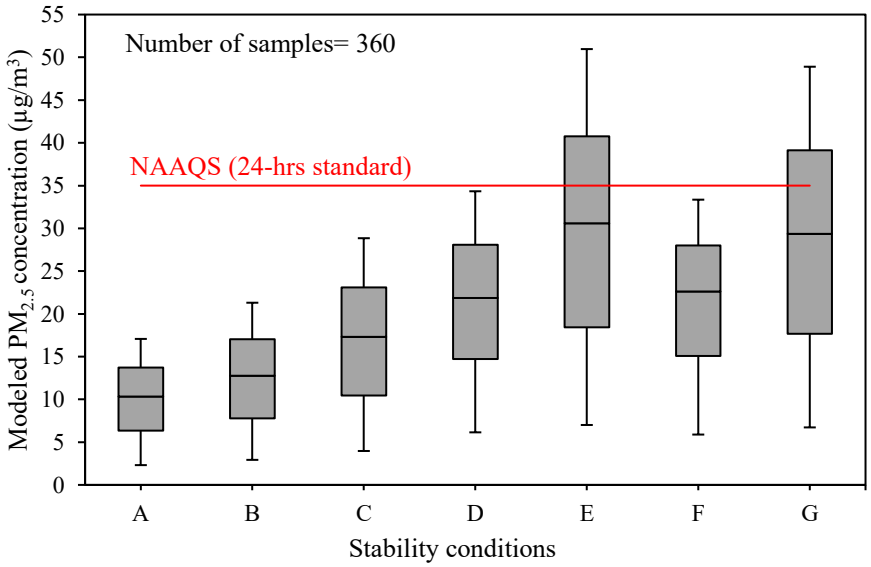

Figure 6.4 Modeling $PM_{2.5}$ concentrations for various stability conditions and comparison with the air quality standard value

The lines divided the group is called quartiles. The middle line is called median of the data, which also divides the box into two parts. The middle box is known as inter-quartiles, showing median of the data. The upper line of the box is known as upper-quartiles, which represents 75th percentile of the data. The lower quartiles represent 25th percentile of the data. The minimum and maximum ranges outside the 50 % of the box is called as lower and upper whiskers.

6.4.4 Effect of mixing height on $PM_{2.5}$

Mixing height is the depth of vertical mixing or dispersion of pollutants above the ground level (EPA, 2004). It is characterized by the frictional velocity, wind profile, temperature gradient, roughness and Monin-Obukhov length. It is one of the leading meteorological factors which vary with the atmospheric stability. Thus, dispersion of the pollutant is dramatically affected as shown in Figure 6.5. In this study, the maximum mixing height of 298 m is achieved during stable conditions. Whereas,

during unstable conditions, it varies from 416 to 1875m. The maximum mixing height was obtained during April (mid of spring) and September (beginning of fall) in both stability conditions. Furthermore, $PM_{2.5}$ concentrations were determined concerning mixing height. Figure 6.5 explains that when mixing height is low, the predicted $PM_{2.5}$ concentration is high. Whereas, when depth is high, minimum values for $PM_{2.5}$ are observed. As stability conditions change their pattern each month and season, mixing height also follows the same pattern. Hence, for each cold month, mixing height is small with a high $PM_{2.5}$ concentration and vice versa. In essence, more extended mixing depth supports the dispersion of pollutants. Otherwise, pollutant gets trapped due to temperature inversion during the occurrence of stable condition as in physical reality (Wang et al., 2015).

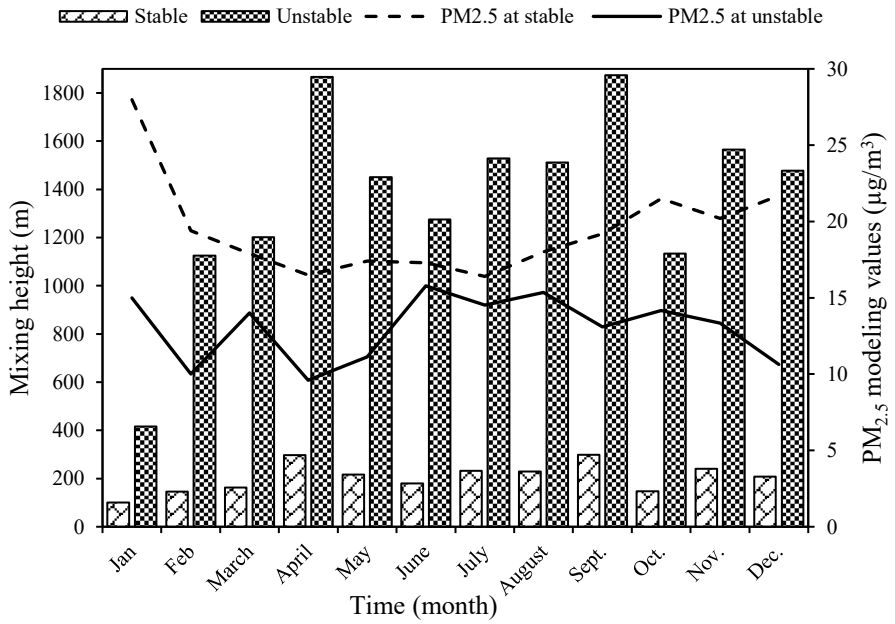

Figure 6.5 Mixing height profile and its relationship with $PM_{2.5}$ based on the stable and unstable condition

6.4.5 Regression analysis

Effect of various meteorological factors on mixing height was also statistically evaluated to understand the correlation of these parameters with the mixing height. The factors selected for regression analysis were wind speed, temperature, rainfall and

surface heat flux. The average wind speed range is from 2.01 to 4.11 m/s at the copper mining site. The elevated pollution level is expected during the low wind speed. However, for this region, calm wind conditions were not observed. Table 6.3 shows a good correlation of wind speed with the mixing height for both stable and unstable conditions. The height of convective boundary layer is changed because of increase and decrease in surface temperature. Thus, it also affects the mixing height. The temperature varies from -0.44ºC in winter to 25ºC in summer. Table 6.3 also illustrates the fair correlation of temperature with mixing height during stable and unstable conditions. These results agree with the study of Roy et al., (2011b) for the coal mine, with R^2 0.44-0.54. Table 6.3 represents a strong correlation of surface heat flux with the mixing height for both the stability conditions. Heat flux not only influenced the mixing height but also proportional to the Monin-Obukhov length (L) (see eq. 3.42). Rainfall was also plotted against the mixing height. This factor is selected because rainfall plays a vital role in the estimation of deposition velocity. Table 6.3 shows a fair correlation between the two parameters. Thus, variations in rainfall every season and year might have led to different correlation. In conclusion, surface heat flux and wind speed have a significant influence on mixing height as compared to temperature and rainfall.

Table 6.3 Correlation of mixing height with various meteorological parameters

Parameters	R^2 for stable condition	R^2 for unstable condition
Wind speed (m/s)	0.707	0.625
Temperature (ºC)	0.563	0.487
Surface heat flux (kwh/m^2/day)	0.804	0.755
Rainfall (inches)	0.487	0.696

Note: For more detail see Appendix Figure A-1

Linear regression analysis between $PM_{2.5}$ modeling values and its monitoring values for the same time duration were obtained as shown in Figure 6.6. The class representation for each season is based on the highest percentage frequency for that time by taking the average of hourly data. It is interesting to note that the modeling results for winter and summer seasons show a good correlation with the monitoring values with 0.82 and 0.80 R^2 respectively. It means that predicted values based on the

stability pattern for these two seasons are close to the actual conditions. Whereas, a good correlation is obtained for fall and spring. The reason behind 0.69 R^2 value for the spring season might be because of high winds which tend to shift the linear dependence (Schmid and Oke, 1990). Hence, it is concluded that in stable condition, the modeled results are more likely close to the field values. Whereas, more dispersion is the reason for weak correlation and variation between the predicted and observed values of the pollutants during unstable conditions.

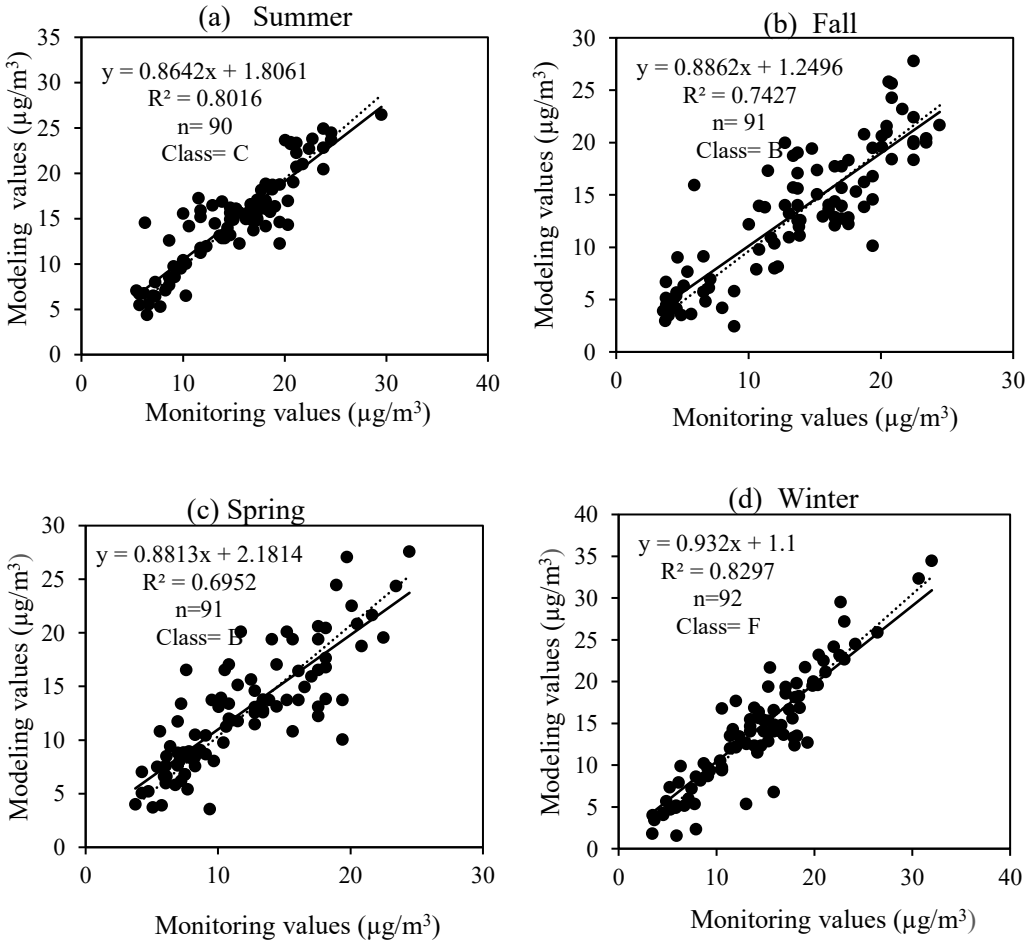

Figure 6.6 Regression analysis of $PM_{2.5}$ concerning seasons and different class (a) Summer; (b) Fall; (c) Spring; (d) Winter

6.5 Discussion

The meteorological factors such as stability class and mixing height were studied and subsequently, correlated with the concentration of $PM_{2.5}$. It is worth to mention that atmospheric stability is essential in selecting all the primary parameters which make the fundamentals of air dispersion modeling (Latini et al., 2000). The monthly classification and diurnal patterns can help to choose the suitable treatment method for the pollutant. Moreover, over and underestimation of a pollutant concentration can be improved if correct stability pattern would be determined. Boundary conditions of an air dispersion model-MADM are decided based on the meteorological factors obtained after the PTM analysis. For instance, if mixing height is low then no need to calculate the pollutant's concentration at an elevated level. If instability occurs, there are more chances of pollutant dispersion both vertically and horizontally. Similarly, mixing height plays a significant role in dispersing the pollutant. For unstable and neutral conditions, mixing height can be taken equal to the PBL height. Hence, contaminated air gets diluted as travel vertically. Some researchers attempted to study winter inversion during the stable conditions as persistence inversion may lead to severe episodes of air pollution. In this study, 297.5 m maximum height is achieved during stable condition and 1873 m during instability. Furthermore, minimum mixing height is achieved in January during stable conditions (see Figure 6.5). These results explain well the concept that during winter inversion higher values of pollutants are achieved. Similarly, this study also shows the maximum concentration of $PM_{2.5}$ (28 $\mu g/m^3$) during this month. Beyond this height, there are very few chances of pollutant dispersion. Wind speed is also another significant parameter in this study as the determination of the suitable stable class entirely depends on wind speed and NRI. Wind speed is not only an integral component of many meteorological factors (such as frictional velocity, roughness length, mixing height) but also a critical parameter in the mine air dispersion model (MADM). Hence, hourly wind speed, direction and hours of sun are also essential to follow the actual pattern of stability. The selection of an empirical method for mixing height also depends upon the stability conditions. For example, for neutral condition virtual temperature was used instead of actual temperature to calculate Monin-Obukhov length (L). The virtual temperature further comprises of mixing ratio

(w) and ambient temperature (Ta) using the equation $T = (1+0.61w)Ta$; whereas for mixing ratio air temperature, dewpoint and actual station pressure (altimeter setting) are required to proceed. Statistical analysis of various parameters shows a strong correlation of surface heat flux with the mixing height. This is one of the reasons to choose PTM method to determine the atmospheric stability. Likewise, for each stability condition different parameters might be required to calculate meteorological factors. As far as PTM method is concerned, it is easy to implement and required a very minimum number of input parameters. As compared to advantages, there are very few limitations of the modeling framework which are observed during the study. For example, any direct relation of meteorological factors with the emission rate of the pollutant is not established using the proposed framework. For future, it is recommended to study the effect of meteorological factors on the mining activities and to suggest the control strategy at the source level.

6.6 Summary

This chapter concerns the determination of stability pattern by implementing the PTM method. Different classes were selected using wind speed and NRI. The NRI values were obtained by calculating solar altitude and gathering weather data such as sky condition, solar insolation. The seasonal variation shows that most of the stable conditions happened to occur during winter as compared to other seasons. The analysis results reveal that night time follows the stability pattern. Whereas, daytime is under the instability conditions. Neutral conditions usually occurred during the day-night transition. $PM_{2.5}$ concentration is then predicted with a mining-zone air dispersion model concerning stability patterns. It is concluded that maximum values of $PM_{2.5}$ are obtained during January at night time. Moreover, $PM_{2.5}$ values exceeded the standard for the E and G class as the chances of dispersions are very minimum during this condition. The attained mixing height is high for the unstable condition, thus allowing more dispersion and dilution of the pollutant vertically. The regression analysis shows the satisfactory agreement between the modeling values and observed values of $PM_{2.5}$ for the same station. Furthermore, a good correlation is established for wind speed and surface heat flux against mixing height.

CHAPTER 7 DECISION ANALYSIS SYSTEM FOR MINING USING A STOCHASTIC MULTI-CRITERIA INTEGRATED APPROACH

7.1 Study Area

The proposed MCDA framework was applied to copper-gold mine B, British Columbia, Canada. Mine "B" is an open pit mine, utilizing a fleet size of 25 haul trucks and various auxiliary equipment to support the mining operation. (The same case study is used in Chapter 5, see section 5.1 for more detail about study area).

7.2 Inputs and Data Preparation

7.2.1 Identification and screening of alternatives

Based on the evaluation criteria approach, alternatives were first identified, and subsequently, evaluation matrix was formed (see Table 7.1). After the careful literature review, information was gathered, and only those methods were taken into consideration which assisted in minimizing air pollution directly or indirectly at the mining site. In this process, quantitative values were assigned to each criterion depending upon the nature of the activity and data availability. Three different groups were analyzed for ranking to minimize the air contaminants, i.e., particulate matter, greenhouse gases and toxic gases (hydrogen cyanide). It is worth to note that alternatives are selected based on their effectiveness in fulfilling the objective such as removal of the pollutants, their evidence of reliability and promising of new technology in the field of mining.

(a) *Group 1: Alternatives for dust (Particulate matter) and other fugitive removal methods*

In this group, five different options were considered as action A= [A_1, A_2, A_3, A_4, A_5] including the baghouse and water spraying. The first option selected for evaluation

was the baghouse as a part of existing mine system. For the alternative opportunity, hood or roofing over the conveyor belts and transport system was considered as an action. The third option was capping and vegetation over the dried tailing impoundments and storage piles. This option is usually viewed as a reclamation program in mining but can be used during the construction phase to avoid the contact of the wind with the exposed surface. The fourth alternative was the usage of chemical agents and stabilizers including emulsified asphalt, calcium chloride, calcium lignosulfonate and other surfactants. Among these, calcium chloride was chosen for further evaluation. The selection of this agent has been made depending upon the application rate and cost.

(b) *Group 2: Reduction in fuel consumption to minimize carbon footprints*

Four systems were identified through this group analysis. One was for transport and hauling system which included idling reduction program using electronic fleet management and routing systems using real-time GPS data. The reduction factors and cost for this program were adopted from Kennecott mine program (Rio Tinto, 2016). Kennecott copper mine, Utah has successfully implemented the idling reduction program by installing idle monitors over 430 Kennecott vehicles (light to medium duty vehicles and haul trucks). These monitors assist in saving fuel by reporting the engines that have been idling for a designated amount of time. The program saved 2,074,814 gallons of fuel with the reduction of 21,247 tons of greenhouse gas emissions (Rio Tinto, 2016). Another alternative selected for analysis was concentrated solar thermal technology (CST) used to generate electricity with CST energy also known as concentrated solar power and has the highest possible expectations to minimize GHG emissions among all the potential applications identified. Eglinton et al. (Eglinton et al., 2013) provided evidence that CST is future generation technology and has potential to use in metal mining such as copper, zinc, lead, nickel, gold, etc. The third alternative was biofuel used for all the stationary engines and heavy-duty vehicles, and this option is adopted by the study available for Inco's Creighton Mine in Sudbury, Ontario and Newmont USA, Ltd Lee Ville underground mining, USA (Bugarski et al., 2014). The blended biodiesel fuel with the upgraded diesel oxidation catalyst (DOC) reduced

98±11% of carbon monoxide and blend of biodiesel with ultra-low sulfur diesel (ULSD) with 57% of biodiesel content fatty acid methyl ester (FAME) reduced up to 61% of total carbon content. The fourth option was the existing strategy of the mine A to reduce carbon footprint by using two of five electric drillers and three electric shovels.

(c) *Group 3: Destruction of cyanide alternatives*

Sodium cyanide is mostly used as metal recovery reagents in almost 90 % of the mine in Canada. However, its usage also demands to properly destroy it within a processing plant by using appropriate destruction method. Some alternatives to cyanide are thiourea, thiosulphate, etc. These reagents were evaluated based on five criteria to choose the right option which included gaseous emissions, extraction efficiency, lethal dosage, the amount of the chemical required and cost of the chemical. Among all, usage of sodium cyanide is still a better choice. Subsequently, alternatives of cyanide destruction were evaluated against some selected criteria. The conventional methods typically being applied for cyanide destruction in mining usually involve the oxidation of cyanide considering alkaline chlorination, hydrogen peroxide, SO_2/air process, biological treatment and anodic oxidation. All these methods have some pros and cons. There has not been any best method available yet for attaining the low emissions of cyanide. Three methods selected for alternatives were gas sparged hydro-cyclone (GSH) reactor, ozonation, and electrochemical oxidation depending upon the highest removal efficiency of free cyanide. GSH is used mostly for the treatment of cyanide by chemical oxidation with the use of chlorine dioxide [ClO_2(g)] (Parga et al., 2003). Ozone is used for in-situ treatment and produced from air using an ozone generator to remove free cyanide which has potential to produce hydrogen cyanide in the air. The destruction of cyanide using electrochemical oxidation is more favorably conducted in strong alkaline solution. For this study, values were adopted from Xu et al. (Xu et al., 2012) research. The anodes used during the process by Xu et al. were Ti/SnO_2-Sb-Ce anode showing cyanide removal 84.2- 98.2 % at initial pH 13 with a reaction time of 4 (hr), but removal efficiency reduced to 48.2- 69.5% at initial pH 6 (Xu et al., 2012).

Table 7.1 Identification of alternatives and their effectiveness to minimize air pollution

Alternatives	ID #	Effectiveness	References
Group 1: Dust control alternatives			
Air pollution control equipment such as Baghouse	A1	99% of captured pollutants	(Driussi and Jansz, 2006)
Hood over conveyor belt /transport system	A2	99-100%	(Cecala et al., 2012)
Capping of tailing waste by vegetation	A3	75%	(Sheoran et al., 2013)
Chemical stabilizer for haul roads (calcium chloride)	A4	85%	(Dwayne and Regensburg, 2001)
Water as existing method	A5	50-75%	(Prostański, 2013)
Group 2: Reduction in fuel consumption to minimize the carbon footprints			
Biodiesel blended with FAME and ULSD or Blend with DOC	A6	61 % of TOC and 98%±11% of carbon monoxide	(Bugarski et al., 2014)
Idling reduction by use of computerized fleet management and routing systems using real-time GPS data	A7	15 % reduction in GHGs (overall mine)	(Vivaldini et al., 2012)
Concentrated solar thermal technologies (CST)	A8	15 % reduction in GHGs (overall mine)	(Eglinton et al., 2013)
Electric drilling as existing system	A9	52% for stationary fuel combustion	Mine B, Canada
Group 3: Alternative of cyanide destruction method			
Gas Sparged Hydro-cyclone (GSH) reactor	A10	99.9% free cyanide; 78.9 % complex cyanide at pH 11.23	(Parga et al., 2003)
Ozonation	A11	99.9 % free cyanide	(Parga et al., 2003)
Electrochemical oxidation	A12	84.2-98.2% at PH 13 with detention time 4 hrs	(Xu et al., 2012)

7.2.2 Criteria values for alternatives

Criteria to evaluate each alternative were identified to ensure the objective of the decision analysis method. The data for each criterion was obtained from literature studies and different mining reports by experts. Existing methods of the mine site A were also included for comparison purpose. For each group, different criteria were chosen depending upon the nature of the activities of that group. The selected criteria for the decision system should follow the presented objectives:

- Minimize the air pollution
- Minimize the cost
- Maximize the extraction rate or efficiency

- Maximize the sustainable performance
- Minimize the risk associated with the pollutants
- Maximize the future use
- Minimize the energy/fuel consumption

Table 7.2 illustrates these criteria and their scoring scale accordingly. Each criterion is rated based on the scale of 1 to 9, using knowledge of environmental and technical evaluation. Each option based on the preference that has low cost rated at 9 and the high cost rated as 1. For less magnitude of the pollutants emitted rated as 9, otherwise scored 1. The risk is associated with the pathway of the pollutant or the resultant pollutant produced during removal of the target pollutant, may pose a threat to surrounding ecosystem. If this is the case, that alternative would be rated as 1; otherwise rated the higher value up to 9. For long-term performance, an option that is more efficient for a long duration is rated as 9, and an alternative that would not be much suitable for the same period is scored as 1. An option that has an excellent removal efficiency is rated as 9; otherwise, it is scored less value. If an alternative required less energy to remove pollutant is rated as 9; otherwise, it is rated at a lesser value. An alternative that would increase future use and aesthetic of the site is rated as 9, and vice versa.

Table 7.2 Criteria and score scaling

Criteria	Id#	Score
Cost	Ct	1 (low) to 9 (extremely high)
Air pollution	AP	1 (low) to 9 (extremely high)
Risk	Rk	1 (low) to 9 (extremely high)
Long-term performance	LP	1 (poor) to 9 (excellent)
Efficiency	Ef	1 (poor) to 9 (excellent)
Energy	Eg	1 (low) to 9 (extremely high)
Future use	Fu	1 (poor) to 9 (excellent)

Table 7.3 presents a pair-wise comparison matrix of the criteria. The matrix was constructed using AHP method illustrates the relative importance of one criterion against another and shows the preference of participated criteria in the decision-making process. The synthesis judgment was based on stakeholder's preferences (from mine

A), and experts' opinion (a group of professional civil engineers and environmental experts). The geometric mean was obtained for each criterion after careful evaluation. A pairwise comparison was performed on a scale of 1 to 9 using Super Decisions software (SuperDecisions tool, 2017). For instance, a decision-maker (DM) strongly prefers (9) for the air pollution minimization (AP) criterion compared to the long performance (LP) criterion. The preference of LP over AP (i.e., 0.11) is obtained by taking the reciprocal preference value of LP over AP. The normalized weights of the criteria were achieved by computing eigenvectors of the matrix. The remainder values of the matrix could be explained similarly. The scaling between 1 to 9 was assigned based on Saaty (Saaty, 2008) rating. For example, 1 represents the equal importance of one criterion over another; 3 shows of moderate significance; 5 shows higher importance; 7 represents much higher importance; 9 shows a complete dominance over others; and 2, 4, 6, 8 shows intermediate values above or below the defined scale (Saaty, 2008).

Table 7.3 Pairwise comparison matrix for criteria evaluation

Criteria	Ct	AP	Rk	Eg	Ef	LP	Fu
Ct	1	0.142	0.125	0.142	0.2	2	4
AP	7	1	2	4	7	9	8
Rk	8	0.5	1	6	7	8	9
Eg	7	0.25	0.166	1	8	8	9
Ef	5	0.142	0.142	0.125	1	3	4
LP	0.5	0.11	0.125	0.125	0.33	1	4
Fu	0.25	0.125	0.11	0.11	0.25	0.25	1

The inputs for multicriteria methods (e.g., PROMETHEE) should be provided as an evaluation table. The Table 7.4 represents criteria; whether the criteria should be maximized (Max) or minimized (Min) depending upon the objective. Criteria weights indicate the importance of one criterion over the other criteria. Whereas, the evaluation of the alternatives based on each criterion and preference function shows the degree of preference of one alternative over another option. The normalized criteria weights were calculated from the AHP computation. The results indicate that minimizing air pollution (AP) is the most prioritized (i.e., 0.34) criterion followed by the following

order: risk (Rk)> energy consumption (Eg) >efficiency (Ef)>cost (Ct)>long term performance (LP)> future use (Fu). Preference function (V shape) is selected for all criteria. This preference type is chosen as it best represents the data compared to other preference functions. The evaluation of the impact on alternative is difficult to quantify, and based on literature reviews. For this purpose, a 9-point qualitative scale ranging from 1 (very low impact) to 9 (very high impact) has been applied.

Table 7.4 Input evaluation matrix for PROMETHEE

Criteria	Min / Max	Normalized criteria weight	Category 1					Category 2				Category 3		
			A1	A2	A3	A4	A5	A6	A7	A8	A9	A10	A11	A12
Ct	Min	.045	7	2	3	4	3	8	9	9	7	6	5	7
AP	Min	0.34	8	8	7	7	6	3	6	7	5	4	6	7
Rk	Min	0.30	1	4	9	7	9	5	3	4	6	1	1	3
LP	Max	0.18	9	7	7	8	2	7	7	9	1	7	7	6
Ef	Max	.075	9	9	7	8	6	7	8	8	4	8	8	7
Eg	Min	0.037	7	7	6	8	8	4	6	7	5	5	7	2
Fu	Max	0.021	9	6	8	7	7	8	9	9	7	6	8	7

7.3 Results

7.3.1 Evaluation of alternatives based on multi-criteria

By utilizing Visual PROMETHEE (Edition15) tool, the model was simulated for the three groups simultaneously so that model implies the ranking of the best alternative. Table 7.5 indicates the preference function values based on deterministic analysis for each criterion. The obtained preference values are expressed in terms of positive and negative values. Higher the positive value, more inclined towards a preference of the alternative over another technology. For instance, capping through vegetation and water spraying cost is minimum as compared to other options. This is shown by the highest value (0.909) obtained for these two alternatives. Minimum air pollutants are produced by using baghouse by the value 0.954. Whereas risk value is low for the baghouse, hooding, water spraying, idling reduction applications and concentrated solar thermal technologies by 0.5. In the context of long-term performance, idling reduction application due to computerized fleet management and concentrated solar thermal technologies show preference values of 0.818 over other alternatives. Concerning efficiency of the techniques, for group 1 (Alternatives for dust and other

fugitive removal methods) baghouse, hooding and chemical stabilizer are equally efficient with a value of 0.272. For group 2 (Reduction in fuel consumption to minimize carbon footprint) idling reduction and concentrated solar thermal technology are showing maximum efficiency. For group 3 (destruction of cyanide alternatives) gas sparged hydro cyclone method, and ozonation is considered efficient with value 0.272. Regarding energy consumption, capping over storage piles and dried tailing needed minimum energy as compared to other methods. For future use, idling reduction application and concentrated solar thermal technologies are considered as promising technologies with preference values of 0.68 over other alternatives.

Table 7.5 Evaluation of alternatives with respect to criteria

Alternatives	Ct	AP	Rk	LP	Ef	Eg	Fu
Baghouse	-0.5909	0.9545	0.500	0.272	0.272	-0.136	-0.318
Hood over conveyor	0.2273	0.6818	0.500	-0.318	0.272	0.272	-0.318
capping	0.9091	0.272	0	-0.318	-0.272	0.909	0.681
Chemical stabilizer	-0.1818	0.272	-0.5	0.272	0.272	0.636	-0.727
Water spray	0.9091	-0.1364	0.5	-1	-0.818	0.636	0.227
biodiesel	-0.1818	-0.9545	-1	0.545	-0.272	-0.727	-0.318
Idling reduction	0.2273	-0.1364	0.5	0.818	0.272	-0.136	0.6818
CST program	-0.5909	0.2727	0.5	0.818	0.272	0.272	0.6818
Elect. drilling	0.2273	-0.545	-0.5	0.5455	-0.272	-0.5	0.227
GSH	-0.1818	-0.818	-0.5	-0.772	0.272	-0.5	-0.727
Ozonation	0.2273	-0.136	0	-0.318	0.272	0.272	0.227
Elect. oxidation	-0.6009	0.272	0	-0.5455	-0.272	-1	-0.318

7.3.2 Preferences of alternatives

The computed positive flow (Φ^{+}), negative flow (Φ^{-}), net flow (Φ^{Net}), output/input ratio and aggregated weight for alternatives through the deterministic PROMETHEE analysis are shown in Table 7.6. All the preference functions values are multiplied by the weighting values to produce preference index. The weighting values are determined using AHP method. The positive flow of an alternative is obtained by summation of preference index in a row for the method. If any treatment option is characterized by a greater positive flow value and a smaller negative flow value, the better this alternative dominates other options. Hence, these values are obtained as the partially ranking the alternatives. Whereas, the net flow is determined as a difference between the positive

and the negative flows. Also, it represents whether an alternative outranks other options. The net results are used to rank the alternatives. Likewise, out/Input ratio and aggregated percentage analysis similarly interpreted the results using a complete PROMETHEE II ranking.

Based on net flow analysis following is the order of ranking
Group 1: Capping>Water spraying>Hood over the conveyor>Baghouse> Chemical stabilizer
Group 2: Idling reduction> CST program> Elect. drilling>Biodiesel
Group 3: Ozonation>Elect. Oxidation>GSH

Based on O/I ratio following is the order of ranking
Group 1: Capping>Hood over the conveyor>Baghouse>Water spray> Chemical stabilizer
Group 2: Idling reduction=CST program>Elect. drilling>Biodiesel
Group 3: Ozonation>Elect. Oxidation>GSH

Thus, based on net flow ranking, capping of vegetation dominated the water spraying, hood over the conveyor, baghouse and chemical stabilizer. In group 2, idling reduction program is a dominated method for saving energy consumption and consequently contributed towards carbon footprints followed by CST program, electrical drilling (which was also the existing application for mine A) and biodiesel. For group 3, ozonation is a preferable option for cyanide destruction as compared to other two methods. It is noteworthy that PROMETHEE II deterministic complete O/I ratio ranking also produced the same order for group 3. For group 1, water spraying positioned 4^{th} in ranking instead of 2^{nd} and in group 2, idling reduction and CST shared the same ranking. The other alternatives have the same ranking in the net flow and O/I ratio PROMETHEE analysis. Table 7.6 illustrates the complete ranking results in the 5^{th} column expressing values in weight aggregated weight in percentage. Group-wise ranking order follows the same ranking results as gained by output/ input ratio through complete ranking. Whereas, by ignoring the grouping, both idling reduction and CST application ranked first among all the alternatives with the probability of 100 %.

Capping of vegetation ranked second with 98.57 % chances followed by Hood over conveyor that has 75.7 % probability. Baghouse and ozonation have equal ranking probability with 60.47 % aggregated weight followed by water spraying then chemical stabilizer with 56.6% and 52.4% respectively. The electric drilling followed by electrical oxidation, biodiesel and gas sparged hydro cyclone methods are the least likely choices.

Table 7.6 Preference of alternatives by PROMETHEE method analysis

Analysis	Partial analysis PROMETHEE 1		Complete analysis PROMETHEE II		
Alternatives	Φ^+	Φ^-	Φ^{Net}	O/I ratio	Weight aggregated %
Baghouse	0.347	0.3536	-0.0065	1.16	60.47
Hood over conveyor	0.3852	0.1938	0.1914	1.46	75.72
Capping	0.5201	0.1616	0.3585	1.90	98.57
Chemical stabilizer	0.3015	0.3098	-0.0083	1.03	52.40
Water spray	0.4243	0.3112	0.1131	1.09	56.65
Biodiesel	0.1519	0.5492	-0.3973	0.41	21.3
Idling reduction	0.4510	0.1399	0.3111	1.93	100
CST program	0.4320	0.1851	0.2470	1.93	100
Elect. drilling	0.2714	0.3614	-0.0899	0.79	40.9
GSH	0.1220	0.5611	-0.4392	0.368	19.08
Ozonation	0.3193	0.2297	0.0896	1.16	60.47
Elect. oxidation	0.1388	0.5083	-0.3695	0.48	24.87

7.3.3 Networking analysis of alternatives

Figure 7.1 depicts the networking of alternatives based on the positive and negative flows for mine A regardless of three different groups. If all the options would be considered as one group to fulfill the objectives of this study then, in this scenario, capping of vegetation along with the combination of idling reduction and CST program are dominated alternatives. Whereas, GSH method for cyanide destruction is considered as a last preferable option. One can also interpret the results as a set of combination of different alternatives as one option. For instance; option 1 includes idling reduction, CST program, capping, hood over conveyor and ozonation. This combination of alternatives represented all the three groups and considered as a preferable option on ranking basis. This option not only controls the dust problem but also reduce the fuel consumption and contribute towards the carbon footprints.

Moreover, ozonation helps to destroy the free cyanide which has potential to produce hydrogen cyanide. The other option 2 comprises of the baghouse, water spraying, chemical stabilizer, electrical drilling and electrical oxidation. This option is the second preferable combination of different alternatives which represents the group 1, 2 and 3. Most of the alternatives combination mentioned in option 2 has been already used by mine A except electrical oxidation as a mitigation measures. In conclusion, the good networking also assists in selecting suitable technologies as a combined set to implement a plan to control the air pollution at the mine site effectively.

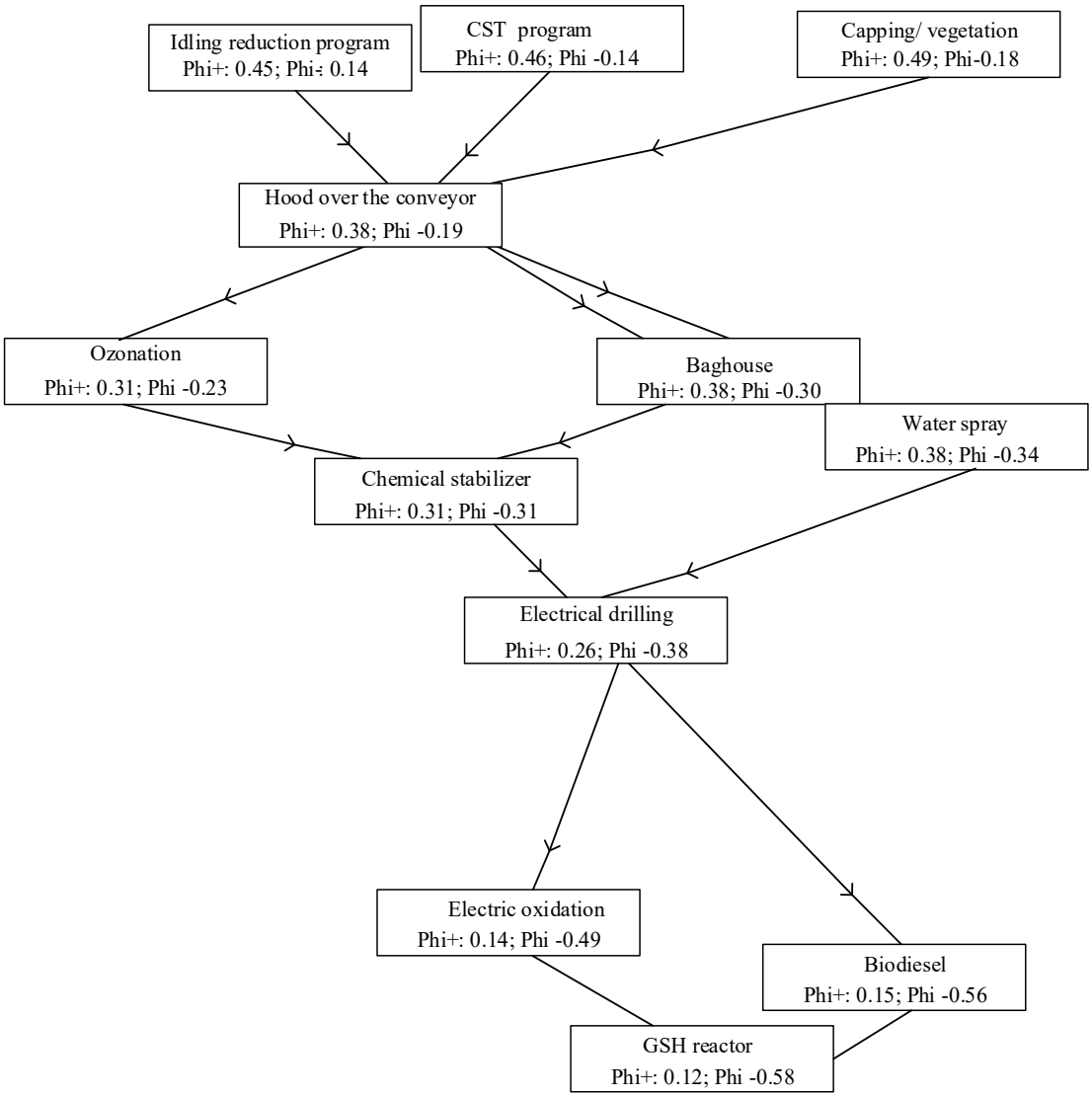

Figure 7.1 Alternatives network analysis using visual PROMETHEE

7.3.4 GAIA visual analysis of alternatives

Decision makers (DMs) can easily determine the individual strength of each criterion, as well as the degree of consistency and the quality of each alternative for each criterion using GAIA plane. For instance, in this study, the GAIA plane stick (red color) inclined entirely towards idling program and CST application coordinate along with capping. The square represents group1 alternatives, whereas group2 and group3 are represented by circle and diamond shapes respectively. The position of alternatives determines the degree of weakness or strength along the criteria axes. The closeness of criteria orientation to an alternative shows the preference of one alternative over others. For example, in Figure 7.2 alternative A7, A8, A2, and A11 lie close to most of the criterion considering as best options with similar profiles. Principle component analysis (PCA) concept is used by GAIA method minimize the missing or loss information by reducing the number of dimensions. The quality analysis represents that how much data got lost. In this research quality level was 92.6%, which indicates that very few information lost during projection.

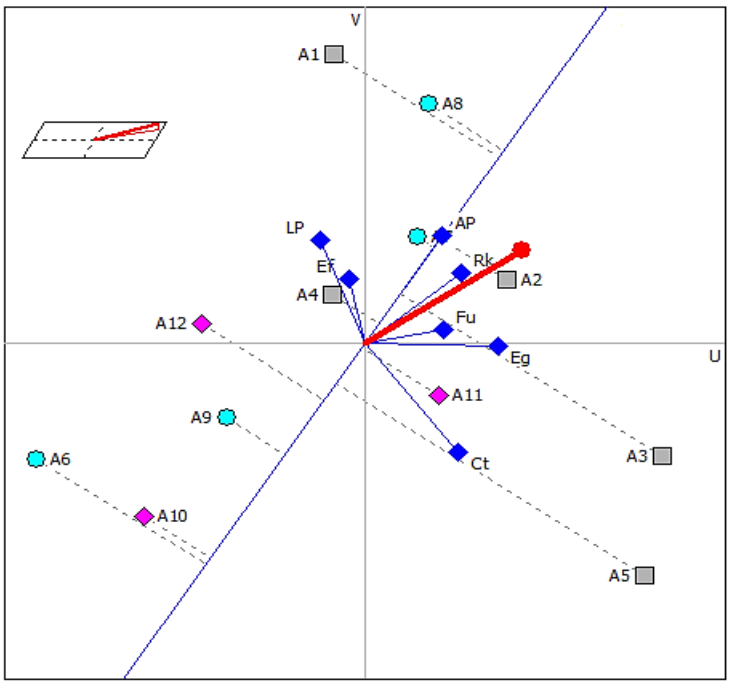

Figure 7.2 GAIA visual analysis with respect to air pollution axis

7.3.5 Probabilistic decision analysis

Figure 7.3 illustrates the possible range of cumulative distribution functions of the net flow of alternatives. For instance, Figure 7.3 (a) shows a range of baghouse alternative from -6.4 to +5.1 net flow, and the capping range lies between -2.24 to +5.12. Also, it is interesting to compare the net flows values at different cumulative distribution functions such as in Figure 7.3 (c) at 80 % frequency exceedance (or 0.8 cumulative probability distribution), electrical oxidation is showing net flow value of 0.5, GSH shows 0.8 and ozonation represents 1.5 flow. Thus, net flow value varies at each distribution function value. This stochastic output enables the stakeholders to obtain the net flow values at the required interval and ranks the alternatives with the level of confidence. This approach helps to understand different possibilities while considering uncertainties (weights and output net flows) and opposed to single values obtained through a deterministic way.

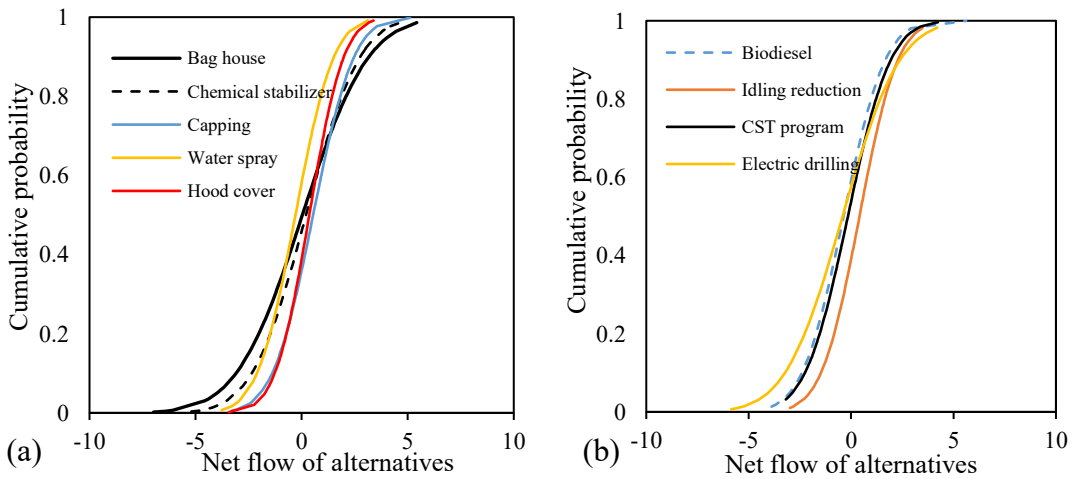

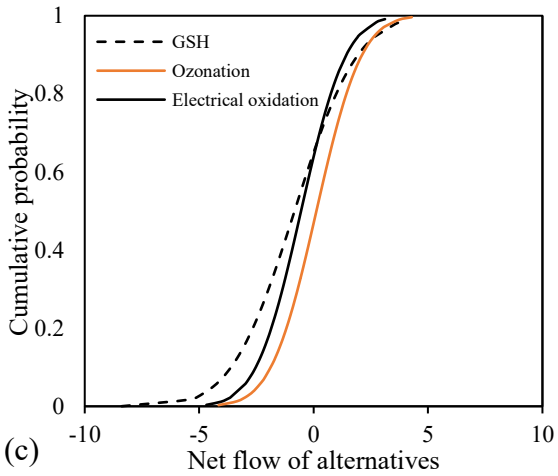

Figure 7.3 Cumulative probability distribution function of net flow for PROMETHEE analysis (a) dust removal methods (b) reduction of energy consumption (c) cyanide destruction

Figure 7.4 depicts the contribution of criteria by ranking the alternatives using Spearman rank correlation method. It is noticed that weight of criteria for each alternative is different. For example, A8 (CST) alternative is sensitive to AP followed by Ct, Ef, Eg, Rk, LP and Fu criteria. Whereas, the A9 (electrical drilling) alternative is sensitive to Ct followed by AP, Rk, LP, Fu, Eg and Ef criteria. Thus, the ranking of each option is sensitive to different criteria. Moreover, it is also noted that overall air pollution (AP) is most sensitive criteria for each alternative and future use (Fu) has least contribution. Furthermore, Figure 7.4 shows a good association between the parameters (including criteria and alternatives), the positive sign occurring for strong correlation and the minus sign representing weak correlation between criterion and alternative.

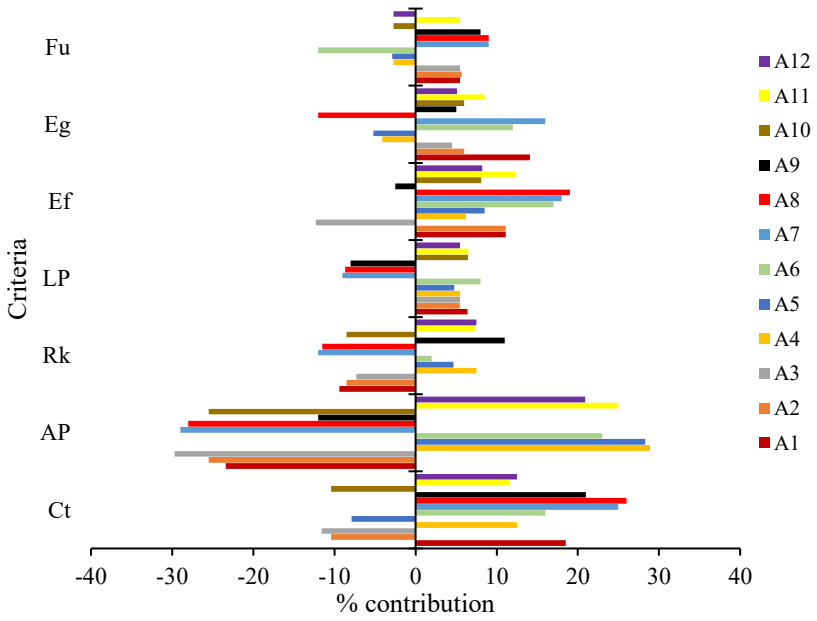

Figure 7.4 Percentage contribution of criteria on ranking the alternatives using Spearman rank correlation method

7.4 Discussion

This study shows that PROMETHEE method is one of the promising technology in the selection of air treatment alternatives in the mining sector. The reason for using this approach in the proposed framework is that PROMETHEE is dominating 60% of the category over other methods in the field of air quality/emission (Huang et al., 2011). Hence, its use in the integrated study of air pollution and mining field is new. Two different methods which are AHP and PROMETHEE combined to assist decision makers since it presents a complete analysis of relevant criteria and parameters. This framework allows the user to select suitable treatment technology in the context of air pollution reduction while enabling the use of AHP for criteria's weight calculations. One of the advantages of conducting this study is to learn about the effectiveness of the integrated tool at the mine site. The reliability of this kind of deterministic framework also proved during the selection of remedial alternatives for controlling acid drainage issue in British Columbia' mine, Canada (Betrie et al., 2013).

Air pollution control strategy is categorized into three groups, i.e., dust control, reduction of fuel consumption which may lead to the carbon footprint contribution and cyanide destruction. This division helps to address the range of different alternatives depending upon the target and overall network analysis for the mine. This study provides concise concept by recognizing that there is no single technology appropriate for use in air pollution reduction context. Thus, a clear means of determining which factors should influence the choice of technology, based on simple responses to a series of criteria. Efforts are made to enlist all the potential and emerging techniques in this research, which have been in practice nowadays in mining especially for the group 2, i.e., Reduction in fuel consumption to minimize carbon footprints.

It is noteworthy that PROMETHEE method can allow users to have both qualitative system (point based) and a quantitative system simultaneously. The quantitative data for cost ($), removal efficiency (%), and energy consumption data (kW) is extracted from literature review. Whereas, the qualitative data is obtained through surveys and experts' opinion such as long-term performance, future use of alternatives and air pollution information. The Gaussian air dispersion modeling is performed to analyze that how much pollutant concentration exceeds the environmental air quality criteria which helps to assign the points against risk criterion. Thus, the characterization of the risk is calculated as probabilistic risk assessment which refers to the generation of distributions of risk representing uncertainty (see supporting Fig. S-1). The risk can be expressed as Pf ($C > L_p$), where C denotes the concentration of any pollutant, L_p is the environmental standard for each pollutant p (prescribed safety limit of the pollutant p), and Pf denotes probability. For this study, to make a homogenous matrix, all the values and quantitative data obtained through literature is represented as a scoring system. For example, 9 score is assigned for the control methods having the removal efficiency in the range from 95 to 99 (%); 8 score is assigned for those alternatives having range of 85-94 (%). Similar concept is used to assign scores to other criteria. The highest point 9 is assigned to the maximum value among the alternatives (see supporting Table A-4).

The ranking of alternatives is profoundly influenced by the allocation of weights to criteria as well as alternatives. Figure 7.5 represents some examples showing the effect of weighting criteria on the net flow of alternatives by conducting a sensitivity analysis using walking weights as a unique feature in the visual PROMETHEE tool. The upper bar charts show the complete PROMETHEE ranking of alternatives and the lower bar charts represents the weights of the criteria determined by AHP pairwise magnitude of the ranking concerning positive and negative flows. For instance, by changing the weights of air pollution minimization (AP) criteria from 41 % to 25% and maximizing the efficiency (Ef), there is a slight increase towards positive flow for alternatives A3, A2, A8, A7, A11, and A4. Whereas, A5, A9, and A12 tending to move towards negative flow. If allocated weight is increased from 41 to 43% for air pollution minimization (AP) criteria and neglecting future use (Fu), then alternative A7 shifted from positive flow towards negative flow. It is important to keep into consideration that higher the positive flow value more chances of alternative method to dominate.

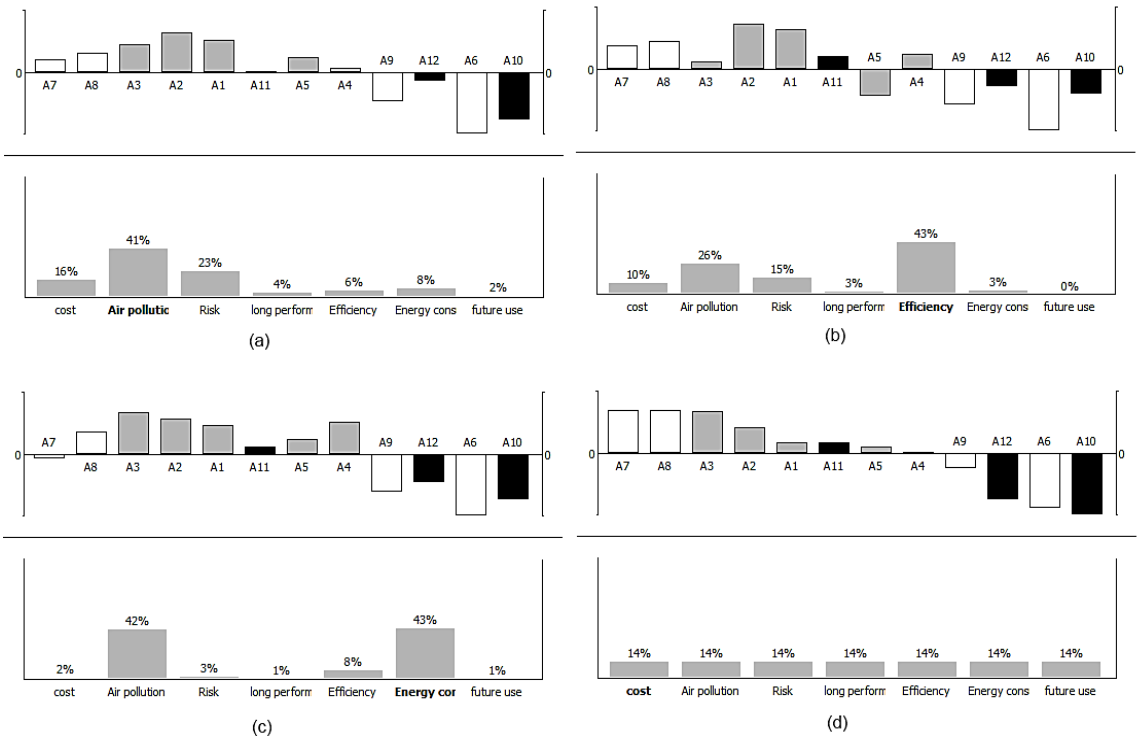

Figure 7.5 Sensitive analysis by walking weights of various criteria (a) maximizing air pollution criterion; (b) maximizing efficiency criterion; (c) maximizing air pollution and energy consumption criterion; (d) equal contribution of each criterion

7.5 Summary

This chapter describes the implementation of the multi-criteria decision analysis system consists of identifying criteria to evaluate alternatives, calculating criteria weights by using AHP, applying Preference Ranking Organization Method for Enrichment Evaluation (PROMETHEE) I and II methods and conducting a sensitivity analysis. The results of the deterministic PROMETHEE analysis ranked the alternatives and showed the other comparable alternatives under different categories. The deterministic PROMETHEE II results illustrate the complete rankings of the alternatives. For instance, the application of the PROMETHEE II method at the mining site indicates that the capping, idling, and ozonation is preferable among group 1, 2 and 3 respectively. The ranking is based on the seven criteria which are air pollution (AP), risk (Rk), energy consumption (Eg), efficiency (Ef), cost (Ct), long-term performance (LP) and future use (Fu). By conducting the sensitivity analysis, it is concluded that higher the positive flow value more chances of the alternative method to get dominate. The study also confirms that by varying the assigned weight of criteria help to achieve the best optimal solution. The GAIA plane enables the visual representation of all the alternatives and criteria exclusively with respect to the reference axis. A stochastic method was used to perform uncertainty analysis for the weighting criteria, and output alternatives flow using Monte Carlo Simulation technique. Furthermore, a significant analysis was accomplished using the Spearman rank correlation method to examine the impact of each criterion on alternatives.

CHAPTER 8 OPTIMIZATION OF AIR POLLUTION CONTROL MODEL

8.1 Study Area and Data Collection

Mine C is an open pit mine located in Utah, USA, comprises approximately 900 ha area. Processing facilities included a concentrator, a 175-megawatt (MW) coal-fired power plant, a smelter, and a refinery as shown in Figure 8.1. For this study air emissions during copper production is considered. The average daily data from the year 2014 to 2015 were collected. The average maximum ambient temperature is 12.7 ºC. The mean wind speed of the site is 3.4 m/s. The weather data were separately collected through NOAA regional climate center as well as airport weather station (W). The pollutants data were obtained from the three-points (Smelter, refiner and mine pit site) for this study. (The same case study is used in Chapter 6 and 9, for detail map see Figure 9.1).

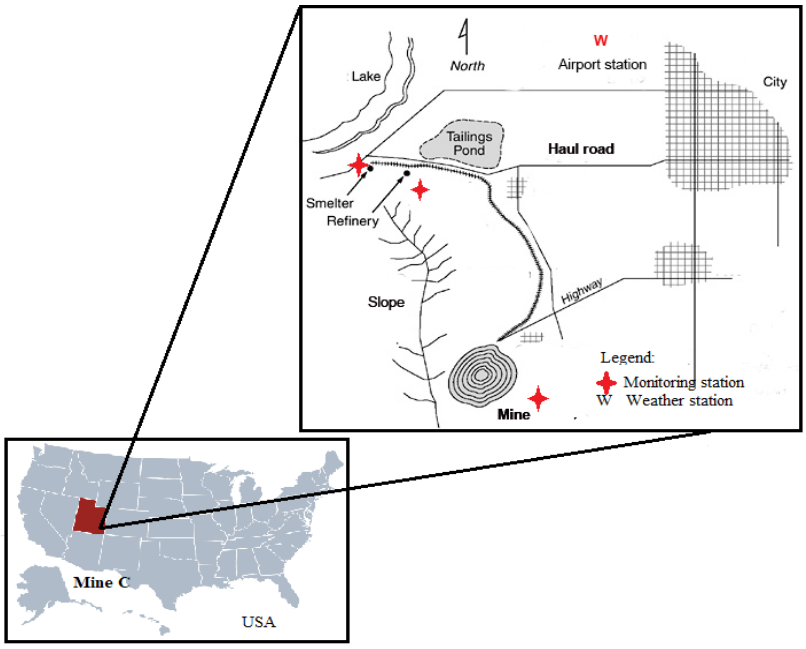

Figure 8.1 Location of mine C and monitoring station

8.2 Input for the Optimization Model

Table 8.1 summarizes all the important parameters used as inputs for the optimization model. The production capacity of the mine and availability of resources as copper production values are mentioned in Table 8.1, which are average values for the year of 2014-2015. Whereas, the unknown variable is X which is copper production from each mining activities after applying control strategy. Furthermore, emission of the pollutants is obtained from the life cycle inventories and reports of mine C. The significant pollutants included in this study are PM_{10}, $PM_{2.5}$, NO_X, and SO_2.

Table 8.1 Inputs for the optimal model-APCM (Utah, 2017)

Input parameters	Average values
The annual production rate of mine (10^5. tons/yr)	2.55
The grade of copper mine (g/tons)	0.97
Total production of copper (tons. 10^5)	2.68
Emission of $PM_{2.5}$ generated (10^4. kg/yr)	7.14
Emission of PM_{10} generated (10^4. kg/yr)	6.50
Emission of NO_x generated (10^4. kg/yr)	1.26
Emission of SO_2 generated (10^4. kg/yr)	3.78

Particulate controls are mainly collectors (cyclones), electrostatic precipitators, baghouse or wet scrubbers. Mechanical collectors are used to controlling larger diameter particulate in a pre-control capacity. Whereas, electrostatic precipitators are used mostly in high emission rate applications such as coal-fired power plants (Turner et al., 1988). Baghouse (fabric filters) cover a wide range of emission sources from the large scale to minimal sources. Moreover, filter size varies depending on particulate loading, temperature and moisture content. Wet scrubbers are efficient for large-particulate emission sources (MJ Bradley and Associates, 2005). NO_x can be controlled by selective non-catalytic reduction (SNCR), which involves the injection of ammonia or urea into the exit air stream to react with NO_x to form nitrogen and water. Without the benefit of a catalyst, the reaction temperature is very high (1,400 to 1,500°F), which makes SNCR only useful in a relatively high, narrow temperature range. Selective catalytic reduction (SCR) is one of the most effective NO_x controls for combustion

sources. The catalyst allows an efficient reaction to take place at lower temperatures; typically, 500–900°F, depending on the type of catalyst (USEPA, 1999). Whereas, a flue gas desulfurization (FGD) system is based on an alkaline reagent. The purpose of using these reagents is to absorb SO_2 in the effluent stream and produce by-products such as calcium sulfate and sodium compound. These solid sulfate compounds are then removed from the air stream using equipment installed at downstream. FGD technologies are further classified as wet and dry based on the reagent used during the application. Wet regenerable FGD systems are more efficient as they have 95-98% SO_2 control capability (Sargent and Lundy LLC, 2003).

Table 8.2 represents the costing information of various identified air pollution control equipment. The direct and indirect costing is obtained which can be added to obtain C_{ij} using eq. (3.56) to find out the total cost of the specific option. Moreover, removal efficiency range is provided in Table 2, which were applied as (1- η) to obtain the reduction of emission (E) after treatment of pollutant and used in eq. (3.60).

Table 8.2 Economic inputs for air pollution control technology (USEPA, 2002)

Air pollution control equipment	Removal efficiency (%)	Direct cost ($).$10^3$ (*DC*)	Indirect cost ($). 10^3 (*IC*)
Wet Scrubbers (WS)	96	159	103
Electrostatic precipitator (Ep)	99	221	202
Baghouse (BH)	95	56	29
Selective catalytic reduction (SCR)	85	8.490/ton	3.540/ton
Non-selective catalytic reduction (NSCR)	65	3.130/ton	2.545/ton
Low NOx burner (LNB)	55	1.170/ton	2.400/ton
Flue gas recirculation (FGR)	60	1.370/ton	0.450/ton
Dry flue gas desulfurization (FGD-dry)	94	6300	1250
Wet flue gas desulfurization (FGD-wet)	98	7760	5600
Dust suppressant (e.g. Magnesium chloride) (DS)	85	0.37/(10^3.yd^3)	0.12/(10^3.yd^3)

Random variables related to meteorological parameters and emission rates of pollutant both were considered. Figure 8.2 illustrates the probability analysis of wind speed (m/s) and standard deviation (m) using Monte Carlo method and showing an average of 3.4 (m/s). The normal distribution method was used to statistically determine

the maximum probability of all outcome to be used as input in the optimization model. A similar approach is used to evaluate the uncertainty in other parameters such as emission rate of the pollutants, standard deviation, etc. The values of standard deviation (σ_y and σ_z) in transfer function are based on the stability percentage occurrence which is calculated in Chapter 6, Figure 6.1.

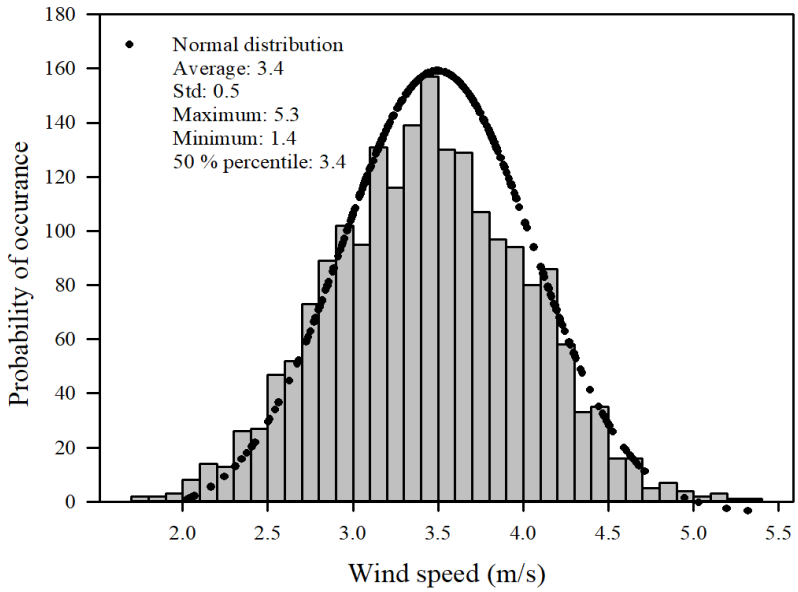

Figure 8.2 Monte Carlo simulation of wind speed

8.3 Environmental Guidelines

The environmental risk assessment (ERA) involves a comparison of the pollutant concentration with the environmental standard or guideline values. However, the ambient air quality standards are different for each country, provinces or states. Table A-3 (Appendix), represents the annual average and 24 hrs as an example, the guidelines for $PM_{2.5}$, SO_2, NO_2, and PM_{10}. To select only standards for a specific case study could be over/under-conservative or impractical for environmental risk analysis since the risk indicators such as the degrees of guideline violation are not compatible among different regions or other copper mines.

8.4 Results

8.4.1 Optimization-based least cost treatment analysis

For each pollutant, a different set of treatment options were planned to determine the best cost-effective solution. For each air pollution control alternative, the model was run separately for each pollutant based on a single objective function. The selected treatment technologies in this study for $PM_{2.5}$ and PM_{10} are the same, as both are the particulate matter and can be removed by using the similar method. Table 8.3 illustrates that electrostatic precipitator option is costly among other methods to treat the particulate matter. The reason behind this is evident that removal efficiency is highest which is 99% in comparison to other technologies. Whereas, the low-cost option with an excellent removal efficiency is baghouse. It is interesting to note that dust suppressant (Magnesium chloride) is cheapest among all with the removal efficiency of 85 %. In the mining sector, dust suppressants are used more frequently. However, it can only be applied to some of the activities such as hauling roads, stockpiling area, grinding area and where there are chances of wind blow the dust. All the three other options which are baghouse, wet scrubbers, and electrostatic precipitators can be installed as units. Whereas, for dust suppressants can be applied only in terms of quantity per area.

Table 8.3 Optimization analysis of air pollution control technology

Pollutants	Treatment options	Optimum Cost ($). 10^3
$PM_{2.5}$ and PM_{10}	1. Baghouse (BH)	567
	2. Wet scrubber (WS)	656.5
	3. Electro precipitator (EP)	1377
	4. Dust suppressant (DS)	100.98
NO_x	1. Selective catalytic reduction (SCR)	2079
	2. Non-selective catalytic reduction (NSCR)	923.93
	3. Flue gas recirculation (FGR)	239.76
	4. Low NOx burner (LNB)	170
SO_2	1. Dry flue gas desulfurization (FGD-dry)	7290
	2. Wet flue gas desulfurization (FGD-wet)	13230

8.4.2 Comparison of control cost and production

APCM model is solved for the case study to meet both production and emission control requirements. Figure 8.3 depicts relation of copper production and control cost of pollutants. Four different solutions are identified to treat particulate matter and NO_x together as one option. These options are selected based on the least cost option for each set of pollutant treatment. For example, option 1 comprises baghouse for particulates and flue gas recirculation for NO_x with the total cost of 88 (10^4. \$) and production of 1.2 x10^5 (tons/yr). The option 2 comprises a combination of baghouse and dust suppressants for particulate matter and flue gas recirculation along with low NO_x burner with the total cost of 109 (10^4. \$). This option can produce 1.3 x 10^5 (tons/yr). Whereas, option 3 includes baghouse for particulate matter with the non-selective catalytic reduction for NO_x with the production of 1.47 x 10^5 (tons/yr) at the cost of 149 (10^4. \$). The last option considered for comparison includes baghouse and dust suppressants for particulate matter and non-selective catalytic reduction for NO_x. The option 4 is like option 3 with the addition of dust suppressants and able to produce 1.36 times more copper at the cost of 162 (10^4. \$).

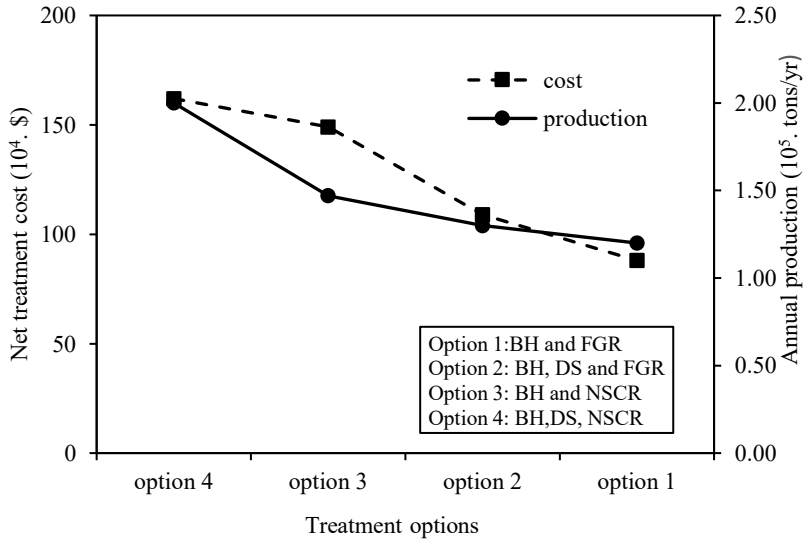

Figure 8.3 Comparison of control cost with annual production

If the planner strategized to select only on the cost basis, then option 1 is the minimum cost solution. If both production and cost of treatment must be evaluated, then option 3 and 4 can be considered.

8.4.3 Environmental risk assessment

As discussed before (Chapter 3, section 3.7.2), to enable a guideline-based environmental risk analysis, the guidelines are categorized based on strictness levels: (1) strict (S), (2) medium (M), and (3) loose (L). The literature data based on expert's knowledge, common values in each criterion and questionnaire survey data is collected to construct membership functions for three values a, b, and c of fuzzy sets in eqs. (3.63 -3.65). The annual average guideline for $PM_{2.5}$, NO_2, and SO_2 was of interest in this study. However, 24 hr average values were selected for PM_{10} based on the hourly representation of different guidelines. Figure 8.4 represents the three strictness levels of guidelines for each pollutant. The results indicated that the strict, medium and loose guideline of the annual average SO_2 concentration is approximately 30 $\mu g/m^3$, 60 $\mu g/m^3$ and 80 $\mu g/m^3$ respectively. For example, if the ambient air quality guideline is 60 $\mu g/m^3$ (medium), then it has a membership grade of 1; if the guideline is 50 $\mu g/m^3$, then it has two membership grades of 0.39 and 0.63 which fall into two different categories of partially strict and partially medium respectively. Similarly, for NO_2, the membership grade of 1 represents the value of 40 $\mu g/m^3$ (S), 60 $\mu g/m^3$ (M) and 100 $\mu g/m^3$ (L). Moreover, the ambient air quality guidelines for $PM_{2.5}$ are 8 $\mu g/m^3$ (S),10 $\mu g/m^3$ (M) and 15 $\mu g/m^3$ (L). However, the S-M-L range for the $PM_{2.5}$ environmental guideline is very close as compared to gaseous pollutants. The guideline values for ambient air quality standard for PM_{10} are 25 $\mu g/m^3$ (S), 50 $\mu g/m^3$ (M) and 150 $\mu g/m^3$ (L).

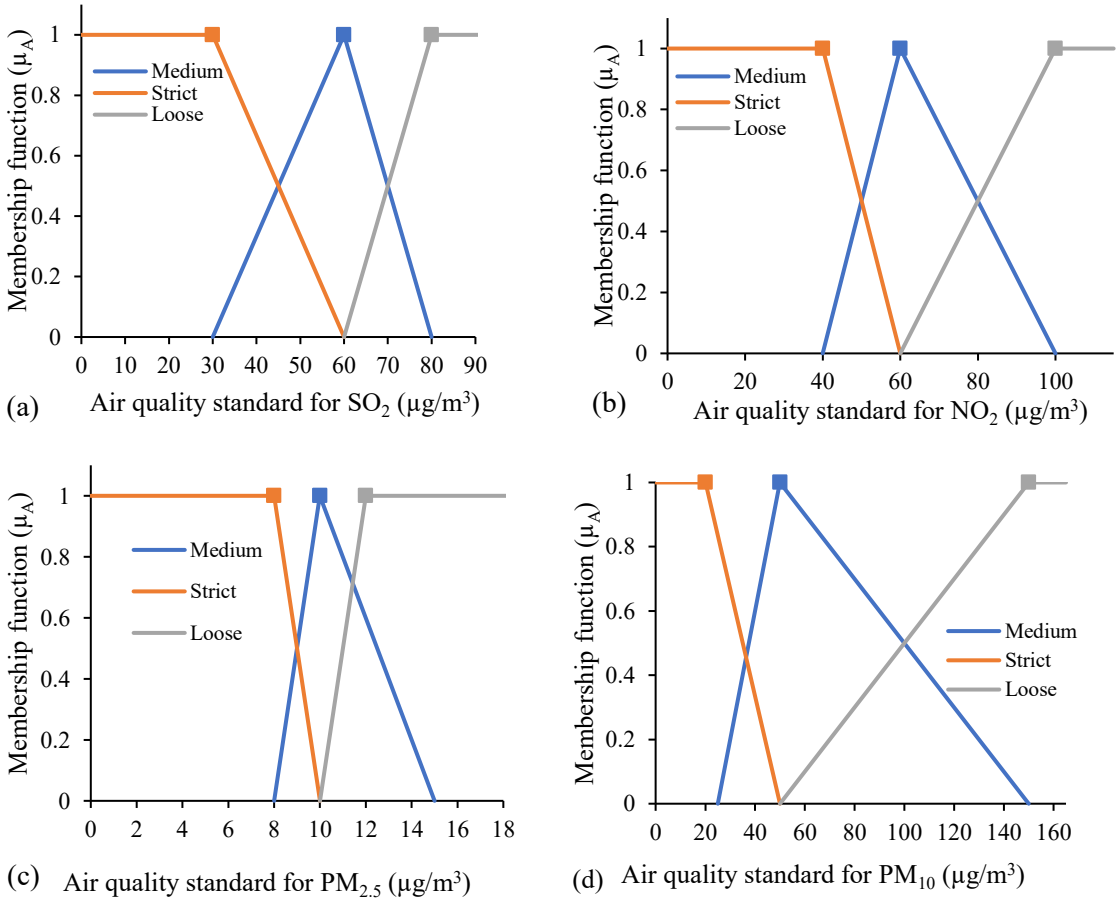

Figure 8.4 Fuzzy based environmental guidelines using membership function (a) SO_2; (b) NO_2; (c) $PM_{2.5}$; (d) PM_{10}

The predicted pollutant concentrations are signified as stochastic events in the form of normal distribution through the Monte Carlo as seen in Figure 8.5. A cumulative probability concept characterizes the analysis of the stochastic event. As an outcome of this event, pollutant concentration exceeds the guideline should be either true (with value 1) or false (with value 0). However, the environmental guideline value can be assigned based on any category of an ERA in the Monte Carlo simulation. In this study, the occurrence of ER due to the violation of the environmental guideline is treated as a fuzzy event. Randomness associated with the pollutant concentration is associated with the fuzzy event using the concept of fuzzy logic. The shaded area is a representation of 1-$F(L_o)$ in eq. (3.68). The environmental guideline (L_o) for $PM_{2.5}$, PM_{10}, and NO_2 are selected based on Medium category. Whereas, SO_2, the strict category is chosen as the predicted concentration at downside through the Gaussian

model is already below the strict guideline. If medium guideline value is selected for SO_2, the obtained risk area become zero. The risk associated with $PM_{2.5}$ is 0.212 which depict that cumulative probability to violate the environmental standard of 10 ($\mu g/m^3$) is 21.2 %. Likewise, the risk associated with PM_{10}, SO_2 and NO_2 is 0.048, 0.032 and 0.159 respectively. Against each environmental standard different value of the risk can be generated.

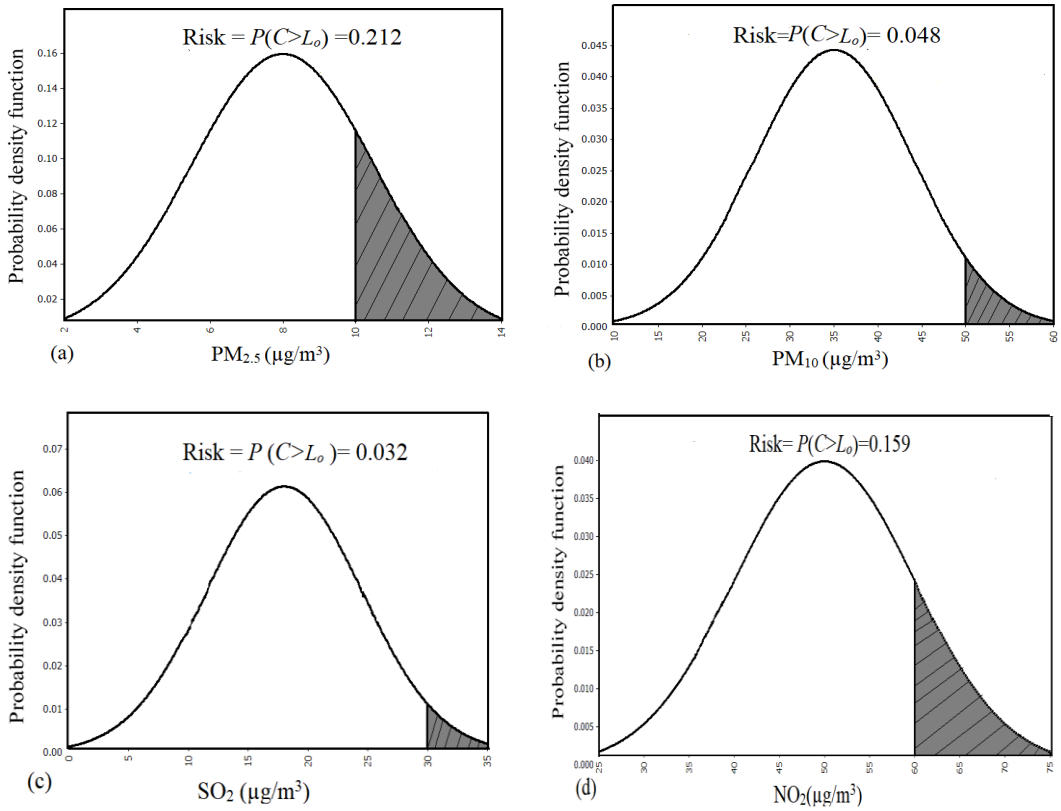

Figure 8.5 Risk assessment based on pollutant concentration through MCS (a) $PM_{2.5}$; (b) PM_{10}; (c) SO_2; (d) NO_2

8.4.4 Expected air quality based on the planned control

After selecting the least cost-effective solution for each pollutant, the final concentration after treatment is analyzed using eq. (3.60). Table 8.4 represents the concentration of pollutants using MADM model and comparison with fuzzy based environmental guidelines of the pollutants and concentration after treatment. It is

noteworthy that $PM_{2.5}$, PM_{10}, and NO_x are above the strict air quality standard values and below the medium and loose guidelines. Whereas, SO_2 is already under the strict limits and do not need any treatment. It is noticed that after treatment, the reduced concentration of $PM_{2.5}$ is 5.813(μg/m^3), PM_{10} is 13.1 (μg/m^3), NO_x is 35.34 (μg/m^3), and SO_2 is 7.6 (μg/m^3). The values of the environmental guideline are also included in the model by using "L_p" variable in air quality constraint. Thus, all the values after treatment met the standard. It concludes that not only cost of equipment and their removal efficiency are crucial factors, but also air quality guidelines are significant for optimizing the control strategy.

Table 8.4 Average pollutant concentration before and after control methods

Pollutants	Before control Avg. (μg/m^3)	Fuzzy environmental guideline S-M-L(μg/m^3)	Control methods	After control (μg/m^3)
$PM_{2.5}$	8	8-10-15 (annual)	BH and DS	5.813
PM_{10}	35	25-50-150 (24hrs)	BH and DS	13.1
NO_x	50	40-60-100 (annual)	NSCR	35.34
SO_2	18	30-60-80 (annual)	FGD-dry	7.6

8.5 Discussion

An integrated optimization modeling and risk assessment system has been developed which involves linear programming based single objective model, air dispersion modeling, Monte Carlo simulation and stochastic simulation-based fuzzy risk assessment. In this research, the framework is designed to select the best treatment among many options available on a rational and cost-effective basis. Also, evaluation of alternatives based on single objective helps to avoid confusion because of conflicting objectives and complex computation. Furthermore, uncertainty is an inevitable component of the decision-making process, the stochastic analysis using Monte Carlo is proposed to enable the decision maker to account for the impact of uncertainty in the final decision-making. Thus, the proposed integrated risk assessment model can systematically quantify both probability and possibility related uncertainties associated

with meteorological conditions and environmental guidelines in an air quality management system. Because of such uncertainties, deterministic ambient environmental guidelines could be impractical and not suit to be implemented. This integrated model of optimization and fuzzy risk assessment represents a unique approach for supporting air quality management and pollution control.

There are some limitations of this modeling study which can be considered as future recommendations. For risk assessment, the environmental risk assessment based fuzzy approach is developed which divide the guidelines into different categories while health risk assessment is ignored. The pollutants can be characterized as carcinogen and non-carcinogen, resulting in two types of human health risk impacts (e.g., hazard index). To quantify the general risk level, it is recommended to consider the environmental risks from guideline violation as well as the health risks from multiple pollutants in the future study by applying fuzzy rules. Moreover, this study only considers input uncertainties in wind speed and standard deviation because of atmospheric stability. It is recommended to analyze other inputs such as dispersion coefficients and surface roughness. Other than environmental guidelines, air quality index can also be used to evaluate air quality. However, this study focused on fuzzy environmental risk assessment based on air quality guidelines.

8.6 Summary

In this Chapter, optimization based an air pollution control model (APCM) is implemented. Multiple simulation runs were conducted for each pollutant and every treatment option. The approach also considered the prescribed ambient air quality standard and availability of resources, which are incorporated as constraints. The effect of meteorological parameters such as wind speed and atmospheric stability is introduced as dispersion transfer function. Mining-zone air dispersion model (MADM) is applied to determine the concentration of pollutants at downwind direction, while incorporation real-time meteorological data. The uncertainties in specific inputs (such as wind speed) and final predicted concentrations are overcome through probability analysis by using Monte Carlo method. A fuzzy set is applied to categorize the

environmental guidelines into S-M-L regions using triangular membership function. A fuzzy logic system is used to deal with the randomness associated with the pollutant concentration with the fuzzy event. In conclusion, the model can be used as a decision tool for planners to select the sustainable and cost-effective technology to control air pollution.

CHAPTER 9 AN INTEGRATED LIFE CYCLE ASSESSMENT BASED AIR QUALITY MODELING AND DECISION SUPPORT SYSTEM

9.1 Overview of the Study Area: A Copper Mining Area, Utah, USA

Mine C is an open pit copper mine located in the Utah county, USA, comprises approximately 900 ha area. The application of integrated LCAQMS is explored by considering air emissions during copper production is considered. Five years' 24 hrs daily data from the year 2011 to 2015 were collected. For validation, seven monitoring stations (S1 to S7) have been examined as shown in Figure 9.1. The average maximum ambient temperature is 12.7 to 17 ^{0}C. Whereas, average monthly precipitation is 1.54 inches. The mean wind speed is 3.4 m/s. Thus, for each monitoring station, the weather data is separately collected through NOAA regional climate center. The meteorological parameters are considered from Chapter 6.

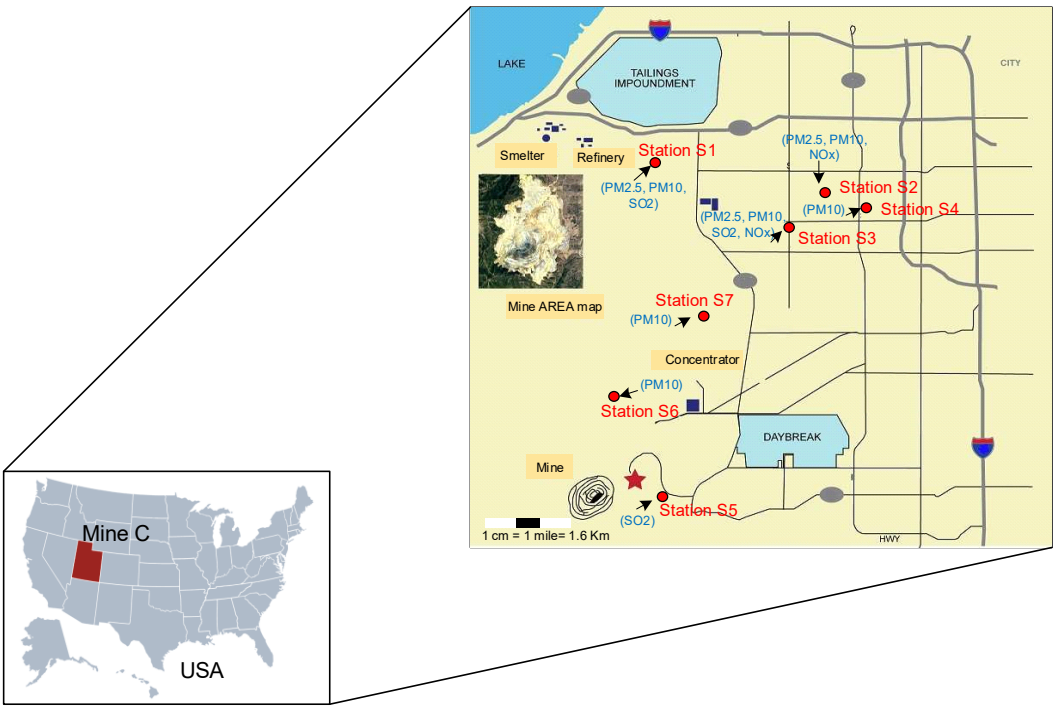

Figure 9.1 Location of mine C and monitoring station

9.2 Input Database and Data Collection

In the proposed LCAQMS approach, there are three components of input database including geographical, meteorological and air emission inventory from the LCA output as discussed in Chapter 4. The geographical database included digital maps, land usage data, elevation dataset, surface roughness length and processed into gridded surface within the modeling domain. Whereas, meteorological data included the wind speed, direction of the wind, ambient temperature, precipitation rate, stability class, etc. The added parameters are emission rate from the sampling points, stack height, stack diameter, exhaust temperature, exit velocity and plume rise. These data sets are spatially allocated and stored in the database in the corresponding compartment and saved as Excel spreadsheet. Following Table 9.1 shows different sources of database and their categories used in this study.

Table 9.1 Input databases for LCAQMS simulation

Category	Data	Pollutants/parameters	Description
Technical	Mining activities; infrastructure	Ore removal, drilling, hauling, handling, concentrating, smelting, refining, stockpiling/overburden, tailing and power plants	Technical reports; websites (mine C)
Emissions	Emission data per unit activity (tones/hr)	NOx, SO_2, PM_{10}, $PM_{2.5}$, CO, VOCs, CH_4, Hg, NH_3	Sampling data at the source or per unit activity (mine C)
Emissions	National pollution emission inventory for year 2011-2014 (tones/year)	NOx, SO_2, PM_{10}, $PM_{2.5}$, CO, VOCs	(USEPA, 2014) Air emission inventories.
Meteorology	Average daily data (2011-2015)	Wind speed (m/s); temperature (^{0}C); precipitation (mm/hr); frequency of wind direction	(NOAA, 2015) Regional climate center.
Land use	Digital mapping	Longitude and latitude; terrain type	(USGS maps, 2017)
Air monitoring	Average daily (2011-2015)	NOx (ppb) based on 1-hr average, SO_2 (ppb) based on 1-hr average, PM_{10} and $PM_{2.5}$ ($\mu g/m^3$) based on 24-hrs average	(Utah, 2017). Air pollution data Archive
Greenhouse data	Greenhouse gases facility data Average monthly (2011-2015)	CO_2, CH_4, N_2O (CO_2 eq. metric tones)	(USEPA, 2015) Greenhouse gases data at the facility level.

9.3 Implementation of LCAQMS Model

9.3.1 Emission inventory

Air emission inventory was generated by using inverse matrix method. Table 9.2 shows the quantitative inventory results for the year 2011-2013, illustrating that mine "C" contributed a maximum amount of NO_x, SO_2, PM_{10}, $PM_{2.5}$, CO, VOCs, NH_3, CH_4, and Hg. Diesel fuel combustion is one of the significant sources of NO_x production. During smelting and refining process nitrogen oxide is produced. Coal power plant is the primary source of SO_2 emissions at the mine site. Most the particulate matter is generated from natural activities at a mining site such as heavy machinery, bulldozing, blasting, and hauling of trucks on unpaved roads. Moreover, PM_{10} is also emitted when the wind blows over different types of stockpiles. PM_{10} and $PM_{2.5}$ are produced mainly from mobile equipment and vehicle exhausts. Whereas, CO is generated due to heavy equipment used during processing of ore and incomplete combustions. During data collection, it was found that landfill methane gas is being utilized for the refinery process from an adjacent municipal waste dump to replace natural gas used to heat the electrolyte. CH_4 is also considered as a greenhouse gas which may produce because of fuel consumption such as diesel, gasoline, and propane. Though, it is not directly generated due to the mining activities. Usually, the presence of VOCs is more profound during smelting processes of metals.

Table 9.2 Emission Inventory for the mining site

Pollutants	Inventory(tons/year)
PM_{10}	1238.4
$PM_{2.5}$	774
SO_2	3768.9
NO_x	4551.2
CO	254.8
CH_4	18.6
Hg	1.49
NH_3	72.8
VOCs	158.5

Figure 9.2 depicts a comparison between modeled values and the observed values gathered through the national monitoring database. For NO_x, there is 3.2 % difference,

because the obtained values also included the power consumption by the laboratory facilities which was not considered during the case study. Whereas, for SO_2 modeled value is 6.6 % more than observed. The reason behind this is that inlet temperature for concentrator varies which give rise to SO_2 generation. At the time of data collection, a high temperature is observed which ultimately produced the considerable amount of SO_2 as compared to the reported value which is based on average temperature.

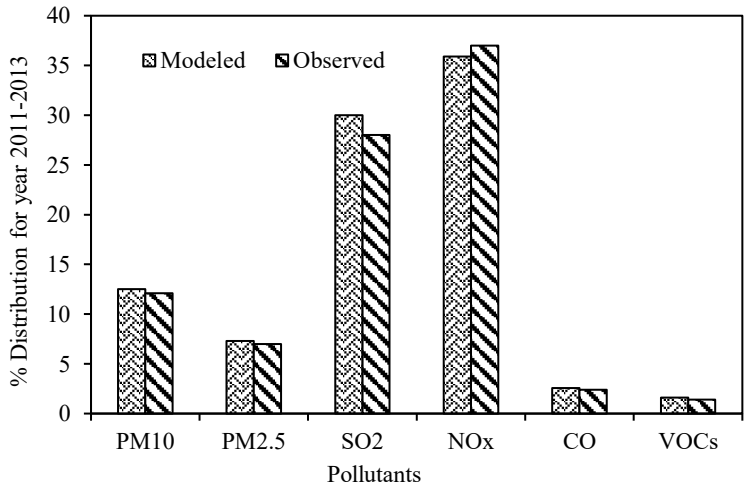

Figure 9.2 Evaluation of inventory with field values

9.3.2 Impact category assessment

Using TRACI method, the impacts of the same mine were calculated, based on the four selected environmental indicators which are climate change, acidification, particulate matter formation and photochemical oxidant formation. The results imply that it is possible to attribute the calculated environmental impact to each mining activity included within the boundary conditions and trace it back to the unit process(es) that generated them (see Figure 9.3). Furthermore, the results were normalized to the midpoint level based on background concentration database available at the Utah monitoring program.

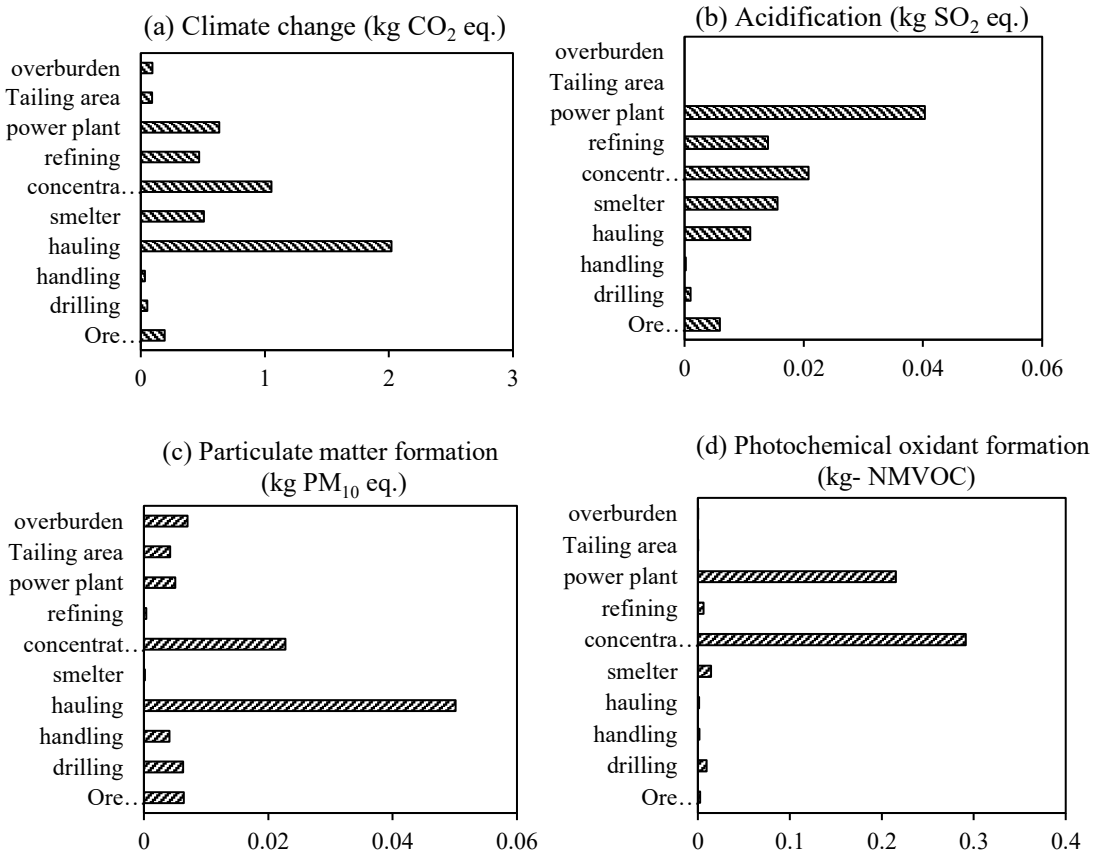

Figure 9.3 Midpoint impact assessment using TRACI (a) Climate change, (b) Acidification, (c) Particulate matter formation, (d) Photochemical oxidant formation

9.3.3 Carbon footprint analysis

Three greenhouse gases (CO_2, CH_4, N_2O) were considered depending upon the availability of data (2011-2015) and which might directly subsidize the carbon credit. The input variables subsequently included the stationary fuel combustion sources, coal power plant and adjacent waste landfill site to collect data for CH_4. Different combinations based on various nodes was performed through BPANN model for each scenario. Figure 9.4 represents modeled average value of carbon credit for each year for mine C and then compared it with the monitoring values for the same year. The trend sharply increased for the year 2013 but then gradually lower for 2014 and 2015.

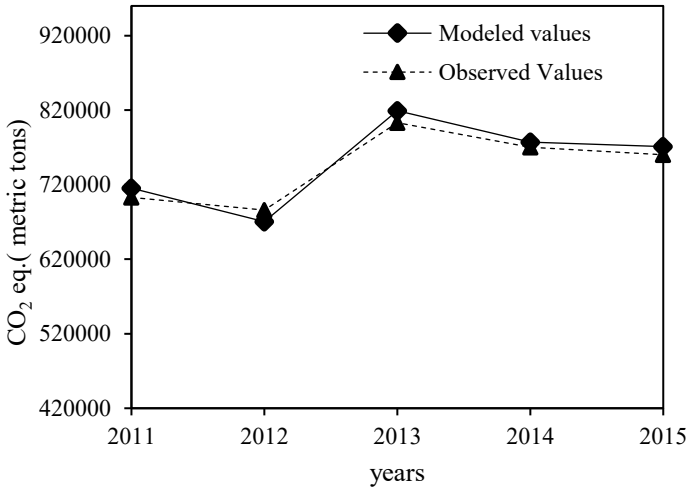

Figure 9.4 Carbon footprints for mine C and field comparison

9.3.4 Prediction of pollutant at the receptor level

The predicted concentrations at ground level were determined using the MADM algorithm while considering the dry deposition effect due to gravitational settling. Figure 9.5 shows the contour map representing elevation values at y-axis and distances interval at x-axis. Maximum values for $PM_{2.5}$ and PM_{10} were observed at the mining site. The predicted concentration gradually reduced as traveled as a plume away from the source. For SO_2 maximum concentrations were predicted around the smelter and refinery area of mine other than mine pit. The reason is that the energy source of these units is coal power plant. Moreover, it is interesting to observe that NO_x was found from 44 to 60 ppb not only around and at the mining site but also near the mine pit. It is noticeable that NO_x is high in this area due to transportation activities during hauling and other mobility of the equipment and other incomplete combustion of engines. Thus, all the values met the national ambient air quality standards (NAAQS).

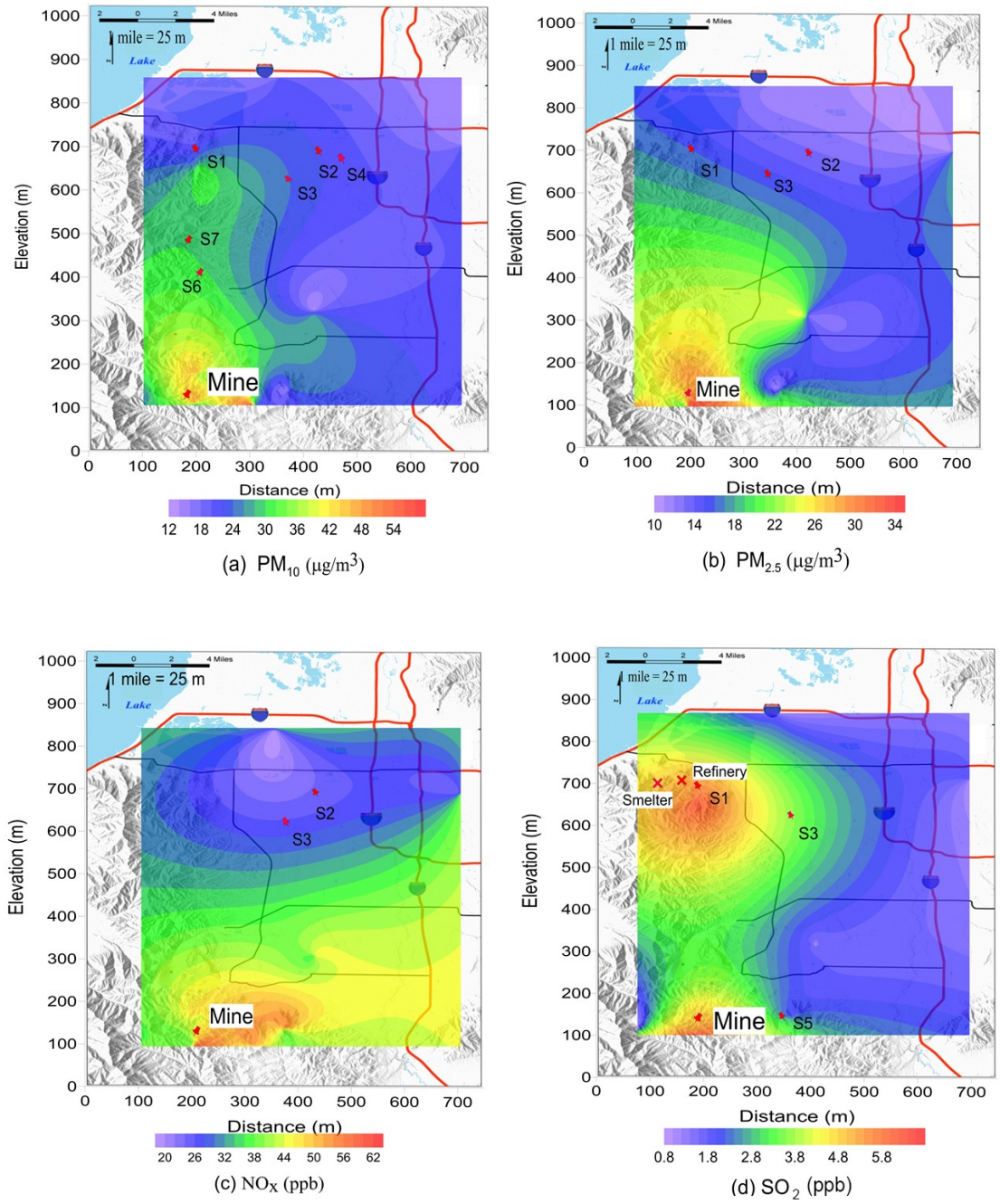

Figure 9.5 Contour mapping of air quality pollutant concentrations for mine C based on daily average from 2011 to 2015 for (a) PM_{10}; (b) $PM_{2.5}$; (c) NO_x; (d) SO_2

9.3.5 Decision analysis

Figure 9.6 illustrates the networking of alternatives based on positive and negative flows for mine C regardless of different groups. If all the options are considered as one group to fulfill the objectives of this study then in this situation, capping of vegetation along with the combination of idling reduction and CST program is dominated alternatives. Whereas, biodiesel method for the reduction of greenhouse gases is considered as a last preferable option as compared to other options. One can also interpret the results as a set of combination of different alternatives as one option. For instance; option 1 is to apply the combination of idling reduction, CST program, capping, hood over the conveyor, baghouse and water spraying which could be efficiently used for the removal of pollutants based on the evaluation of seven criteria mentioned in the methodology section. This combination of alternatives represented all the two groups and considered as the preferable cost-effective option on ranking basis. This option not only controls the dust problem but also reduce the fuel consumption and contribute towards the reduction of carbon footprints. The option 2 is baghouse, water spraying, chemical stabilizer, electrical drilling, and biodiesel. This option is the second preferable combination of different alternatives. In conclusion, the good networking also assists in selecting suitable technologies to implement a plan to control the air pollution at the mine site effectively.

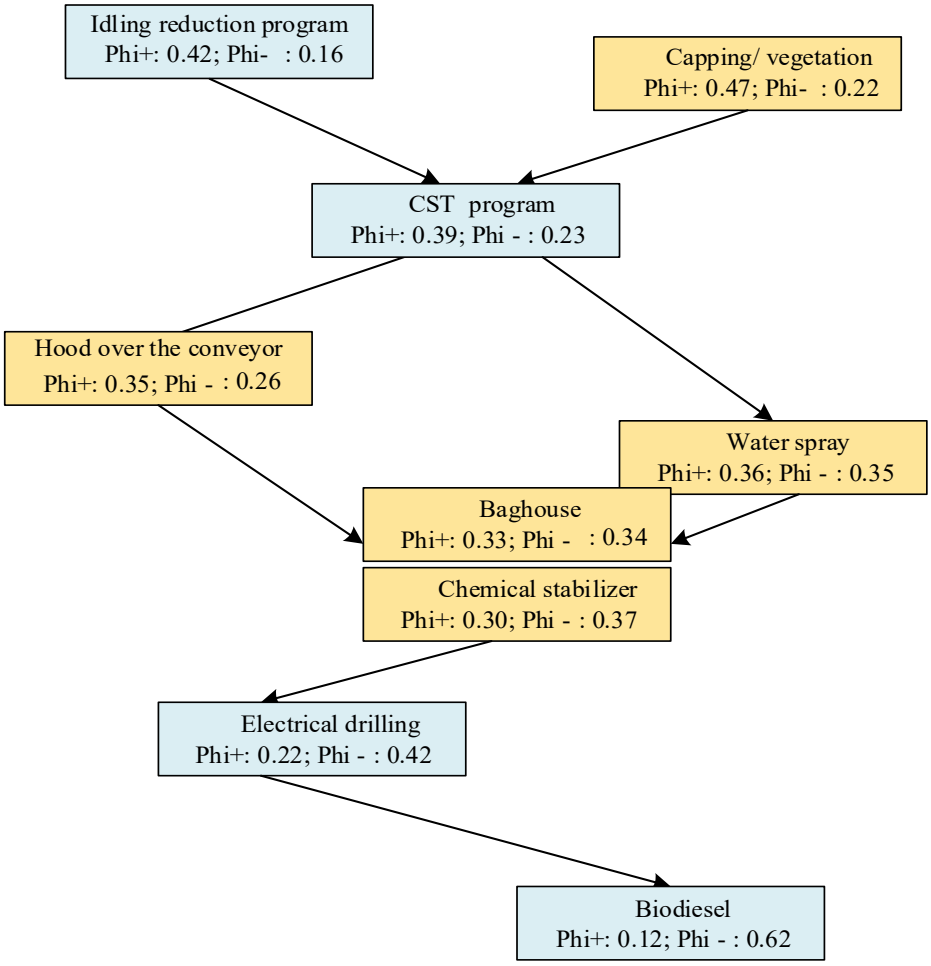

Figure 9.6 Results of alternatives network analysis using visual PROMETHEE

9.3.6 Validation of air quality Model

The MADM simulation is examined and validated by comparing the modeling results with the observations values of monitoring stations (S_1 to S7) under the same environmental conditions using the average daily data for from the January 2011 to December 2015. Results for $PM_{2.5}$, PM_{10}, SO_2, and NO_x were considered for regression analysis. Figure 9.7 illustrates the comparison of all the observed and modeled values at the monitoring station S_1 for the available pollutants as an example. Similar testing was performed for each monitoring station.

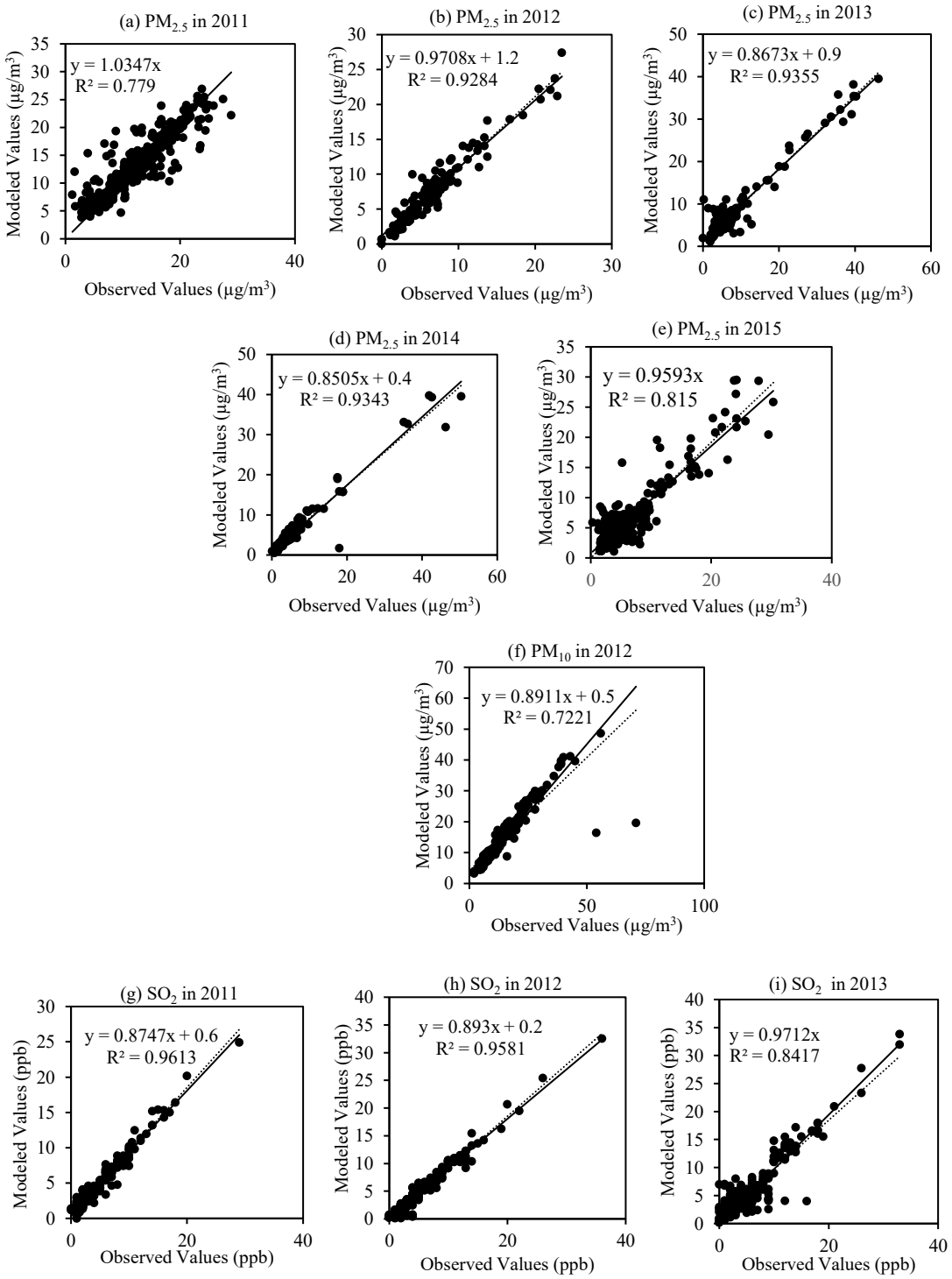

Figure 9.7 Correlation between modeling and monitoring data at S_1 (a) $PM_{2.5}$ in 2011, (b) $PM_{2.5}$ in 2012, (c) $PM_{2.5}$ in 2013, (d) $PM_{2.5}$ in 2014, (e) $PM_{2.5}$ in 2015, (f) PM_{10} in 2012, (g) SO_2 in 2011, (h) SO_2 in 2012, (i) SO_2 in 2013

Table 9.3 represents the coefficient of determination (R^2) for all the four pollutants at different monitoring stations. This result indicates that the MADM model can satisfactorily reproduce the variations of particulate matter and gaseous particles (SO_2 and NO_x). Moreover, the correlation value shows that model could generate predicted results using selected input parameter at various locations.

Table 9.3 Regression analysis for pollutants (2011-2015) at different monitoring stations

Station Id	R^2 for $PM_{2.5}$					R^2 for PM_{10}					R^2 for SO_2					R^2 for NO_2				
	2011	2012	2013	2014	2015	2011	2012	2013	2014	2015	2011	2012	2013	2014	2015	2011	2012	2013	2014	2015
S1	0.779	0.92	0.93	0.93	0.82	--	0.722	--	--	--	0.96	.95	.84	--	--	--	--	--	--	--
S2	0.68	.74	--	--	.89	0.78	.70	--	--	.83	--	--	--	--	--	0.81	0.74	.79	.87	--
S3	--	.71	.642	.775	.72	.71	.74	.79	--	.72	.84	.70	.71	.69	.72	.74	.69	.88	.71	.74
S4	--	--	--	--	--	.94	.72	.87	.77	.75	--	--	--	--	--	--	--	--	--	--
S5	--	--	--	--	--	--	--	--	--	--	.69	.72	.70	--	.84	--	--	--	--	--
S6	--	--	--	--	--	.90	.91	.75	.81	--	--	--	--	--	--	--	--	--	--	--
S7	--	--	--	--	--	.79	.82	.88	.91	--	--	--	--	--	--	--	--	--	--	--

9.4 Discussion

The LCAQMS framework offers a flexible way to store a large quantity of data (e.g., physical environmental and technical data) while preserving their dependability with their corresponding operational processes in the mining system. The model allows the calculation of site-specific LCA impacts based on a real case study and provides a realistic way to allocate environmental burdens as inputs per unit process. It provides the level of details, essential to facilitate the LCA for midpoint impact categories.

LCAQMS application reveals that by developing inventory, assessing midpoint impact and analyzing carbon footprint, it could be useful as an assessment tool based on life cycle approach for further investigation of air pollution. Also, this framework helps during feasibility study of the mining project to find out potential air pollutants and carbon credit. The main aim that motivated the development of MADM method is to provide the air quality model that would provide predicted concentration profiles for

pollutants through the advanced Gaussian algorithm, suitable for the mining sites. It extended the tradition Gaussian model to consider point sources, line sources and fugitive emissions with mining emission rate calculations in one model. This approach explicitly shows understanding of the mining system, while successfully involve all the related atmospheric parameters. It allows understanding the effect of physical removal mechanism on the pollutant's load. It is anticipated that the results provided by the MADM help to gain further insight into air quality at mining industry.

Furthermore, by adding decision analysis module in the framework, help to get more quantitative and endpoint modeling results. The model can be used for adaptation of alternative technologies and air pollution control remedies at the mining site which would help in environmental management. Particularly coupling of models within the integrated environment is also a significant contribution to the limited literature available on the integrated environmental modeling system for the mining industry.

9.5 Summary

This chapter discusses the implementation of an integrated life cycle assessment based air quality modeling system (LCAQMS) for the mining sector. Modeling tools were applied in an open pit copper mine through LCAQMS framework. Based on the inventory results of air emissions developed in the study, it was observed that NO_x, SO_2, PM_{10}, and $PM_{2.5}$ were significant contributors towards the environmental load. The profound midpoint modeling impacts of copper mine were determined using TRACI method. Whereas, BPANN simulation technique was used for carbon footprint analysis of the mine C. The study confirms that ANN can predict the future concentration based on the past data. Conclusively, this mine was responsible for producing average 0.7×10^6 metric tons of CO_2 eq. from the year 2011 to 2015 because of greenhouse gases emissions and fuel consumption during the mining activities. Thus, it is expected that different mines would show different results, due to different operating conditions and emission rates. The MADM was applied for the continuous point sources emission in the mining sector. Air quality profiles of $PM_{2.5}$, PM_{10}, SO_2, and NOx are presented as a contour mapping for a mine C. The predicted concentrations

have been found in good agreement with the field observations to validate the developed MADM approach. For selecting the best technology based on various selection criteria, PROMETHEE method was used as a multicriteria decision-making tool.

CHAPTER 10 CONCLUSIONS AND RECOMMENDATIONS

10.1 Conclusions

This thesis is dedicated to developing the novel integrated life cycle assessment based air quality modeling system (LCAQMS) for the mining industry and applied to three different North American mining site. A graphical user interface is built. Inventory development, carbon footprint analysis, air quality modeling and the decision of the cost-effective control technology to minimize air pollution are the key points of the system. A series of the research tasks are conducted, which are summarized as follows:

1. The life cycle inventory model is developed using the inverse matrix method and impact assessment is investigated using defined characterization methodologies. Furthermore, the modeling approach explores the feasibility of back propagation artificial neural networking (BPANN) model to analyze the carbon footprints (CO_2 equivalent) by constructing different scenarios. The structural composition of LCAMM model assists to translate all mining data to generate the inventory and environmental impact for further analysis of pollutant's dispersion and assist decision makers to select an appropriate remedial technique in the mining industry. Both models (LCI and ANN) are implemented to the open-pit gold mining site, Canada, as integrated manner using a graphical user interface.

2. The k-theory Gaussian algorithm is used for the mining application. The analytical solution is modified by incorporating the emission rate based on various mining activities. Thus, a mining-zone air dispersion modeling system (MADM) has been developed for the prediction of air pollutants by considering mining activities and deposition mechanism. The implications of MADM shows that the model can perform well during low wind conditions as well as calm conditions which mostly other Gaussian models failed. Both particulate matter and gaseous pollutants have been addressed. As far as physical removal is concerned, by ignoring it, overestimated predicted concentrations are found near the ground surface as well

as at different receptor locations. The particles such as PM_{10} removal flux through dry deposition is slightly more as compared to the fine particle $PM_{2.5}$ because the deposition velocity for coarse particles is higher than the fine particles. The results reveal that all the values met air quality standards except $PM_{2.5}$ during the stable conditions. The performance of the model can be adjusted by incorporating background values if needed to improve the model to field values ratio.

3. The PTM method is integrated with the mining-zone air dispersion model (MADM) to examine the vertical dispersion effect on the pollutant concentration at ground level under the different stability patterns. The correlation of various meteorological parameters (wind speed, temperature, surface heat flux, and rainfall) is established with the mixing height. A detailed investigation is performed in a copper mining area (Utah, USA) by determining the atmospheric stability conditions based on seasonal variation and the diurnal cycle.

4. To manage the air pollution, a decision analysis method is developed by implementing the multi-criteria decision analysis (MCDA) method which helps in reducing air pollution and carbon footprints. The existing methods or frameworks in the mining sector, which have been used in the past to select the sustainable solution, are lacking aid of MCDA and there is need to contribute more in this field with a promising decision system. The analysis involves processing inputs to the PROMETHEE which assists in ranking the alternatives, while criteria weighting has been determined using the AHP method. The probability distribution of criteria weights and output flows are defined by performing uncertainty analysis using Monte Carlo Simulation (MCS). The sensitivity analysis is conducted using Spearman rank correlation method and walking criteria weights. The results indicate that the integrated framework provides a reliable way of ranking air pollution control alternatives and help in quantifying the impact of different criteria for the selected alternatives.

5. To further explore the decision analysis system, a stochastic air pollution control model is developed to achieve a cost-effective management solution. The air

pollution control model is formulated to predict the cost of treatment using linear programming with a single objective function and multi-constraints. Furthermore, an integrated fuzzy based risk assessment approach is applied to examine uncertainties and evaluate an ambient air quality systematically. This method incorporates meteorological data as a dispersion transfer function to support the local conditions. Monte Carlo simulation method is applied to perform the probabilistic analysis and the uncertainties in the inputs and predicted concentration. Fuzzy logic is then used to identify environmental risk through stochastic simulated cumulative distribution functions of pollutant concentration.

6. LCAQMS is developed by integrating LCAMM (life cycle inventory model, characterization methods, BPANN), MADM (including PTM method to determine meteorological parameters), and decision support system (MCDA and APCM). LCAQMS is a significant contribution to the limited literature available on the integrated system for the mining industry. Thus, a graphical user interface is developed. The system integrates inverse matrix which is used to develop air emission inventory; characterization method to assess the environmental implications; artificial neural network model for carbon footprint analysis; air dispersion modeling to predict the pollutant concentration at receptor level; and decision analysis tool to provide air pollution control solutions. The study indicates that the developed LCAQMS can serve as a useful tool to assess, predict and assist in the selection of environmental mitigation options for mining sites.

10.2 Contributions

The main contribution of this study is the development of a life cycle assessment based system which integrates air dispersion modeling and decision analysis modeling techniques for mining. This novelty approach contributes to the limited studies available in the discipline of integrated environmental modeling and mining. Several specific contributions are summarized below:

1. An integrated life cycle inventory and artificial neural network model is one of the significant contributions which allows to identify air emission load for each mining activity and to evaluate the emission impact by linking the life cycle inventory to each impact category. The modeling approach is applied to simulate the carbon footprint analysis for the mining site. The structural composition of matrix-based computed framework offers a flexible way to store the data (e.g., physical environmental and technical data) while preserving their dependability with their corresponding operational processes in the mining system. Moreover, this approach helps during the feasibility study of the mining project to find out potential air pollutants and carbon credit.

2. A local scale air dispersion model is developed which integrates with the meteorological method to provide predicted concentration profiles for multi-pollutants and can be easily applied to mining sites. This approach explicitly shows understanding of the mining system, while successfully involve all the atmospheric parameters. It allows the effect of physical removal mechanism (deposition) and vertical dispersion on the pollutant's load. It can be anticipated that the results provided by the MADM help to gain further insight into air quality in the mining industry.

3. A stochastic air quality management system for mining region is developed which aid planners to minimize the pollutants at a marginal cost by suggesting control pollution techniques The MCDA system is useful for decision makers to rank the alternatives for mine sites which help to minimize the dust, energy consumption and reduce cyanide during gold production. Additionally, Air pollution control model is developed to achieve the cost effective solution and a fuzzy set is applied to categorize the environmental guidelines to quantify the risk.

4. A graphical user interface is developed to integrate the primary and sub-models as a system called LCAQMS.

In conclusion, this thesis presents some distinguished features over traditional air quality models by incorporating life cycle inventory of related mining activities, carbon footprint analysis, seamless integration of mining-zone air dispersion modeling, and decision analysis for the in-depth evaluation of pollution control techniques. Moreover, the system integrated with optimization of cost-effective solution, effective quantification of uncertainties using stochastic technique and risk assessment using fuzzy method. Generally, the integrated LCAQMS graphical user interface can be used by environmental engineers to provide insight and technical bases for supporting air quality assessment, prediction and management. In summary, with these expanded evaluation dimensions, the integrated approach can be more effectively used and more confidence can be expected in dealing with air pollution and potential environmental.

10.3 Recommendations

The mining-zone air dispersion model incorporates the physical removal mechanism such as settling velocity and deposition. For future study, it is recommended to consider the chemical and biological transformation of the pollutants particularly for gaseous pollutants and their effect on the predicted concentrations.

For future work, it is recommended to incorporate downwash algorithm in the model by extending the features of the model to engulf the wind circulation effect around buildings in the residential area. Moreover, the model can be integrated with CFD model to get further insight of the air dispersion in the mining pit area.

The pollutants can be categorized as carcinogen and non-carcinogen, resulting in human health risk impact (such as lifetime cancer risk for the carcinogen, and hazard index for non-carcinogen). To quantify the general risk level, in addition to the environmental risks from guideline violation, health risks from multiple pollutants should be considered by incorporating more linguistic variables.

Due to the complex nature of mining activities and air pollution problems, the data required for the field applications is extensive. Although, most data sources are

relatively accurate, and reliable others are less so. Therefore, increasing the accuracy and certainty of the data sets through further investigation and verification would help to improve the quality of the generated forecasting and assessment results.

REFERENCES

Ashrafi, K., and Hoshyaripour, G. a. (2010). "A Model to Determine Atmospheric Stability and its Correlation with CO Concentration." International Journal of Civil and Environmental Engineering, 2(2), 83–88.

Asif, Z., and Chen, Z. (2016). "Environmental management in North American mining sector." Environmental Science and Pollution Research, 23(1), 167–179.

Asif, Z., Chen, Z., and Guo, J. (2018). "A study of meteorological effects on $PM_{2.5}$ concentration in mining area." Atmospheric Pollution Research, 9(4), 688–696. doi: https://doi.org/10.1016/j.apr.2018.01.004.

Asif, Z., Chen, Z., and Han, Y. (2018b). "Air quality modeling for effective environmental management in the mining region." Journal of Air and Waste Management Association, 68(9), 1001–1014.

Asif, Z., Chen, Z., and Zhu, Z.H. (2018c). "An integrated life cycle inventory and artificial neural network model for mining air pollution management." International Journal of Environmental Science and Technology, 1–10. doi:https://doi.org/10.1007/s13762-018-1813-9.

Atabi, F., Jafarigol, F., Moattar, F., and Nouri, J. (2016). "Comparison of AERMOD and CALPUFF models for simulating SO_2 concentrations in a gas refinery." Environmental Monitoring and Assessment, 188(9), 516–522.

Atkinson, D. G., Bailey, D. T., Irwin, J. S., and Touma, J. S. (1996). "Improvements to the EPA Industrial Source Complex Dispersion Model." Journal of Applied Meteorology, 36(8), 1088–1095.

Awuah-Offei, K., and Adekpedjou, A. (2011). "Application of life cycle assessment in the mining industry." International Journal of Life Cycle Assessment, 16(1), 82–89.

Baawain, M. S., and Al-Serihi, A. S. (2014). "Systematic approach for the prediction of ground-level air pollution (around an industrial port) using an artificial neural network." Aerosol and Air Quality Research, 14, 124–134.

Badr, T., and Harion, J. L. (2007). "Effect of aggregate storage piles configuration on dust emissions." Atmospheric Environment, 41(2), 360–368.

Baklanov, A. (2000). "Application of CFD Methods for Modeling in Air Pollution

Problems : Possibilities and Gaps." Environmental Monitoring and Assessment, 65(1), 181–189.

Baklanov, A., Joffre, S. M., Piringer, M., Deserti, M., Middleton, D. R., Tombrou, M., Karppinen, A., Emeis, S., Prior, V., and Rotach, M. W. (2005). "Scientific Report 06-06 Towards estimating the mixing height in urban areas." Danish Meteorological Institute, ISBN: 87-7478-540-0.

Bare, J. C., Norris, G. A., Pennington, D. W., and Mckone, T. (2003). "TRACI: The Tool for the Reduction and Assessment of Chemical and Other Environmental Impacts." Journal of Industrial Ecology, 6(3), 49–78.

Barnes, M. J., Brade, T. K., Mackenzie, A. R., Whyatt, J. D., Carruthers, D. J., Stocker, J., Cai, X., and Hewitt, C. N. (2014). "Spatially-varying surface roughness and ground-level air quality in an operational dispersion model." Environmental Pollution, 185, 44–51.

Baumann, H., and Tillman, A.M. (2004). "The Hitch Hiker's Guide to LCA. An orientation in life cycle assessment methodology and application." Data Management, 13, 543–550.

Belton, V., and Stewart, T. (2002). "Multiple criteria decision analysis: an integrated approach. " Springer Science and Business Media, Boston, MA. eBook ISBN: 978-1-4615-1495-4.

Betrie, G. D., Sadiq, R., Morin, K. A., and Tesfamariam, S. (2013). "Selection of remedial alternatives for mine sites: A multicriteria decision analysis approach." Journal of environmental management, 119, 36–46.

Bhandari, S., Bhandari, A., and Arya, S. (2004). "Dust resulting from blasting in surface mines and its control." Proceedings of explosive conference, 25–34.

Bhaskar, R., and Ramani, R. V. (1988). "Dust flows in mine airways: a comparison of experimental results and mathematical predictions." Publications produced in the Generic Mineral Technology Center for Respirable Dust in the year, 31–39.

Bhattacharjee, S., Das, M., Ghosh, S. K., and Shekhar, S. (2016). "Prediction of meteorological parameters." 24th ACM SIGSPATIAL International Conference on Advances in Geographic Information Systems, ACM sigspatial GIS 2016.

Bogdanovic, D., Nikolic, D., and Ivana, I. (2012). "Mining method selection by integrated AHP and PROMETHEE method." Anais da Academia Brasileira de

Ciencias, 84(1), 219–233.

British Columbia air data. (2017). Available at http://www.gov.bc.ca/assests/gov. Accessed Oct.14, 2017.

Bugarski, A. D., Janisko, S. J., Cauda, E. G., Patts, L. D., Hummer, J. A., Westover, C., and Terrillion, T. (2014). "Aerosols and criteria gases in an underground mine that uses FAME biodiesel blends." The Annals of Occupational Hygiene, 58(8), 971–982.

Buske, D., Vilhena, M. T., Moreira, D. M., and Tirabassi, T. (2007). "Simulation of pollutant dispersion for low wind conditions in stable and convective planetary boundary layer." Atmospheric Environment, 41(26), 5496–5501.

CAAQS. (2017). "Canadian Ambient Air Quality Standards." Available at https://www.ccme.ca/en/resources/air/air/sulphur-dioxide.html. Accessed Feb. 12, 2017.

Carson, J. E., and Moses, H. (1969). "The validity of several plume rise formulas." Journal of the Air Pollution Control Association, 19(11), 862–866.

Caterpillar. (2010). Caterpillar Performance Handbook - edition 40, Caterpillar Inc, Peoria, 2010. Accessed Dec. 12, 2017.

CDED. (2017). Available at https://open.canada.ca/data/. Accessed Dec. 27, 2017.

Cecala, A. B., O'brien, A. D., Schall, J., Colinet, J. F., Fox, W. R., Franta, R. J., Joy, J., Reed, W. R., Reeser, P. W., and Rounds, J. R. (2012). "Dust control handbook for industrial minerals mining and processing." NIOSH Report of Investigation, Publication No. 2012-112 (RI 9689), 1–284.

Chan, K. Y., and Jian, L. (2013). "Identification of significant factors for air pollution levels using a neural network based knowledge discovery system." Neurocomputing, 99, 564–569.

Chandra, J. P., and Katiyar, V. K. (2011). "Mathematical model for dispersion of air pollutant considering settling of particles and dry deposition." International Journal of Mathematical Sciences and Applications, 1(3), 1591–1595.

Chaulya, S. K., Ahmad, M., Singh, R. S., Bandopadhyay, L., Bondyopadhay, C., and Mondal, G. C. (2003). "Validation of two air quality models for Indian mining conditions." Environmental monitoring and assessment, 82(1), 23–43.

Chen, Z., Huang, G., and Chakma, A. (2003). "Hybrid Fuzzy-Stochastic Modeling

Approach for Assessing Environmental Risks at Contaminated Groundwater Systems. ” ASCE Journal of Environmental Engineering, 129(1),79–88.

Chen, Z., Zhao, L., and Lee, K. (2010). “Environmental risk assessment of offshore produced water discharges using a hybrid fuzzy-stochastic modeling approach.” Environmental Modelling and Software, 25 (6), 782–792.

Cheng, S., Li, L., Chen, D., and Li, J. (2012). “A neural network based ensemble approach for improving the accuracy of meteorological fields used for regional air quality modeling.” Journal of environmental management, 112, 404–414.

CIEEDAC. (2015). “Canadian Industrial Energy End use Data and Analysis Center.” Metal Ore Mining 12200, Available at http://www.cieedac.sfu.ca/index.html. Accessed Apr. 21, 2015.

Clímaco, J., and Craveirinha, J. (2005). “Multiple criteria decision analysis–state of the art surveys.” International Series in Operations Research and Management Science, Publisher Springer-Verlag New York**,** 899–951.

CMLCA. (2015). Available at http://cml.leiden.edu/software/data-cmlia.html. Accessed Jun. 5, 2015.

Cole, C. F., and Fabrick, A. J. (1984). “Surface mine pit retention.” Journal of the Air Pollution Control Association, 34(6), 674–675.

Cole, C. F., and Zapert, J. G. (1995). “Air quality dispersion model validation at three stone quarries.” TRC Environmental Corp. TRC project No. 14884 for the National Stone Association, Washington DC.

Cooper, C. D., and Alley, F. C. (2002). Chapter 3: “Air pollution control: A design approach. ” Waveland Press Inc., Illinois, p. 126.

Cooper, J. S. (2003). “The Computational Structure of Life Cycle Assessment, by Reinout Heijungs and Sangwon Suh. Dordrecht.” Journal of Industrial Ecology, 7(2), 131–132.

Corporan, E., Quick, A., DeWitt, M., Lee, C., Serre, S., Zhao, Y., Lee, S., Hastings, T., Chin, P., Ollis, D., Qian, J., Ferro, A., Fowler, K., Annamalai, K., Sweeten, J., Stokke, J., Mazyck, D., et al. (2008). “Effect of Meteorological Parameters on Fine and Coarse Particulate Matter Mass Concentration in a Coal-Mining Area in Zonguldak, Turkey.” Journal of the Air and Waste Management Association, 58(4), 543–552.

Costa, a., Macedonio, G., and Folch, a. (2006). "A three-dimensional Eulerian model for transport and deposition of volcanic ashes." Earth and Planetary Science Letters, 241, 634–647.

Cristóbal, J., Guillén-Gosálbez, G., Jiménez, L., and Irabien, A. (2012). "Optimization of global and local pollution control in electricity production from coal burning." Applied Energy, 92, 369–378.

Dieterle, F. J. (2003). "Multianalyte quantifications by means of integration of artificial neural networks, genetic algorithms and chemometrics for time-resolved analytical data." PhD. Thesis, University of Tübingen.

Diez, S., Barra, E., Crespo, F., and Britch, J. (2014). "Uncertainty propagation of meteorological and emission data in modeling pollutant dispersion in the atmosphere." Ingeniería e Investigación, 34(2), 44–48.

Driussi, C., and Jansz, J. (2006). "Technological options for waste minimisation in the mining industry." Journal of Cleaner Production, 14(8), 682–688.

Durucan, S., Korre, A., and Munoz-Melendez, G. (2006). "Mining life cycle modelling: a cradle-to-gate approach to environmental management in the minerals industry." Journal of Cleaner Production, 14(12–13 SPEC. ISS.), 1057–1070.

Dwayne, D. T., and Regensburg, B. (2001). "Guidelines for mine haul road design." Applied Science, Faculty of Engineering, School of (Okanagan), University of British Columbia.

ECC. (2017). "Environment and climate change Canada." Available at http://open.canada.ca. Accessed Jul. 16, 2017.

Eco-indicator. (2016). Available at http://www.pre.nl/eco-indicator99/. Accessed Jun. 16, 2016.

Ecoinvent. (2016). Available at https://www.ecoinvent.org/database/ecoinvent-34/ecoinvent-34.html. Accessed Jun. 15, 2016.

Economics, I., and Ecology, I. (2009). "Handbook of Input-Output Economics in Industrial Ecology edited by Sangwon Suh." Journal of Industrial Ecology, 13(5), 830–832.

EDIP. (2016). Available at http://cpmdatabase.cpm.chalmers.se. Accessed Jul. 7, 2016.

Eglinton, T., Hinkley, J., Beath, A., and Dell'Amico, M. (2013). "Potential applications

of concentrated solar thermal technologies in the Australian minerals processing and extractive metallurgical industry." JOM, 65(12), 1710–1720.

Elevli, B., and Demirci, A. (2004). "Multicriteria choice of ore transport system for an underground mine: Application of PROMETHEE methods." Journal-south african institute of mining and metallurgy, 104, 251–256.

Environment Canada. (2016). "Weather and meterological data." Available at https://www.ec.gc.ca. Accessed Oct. 15, 2016.

EPA. (1995). "Modeling fugitive dust impacts from surface coal mining operations: phase III – evaluating model performance. " Research Triangle Park, NC: U.S. Environmental Protection Agency, Office of Air Quality Planning and Standards, Emissions, Monitoring, and Analysis Division, EPA publication No. EPA–454/R–96–002.

EPA. (2004). "Good Practice Guide for Atmospheric Dispersion Modeling." New Zealand. Number 522; National Institute of Water and Atmospheric Research: Wellington, New Zealand, 2004.

EPA. (2006). "Compilation of air pollutant emission factors, Volume 1: Stationary Point and Area Sources. Chapter 13: Miscellaneous Sources. Section 13.2.2: Unpaved Roads." Available at https://www.epa.gov/air-emissions-factors-and-quantification/ap-42-compilation-air-emissions-factors. Accessed Jul. 7, 2016.

Ericson, B., Hanrahan, D., and Kong, V. (2008). "The world's worst pollution problems: the top ten of the toxic twenty." Blacksmith Institute and Green Cross.Available at http:// www.worstpolluted.org. Accessed Sep. 19, 2017.

Ermak, D. L. (1977). "An analytical model for air pollutant transport and deposition from a point source." Atmospheric Environment (1967), 11(3), 231–237.

Essa, K. S. M., Embaby, M. M., Kozae, A. M., Mubarak, F., and Kamel, I. (2006). "Estimation of seasonal atmospheric stability and mixing height by using different schemes." VIII Radiation Physics and Protection Conference, 13-15 November 2006, Egypt.

Essa, K. S. M., Etman, S. M., and El-Otaify, M. S. (2014). "Modeling of atmospheric dispersion with dry deposition: an application on a research reactor." Revista Brasileira de Meteorologia, 29(3), 331–337.

Essa, K. S. M., Etman, S. M., and Embaby, M. (2007). "New analytical solution of the

dispersion equation." Atmospheric Research, 84(4), 337–344.

Finkbeiner, M., Inaba, A., Tan, R., Christiansen, K., and Klüppel, H.-J. (2006). "The new international standards for life cycle assessment: ISO 14040 and ISO 14044." The international journal of life cycle assessment, Springer, 11(2), 80–85.

Fisher, B. (2002). "Meteorological factors influencing the occurrence of air pollution episodes involving chimney plumes." Meteorological Applications, 9(2), 199–210.

Fishwick, S., and Scorgie, Y. (2011). "Performance of CALPUFF in predicting time-resolved particulate matter concentrations from a large scale surface mining operation." Proceedings of CASANZ Conference, 1–5.

García-Díaz, J. C., and Gozalvez-Zafrilla, J. M. (2012). "Uncertainty and sensitive analysis of environmental model for risk assessments: An industrial case study." Reliability Engineering and System Safety, 107, 16–22.

Garland, J. A., and Branson, J. R. (1976). "The mixing height and mass balance of SO2 in the atmosphere above Great Britain." Atmospheric Environment (1967), 10(5), 353–362.

Geldermann, J., Spengler, T., and Rentz, O. (2000). "Fuzzy outranking for environmental assessment. Case study: Iron and steel making industry." Fuzzy Sets and Systems, Elsevier Science Publishers B.V., 115(1), 45–65.

Gobakis, K., Kolokotsa, D., Synnefa, A., Saliari, M., Giannopoulou, K., and Santamouris, M. (2011). "Development of a model for urban heat island prediction using neural network techniques." Sustainable Cities and Society, 1(2), 104–115.

González, B., Adenso-Díaz, B., and González-Torre, P. . (2002). "A fuzzy logic approach for the impact assessment in LCA." Resources, Conservation and Recycling, 37(1), 61–79.

Gopal, S., Tang, X., Phillips, N., Nomack, M., Pasquarella, V., and Pitts, J. (2016). "Characterizing urban landscapes using fuzzy sets." Computers, Environment and Urban Systems, 57, 212–223.

Goyal, R., and Kumar, P. (2013). "Indoor-outdoor concentrations of particulate matter in nine microenvironments of a mix-use commercial building in megacity Delhi." Air Quality, Atmosphere and Health, 67, 747–757.

Grandinetti, L., Guerriero, F., Lepera, G., and Mancini, M. (2007). "A niched genetic

algorithm to solve a pollutant emission reduction problem in the manufacturing industry: A case study." Computers and Operations Research, 34(7), 2191–2214.

Gurumurthy, A., and Kodali, R. (2008). "A multi-criteria decision-making model for the justification of lean manufacturing systems." International Journal of Management Scienceand Engineering Management, 3(2), 100–118.

Gwak, J. M., Kim, M. R., and Hur, T. (2003). "Analysis of internally recurring unit processes in life cycle assessment." Journal of Cleaner Production, 2, 437–457.

Hassoon, A. F., Mohammed, S. K., and Al-Saleem, H. H. H. (2014). "Atmospheric Stability and Its Effect on The Polluted Columns of Concentrations in North West of Baghdad City." Iraqi Journal of Science, 55(2A), 572–581.

Heijungs, R., Huppes, G., and Guinée, J. B. (2010). "Life cycle assessment and sustainability analysis of products, materials and technologies. Toward a scientific framework for sustainability life cycle analysis." Polymer Degradation and Stability, 95(3), 422–428.

Heijungs, R., Koning, A., Suh, S., and Huppes, G. (2006). "Toward an Information Tool for Integrated Product Policy: Requirements for Data and Computation." Journal of Industrial Ecology, 10(3), 147–158.

Heijungs, R., and Suh, S. (2006). "Reformulation of matrix-based LCI: From product balance to process balance." Journal of Cleaner Production, 14(1), 47–51.

Heijungs, R., and Sun, S. (2002). "The computational structure of life cycle assessment." The International Journal of Life Cycle Assessment. Publisher Springer Netherlands, doi:10.1007/BF02978899.

Helmis, C. G., Sgouros, G., Tombrou, M., Schäfer, K., Münkel, C., Bossioli, E., and Dandou, A. (2012). "A Comparative Study and Evaluation of Mixing-Height Estimation Based on Sodar-RASS, Ceilometer Data and Numerical Model Simulations." Boundary-Layer Meteorology, 145(3), 507– 526.

Hendrickson, C. T., Horvath, A., Joshi, S., Klausner, M., Lave, L. B., and McMichael, F. C. (1997). "Comparing two life cycle assessment approaches: a process model vs.economic input-output-based assessment." Proceedings of the 1997 IEEE International Symposium on Electronics and the Environment. ISEE-1997.

Huang, I. B., Keisler, J., and Linkov, I. (2011). "Multi-criteria decision analysis in environmental sciences: ten years of applications and trends." Science of the total

environment, 409(19), 3578–3594.

Huertas, J. I., Huertas, M. E., Izquierdo, S., and González, E. D. (2012). "Air quality impact assessment of multiple open pit coal mines in northern Colombia." Journal of Environmental Management, 93, 121–129.

Hunter, C. (2012). A Recommended Pasquill-Gifford Stability Classification Method for Safety Basis Atmospheric Dispersion Modeling at SRS, Report No. SRNL-STI--2012-00055.

ILCD. (2015). "Characterization factors. " Available at http://www.lct.jrc.ec.europa.eu. Accessed Dec. 12, 2015.

IMPACT. (2002). Available at https://www.quantisintl.com. Accessed Apr. 12, 2015.

Ingwersen, W.W. (2011). "Emergy as a Life Cycle Impact Assessment Indicator: A Gold Mining Case Study." Journal of Industrial Ecology, 15(4), 550–567.

ISO. (2006). "ISO 14044: Environmental Management — Life Cycle Assessment — Requirements and Guidelines." Environmental Management, 3, 54–60.

Kaimal, J. C., and Finnigan, J. J. (1994). "Atmospheric boundary layer flows: their structure and measurement. " Oxford university press.

Kaya, I., and Kahraman, C. (2009). "Fuzzy robust process capability indices for risk assessment of air pollution." Stochastic Environmental Research and Risk Assessment, 529–541.

Kaya, I., and Kahraman, C. (2011). "A new tool for risk assessment of air pollution: Fuzzy process capability indices." Human and Ecological Risk Assessment, 17(3), 613–630.

Keeney, R. L., and Raiffa, H. (1993). "Decisions with multiple objectives: preferences and value trade-offs. " Cambridge university press.

Kiker, G. A., Bridges, T. S., Varghese, A., Seager, T. P., and Linkov, I. (2005). "Application of multicriteria decision analysis in environmental decision making." Integrated environmental assessment and management, 1(2), 95–108.

Kim, G. (2010). "Air Dispersion Modeling Guidelines." Journal of Chemical Information and Modeling. doi 10.1002/9781118723098.

Lal, B., and Tripathy, S. S. (2012). "Prediction of dust concentration in open cast coal mine using artificial neural network." Atmospheric Pollution Research, 3(2), 211–218.

Latini, G., Grifoni, R. C., and Passerini, G. (2000). "Dependency of mixing height as function of Monin-Obukhov length on stability conditions." Advances in Air Pollution. Air Pollution VIII, C.A. Brebbia, H. Power and J.W.S Longhurst (Editors) 2000 WIT Press, www.witpress.com, ISBN 1-85312-822-8.

Leili, M., Naddafi, K., Nabizadeh, R., Yunesian, M., and Mesdaghinia, a. (2008). "The study of TSP and PM10 concentration and their heavy metal content in central area of Tehran, Iran." Air Quality, Atmosphere and Health, 1(3), 159–166.

Lenzen, M. (2002). "A guide for compiling inventories in hybrid life-cycle assessments: Some Australian results." Journal of Cleaner Production, 10(6), 545–572.

Lesage, P., Ekvall, T., Deschênes, L., and Samson, R. (2006). "Environmental assessment of brownfield rehabilitation using two different life cycle inventory models." The International Journal of Life Cycle Assessment, 12(7), 497–513.

Li, J. B., Huang, G. H., Zeng, G. M., Maqsood, I., and Huang, Y. F. (2007). "An integrated fuzzy-stochastic modeling approach for risk assessment of groundwater contamination." Journal of Environmental Management, 82(2), 173–188.

Li, Y., and Guan, J. (2009). "Life cycle assessment of recycling copper process from copper-slag." 2009 International Conference on Energy and Environment Technology, ICEET 2009, 198–201.

Liao, K. J., and Hou, X. (2015). "Optimization of multipollutant air quality management strategies: A case study for five cities in the United States." Journal of the Air and Waste Management Association, 65(6), 732–742.

Liu, J., Zhu, L., Wang, H., Yang, Y., Liu, J., Qiu, D., Ma, W., Zhang, Z., and Liu, J. (2016). "Dry deposition of particulate matter at an urban forest, wetland and lake surface in Beijing." Atmospheric Environment, 125, 178–187.

Liu, L., Huang, G. H., Liu, Y., Fuller, G. A., and Zeng, G. M. (2003). "A fuzzy-stochastic robust programming model for regional air quality management under uncertainty." Engineering Optimization, 35(2), 177–199.

Lu, W. (2006). "Study on the advanced technique of environmental assessment based on life cycle assessment using matrix method." Doctoral dissertation, Graduate School of Engineering, The University of Tokyo.

Ma, X. M., and Zhang, F. (2002). "A genetic algorithm based stochastic programming

model for air quality management." Journal of environmental sciences (China), 14(3), 367–374.

Macharis, C., Springael, J., De Brucker, K., and Verbeke, A. (2004). "PROMETHEE and AHP: The design of operational synergies in multicriteria analysis - Strengthening PROMETHEE with ideas of AHP." European Journal of Operational Research, 6(1), 307–317.

Macintosh, D.L., Stewart, J.H., Myatt, T.A., Sabato, J.E., Flowers, G.C., Brown, K.W., Hlinka, D.J., and Sullivan, D.A. (2010). " Use of CALPUFF for exposure assessment in a near field complex terrian setting. " Atmospheric Environment, 44(2), 262–270.

Manomaiphiboon, K., and Russell, A. G. (2004). "Effects of uncertainties in parameters of a Lagrangian particle model on mean ground-level concentrations under stable conditions." Atmospheric Environment, 38(33), 5529–5543.

Martano, P. (2000). "Estimation of Surface Roughness Length and Displacement Height from Single-Level Sonic Anemometer Data." Journal of Applied Meteorology, 39(5), 708 –715.

MathWorks-trainlm. (2015). "Levenberg-Marquardt backpropagation." Available at http://www.mathworks.com/help/nnet/ref/trainlm.html. Accessed Aug. 24, 2015.

McKendry, I. G. (2002). "Evaluation of Artificial Neural Networks for Fine Particulate Pollution (PM_{10} and $PM_{2.5}$) Forecasting." Journal of the Air and Waste Management Association, 5(7), 31 –37.

Mesto. (2016). Available at http://www.metso.com/industries/mining/services-mining/. Accessed Aug. 21, 2016.

Mining Association Canada Report. (2012). "Towards Sustainable Mining Progress Report 2012." Available at http://mining.ca/sites/default/files/documents/TSMProgressReport2012.pdf. Accessed Jun. 6, 2014.

MJ Bradley and Associates. (2005). "Best Available Technology for Air Pollution Control." Analysis Guidance and Case Studies for North America. Accessed Sep. 6, 2014.

Mladineo, M., Mladineo, N., and Jajac, N. (2015). "Project management in mine actions using Multi-Criteria-Analysis-based decision support system." Croatian

Operational Research Review, 5(2), 415–425.

MOE BC. (2017). "Ministry of the Environment, BC Air data Archieve." Available at https://envistaweb.env.gov.bc.ca/. Accessed Dec. 20, 2017.

Moreira, D. M., Tirabassi, T., Vilhena, M. T., and Goulart, A. G. (2010). "A multi-layer model for pollutant dispersion with dry deposition to the ground." Atmospheric Environment, 44(15), 1859–1865.

Moreira, D. M., Vilhena, M. T., Buske, D., and Tirabassi, T. (2006). "The GILTT solution of the advection–diffusion equation for an inhomogeneous and nonstationary PBL." Atmospheric Environment, 40(17), 3186–3194.

Moreira, D. M., Vilhena, M. T., Buske, D., and Tirabassi, T. (2009). "The state-of-art of the GILTT method to simulate pollutant dispersion in the atmosphere." Atmospheric Research, Elsevier B.V., 92(1), 1–17.

Moreira, D. M., Vilhena, M. T., Tirabassi, T., Buske, D., and Cotta, R. (2005). "Near-source atmospheric pollutant dispersion using the new GILTT method." Atmospheric Environment, 39(34), 6289–6294.

NAAQS. (2017). "National ambient air quality standards." Available at https://www.epa.gov/sites/production/files/2015-02/documents/criteria.pdf. Accessed Sep. 24, 2017.

NAPS. (2015). "National air pollution Surveillance (NAPS) program." Available at http://maps-cartes.ec.gc.ca. Accessed Apr. 12, 2016.

Narita, N., Ikuta, Y., Nakano, K., Yamawaki M., Aoki, R. (2005). "Dissemination of LCA methodology through LCA software and database." . Journal of Life Cycle Assessment, 1, 96–101.

Nassar, N., Nagy, M., Agamy, S., Ramadan, A. B. A., and Tawfik, F. S. (2010). "Estimation of Atmospheric Stability Classification for the North Coast of Egypt." Journal of Environmental Science and Engineering, 4(6), 43–50.

National Pollutant Release Inventory. (2013). "NPRI Facility Reported Data by Substance, Environment Canada." Available at http://www.ec.gc.ca.Accessed Apr. 12, 2015.

Neshuku, M. N. (2012). "Comparison of the performance of two atmospheric dispersion models (AERMOD and ADMS) for open pit mining sources of air pollution." MSc. Thesis, Chemical engineering, University of Pretoria.

Nikolić, D., Milošević, N., Mihajlović, I., Živković, Ž., Tasić, V., Kovačević, R., and Petrović, N. (2010). "Multi-criteria analysis of air pollution with SO2 and PM10 in urban area around the copper smelter in Bor, Serbia." Water, air, and soil pollution, 206(1–4), 369–383.

NOAA. (2015). "Regional climate center. Salt Lake City Weather Forecast Office. " Available at http://www.weather.gov/climate. Accessed June 25, 2017.

NOAA calculator. (2017). "Calculating solar position." Available at https://www.esrl.noaa.gov/gmd/grad/solcalc/azel.html. Accessed Sep. 20, 2017.

NOAA (2017). "Mixing ratio calculator." Available at https://www.weather.gov/epz/wxcalc_mixingratio. Accessed Nov. 15, 2017.

Norgate, T., and Haque, N. (2010). "Energy and greenhouse gas impacts of mining and mineral processing operations." Journal of Cleaner Production, 18(3), 266–274.

Norgate, T., and Haque, N. (2012). "Using life cycle assessment to evaluate some environmental impacts of gold production." Journal of Cleaner Production, 29–30, 53–63.

Nuss, P., and Eckelman, M. J. (2014). "Life cycle assessment of metals: A scientific synthesis." PLoS One, Public Library of Science, 9(7),101–298.

Onkal-Engin, G., Demir, I., and Hiz, H. (2004). "Assessment of urban air quality in Istanbul using fuzzy synthetic evaluation." Atmospheric Environment, 38(23), 3809–3815.

Ontario. (2017). Available at http://www.airqualityontario.com. Accessed Nov. 12, 2017.

Ontario Ministry of Labour. (2013). "Blitz Results: Underground mining ventilation hazards." Available at http://www.labour.gov.on.ca. Accessed April 2, 2015.

OpenLCA. (2016). Available at http://www.openlca.org. Accessed Sep. 6, 2016.

Parga, J. R., Shukla, S. S., and Carrillo-Pedroza, F. R. (2003). "Destruction of cyanide waste solutions using chlorine dioxide, ozone and titania sol." Waste Management, 23(2), 183–191.

Patra, A. K., Gautam, S., Majumdar, S., and Kumar, P. (2016). "Prediction of particulate matter concentration profile in an opencast copper mine in India using an artificial neural network model." Air Quality, Atmosphere and Health, 9(6), 697–711.

Pereira, M. J., Soares, A., and Branquinho, C. (1997). "Stochastic simulation of fugitive dust emissions." Geostatistics Wollongong, 96, 1055–1065.

Ping, J., Chen, B., and Husain, T. (2010). "Risk Assessment of Ambient Air Quality by Stochastic-Based Fuzzy Approaches." Environmental Engineering Science, 27(3), 233–246.

Polat, G., Damci, A., Gurgun, A. P., and Demirli, I. (2016). "Urban Renewal Project Selection Using the Integration of AHP and PROMETHEE Approaches." Procedia Engineering, 339–346.

Prostański, D. (2013). "Use of air-and-water spraying systems for improving dust control in mines." Journal of Sustainable Mining, 12(2), 29–34.

Qin, X. S., and Huang, G. H. (2009). "Characterizing uncertainties associated with contaminant transport modeling through a coupled fuzzy-stochastic approach." Water, Air, and Soil Pollution, 197(1–4), 331–348.

Quebec. (2018). Available at http://www.mddelcc.gouv.qc.ca/air/criteres/Normes-criteres-qc-qualite-atmosphere.pdf. Accessed Jan. 13, 2018.

Quick LCA. (2015). Available at http://criepi.denken.or.jp/en. Accessed Dec. 2, 2015.

Rao, K. S. (1981). "Analytical solutions of a gradient-transfer model for plume deposition and sedimentation." US Department of Commerce, National Oceanic and Atmospheric Administration, Environmental Research Laboratories.

Recipe. (2016). Avaialble at http://www.lcia-recipe.net. Accessed Jun. 16, 2016.

Reed, W. R., Westman, E. C., and Haycocks, C. (2002). "The introduction of a dynamic component to the ISC 3 model in predicting dust emissions from surface mining operations." APCOM 2002: 30 th International Symposium on the Application of Computers and Operations Research in the Mineral Industry, 659–667.

Reid, C., Be´caert, V. rie, Aubertin, M., Rosenbaum, R. K., and DeschÃªnes, L. (2009). "Life cycle assessment of mine tailings management in Canada." Journal of Cleaner Production, 17(4), 471–479.

Ren, H., Zhou, W., Nakagami, K., Gao, W., and Wu, Q. (2010). "Multi-objective optimization for the operation of distributed energy systems considering economic and environmental aspects." Applied Energy, 87(12), 3642–3651.

Rio Tinto. (2016). Available at http://www.kennecott.com/air-quality. Accessed July 5, 2017.

Roy, S., Adhikari, G. R., Renaldy, T. A., and Jha, A. K. (2011a). "Development of multiple regression and neural network models for assessment of blasting dust at a large surface coal mine." Journal of Environmental science and Technology, 4(3), 284–301.

Roy, S., Adhikari, G. R., Renaldy, T. A., and Singh, T. N. (2011b). "Assessment of atmospheric and meteorological parameters for control of blasting dust at an Indian large surface coal mine." Research Journal of Environmental and Earth Sciences, 3(3), 234–248.

Saaty, T. L. (2008). "Decision making with the analytic hierarchy process." International Journal of Services Sciences,1(1), 83–98.

Sadiq, R., and Tesfamariam, S. (2009). "Environmental decision-making under uncertainty using intuitionistic fuzzy analytic hierarchy process (IF-AHP)." Stochastic Environmental Research and Risk Assessment, 23(1), 75–91.

Sargent and Lundy LLC. (2003). "Wet flue gas desulfurization technology evaluation." Report. Available at https://www.graymont.com. Accessed July 5, 2017.

Saxton, K., and Chandler, D. (2000). "Wind erosion and fugitive dust fluxes on agricultural lands in the Pacific Northwest." American Society of Agricultural Engineers, 43(3), 623–630.

Schmid, H. P., and Oke, T. R. (1990). "A model to estimate the source area contributing to turbulent exchange in the surface layer over patchy terrain." Quarterly Journal of the Royal Meteorological Society, 116(494), 965–988.

Shaban, H. I., Elkamel, A., and Gharbi, R. (1997). "An optimization model for air pollution control decision making." Environmental Modeling and Software, 12(1), 51–58.

Sharan, M., and Modani, M. (2007). "Variable K-theory model for the dispersion of air pollutants in low-wind conditions in the surface-based inversion." Atmospheric Environment, 41(33), 6951–6963.

Sheoran, V., Sheoran, A. S., and Poonia, P. (2013). "Phytostabilization of metalliferous mine waste." Journal of Industrial Pollution Control, 29(2), 183–192.

Silvester, S. a., Lowndes, I. S., and Hargreaves, D. M. (2009). "A computational study of particulate emissions from an open pit quarry under neutral atmospheric conditions." Atmospheric Environment, 43(40), 6415–6424.

Soriano, A., Pallarés, S., Pardo, F., Vicente, A. B., Sanfeliu, T., and Bech, J. (2012). "Deposition of heavy metals from particulate settleable matter in soils of an industrialised area." Journal of Geochemical Exploration, 113, 36–44.

Suh, S., and Huppes, G. (2002). "Missing inventory estimation tool using extended input-output analysis." The International Journal of Life Cycle Assessment, 7(3), 134–140.

Suh, S., Lenzen, M., Treloar, G. J., Hondo, H., Horvath, A., Huppes, G., Jolliet, O., Klann, U., Krewitt, W., Moriguchi, Y., Munksgaard, J., and Norris, G. (2004). "System Boundary Selection in Life-Cycle Inventories Using Hybrid Approaches." Environmental Science and Technology, 38(3), 657–664.

Super Decisions tool. (2017). Available at https://www.superdecisions.com. Accessed Dec. 16, 2017.

Tartakovsky, D., Broday, D. M., and Stern, E. (2013). "Evaluation of AERMOD and CALPUFF for predicting ambient concentrations of total suspended particulate matter (TSP) emissions from a quarry in complex terrain." Environmental Pollution, 179, 138–145.

Tecer, L. H. (2007). "Prediction of SO_2 and PM concentrations in a coastal mining area (Zonguldak, Turkey) using an artificial neural network." Polish Journal of Environmental Studies, 16, 633–638.

Technical overview Quebec Report. (2013). "Regulation Respecting a Cap-and-Trade System for Greenhouse Gas Emission Allowances (C&T)." ISBN : 978-2-550-67550. Available at http://www.mddelcc.gouv.qc.ca. Accessed Jun. 16, 2014.

Tesfamariam, S., and Sadiq, R. (2006). "Risk-based environmental decision-making using fuzzy analytic hierarchy process (F-AHP)." Stochastic Environmental Research and Risk Assessment, 21(1), 35–50.

Tirabassi, T., Tiesi, A., Buske, D., Vilhena, M. T., and Moreira, D. M. (2009). "Some characteristics of a plume from a point source based on analytical solution of the two-dimensional advection-diffusion equation." Atmospheric Environment, Elsevier Ltd, 43(13), 2221–2227.

TRACI. (2016). Available at http://www.epa.gov/nrmrl/std/traci/traci.html. Accessed Oct. 15, 2016.

Trivedi, R., Chakraborty, M. K., and Tewary, B. K. (2009). "Dust dispersion modeling

using fugitive dust model at an opencast coal project of Western Coalfields Limited, India." Journal of Scientific and Industrial Research, 68(1), 71–78.

Turner, D. B. (1964). "A diffusion model for an urban area." Journal of Applied Meteorology, 3(1), 83–91.

Turner, D. B. (1997). "The Long Lifetime of the Dispersion Methods of Pasquill in U.S. Regulatory Air Modeling." Journal of Applied Meteorology, 36, 1016–1020.

Turner, J. H., Lawless, P. A., Yamamoto, T., Coy, D. W., Greiner, G. P., McKenna, J. D., and Vatavuk, W. M. (1988). "Sizing and costing of electrostatic precipitators part I. Sizing considerations." Journal of the Air Pollution Control Association, 38(4), 458–471.

Upadhyaya, G., and Dashore, N. (2011). "Fuzzy logic based model for monitoring air quality index." Indian Journal of Science and Technology, 4(3), 215–218.

USEPA. (1999). "Nitrogen Oxides (NO_x), Why and How They Are Controlled." Technical report, EPA 456/F-99-006R. Available at https://www.epa.gov. Accessed Jan. 25, 2015.

USEPA. (2002). "EPA air pollution control cost manual." Manual 6th edition, EPA/452/B-02-001. Available at https://www.epa.gov. Accessed Oct. 11, 2014.

USEPA. (2014). "Air emission inventories." Available at https://www.epa.gov/air-emissions-inventories/air-pollutant-emissions-trends-data. Accessed Oct. 11, 2014.

USEPA. (2015). "Greenhouse gases data at facility level." Available at https://ghgdata.epa.gov. Accessed Nov. 25, 2015.

USGS maps. (2017). Available at https://viewer.nationalmap.gov. Accessed Feb. 15, 2017.

USEtox. (2015). Available at http://www.usetox.org. Accessed Sep. 20, 2015.

Utah. (2017). Available at http://www.airmonitoring.utah.gov. Accessed Oct. 12, 2017.

Visscher, A. De. (2014). Air Dispersion Modeling. Foundations and Applications. Journal of Chemical Information and Modeling.

Vivaldini, M., Pires, S. R. I., and de Souza, F. B. (2012). "Improving logistics services through the technology used in fleet management." JISTEM-Journal of Information Systems and Technology Management, 9(3), 541–562.

Wang, S.-Y. S., Hipps, L. E., Chung, O.-Y., Gillies, R. R., and Martin, R. (2015).

"Long-Term Winter Inversion Properties in a Mountain Valley of the Western United States and Implications on Air Quality." Journal of Applied Meteorology and Climatology, 54(12), 2339–2352.

Wang, X., Zhang, L., and Moran, M. D. (2014). "Bulk or modal parameterizations for below-cloud scavenging of fine, coarse, and giant particles by both rain and snow." Journal of Advances in Modeling Earth Systems, 6(4), 1301–1310.

WHO. (2017). "Ambient (outdoor) air quality and health." Available at http://www.who.int/mediacentre/factsheets/fs313/en/. Accessed Jan. 12, 2017.

Worldsteel Association report. (2011). "About the Worldsteel Life Cycle Inventory." Available at http://www.worldsteel.org. Accessed May 15, 2014.

Wortmann, S., Vilhena, M. T., Moreira, D. M., and Buske, D. (2005). "A new analytical approach to simulate the pollutant dispersion in the PBL." Atmospheric Environment, 39(12), 2171–2178.

WRPLOT. (2017). Available at "https://www.weblakes.com/products/wrplot.html." Accessed Dec. 5, 2017.

Xu, H., Li, A., Feng, L., Cheng, X., and Ding, S. (2012). "Destruction of cyanide in aqueous solution by electrochemical oxidation method." Int.J.Electrochem.Sci, 7, 7516–7525.

Yang, A. L., Huang, G. H., Qin, X. S., and Fan, Y. R. (2012). "Evaluation of remedial options for a benzene-contaminated site through a simulation-based fuzzy-MCDA approach." Journal of hazardous materials, 213, 421–433.

Z. Chen, Y. Chen, S. S. Zhang, K. Wang, et al. (2015). "A Combined Robust Fuzzy Programming Model (CRFLP-AIR) for Regional Air Pollution Control Planning under Uncertainty." Wulfenia Journal, 22(12), 158–215.

Zannetti, P. (2013). Air pollution modeling: theories, computational methods and available software. Springer Science and Business Media.eBook ISBN: 978-1-4757-4465-1.

Zhang, H., Liu, Y., Shi, R., and Yao, Q. (2013). "Evaluation of PM_{10} forecasting based on the artificial neural network model and intake fraction in an urban area: A case study in Taiyuan City, China." Journal of the Air and Waste Management Association, 63(7), 755–763.

Zhang, H., Xu, T., Zong, Y., Tang, H., Liu, X., and Wang, Y. (2015). "Influence of

Meteorological Conditions on Pollutant Dispersion in Street Canyon." Procedia Engineering, 121, 899–905.

Zhou, Y., Levy, J. I., Hammitt, J. K., and Evans, J. S. (2003). "Estimating population exposure to power plant emissions using CALPUFF: A case study in Beijing, China." Atmospheric Environment, 37, 815–826.

Zhu, L., Liu, J., Cong, L., Ma, W., Wu, M., and Zhang, Z. (2016). "Spatiotemporal characteristics of particulate matter and dry deposition flux in the Cuihu Wetland of Beijing." PLoS ONE, 11(7), 109–116.

APPENDIX

Table A-1 Surface roughness length based on land use and seasons (USEPA, 2000; Li, 2009)

	Seasons (values in meters)			
Land type	Summer	Fall	Winter	Spring
Deciduous Forest	1.30	0.80	0.50	1.00
Grassland	0.10	0.01	0.001	0.05
Urban	1.00	1.00	1.00	1.00
Shrub land	0.30	0.30	0.15	0.30
Cultivated Land	0.20	0.05	0.01	0.03
Coniferous Forest	1.30	1.30	1.30	1.30
Water	0.0001	0.0001	0.0001	0.0001
Residential area	0.50	0.50	0.50	0.50

Case study: A copper-gold mine, British Columbia

Table A-2 Background emission rates (Environment Canada, 2016)

Sources	TSP	PM_{10}	$PM_{2.5}$	NO_2
Background		Emissions (tons/year)		
Industrial	1024	576.3	339.8	2248
Heating	176.2	166.6	165.4	110
Transportation	23.3	23.1	16.1	815
Any disturbed land	35.9	16.3	2.6	---

Table A-3 Environmental guidelines based on different standards

Pollutants	Standards	Averaging time	Values ($\mu g/m^3$)	Reference
$PM_{2.5}$	World health organization (WHO)	Annual	10	(British Columbia, 2017; CAAQS, 2017; NAAQS, 2017; Ontario, 2017; Quebec, 2018; WHO, 2017)
		24hrs	25	
	Canada NAAQO	Annual	10	
	USEPA-NAAQS	24 hrs	28	
		Annual	12	
	Provincial-Ontario	24 hrs	35	
	Quebec	24 hrs	30	
	British Columbia	24hrs	30	
	Utah	Annual	8	
		24hrs	25	
		Annual	15	
		24hrs	35	
PM_{10}	WHO	Annual	20	
		24hrs	50	
	Canada NAAQO	24hrs	25	
	USEPA-NAAQS	24hrs	150	
	Provincial-Ontario	24hrs	50	
	British Columbia	24hrs	50	
	Utah	24hrs	150	
NO_2	WHO	Annual	40	
		1 hr	200	
	Canada NAAQO	Annual	100A;60D	
		24 hrs	200A	
	USEPA-NAAQS	1 hr	400A	
		Annual	100	
	Provincial-Ontario	1 hr	188 (100ppb)	
		24 hrs	200	
	British Columbia	1 hr	400	
		Annual	60	
	Utah	1 hr	188 (100ppb)	
		Annual	100 (53 ppb)	
		1 hr	188 (100ppb)	
SO_2	WHO	Annual	50	
	Canada NAAQO	24hrs	125	
		Annual	60A;30D	
		24hrs	300A;150D;800T	
	USEPA-NAAQS	1hr	900A;450D	
		Annual	80	
	Provincial-Ontario	1hr	197	
		Annual	55	
	British Columbia	24hrs	275	
	Quebec	1 hr	197	
	Utah	Annual	52	
		Annual	60(.03ppm)	
		24 hrs	280(.14ppm)	
		1 hr	197(75ppb)	

A: Acceptable; D: Desirable; T: Toxic level

Table A-4 Scaling with respect to various range values of criteria

Scale	Efficiency (%)	Cost (10^3.$)	Energy consumption (kW)	Performance & air pollution	Future use Probability (%)	Risk
9	95-99	≥5000	350-400	Long term for multi-pollutants/activities	81-90	0.45-0.50
8	85-94	≥1000	300-350	Long term for two-pollutants/activities	71-80	0.40-0.45
7	75-84	≥500	250-300	Long term for single pollutant/activity	61-70	0.35-0.40
6	65-74	200-400	200-250	Medium-long	51-60	0.30-0.35
5	55-64	150-200	150-200	medium	41-50	0.25-0.30
4	45-54	100-150	100-150	Short-medium	31-40	0.20-0.25
3	35-44	50-100	50-100	Short term for multi-pollutants/activities	21-30	0.15-0.20
2	25-34	10-50	10-50	Short term for two-pollutants/activities	11-20	0.10-0.15
1	10-24	<10	<10	Short term for single pollutant/activities	5-10	≤0.09

Statistical analysis of various meteorological parameters with Mixing height

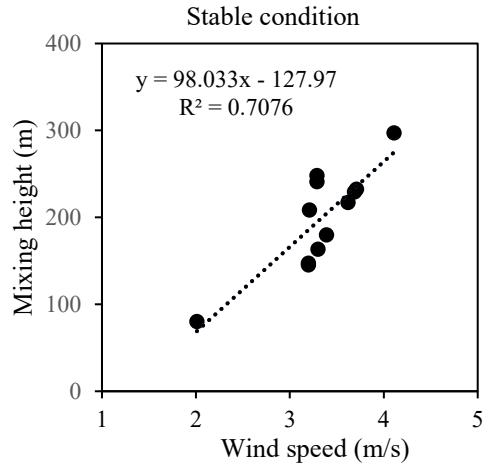

(a)

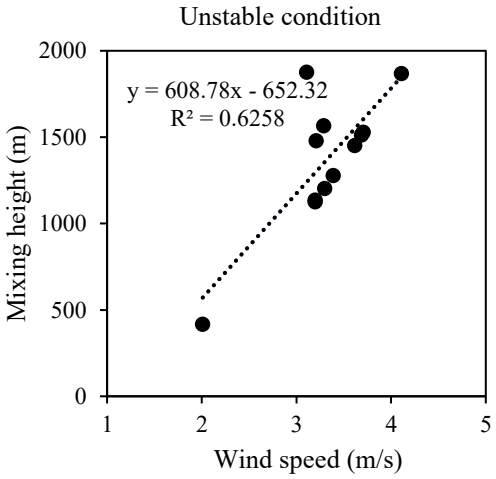

(b)

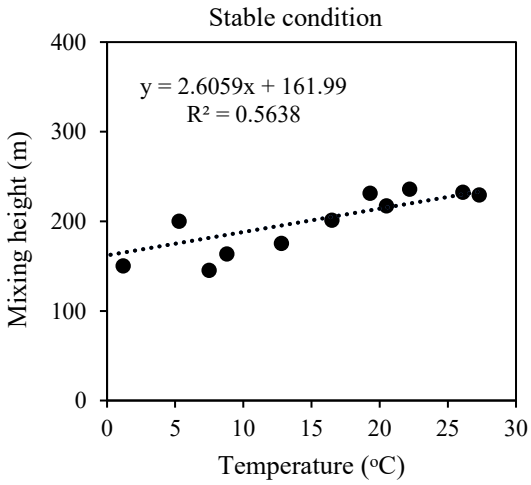

(c)

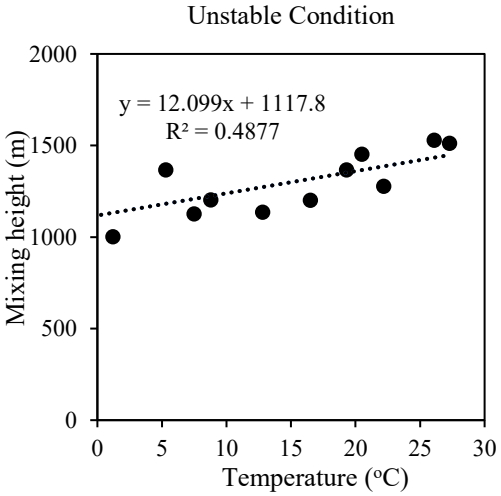

(d)

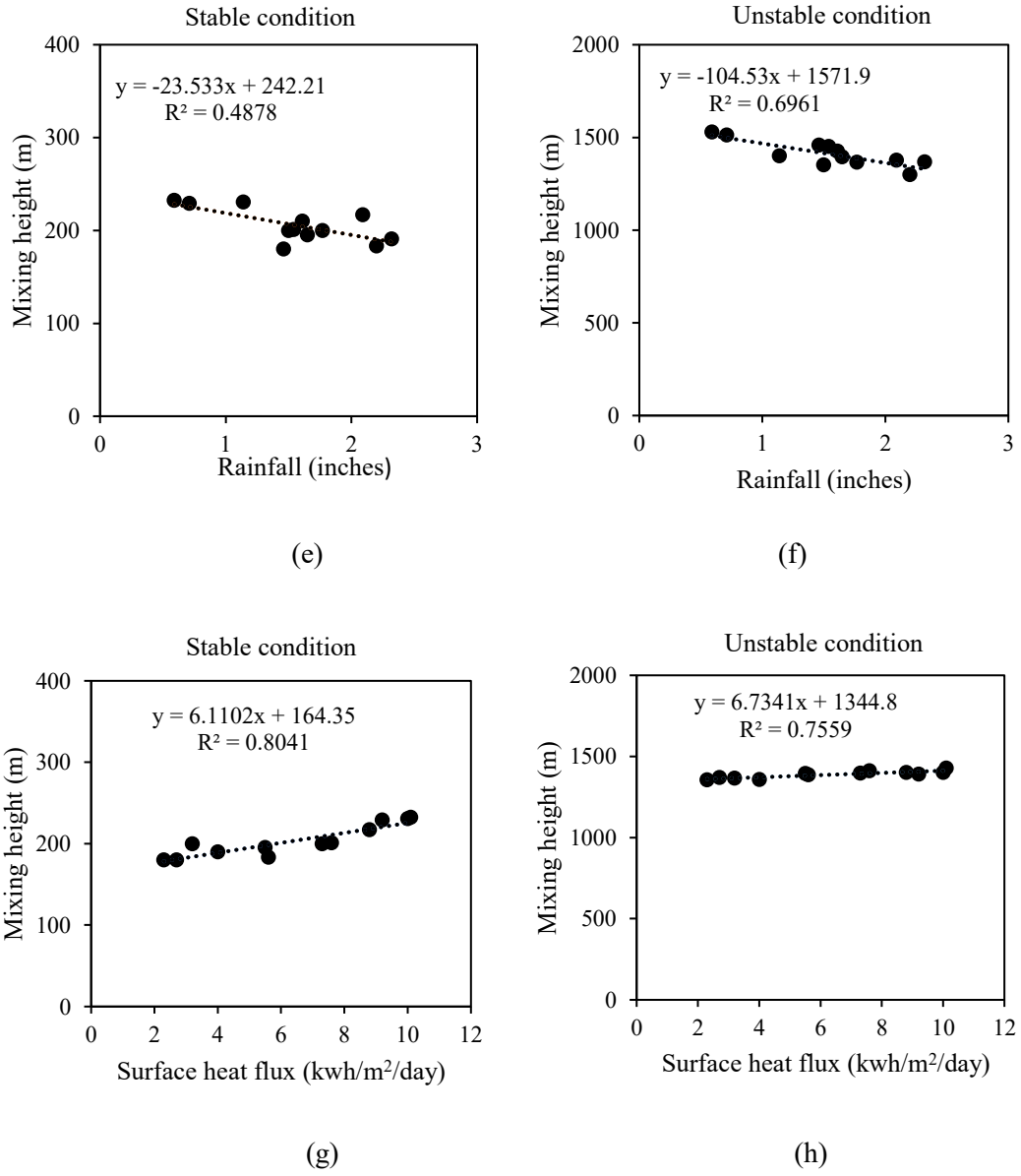

Figure A-1 Statistical correlation of mixing height with various meteorological factor (a) wind speed during stable condition (b) wind speed during unstable condition; (c) temperature during stable condition; (d) temperature during unstable condition; (e) rainfall during stable condition; (f) rainfall during unstable condition; (g) surface heat flux during stable condition; (h) surface heat flux during unstable condition.